

Evaluating 2B3, a novel immunotherapy in the PDAPP model of amyloid pathology

Charles Evans

Cardiff University

A thesis submitted for the degree of Doctor of Philosophy at Cardiff University

2016



DECLARATION

This work has not previously been accepted in substance for any degree and is not concurrently submitted in candidature for any degree.

Signed (Candidate) Date

STATEMENT 1

This thesis is being submitted in partial fulfilment of the requirements for the degree of PhD

Signed (Candidate) Date

STATEMENT 2

This thesis is the result of my own independent work/investigation, except where otherwise stated. Other sources are acknowledged by explicit references.

Signed (Candidate) Date

STATEMENT 3

I hereby give consent for my thesis, if accepted, to be available for photocopying and for inter-library loan, and for the title and summary to be made available to outside organisations.

Signed (Candidate) Date

Table of Contents

Acknowledgements.....	iv
Abbreviations	vi
Tables	v
Figures.....	vi
Thesis Abstract.....	vii
Chapter 1: Introduction	9
1.1 Thesis Overview.....	10
1.2 An Overview of Alzheimer’s Disease.....	11
1.3 Alzheimer’s Disease Pathology.....	16
1.4 Modeling Alzheimer’s Disease.....	31
1.5 Current and Developing Treatment for Alzheimer’s Disease.....	45
1.6 Thesis Summary, Aims and Hypotheses.....	54
Chapter 2: General Methods	55
2.1: Introduction	56
2.2 Maintenance and breeding of the PDAPP colony	56
2.3 Characterising the behavioural phenotype of male PDAPP mice.....	58
2.4 Biochemical Analysis of PDAPP and Wild-Type Brains	63
Chapter 3: Characterising Foraging Behaviour in PDAPP Mice	70
Chapter Overview	71
3.1 Chapter Introduction	71
3.2 Experiment 1: The effects of hippocampal cell loss of foraging behaviour.....	75
3.2 - Experiment 2: Assessment of non-spatial WM in HPC lesion mice	91
3.4 - Experiment 3: Assessing foraging behaviour in PDAPP mice	97
3.4 Chapter Discussion	104
Chapter 4: Characterising object recognition memory and age-related amyloid pathology in PDAPP mice	110
Chapter Overview	111
4.1 Chapter Introduction	111
4.2 - Experiment 4: Object Novelty Memory in PDAPP Mice	119
4.3 Experiment 5: Object-in-Place Memory in PDAPP mice	125
4.4 Experiment 6: Amyloid Pathology in PDAPP Mice	130
4.5 Chapter Discussion	133
Chapter 5: 2B3 reverses an age-dependent cognitive deficit in PDAPP mice	136
Chapter Overview	137
5.1 Chapter Introduction	137
5.2 Experiment 7: <i>In vivo</i> assessment of 2B3	141
5.3 Experiment 8: <i>Ex vivo</i> tissue analysis of 2B3 treated mice	155
5.4 Chapter Discussion	163

Chapter 6: Thesis Discussion.....	171
6.1 Thesis Overview	172
6.2 Summaries and Discussion of Findings.....	172
6.4 Are Transgenic Mouse Models of AD a useful tool for preclinical investigations?.....	181
6.6 Future directions	184
6.7 Thesis Summary and Conclusions	186
Bibliography	188

Acknowledgements

There are so many people that I wish to thank for their help, support, motivation, enthusiasm and guidance throughout the time of my PhD. My first thanks are to Professor Mark Good, Dr Emma Kidd and Dr Rhian Thomas for bravely offering me the PhD place way back in June 2012. Since then they have been incredible mentors, fountains of knowledge and have had the patience of saints for all the questions I may have had as well as toward the “small” errors I may have made along the way! I remember asking in my PhD interview the ratio of behavioural neuroscience to biochemistry that would come with this PhD, to which the answer was around 30% behaviour, 70% biochemistry. If you are brave enough to read this thesis, you may be quick to realise that was not quite the case in the end and therefore I an extended thanks to Mark for taking me from the highs of a biochemist in training to the now levels of a “social scientist” as Emma and Rhian may be quick to jibe. But in seriousness, I cannot say thank you enough to all three of my supervisors for their input over the entire PhD and especially Mark for teaching me so much as well as when it has come to entertaining the odd trip to The Woodville with an imminent sore head the day to follow!

I would like to thank all the people that have helped out across the BNL and labs in Redwood. The Animal Welfare team and Nicky Walker in the BNL could not be more helpful, especially to Pat Mason and Helen Read the two head NACWO’s that have been in the BNL since I began. As well as a few histology Gods, Moira, Eman and Dr Lisa Kinnavance who helped teach me how to slice, mount and and stain a mouse brain, no easy feat! And to the health and safety and lab managers from both the BNL, Dr Claudia Calder and Les Craven who have always been there with help and support when in need! And the amazing comedy and cleaning duo of Andy and Mary, who have always provided a laugh for the early morning starts, as well as the odd terrifying prank! I must also thank the project students that have helped significantly along the way with behavioural assays and protein extractions and Western blots; Sum Mistry, Laura Westacott, George and Mirka, thank you for all your help!

A huge thanks to all the close friends that have been made through the time and for understanding the mutual suffering we all go/have been through! Asta, Stacy, Lee, Emma, Alison, Shay Shay, Justin(e), Qutaiba, Mouhamed. A big shout out to Dr Marisol Vazquez for many an afternoon of coffee, dinner, CAKE and more. And to #TeamGood which was the permanent support group through this PhD, so another thank you to Mark, but also and by no

means least Jess Hall. Jess you have been a huge help and great lab bud when it comes to sharing the load across the board as well as for the rare times we make it back above ground level and into the outside world!! Now good luck with your thesis! And finally to old friends that have been there from day one, some of whom still think I am a University student, thanks guys; Harri, TJ, Megan, Chucks, Annabel, Emily, Emma and William Streatfeild who still thinks he is better than me at biochemistry because of one grade at A Level and will love that that is now written in here for eternity!

I would also like to extend a thank you to people that inspired me to take on this life in science and research. My early tutors and project supervisors, Dr Malcolm von Schantz, Dr Sonia Bennet and Dr Raphaelle Winsky-Sommerer of the University of Surrey. And especially Dr Amy Pooler who was my project PI when I was at King's College London undertaking my first ever research project. I would never have become so fascinated with this area of research and science as a whole without their input.

My final thanks is to family. Mum, you have been an incredible pillar of support throughout the entire process and I do not know where I would be without you through this. So tanks and loves ya mah! And to Godfrey for all your incredible support and interest throughout. My Dad for eventually realising research was a real job and then for your continuous support throughout, especially through the writing of the thesis. And finally to my Auntie Bernie and late Auntie Frances, it has always been a pleasure to hear your interests and share what I have been doing with you.

And now my thanks to you, the reader. If you are about to undertake the reading of this thesis, then thank you. It has been by no means a hell of a challenge in managing to write it, but hopefully it won't prove as laborious to read it (although please be kind!).

Abbreviations

Aβ – Amyloid- β peptide	LTP – Long-Term Potentiation
ACh – Acetyl Choline	MCI – Mild Cognitive Impairment
AD – Alzheimer’s Disease	mGluR5 – Metabotropic Glutamate Receptor 5
ADDL – A β -Derived Diffusible Ligand	MMSE – Mini-Mental Status Exam
AMPA – α -amino-3-hydroxy-5-methyl-4-isoxazolepropionic acid	mPFC – Medial Prefrontal Cortex
API – Alzheimer’s Prevention Initiative	MRI – Magnetic Resonance Imaging
Apo-E – Apolipoprotein E	MSE – Mental Status Exam
APP – Amyloid Precursor Protein	MTL – Medial Temporal Lobe
BACE – β -Site APP Cleaving Enzyme	MWM – Morris Water Maze
BBB – Blood Brain Barrier	NFT – Neurofibrillary Tangles
CANTAB – Cambridge Neuropsychological Tests Automated Battery	NIA – National Institute of Ageing
CSF – Cerebrospinal Fluid	nAChR – Nicotinic Acetyl Choline Receptor
CTF – Carboxy-Terminal Fragment	NMDA – N-methyl-D-aspartate
DG – Dentate Gyrus	OiP – Object-in-Place
DIAN – Dominantly Inherited Alzheimer’s Network	PiB – Pittsburgh B Compound
DSM – Diagnostic and Statistical Manual of Mental Disorders	PET – Positron Emission Tomography
EHC – Entorhinal Cortex	PrP^C – Cellular Prion Protein
FAD – Familial Alzheimer’s Disease	PRC – Perirhinal Cortex
FTD – Frontotemporal Dementia	PSD95 – Postsynaptic Density Scaffolding Protein
GABA – γ -aminobutyric acid	PSEN – Presenilin
GSK3 – Glycogen Synthase Kinase 3	RAM – Radial Arm Maze
GWAS – Genome-Wide Associated Studies	SAD – Sporadic Alzheimer’s Disease
HPC – Hippocampus	STEP – STriatal Enriched Protein Tyrosine Phosphatase
ICV – Intracerebroventricular	SWM – Spatial Working Memory
KI – Knock-In	WM – Working Memory
KO – Knockout	
LTD – Long-Term Depression	

Tables

- Table 1.1:** Overview of commonly used transgenic mouse models of AD
- Table 1.2:** Overview of the progressive cognitive decline observed in Tg models of AD from longitudinal and cross-sectional studies.
- Table 2.1:** Primary antibodies used in this thesis for Western blot analysis.
- Table 2.2:** Secondary antibodies used in this thesis for Western blot analysis.
- Table 3.1:** Stereotactic coordinates for bilateral hippocampal lesions
- Table 3.2:** Overview of the types of errors scored to assess spatial working memory in a foraging-based task.
- Table 3.3:** Results table showing motor and foraging behaviours in the foraging task (experiment 1)
- Table 3.4:** Mean numbers of working memory errors across trials in the foraging task (experiment 1)
- Table 3.5:** Results table showing motor and foraging behaviours in the foraging task (experiment 2)
- Table 3.6:** Mean numbers of working memory errors across trials in the foraging task (experiment 2)
- Table 3.7:** Results table showing motor and foraging behaviours in the foraging task in wild type and PDAPP mice (experiment 3)
- Table 3.8:** Mean numbers of working memory errors across trials in the foraging task in wild type and PDAPP mice (experiment 3)
- Table 4.1:** Table describing the variations of object recognition memory tasks.
- Table 4.2:** Mean contact times of WT and PDAPP mice across all ages with two identical objects in the sample phase.
- Table 4.3:** Mean contact times with objects in the test phase of the novel object recognition memory task.
- Table 4.4:** Mean contact times of WT and PDAPP mice across all ages with four different objects in the sample phase.
- Table 4.5:** Mean contact times with objects in the test phase of the object-in-place memory task.
- Table 5.1:** Mean contact time with objects of WT and PDAPP mice across sample phases in both pre- and post-operative conditions.
- Table 5.2:** Mean contact times with objects in novel and familiar locations of WT and PDAPP mice in both pre- and post-operative conditions.
- Table 5.3:** Mean contact times (corrected for group bias) with objects in novel and familiar locations of WT and PDAPP mice in both pre- and post-operative conditions.

Figures

- Figure 1.1:** A revised schematic overview of the “Amyloid Cascade Hypothesis”
- Figure 1.2:** Schematic diagram illustration the two main pathways of APP metabolism
- Figure 1.3:** Schematic illustration demonstrating the interactions between A β , tau and Fyn leading to neuronal excitotoxicity.
- Figure 1.4:** Overview of the progressive cognitive decline in AD.
- Figure 2.1:** Example of visualised DNA bands following PCR and gel electrophoresis to identify wild type and PDAPP mice.
- Figure 2.2:** Schematic diagram illustrating the counterbalancing of the behavioural design to characterise memory in PDAPP mice across a range of ages.
- Figure 2.3:** Illustration to demonstrate object recognition memory testing paradigms.
- Figure 3.1:** Figure to illustrate pots and the pot arrangement through training and testing.
- Figure 3.2:** Cresyl stained example of hippocampal lesion and SHAM control mice.
- Figure 3.3:** Schematic illustration of the maximum hippocampal lesion.
- Figure 3.4:** Schematic illustration of the maximum hippocampal lesion.
- Figure 3.5:** Foraging behaviour in HPC lesion mice (experiment 1).
- Figure 3.6:** Novel pot designs used in experiment 2.
- Figure 3.7:** Foraging behaviour in HPC lesion mice (experiment 2).
- Figure 3.8:** Foraging behaviour and spatial working memory performance in PDAPP and WT control mice.
- Figure 4.1:** Illustration to show the varying object recognition memory tests used to assess object recognition memory in rodents.
- Figure 4.2** PDAPP mice show comparable novel object recognition memory to WT littermate controls across all ages and delays tested.
- Figure 4.3** PDAPP mice show an age-dependent deficit in object-in-place memory.
- Figure 4.4:** Levels of A β increase with age in the HPC of PDAPP mice.
- Figure 5.1:** 2B3 treatment improved object-in-place memory in PDAPP mice.
- Figure 5.2:** Levels of total APP in vehicle and 2B3-treated PDAPP mice.
- Figure 5.3:** Quantification of A β 40, A β 42 and β CTF by ELISA in hippocampal homogenates of 2B3 treated PDAPP mice.
- Figure 5.4:** 2B3 reduced NR2B phosphorylation in PDAPP mice.
- Figure 5.5:** Schematic illustration demonstrating the interactions between A β , tau and Fyn leading to NMDAR-mediated neuronal excitotoxicity.

Figure 6.1: Increased activation of STEP reduces NR2B phosphorylation and increases NMDAR endocytosis.

Thesis Abstract

There are currently no disease-modifying therapies to halt or prevent the onset of Alzheimer's disease (AD). Immunotherapy and antibodies targeting the neurotoxic amyloid- β (A β) peptide for its removal from the brain have provided a promising opportunity to provide disease-modifying therapies. However, despite promising pre-clinical data, any benefits have failed to translate to the clinic. This thesis evaluated an antibody approach that, rather than targeting amyloid *per se*, binds to the amyloid precursor protein (APP) at the β -secretase cleavage site to reduce amyloid production by steric hindrance (Thomas et al. 2011, 2013). The main hypothesis of this thesis was that 2B3 administration to aged PDAPP mice (Games et al. 1995), which overexpress a mutated form of *APP* (Indiana mutation; V717F), would (1) reduce APP metabolism and (2) A β production and (3) alleviate age-associated cognitive deficits in PDAPP mice.

In order to test this hypothesis, PDAPP mice underwent behavioural and pathological characterisation at a range of ages to identify the nature and onset of cognitive deficits. Behavioural characterisation included an in-house spatial working memory (SWM) foraging paradigm and a battery of object and spatial recognition tests. PDAPP mice showed age-dependent deficits in SWM starting at 10-12 months. Novel object memory remained intact across all ages tested, however an age-dependent deficit was observed at 14-16 months of age in a visuo-spatial object-in-place (OiP) recognition task. ELISA analyses confirmed an age-related significant increase in amyloid production in the hippocampus of PDAPP mice at 15 months of age.

In the second phase of the programme of work, 17-18 month old PDAPP mice received intracerebroventricular infusion of antibody 2B3 using osmotic minipumps for a period of 14 days. 2B3 administration reversed the OiP recognition memory impairment in PDAPP mice. Improved memory performance was accompanied by a significant reduction in soluble A β 40 and β CTF, but not soluble A β 42. Further investigation also revealed that 2B3 significantly reduced the phosphorylation of NMDA receptor subunit NR2B at the tyrosine 1472 residue to a level similar to age-matched WT controls. Increased phosphorylation of the NR2B residue has been linked with neuronal excitotoxicity and impaired cognitive function in other mouse models (Ittner, Ke, Delerue, Bi, Gladbach, van Eersel, Wölfling, Chieng, Christie, Napier, et al. 2010). It is hypothesised that reduced phosphorylation of the NR2B following 2B3 administration in PDAPP mice most likely played a significant role in improving OiP performance.

Data from this thesis provides evidence that *in vivo* administration of 2B3 and inhibition of APP metabolism/A β production by steric hindrance provides a viable approach for the further development of immunotherapies targeting early stage AD pathology.

In Loving Memory of Frances Maundrell

1950 - 2016

Chapter 1: Introduction

“When Alois Alzheimer revealed the plaques and neurofibrillary tangles under his microscope more than a century ago, one wonders whether he anticipated that the proteins forming these lesions would have such profound roles and be directly linked in the pathogenesis of the disease”

Lars M. Ittner and Jürgen Götz, 2011

1.1 Thesis Overview

Currently, the clinically available treatments for Alzheimer's disease (AD) target AD-related symptoms only and not the underlying pathological mechanisms or causes. Therefore, there is a great demand for the development of these treatments in order to slow the progression or onset of AD. Transgenic mouse models have provided a useful tool in which to investigate pathological mechanisms associated with AD, as well as to evaluate potential disease-modifying compounds.

This introduction will initially outline the clinical observations of AD prevalence, clinicopathology and aetiology (section 1.2). A more in-depth discussion of the molecular pathology of AD will then be discussed (section 1.3). A focus will be on the amyloid- β ($A\beta$) peptide. $A\beta$ has been argued to trigger the pathological cascade of events associated with the progressive neurodegeneration and cognitive decline reported in AD (Hardy & Allsop 1991; Hardy & Higgins 1992; Hardy & Selkoe 2002). Further mechanisms and pathological hallmarks, such as neurofibrillary tangles (NFTs) and hyperphosphorylated tau protein will also be discussed. This will then lead onto an overview of the current transgenic mouse models of AD-like pathology (section 1.4). These models are extensively used in order to provide a better understanding of the pathological mechanisms and behavioural phenotypes associated with AD. A focus will be on the PDAPP model, which was used throughout the research conducted in this thesis (Games et al. 1995). A further common use for Tg AD models is to assess novel compounds to potentially treat AD. A review of the currently available and developing treatments for AD will then be provided in the final section (section 1.5). A focus of this will be on immunotherapy, particularly passive anti- $A\beta$ immunotherapies. Despite the success of these anti- $A\beta$ antibodies in preclinical studies, little success has been translated in clinical trials (Karran & Hardy 2014). The remaining review of developing immunotherapies will focus on an anti-APP β -secretase cleavage site antibody, 2B3. 2B3 is able to reduce $A\beta$ *in vitro* in a range of cell lines, including mouse primary cortical neurons (Thomas et al. 2011; Thomas et al. 2013). Thus, this introduction will hypothesise that administration of 2B3 in PDAPP mice will reduce levels of $A\beta$ and improve memory performance.

1.2 An Overview of Alzheimer's Disease

1.2.1 Prevalence and cost

Alzheimer's disease (AD) is the most prevalent neurodegenerative condition afflicting an estimated 44 million people worldwide (World Alzheimer's Disease Report 2014). It is the most common form of dementia making up 64% of all cases (Alzheimer's Society: Dementia UK, 2014). Within the UK, it is estimated that 850,000 people will have been diagnosed with dementia by 2015, which is equal to 1.3% of the entire UK population (Alzheimer's Society: Dementia UK update, 2014). Of the cases diagnosed, approximately 1 in 14 people are aged 65 and above and 1 in 6 people are over the age of 80, indicating that AD is a disease of age. These figures appear more aggressive in the United States where 5.2million American citizens have been reported to have AD. Of these, 1 in 9 people are over the age of 65 and 1 in 3 are over the age of 85 (Alzheimer's Association: Facts and Figures, 2014).

AD is a debilitating condition not just for the patient, but also the primary care giver. Caregivers are reported to be under supported and overworked, collectively spending over 1.3 billion hours caring for those with dementia in the UK in 2013 (Alzheimer's Society: Dementia UK, 2014). It has further been reported that AD caregivers are susceptible to stress, anxiety as well as depression (Ferrara et al. 2008). In addition to this, in 2014, AD had a reported annual cost of £26.3 billion in the UK (Alzheimer's Society: Dementia UK update, 2014) and a further \$214 billion in the US (Alzheimer's Association: Facts and Figures, 2014). These figures are estimated to double by 2030 due to modern medicines increasing life expectancy. For reasons such as these, research into the mechanisms of AD are important to identify therapeutic targets, as currently there is no preventative treatment. Therefore, there is an ongoing need to continue to improve the understanding of AD aetiology and disease mechanisms in order to develop potential treatments.

1.2.2 Clinical symptoms

Clinical symptoms of AD are consistent with the pathological progression of the disease, starting initially in the medial temporal lobes (MTL) (i.e., entorhinal cortex (EHC) and hippocampus (HPC)), before further progressing into isocortical association areas, including the

parietal and frontal lobes (explained in more detail in section 1.3; Braak & Braak 1991; Braak & Braak 1995). The earliest clinical symptoms observed in patients with AD are a deficit in MTL-dependent episodic memory and semantic memory (Hodges et al. 1990; Bondi et al. 2008). These deficits are commonly observed in the preclinical phase of AD prior to the development of mild AD and mild cognitive impairment (MCI;) (Förstl & Kurz 1999; Bäckman et al. 2001; Bondi et al. 2008). As the disease continues to worsen into the moderate and severe stages of AD, patients express severe impairment of recent memory and appear to “live in the past” (alzheimers.org.uk) and develop further changes in personality, speech and gradual loss of everyday activities of daily living (Beatty et al. 1988; Förstl & Kurz 1999). The average duration of life following clinical diagnosis of AD is approximately 5-10 years. Despite the relatively rapid decline following diagnosis, it is thought that pathological changes in neurochemistry and AD biomarkers may precede this stage decades before clinical symptoms present (Förstl & Kurz 1999; Zanetti et al. 2009; Jack et al. 2010; Jack et al. 2013).

1.2.3 Diagnosing Alzheimer’s Disease

Criteria for diagnosing AD were originally established in 1984 with the National Institute of Neurological and Communicative Disorders and Stroke-Alzheimer’s Disease and Related Disorders Association (NINCDS-ADRDA) criteria (McKhann et al. 1984). These criteria allowed for a “possible” and “probable” diagnosis of AD with a “definite” diagnosis through combined clinical and histopathological examination (McKhann et al. 1984). Similar clinical diagnostic criteria have since been established including the Diagnostic and Statistical Manual of Mental Disorders, 4th edition (DSM-IV) and the International Classification of Diseases, 10th revision (ICD-10) (World Health Organization, ICD-10, 1992; American Psychiatric Association, DSM, 1994; American Psychiatric Association, DSM-IV-TR 2000). The three share many approaches to diagnose AD: including mental status exams (MSE) and memory tests. These assessments are highly sensitive to cognitive and behavioural symptoms associated with AD and allow the progression of decline to be monitored (Schmitt et al. 2000; Salmon & Bondi 2009). Two of the most frequently used assessments to diagnose cognitive impairment are the Mini-Mental Status Examination (MMSE) and the Cambridge Neuropsychological Tests Automated Battery (CANTAB) (Folstein et al. 1975; Cockrell & Folstein 1988; Fray & Robbins 1996; Fray et al. 1996). The MMSE consists of a brief questionnaire able to assess both episodic and semantic memory, working memory, as well as attention and orientation to time and place

(Folstein et al. 1975; Snyderman & Rovner 2009). CANTAB however, is a non-verbal assessment tool, utilizing a touch-screen testing system examining memory, attention and executive function (Fray & Robbins 1996). Similar clinical test procedures are also used in order to track memory and cognitive decline in AD patients including the Montreal Cognitive Assessment, Alzheimer's Disease Assessment Scale and Logical Memory Test I and II (Rosen et al. 1984; Wechsler 1997; Nasreddine et al. 2005). In 1999 a further stage of cognitive decline, MCI, was defined as a translational stage between normal cognition (relative to age and education) and dementia (Petersen et al. 1999). This definition further helped to define and identify those at risk of developing AD (Morris et al. 2001; Petersen 2002). However, AD cognitive symptoms alone show much overlap with other dementias, including frontotemporal dementia (FTD), and accuracy of diagnoses remains variable until postmortem neuropathological examination; which remains the "gold standard" of diagnosis of AD (McKhann et al. 1984; Dubois et al. 2007; Beach et al. 2012).

To better improve AD diagnosis recommendations from the National Institute of Aging (NIA) and Alzheimer's Association workgroups proposed improvements to the diagnostic guidelines for AD based on the advances made in understanding AD since 1984 (Dubois et al. 2007; Jack et al. 2011; Sperling et al. 2011; McKhann et al. 2011; Albert et al. 2011). These recommendations focus on detecting AD in its earliest stages by observing a clinical deficit in episodic memory as well as at least one or more abnormal biomarkers relative to AD neuropathology. These include: molecular neuroimaging with positron emission tomography (PET) with Pittsburgh B compound (PiB) to quantify amyloid levels within the brain, structural neuroimaging with magnetic resonance imaging (MRI) to assess potential MTL atrophy, as well as the analysis of cerebrospinal fluid (CSF) to detect altered levels of amyloid and phospho-tau. However, these recommendations appear to target diagnosis of AD predominantly for research purposes, while the recommendations for a more clinical criterion remain unfeasible in many memory clinics. Due to the relative expense of imaging techniques and the invasive procedure of lumbar puncture to obtain CSF, development of screening procedures incorporating blood-based biomarkers are being developed. These should allow a more clinically-valid and reliable method to diagnosing AD (Burnham et al. 2014; Henriksen et al. 2014; Kiddle et al. 2015).

1.2.4 Aetiology of Alzheimer's Disease

Two predominant forms of AD have been classified, familial AD (FAD) and sporadic AD (SAD). FAD accounts for approximately 1-5% of all cases. SAD accounts for more than 95% of AD cases. Although causal genetic mutations lead to the development of FAD, no single definitive cause has been determined for SAD and it is most likely caused by a combination of genetic and environmental factors (Bettens et al. 2013b; Reitz & Mayeux 2014). Despite this difference, the clinical and neuropathological cascade of events remains similar across both forms of AD (Lippa et al. 1996).

FAD is an autosomal dominant inherited form of AD. To date, 260 causal mutations have been reported for FAD (<http://www.molgen.ua.ac.be/ADMutations>). These mutations are divided between three genes leading to the clinical and neuropathological onset of AD: *APP*, *PSEN1* and *PSEN2* (Levy et al. 1990; Goate et al. 1991; Rogaev et al. 1995; Levy-Lahad et al. 1995; Sherrington et al. 1995). *APP* encodes the amyloid precursor protein (APP), which is metabolized to generate the neurotoxic β -amyloid ($A\beta$) peptide, the main component of neuritic plaques (Selkoe 2001). *PSEN1* and *PSEN2* encode presenilin 1 and 2 respectively. These proteins help compose a large enzyme complex, γ -secretase, directly related to the production of $A\beta$ (De Strooper 2003). These causative mutations commonly result in an increased ratio of $A\beta_{42}$ to $A\beta_{40}$, where $A\beta_{42}$ is reportedly a more neurotoxic species of $A\beta$ (Scheuner et al. 1996; Klein et al. 1999; Chávez-Gutiérrez et al. 2012). The identification of these mutations acted as a foundation of the “Amyloid Cascade Hypothesis” and the generation of $A\beta$ (discussed in detail in section 1.3.1), remains the dominant hypothesis for the pathological cascade of events in AD (Hardy & Higgins 1992; Musiek & Holtzman 2015;).

Unlike FAD there have been no causal genetic mutations reported for SAD. However, twin studies have predicted that the heritability of SAD may be as high as 80% (Gatz et al. 2006). Initial genetic studies revealed the *APOE* $\epsilon 4$ allele as a common risk factor for the onset of AD in later age. People who are homozygous for the *APOE* $\epsilon 4$ allele have a 15 times increased risk of developing AD while those who are heterozygous show a three times increased risk when compared to homozygotes for *APOE* $\epsilon 3$, the most common genotype (Farrer et al. 1997). Due to the continued high risk of developing AD associated with the expression of *APOE* $\epsilon 4$, it was proposed as a semi-dominant inherited gene with moderate penetrance (Genin et al. 2011). Studies have also indicated that apolipoprotein E (Apo-E) has an important role in $A\beta$ metabolism and *APOE* $\epsilon 4$ genotypes have a greater density of neuritic plaques suggesting it may

increase A β brain deposition (Klunk et al. 2004; Kok et al. 2009; Liu et al. 2013) However, despite these findings, *APOE* expression is not sufficient to cause AD. More recently, large-scale GWAS studies have identified several other risk loci associated with SAD. Single nucleotide polymorphisms were initially reported in *CLU*, *PICALM*, *CR1* and *BINI*, while more recent studies have further identified *PLD3*, *FRMD4A*, *EPHA1*, *ABCA7*, *CD2AP*, *CD33* and *MSA4* cluster (Harold et al. 2009; Seshadri et al. 2010; Naj et al. 2011; Lambert et al. 2013; Lambert et al. 2015). Although the precise biological role of these polymorphisms in AD is yet to be defined, functional roles have been reported in lipid processing, immune system regulation, synaptic function and endocytosis, functions which are reportedly affected in AD (Lynch et al. 2003; Tateno et al. 2007; Tebar et al. 1999; Ivanov & Romanovsky 2006; Jones et al. 2010; Bettens et al. 2013a).

Numerous lifestyle and environmental factors have also been associated with SAD. Given that most people diagnosed with AD are 65 years or older, with the risk of diagnosis increasing with age, the most significant risk factor of AD is ageing. Other medical conditions such as elevated blood-pressure, type 2 diabetes and body weight have also indicated increased risk of developing AD (Leibson et al. 1997; Razay & Vreugdenhil 2005; Whitmer et al. 2005; Reitz & Mayeux 2014). However, lifestyle choices have also been reported as protective against the onset of AD. For example, Mediterranean-style diets are associated with a reduced incidence of AD and MCI (Scarmeas et al. 2009; Gu et al. 2010). Similar effects have also been reported in those who undergo regular physical activity as well as engage in cognitively stimulating activities (Fratiglioni et al. 2004; Carlson et al. 2008).

The identification of both genetic as well as lifestyle/medical-based risk factors exemplifies the complexity of SAD. As a result, it is likely that a therapeutic approach using just one method of therapy may be insufficient to combat AD and a more multi-targeted strategy may be required; based on individual risk profiling. Further research is required to understand how these multiple risk factors interact and affect AD-related pathogenic mechanisms.

1.3 Alzheimer's Disease Pathology

The “Amyloid Cascade Hypothesis” has dominated many avenues of AD research since its original report in 1992. Following the identification of extracellular senile plaques, composed of aggregated A β , and intracellular NFTs composed of hyperphosphorylated tau protein, it hypothesized that the gradual build up of plaques caused a downstream cascade of events including NFT development, neurodegeneration and clinical dementia. The two major pathological hallmarks of AD therefore have been intensively studied. This section will start by explaining the amyloid cascade hypothesis before further reviewing the current findings implicating A β and tau in the progressive pathology of AD. Given the focus of this thesis concentrating on *hAPP* overexpression and downstream effects of modulating its metabolism a predominant focus will be given to APP metabolism and neurotoxic effects of A β , however the toxic roles of tau and the pathological relationship between tau and A β will also be discussed.

1.3.1 The Amyloid Cascade Hypothesis

A number of hypotheses have been proposed to explain AD pathology, including elevated oxidative stress, the “mitochondrial cascade hypothesis” (declining mitochondrial activity), the “calpain-cathepsin hypothesis” (age-related decline in the autophagic-lysosomal system) and declining blood-brain barrier (BBB) function (Erickson & Banks 2013; Sutherland et al. 2013; Yamashima 2013; Swerdlow et al. 2014). However, the most commonly accepted AD hypothesis is the amyloid cascade hypothesis, which has remained a focal point of AD research since 1991 (Hardy & Allsop 1991).

The focus on A β followed from its sequencing from meningeal blood vessels of AD and Downs syndrome (DS) patients prior to the finding that it was the primary component of senile plaques (Glenner & Wong 1984; Masters et al. 1985). It was later discovered that the gene encoding the precursor of A β , the amyloid precursor protein (APP) was located on chromosome 21 (Goldgaber et al. 1987; Tanzi et al. 1987). Coupled with the observation that individuals with DS express a trisomy of chromosome 21 and frequently develop AD neuropathology in later life it was proposed that the generation of A β was the primary pathological event of AD (Olson & Shaw 1969). It was later discovered that mutations in *APP* gene locus were causative of FAD and lead to increased levels of A β (Goate et al. 1991; Mullan et al. 1992). Preliminary studies had already reported A β -mediated neurotoxicity and further disruption of calcium homeostasis

leading to NFT development (Yankner et al. 1989; Mattson et al. 1991; Pike et al. 1991; Mattson et al. 1992). Collectively, these findings provided a genetic and pathological basis for the amyloid cascade hypothesis. The amyloid cascade hypothesis stated that the “*deposition of amyloid β protein, the main component of the plaques, is the causative agent of Alzheimer’s pathology and the neurofibrillary tangles, cell loss, vascular damage and dementia follow as a direct result of this deposition*” (Hardy & Higgins 1992).

The amyloid cascade hypothesis has fuelled AD research for over 20 years and still provides a framework for investigation of putative treatments. However, the findings reported over the past two decades have generated considerable controversies and challenges for the amyloid cascade hypothesis. The most salient challenges concern the spatiotemporal pathology of senile plaques and lack of A β plaque correlation with neuronal loss and clinical disease progression (Braak & Braak 1991; Serrano-Pozo et al. 2011). Contradicting the amyloid cascade hypothesis is the fact that NFT pathology shows a significant correlation with neuronal loss (Arriagada, Marzloff, et al. 1992; Gómez-Isla et al. 1997; Serrano-Pozo et al. 2011). However, despite this aggregated phosphorylated tau has been reported to be present in the brainstem and EHC of young adults who are both cognitively normal and amyloid-free (Braak & Del Tredici 2011). With age, this aggregated tau becomes ubiquitous in the HPC (Price & Morris 1999; Knopman et al. 2003). However, the toxic spread of these tau aggregates into neocortical regions is dependent on the presence of plaque and increased amyloid SAD (Price & Morris 1999; Knopman et al. 2003; Petersen et al. 2006). Similar to the spread of aggregated tau, only individuals with plaque pathology display HPC neuronal loss (West et al. 1994; Gómez-Isla et al. 1996). It would therefore seem that despite neuroanatomical discrepancies, A β aggregation is required to initiate and accelerate the neurotoxic properties of NFTs.

Research suggests that A β deposition may commence over a decade prior to the onset of clinical AD (Jack et al. 2013a; Jack et al. 2013b). However, it is argued that despite elevated levels of plaques in asymptomatic individuals, this should be considered a “preclinical” phase of AD (Jack et al. 2013; Roe et al. 2013; Vos et al. 2013). Interestingly, it has been observed that individuals who are ostensibly normal, but show plaque pathology demonstrate subtle deficits when using the AD Cooperative Study-Preclinical Alzheimer Cognitive Composite (ADCS-PACC), which combines tests that assess episodic memory, timed executive function and global function, as well as accelerated HPC atrophy compared to plaque free controls (Chételat et al. 2012; Donohue et al. 2014). This suggests that A β deposition may exhibit progressive, mild, pathology prior to much more rapid disease progression, following the onset of NFT pathology.

In contrast to amyloid plaques, soluble (pre-plaque) forms of A β are better correlated with tau pathology (Handoko et al. 2013; Lesné et al. 2013). As discussed in more detail below, A β oligomers can directly initiate tau phosphorylation *in vitro* and *in vivo* (Ittner et al. 2010; Choi et al. 2014; Zhang et al. 2014;). These findings have led to a revised amyloid cascade hypothesis in which soluble A β oligomers are responsible for the cascade of neuropathological events associated with AD (Hardy & Selkoe 2002) (see Figure 1.1). Despite this revised hypothesis, it still remains unclear as to why the long prodromal phase of AD, when plaques are known to be present, causes little or no neurodegeneration.

There are several studies that suggest A β production and deposition precedes NFT pathology in support of the amyloid cascade hypothesis. For example, amyloid-based immunotherapies in preclinical mouse models of AD have shown that A β monoclonal antibodies reduced levels of soluble A β and phosphorylated tau, improved cognition and electrophysiology markers of synaptic plasticity (Schenk 2002; Oddo et al. 2004; Buttini et al. 2005; Hartman et al. 2005; Klyubin et al. 2005). In contrast to these positive changes in mouse models, immunotherapy has not been successful in clinical trials (Mangialasche et al. 2010). The reasons for this discrepancy may be numerous but one important aspect of the data is that patients are often treated in the mild-moderate stages of AD when neuronal loss is already manifested (in contrast to mouse models). However, more recent results released at the Alzheimer's Association International Conference 2015 revealed promising improvements in cognitive measures and CSF biomarkers in Phase III clinical trials for anti-A β antibodies Solanezumab and Gantenerumab and Aducanumab (Phase Ib trial) treating patients in much earlier stages of AD pathogenesis (Qian et al. 2015; Reardon 2015). Current ongoing pharmacological studies and A β immunotherapy trials using pre-symptomatic FAD cohorts, including the Dominantly Inherited Alzheimer's Network (DIAN) and Alzheimer's Prevention Initiative (API), will provide a key test of the amyloid cascade hypothesis (Reiman et al. 2011; Mills et al. 2013).

Amyloid cascade hypothesis

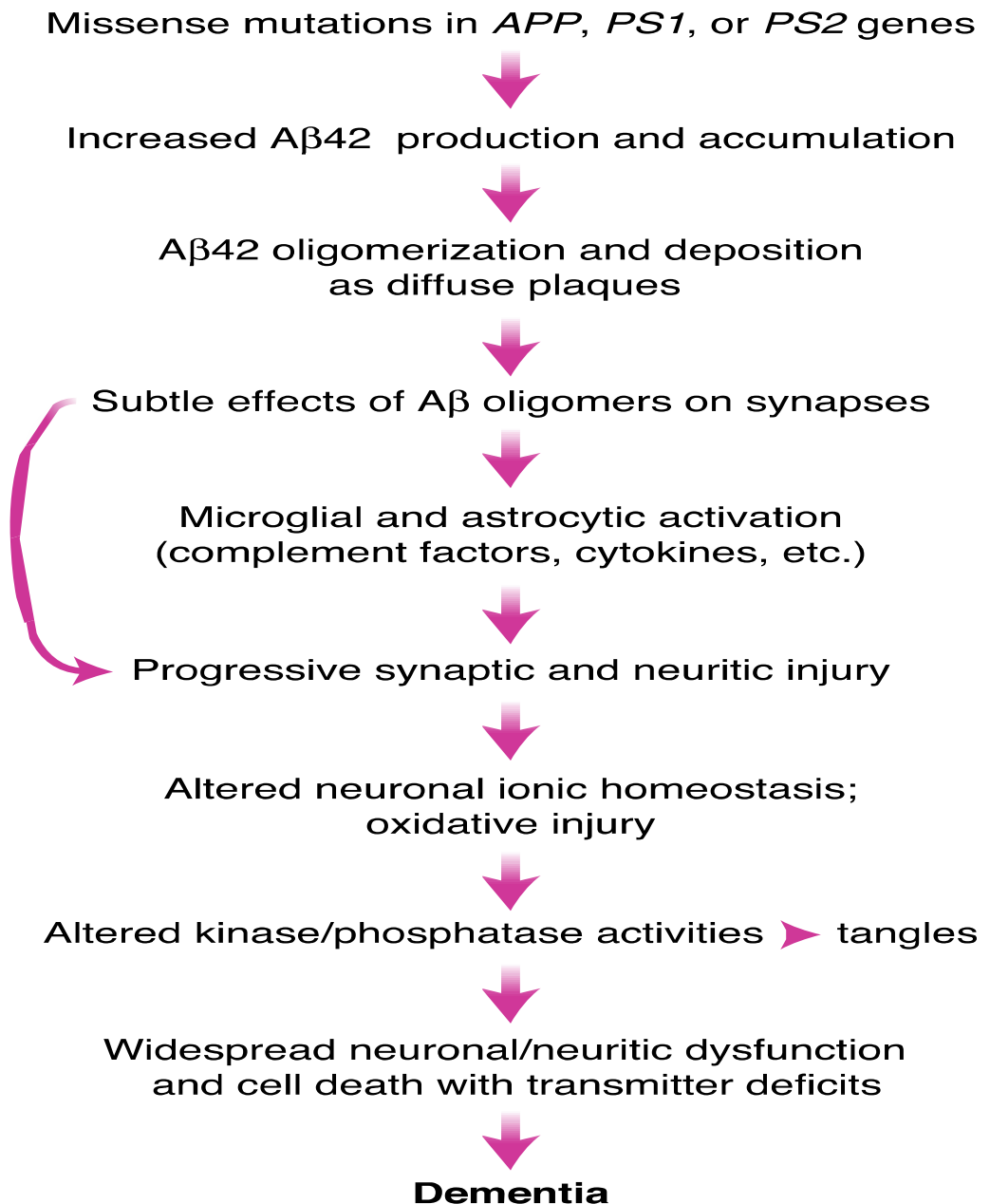


Figure 1.1: A revised schematic overview of the amyloid cascade hypothesis. This shows the sequence of events leading to the clinical onset of AD. The curved arrow represents the theory that soluble A β oligomers may directly cause synaptic and neuronal injury in addition to the activation of neuroinflammatory mediators. (Hardy and Selkoe 2002)

The evidence summarized above suggests the early version of the amyloid cascade hypothesis that originally focused on plaque pathology, as the cardinal event in AD was inaccurate. A β appears to gradually accumulate for several years before somehow triggering the spread of neurotoxic tau pathology, neuronal loss and cognitive decline. It is likely that accumulating A β may need to reach a threshold before triggering intermediary signaling and / or kinase cascades, declining mitochondrial function or altered immune system function that lead to pathological changes in brain function and viability (Musiek & Holtzman 2015). Nevertheless, the long preclinical phase of AD offers a window of opportunity to prevent accumulation of amyloid and thus slow-down or prevent the cascade of events that ultimately causes neuronal loss. Results from the DIAN and API studies will be key to testing whether A β -related interventions provide a viable method of disease modification/prevention in humans.

1.3.2 β -Amyloid Production

APP is a highly conserved single transmembrane protein found in both neuronal and non-neuronal tissue (Jacobsen & Iverfeldt 2009). Three major APP isoforms (APP₆₉₅, APP₇₅₁ and APP₇₇₀) have been reported as a result of alternative splicing of exons 7 and 8 (Moir et al. 1998; Tanaka et al. 1989). Of these, APP₇₅₁ and APP₇₇₀ are mainly (but not exclusively) expressed within non-neuronal tissue. APP₆₉₅ is the most highly expressed isoform in neurons, and recent reports suggest ratios of APP isoform mRNAs to be approximately 1 : 10 : 20 (APP₇₇₀ : APP₇₅₁ : APP₆₉₅) (Tanaka et al. 1989; Haass et al. 1991; Selkoe 2001). APP is metabolised in one of two separate pathways (Figure 1.2), the non-amyloidogenic and the amyloidogenic pathway. The activation of each pathway is determined by the sequential cleavage of APP by enzyme complexes, termed α - and γ -secretase (non-amyloidogenic pathway) and β - and γ -secretase (amyloidogenic pathway). (Zhang et al. 2011).

The non-amyloidogenic pathway sequentially cleaves APP by initial α -secretase activity. α -Secretase activity is mediated by one or more membrane bound enzymes from the family of disintegrin and metalloproteinase domain proteins (ADAM), including ADAM9, 10, 17 and 19 (Asai et al. 2003; De Strooper et al. 2010). α -secretase cleaves APP in the A β encoding domain of APP, thus preventing the generation of A β in this metabolic pathway. The resulting products of α -secretase cleavage are the membrane bound C-terminal fragment, 83 amino acid residues in size (CTF83) and an amino (N) terminal metabolite, soluble APP α (sAPP α), which is released into the extracellular domain. The CTF83 fragment is further processed by the intramembrane

enzyme complex, γ -secretase which generates a small peptide, p3 and a remaining APP intracellular domain (AICD) (Haass et al. 1993; Kojro & Fahrenholz 2005; De Strooper et al. 2010b). The γ -secretase is composed of enzymes PS1 or PS2, nicastrin, anterior pharynx defective, and presenilin enhancer 2, all four of which are reported necessary to reconstitute γ -secretase activity (Levitan et al. 2001; Francis et al. 2002; Steiner et al. 2002).

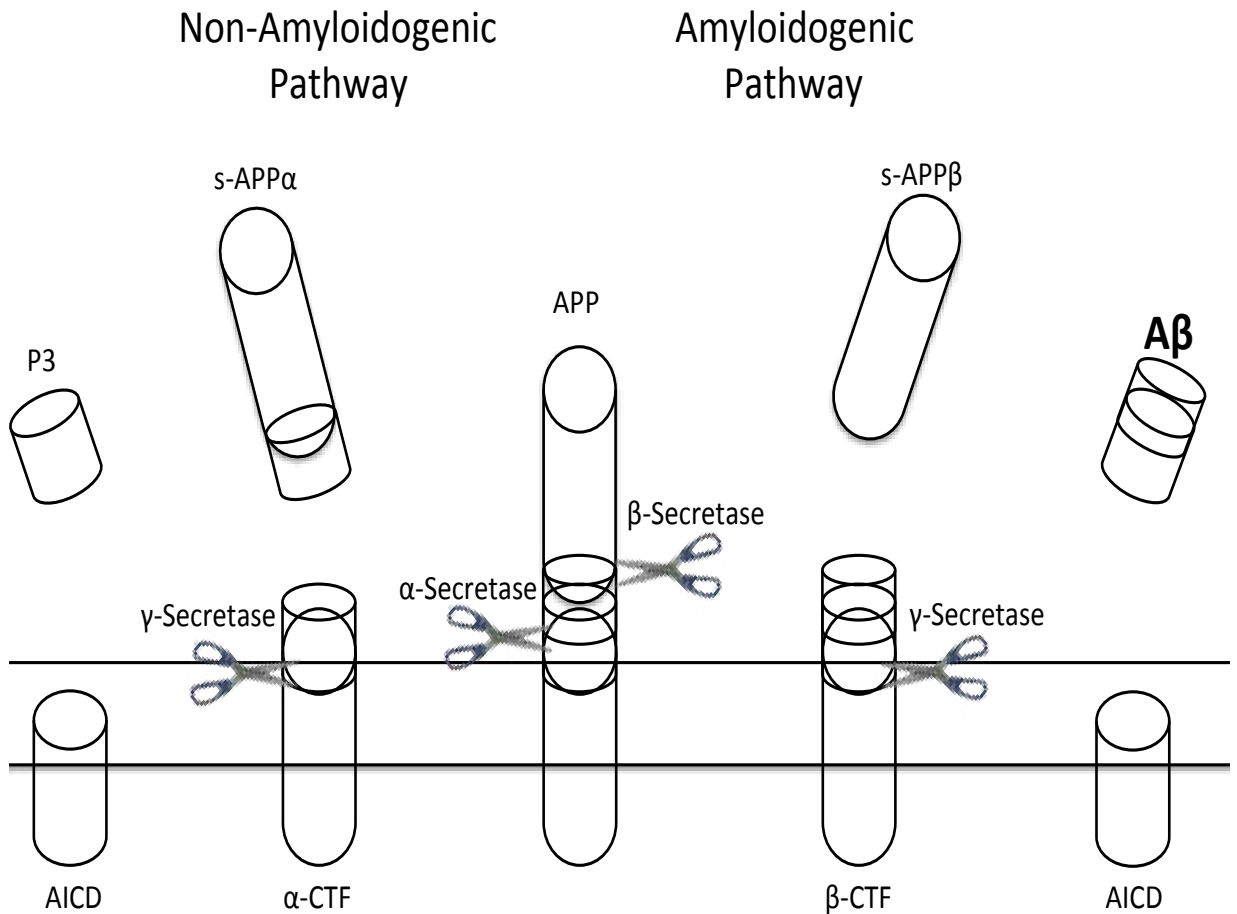


Figure 1.2: Schematic diagram illustrating the two main pathways of APP metabolism. The non-amyloidogenic pathway shows sequential APP cleavage by α -secretase, followed by γ -secretase. The amyloidogenic pathway shows the sequential APP cleavage initiated by β -secretase, followed by γ -secretase and the production of neurotoxic A β .

APP can also be metabolised via the amyloidogenic pathway, which leads to the production of the neurotoxic A β peptide. The initial cleavage of APP is located 99 amino acid residues from the C-terminal of APP by β -secretase, or β -site APP cleaving enzyme 1 (BACE1) (Sinha et al. 1999; Vassar et al. 1999; Vassar et al. 2009). The cleavage generates soluble APP β (sAPP β), which is released into the extracellular space, and a remaining 99 amino acid residue, C-terminal fragment (CTF99) or β CTF, which encodes A β and remains within the membrane compartment. The CTF99 then further undergoes multiple intramembrane cleavages by γ -secretase at sites referred to as γ , ϵ and ζ (Gu et al. 2001; Zhao et al. 2004; Kakuda et al. 2006; Zhao et al. 2007). The initial cleavage at the ϵ -cleavage site allows for the release of the AICD fragment into the cytosol. The remaining fragment is processed at the ζ -site prior to the final γ -site cleavage to generate A β . The γ -site cleavage occurs at variable positions in the A β peptide domain, mainly after amino acids 38, 40 and 42. This generates A β peptides of varying length, which has an important effect on the pathogenicity of A β (Walsh & Selkoe 2007). Most A β produced is 40 amino acid residues in size (A β 40), however, approximately 10% is composed of 42 amino acid residues (A β 42). It is A β 42 that is believed to express the most potent neurotoxic effects *in vivo* and is the most commonly found isoform in amyloid plaques (Jarrett et al. 1993; Walsh & Selkoe 2007).

The non-amyloidogenic pathway accounts for more than 90% of APP metabolism, which is thought to occur at the cell surface. Evidence has shown α -secretase to be enriched at the plasma membrane where it is able to outcompete β -secretase cleavage of APP (Parvathy et al. 1999; Zhang et al. 2011). Studies have also shown that increased APP trafficking to the cell surface or inhibition of its internalisation leads to significant reductions in A β (Cataldo et al. 1997). However, BACE1 cleavage of APP occurs within endocytic vesicles. This is due to the optimum activity of BACE1 occurring at low pH and for this reason BACE1 is predominantly localised within acidic compartments of the cell, such as endosomes and the trans-Golgi network (Vassar et al. 1999; Hook et al. 2002). Impaired APP trafficking to the cell surface or stimulating APP internalisation showed an increase in BACE1 cleavage products of APP (Haass et al. 1992; Lee et al. 2005). However, despite our understanding of these two metabolic pathways, no evidence has yet materialised as to what factors increase the processing of APP down the amyloidogenic pathway.

1.3.3 β -Amyloid Pathology and Senile Plaques

Following its production from APP metabolism, $A\beta$ is released into the extracellular space in a soluble monomeric form. Although not much is understood about the physiological roles of $A\beta$ in the healthy brain, it is thought that $A\beta$ plays a role in modulating synaptic activity and promoting neuronal survival (Kamenetz et al. 2003; Plant et al. 2003; Plant et al. 2006; Pearson & Peers 2006). Kamenetz and colleagues (2003) reported that evoked activity in hippocampal neurons in brain slices increased β -secretase cleavage of APP and stimulated $A\beta$ production. This increase in $A\beta$ production was thought to act as a negative feedback mechanism to depress synaptic activity and prevent excitotoxicity. γ -Secretase inhibitors supported this hypothesis in hippocampal neurons by observing greater excitatory activity as determined by excitatory postsynaptic current frequencies (Kamenetz et al. 2003). Regulation of synaptic activity was further observed in primary cortical neurons following NMDA receptor stimulation. (Lesné et al. 2005). This stimulation inhibited α -secretase APP processing and promoted $A\beta$ production. The authors from this study suggested that even a modest deregulation of glutamatergic neurotransmission may significantly increase the production of $A\beta$ and plaque deposition (Lesné et al. 2005). Plant and colleagues have also reported a significant role in physiological $A\beta$ and neuronal survival (Plant et al. 2003). Both γ - and β -secretase inhibitors incubated with neuronal cell lines for 24 hours led to an increase in cell death, compared to non-neuronal cell lines. This effect was prevented by co-incubation with $A\beta_{40}$. (Plant et al. 2003). This effect was later associated with $A\beta$ -mediated regulation of potassium channel Kv4 subunit expression and hence, further involvement in neuronal excitability (Plant et al. 2006). Collectively, these studies provide evidence that $A\beta$ plays an important role in regulating neuronal activity. Deregulation of these mechanisms clearly contributes to the pathogenesis observed in AD and understanding $A\beta$, both at a physiological and pathological level, is greatly important.

In AD $A\beta$ monomers aggregate into oligomeric forms of dimers, trimers and larger soluble aggregates before further aggregating into insoluble protofibrils and amyloid plaques (Haass & Selkoe 2007; De Strooper 2010). The spatiotemporal pattern of amyloid deposition has been reported in two separate staging systems, initially a three-stage progression distinguished by Braak and Braak in 1991. More recently, Thal and colleagues proposed a five stage process (Braak & Braak 1991; Thal et al. 2002). Thal and colleagues have reported that the spread of amyloid initiates exclusively in the neocortex in stage 1 before progressing into allocortical brain regions, including the HPC and EHC in the second stage. $A\beta$ deposits continue to spread to the

cholinergic nuclei of the basal forebrain and striatum in phase 3 prior to numerous brainstem nuclei in stage 4. Finally, cerebellar A β deposits occur in stage 5 (Thal et al. 2002; Serrano-Pozo et al. 2011). An interesting observation reported by Thal and colleagues was the anterograde pattern by which amyloid spread into regions receiving neuronal projections from those already exhibiting A β deposition (Thal et al. 2002). It was further confirmed that large areas of amyloid accumulation, including in the HPC and EHC can be observed prior to the onset of clinical symptoms, such as episodic memory deficits, and suggests that early treatment for AD in preclinical stages may prevent the further spread of amyloid and subsequent clinical changes (Braak & Braak 1991; Thal et al. 2002).

In contrast, A β in its two opposing forms, soluble monomeric A β and insoluble plaques, shows relatively low levels of neurotoxicity (Martins et al. 2008). However, an interesting hypothesis suggests that plaques may act as an inert “sink” that most likely exist in equilibrium with neurotoxic soluble oligomeric A β (Benilova et al. 2012; Hefti et al. 2013). Indeed, neurons in close proximity of plaques exhibit synaptic loss and changes in neuronal activity in a mouse model of amyloid pathology (Bezprozvanny 2009). Moreover it has been reported that soluble, toxic species of A β appear to “seed” amyloid plaques and return to a soluble state in the presence of biological lipids leading to cognitive impairments in mice (Martins et al. 2008; Gaspar et al. 2010). This is suggestive that it is soluble oligomeric forms of A β that act as neuropathological triggers in AD pathology.

Over a decade of research has revealed specific neurotoxic “species” of A β (Haass & Selkoe 2007; De Strooper 2010; Hefti et al. 2013). The collective term for these species is otherwise known as “A β -derived diffusible ligands” (ADDL) or “soluble oligomeric A β ” and includes A β dimers, trimmers, A β *56 and A β protofibrils. These studies have examined the relative toxicity of different ADDLs generated in a variety of methodologies either from *in vitro* culture techniques or from transgenic mouse or human AD brains (Podlisny et al. 1998; Chromy et al. 2003; Lesné et al. 2006; Shankar et al. 2008). Evidence supporting the neurotoxic properties associated with ADDLs comes from a variety of sources. For example, *in vitro* evidence has shown that treatment of hippocampal neurons with soluble A β dimers extracted from the cortices of AD patients caused aberrant tau phosphorylation and neuritic degeneration; which was prevented by co-administration of an A β immunotherapy (Jin et al. 2011). Furthermore, treatment of rodent HPC slices with soluble A β oligomers blocks the induction of long-term potentiation (LTP), a model of synaptic plasticity processes thought to underpin learning and memory (Bliss & Collingridge 1993; Lambert et al. 1998; Townsend et al. 2006).

Observations from Townsend and colleagues (2006) that A β oligomers blocked LTP appear to be supported by *in vivo* studies showing intracerebroventricular (ICV) administration of soluble oligomeric A β in rats as well as in transgenic mice caused memory deficits (Lesné et al. 2006; Reed et al. 2009). Finally, soluble A β is believed to exhibit high-affinity binding to cell surface receptors. These receptors include the nerve growth factor (NGF) receptor, and the Frizzled receptor, involved in Wnt signaling, binding to which leads to proapoptotic signaling and inhibition of canonical Wnt signaling, involved in hippocampal neurogenesis and synaptic plasticity (Yankner et al. 1990; Magdesian et al. 2008; Knowles et al. 2009). A β -mediated inhibition of Wnt signaling is also implicated in reduced inactivation of tau kinase, glycogen synthase kinase 3 (GSK3), which can lead to increased tau phosphorylation and NFT development (Magdesian et al. 2008). Other synaptic receptors have been identified as A β receptors and will be discussed in more detail in section 1.3.5. However, it must be considered that ADDL preparation protocols vary considerably and treatment concentrations *in vitro* are often orders of magnitude in excess of the nanomolar A β levels believed to be in AD brain. Therefore findings from these studies must be treated with caution. Nevertheless, the collective studies provide convincing evidence for the presence of soluble oligomeric forms of A β in the brain and their role in mediating neuronal dysfunction.

1.3.4 Tau Pathology and Neurofibrillary Tangles

Similar to amyloid plaques, pathological NFTs spread through the brain in a characteristic fashion that is a hallmark of AD. The progressive spread of NFTs was characterized by Braak and Braak (1991, 1995) into six neuropathological stages. Pathology is first present in the transentorhinal layer (stage I-II), including EHC and HPC, before spreading into the limbic system (stage III-IV) and isocortical associated areas (V-VI) (Braak & Braak 1991; Braak & Braak 1995). In contrast to plaque pathology, NFTs account for a significant amount of neuronal degeneration during disease progression and their presence is highly correlated with the cognitive decline in patients (Arriagada, Growdon, et al. 1992; Bierer et al. 1995). It is not surprising therefore that a wealth of AD research has focused on understanding the pathogenesis of tau and developing tau-based therapy (Giacobini & Gold 2013; Pooler et al. 2013; Herrmann & Spiers-Jones 2015)

Tau is most commonly known for its roles in the central nervous system where it is predominantly localized in the cytosol of neuronal axons, but is also present in oligodendrocytes, somatodendritic compartments and the plasma membrane (Klein et al. 2002, Ittner et al. 2010, Pooler et al. 2012). Tau is a microtubule-associated protein that physiologically stabilises microtubules regulated by the phosphorylation/dephosphorylation of serine/threonine (Ser/Thr) residues by enzymes GSK3, casein kinase 1 (CK1), cyclin dependent kinase 5 (Cdk5) and protein phosphatase 2A (PP2A) (Mandelkow et al. 1992; Baumann et al. 1993; Gong et al. 1994; Singh et al. 1995). In AD, this regulated phosphorylation of tau becomes deregulated leading to abnormal or hyperphosphorylation of the tau microtubule binding domain to develop a toxic loss-of-function (Ballatore et al. 2007). Hyperphosphorylated tau protein aggregates into paired helical filaments (PHFs), which aggregate further to form NFTs (Mandelkow & Mandelkow 1998). This abnormal/hyperphosphorylation of tau is caused by increased activity of specific tau kinases, such as GSK3 and cdk5, which are also reported to show increased activity in the presence of A β (Takashima et al. 1998; Alvarez et al. 2001; Noble et al. 2003). Other dementias expressing NFT pathology (known as tauopathies), are independent of A β pathology, and include Frontotemporal dementia with parkinsonism, which is linked to chromosome 17 (FTDP-17), and Pick's disease (reviewed in Yancopoulos & Spillantini 2003). These tauopathies also show abnormally phosphorylated tau, similar to AD (except for the absence of amyloid pathology), and therefore implicate tau as a significant factor in neurodegeneration.

An initial difficulty in studying the neurotoxic properties of tau emerged following a lack of NFT development in APP mouse models of amyloid pathology (Schwab et al. 2004; Götz & Ittner 2008). Therefore, subsequent models have used causative genetic mutations associated with FTD to study neurotoxic properties of abnormally phosphorylated tau protein (as reviewed in Götz et al. 2007). Investigation of the relationship between amyloid and tau pathology has demonstrated a more hierarchical relationship whereby A β is able to increase tau phosphorylation *in vitro* and *in vivo* in APP models. However, there is no evidence of plaque pathology in tau mouse models (Greenberg et al. 1994; Busciglio et al. 1995; Stein et al. 2004). Moreover, transgenic mice simultaneously expressing FAD mutations and FTD tau mutations show exacerbated NFT pathology without any significant change in plaque pathology (Lewis et al. 2001; Oddo et al. 2003; Ribé et al. 2005). A common mouse model used to study AD is the triple transgenic model (3xTg) containing two FAD mutations and one FTD tau mutation and generating both plaque and tangle pathology (Oddo et al. 2003). A β immunotherapy in this model has been reported to both reduce amyloid pathology as well as reduce levels of

hyperphosphorylated tau protein (Oddo et al. 2004). However, tau also acts as a mediator of A β pathology (Roberson et al. 2007; Ittner et al. 2010). Thus, it appears that both A β and tau interact and express a synergistic relationship (this will be discussed in more detail in Section 1.3.5).

It has previously been reported *in vivo* that reduced synaptic density and impaired synaptic function precedes NFT formation in the P301S model of tau pathology (Yoshiyama et al. 2007). Research into the neurotoxic properties of NFTs and tau has suggested that synaptotoxic events and cognitive decline modeled in transgenic tau models are better correlated to toxic soluble tau oligomers than PHFs and NFTs (Spires et al. 2006; Berger et al. 2007; Sydow et al. 2011). These tau oligomers have been reported to be present in the AD brain at levels four-fold higher than present in healthy control brains and are likely to contribute to cognitive decline and AD neuropathology (Lasagna-Reeves, et al. 2012a). When extracted from AD brains, tau oligomers impair LTP in HPC slices of C57Bl/6 mice and when infused via ICV administration into the brains of wild type (WT) C57Bl/6 mice lead to impairment in novel object recognition memory (Lasagna-Reeves et al. 2012b). These effects reported by Lasagna-Reeves and colleagues were not observed in tau knockout (KO) models indicating that endogenous tau plays a significant role in mediating oligomeric tau toxicity. It was also observed that tau pathology had spread from the initial injection site into HPC as well as cortical structures. These results compliment previous findings by both Liu et al and deCallignon et al who reported that tau pathology was able to spread in a circuit-based manner both *in vitro* and *in vivo* (Liu et al.,2012; de Calignon et al.,2012). Interestingly, recent reports have suggested that a further physiological function of tau may be as a cell signaling molecule (Pooler et al. 2013; Pooler et al. 2014). Pooler and colleagues reported that following glutamate stimulation *in vitro* neurons appeared to release tau into the synapse. If these oligomeric forms of abnormally phosphorylated tau act as potent toxic aggregates contributing to AD, this mechanism may be a significant contribution to the progressive spread of tau pathology in AD. Given that A β treatment of neurons *in vitro* caused a reduction in glutamate uptake, this may cause a knock-on effect and stimulate a release of toxic oligomeric tau further contributing to AD pathology (Lauderback et al. 2001; Fernández-Tomé et al. 2004; Li et al. 2009). It is therefore tempting to postulate that combined therapies (targeting both amyloid and tau-mediated pathologies), dependent on disease state, may offer a more optimal treatment for AD.

1.3.5 A β and Tau, a toxic synergy at the synapse

For well over a decade now, the synapse has been a prime target of amyloid pathology (Selkoe 2002). As discussed above, soluble oligomeric A β has been reported to cause a loss of synapses as well as altering electrophysiological recordings of neurons as observed by impaired LTP and enhanced long term depression (LTD) (Walsh et al. 2002; Walsh et al. 2005; Shankar et al. 2008; Li et al. 2009). A β has been reported to interact with a number of synaptic receptors, including the *N*-methyl-D-aspartate (NMDA) receptor (NMDAR), metabotropic glutamate receptor 5 (mGluR5), and the α 7 nicotinic acetylcholine (ACh) receptor (α 7nAChR) (Wang et al. 2000; Renner et al. 2010; Rammes et al. 2011; Shankar et al. 2008). The cellular prion protein (PrP^c) has also recently been observed to act as an A β receptor, altering the interaction between the PrP^c and NMDAR or mGluR5, leading to neurotoxic downstream events (Laurén et al. 2009; You et al. 2012; Um et al. 2013). Studies have also suggested that the precise toxic insult may be dependent on the receptor influenced by A β . The mGluR5 has been implicated in LTD induction, while NMDAR have been more linked to A β -mediated spine loss (Shankar et al. 2008). Collectively, evidence continues to demonstrate a convincing role for A β -mediated toxicity at the synapse, although synaptotoxicity is also thought to be, at least in part, mediated by tau.

Although A β and tau are thought to exert toxicity through separate mechanisms, a more synergistic relationship has been reported at the synapse. A β -mediated NMDAR excitotoxicity appears to be dependent on tau, aspects of which will further be examined in Chapter 5 (Ittner et al. 2010). Ittner and colleagues identified a unique interaction between tau and an Src kinase, Fyn. It had previously been reported that phosphorylated tau, both in the physiological and pathological form, resulted in an increased tau-Fyn interaction influencing the spatial distribution of tau *in vitro* (Lee et al. 1998; Bhaskar et al. 2005). It had also been observed that hyperphosphorylated tau accumulates in somatodendritic compartments (Götz et al. 1995). Fyn phosphorylates the NMDA NR2B subunit, increasing its interaction with postsynaptic density scaffolding protein, PSD95, an event associated with NMDAR-induced synaptic excitotoxicity (Salter & Kalia 2004; Ittner et al., 2010). Moreover, tau KO mice are less susceptible to synaptic A β toxicity (Roberson et al. 2007; Ittner et al., 2010). From these observations Ittner and colleagues postulated that this tau-Fyn interaction was required for the translocation of both Fyn and tau to the somatodendritic compartments in a manner based on tau phosphorylation. Successful completion of this would lead to increased phosphorylation of the NR2B subunit,

enhanced PSD-95-NR2B interaction and increased synaptic excitotoxicity, which may be mediated by increased levels of soluble A β as illustrated in Figure 1.3. Ittner and colleagues used both a tau KO mouse model and truncated tau model lacking the microtubule binding domain of tau, but maintaining the Fyn binding region in order to test this hypothesis. It was thus reported in both models that increased Fyn was observed in the soma and reduced Fyn, tau and phosphorylated NR2B in synaptosomal preparations in comparison to WT controls. These effects were repeated when these tau models were crossed with an APP model of FAD and further showed improved spatial working memory (SWM) performance on a T-maze task (Ittner et al., 2010).

Collectively these results suggest an initial tau-dependent synaptotoxic mechanism influenced by A β . However, it is likely that with disease progression, continued exposure of neurons to A β will lead to increased hyperphosphorylation of tau and an overall downstream increase in NMDA-NR2B mediated excitotoxicity. It has also recently been reported that A β -PrP^c interaction leads to increased Fyn activation and phosphorylation of the NR2B subunit (Um et al. 2012). This effect is likely to further contribute to the synaptotoxic effects of this mechanism. These observations highlight the attraction towards the development of tau-based therapies as well as the importance of targeting A β production early in disease progression.

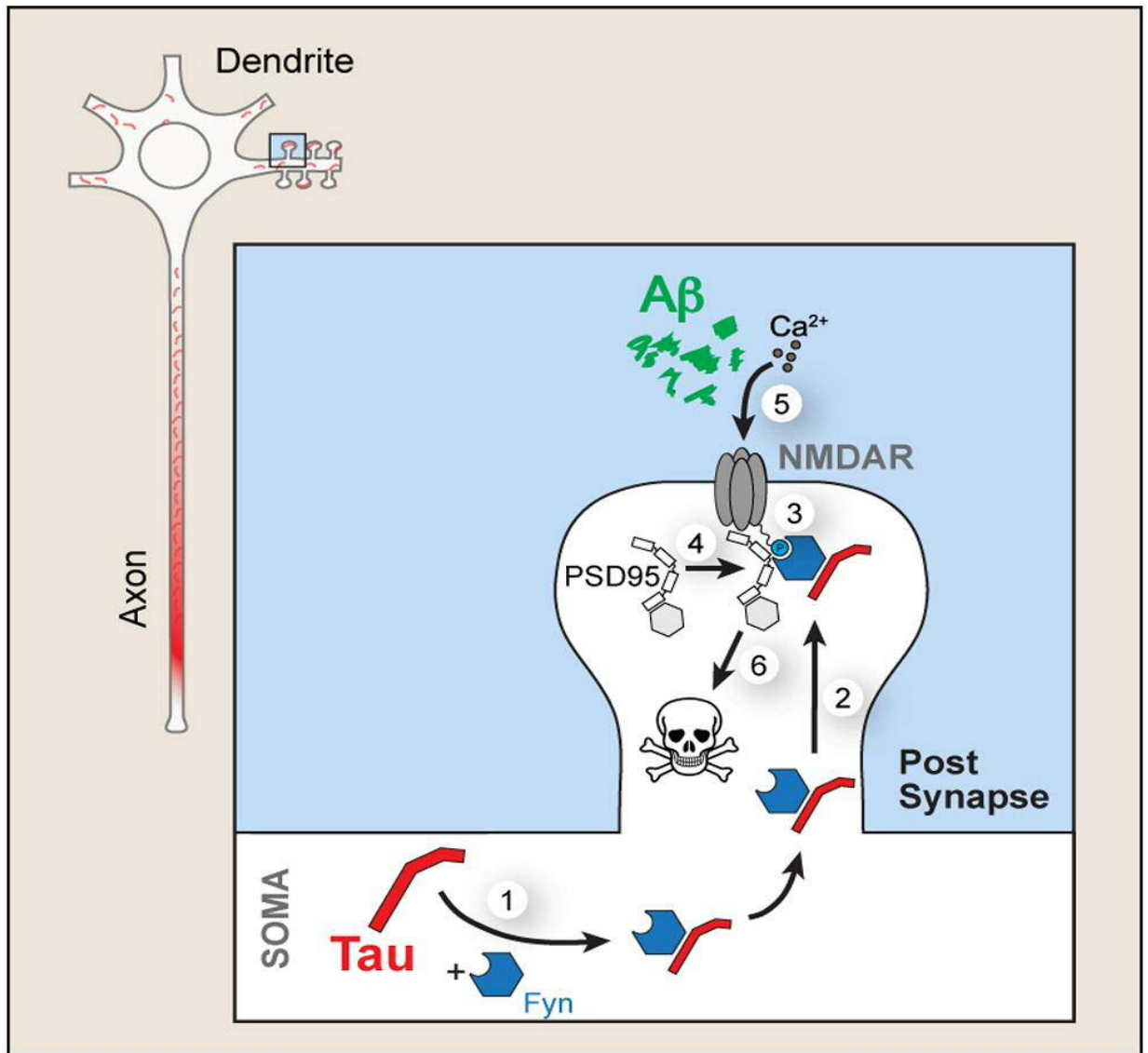


Figure 1.3: Schematic illustration demonstrating the interactions between A β , tau and Fyn leading to neuronal excitotoxicity. Src kinase Fyn interacts with phosphorylated tau protein leading to the translocation of both proteins to the post synapse (1-2). Fyn at the synapse phosphorylates the NR2B subunit of the NMDAR complex, stabilizing its interaction with PSD95 and expression at the synapse (3-4). Increased A β and enhanced expression of NR2B containing NMDARs at the synapse causes disproportionate influx of Ca²⁺ leading to downstream neurotoxicity.

1.4 Modeling Alzheimer's Disease

One goal of the research presented in this thesis was to characterize the cognitive phenotype of the PDAPP mouse model of amyloid pathology; prior to using the model to test the effects of an APP antibody on cognition and pathology. This section aims to provide an overview of methods used to model AD pathology and cognitive decline in animal models. Given the review of AD pathology described in section 1.3, the main focus will be a summary of the behavioural abnormalities observed in transgenic models and their relationship to human AD abnormalities.

There has been extensive use of Tg animals to model the pathological features of AD and evaluate potential therapies based the amyloid cascade hypothesis. Tg models were first developed on the basis of *APP* mutations linked with FAD. There are currently 49 *APP* mutations that have been identified, located throughout the *APP* loci and a further 216 Presenilin 1 mutations within the *PSEN1* loci (<http://www.molgen.ua.ac.be/ADMutations>). Genetic constructs of these human FAD mutations have been expressed under the control of a variety of promoters in mice (Capecchi 1989; Kobayashi & Chen 2005; Webster et al. 2014). However, no *APP* animal model has to date replicated all core pathological features of AD patients, including amyloid-induced tau pathology and substantial neuronal loss (Lee & Han 2013). Regardless of this, these models have been used to provide a more detailed understanding of the effects of excess amyloid production on brain function, cognition and the potential of therapeutic interventions targeting amyloid processing.

1.4.1 Human APP mutant models of amyloid pathology

A number of *hAPP* mutations in mice result in increased levels of A β and age-dependent cognitive deficits (see Table 1.1; Games et al. 1995; Kobayashi & Chen 2005; Moechars et al. 1999; Hsiao et al. 1996). The most commonly used mouse models overexpress the Swedish double K670M/N671L mutation, located at the BACE1 cleavage site, the Indiana V717F mutation, located at the γ -secretase cleavage site, and the Arctic E693G mutation, located within the A β sequence (see Table 1.1; Murrell et al. 1991; Mullan et al. 1992; Nilsberth et al. 2001; Games et al. 1995; Hsiao et al. 1996; Mucke et al. 2000). Other Tg models have expressed two or more separate *hAPP* and/or human *presenilin* mutations in one model in an effort to promote

the onset and severity of pathology. Indeed, these models show a more rapid onset of pathology and cognitive symptoms (See Table 1.1 for gene mutations expressed and comparison of age-related pathology; Mucke et al. 2000; Puoliväli et al. 2002; Trinchese et al. 2004; Oakley et al. 2006). Collectively, these models, similar to human AD patients, show an age-related increase in levels of A β plaque deposition as well as soluble A β , relative to WT littermate controls. However, they do not show any apparent NFT pathology, nor MTL atrophy; a feature that has been correlated with early episodic and semantic memory deficits in patients (see section 1.2.3).

Nevertheless, similar to AD patients, most APP models display age-related cognitive deficits (as illustrated in Figure 1.4 and the progression of different memory deficits detailed in Table 1.2; see also Webster et al. 2014). Generalising across a number of cross-sectional and longitudinal designs, one common pattern emerges and that is there is an onset of SWM deficits that frequently precedes the onset of deficits in object recognition memory (Webster et al. 2014). The precise age at which these pathological and cognitive deficits present varies across AD models. However, the precise background strains and nature of the *APP* and/or *presinillin* transgene overexpression likely contributes to this variance.

SWM will be thoroughly discussed in Chapter 3 and object recognition memory in Chapter 4. However, in order to better understand the comparisons of behavioural tasks used to determine cognitive deficits in AD models, SWM refers to an animal's ability to process spatial information within one trial of an experiment, but not for subsequent trials thereafter (Honig 1978; Olton et al. 1979). Tasks commonly used to assess SWM include the radial arm maze, which consists of an eight-arm maze whereby each arm is baited with a food/liquid reward. Rodents must forage all rewards before completing the task. Any time an animal enters an arm that has previously been visited, this is counted as a working memory error. Many more SWM tasks are also used, an extensive review of which has been reported by (Dudchenko 2004). The tasks that test SWM function show particular sensitivity to hippocampal lesions, which has been shown to be critical to the processing of spatial information (Olton & Paras 1979; Aggleton et al. 1986). AD patients also exhibit visuospatial memory impairment and significant hippocampal pathology, which is most likely a cause of the memory disorders in AD (Hyman et al. 1984; Jack et al. 1992; Carlesimo et al. 1994).

Model	Mutation	Pathology	Cognitive Impairments	Synaptic Deficits
PDAPP (Games et al. 1995)	APP Indiana V717F, PDGFβ promoter ¹	Soluble Aβ and dense core and diffuse Aβ plaques in at 4-6 months ^{2,3} . Dystrophic neurites, gliosis, loss of synaptic densities, hippocampal atrophy ^{1,4,5} .	Spatial learning ^{6,7,8} , Spatial reference memory ⁷ , spatial working memory ^{6,8} , object recognition memory ⁶ , contextual fear conditioning ⁹	Rapid decay of LTP at 4-5 months ¹⁰ . Reduced cholinergic signalling ¹¹
Tg2576 (Hsaio et al. 1996)	APP Swedish, 695.K670N-M671L, Hamster PrP promoter ¹²	Increased soluble Aβ at 6 months of age, plaque deposition by 9-12 months of age ¹³ . Astrogliosis, microgliosis and dystrophic neurites observed ^{14,15}	Spatial reference memory ^{16,17} , spatial working memory ^{18,19} , object recognition memory ^{20,21} , contextual fear conditioning ²²	Reduced dendritic spine density from 4 months and impaired LTP at 5 months in the DG ²³
APP23 (Sturchler-Pierrat et al., 1997)	APP Swedish, 695.K670N-M671L, Murine Thy-1 promoter ²⁴	Aβ plaques, astrogliosis and increased phospho-tau at 6 months of age ²⁴ . 14-25% neuronal loss at 18 months of age ²⁵	Spatial working memory ²⁶ , spatial reference memory ^{26,27,28} , passive avoidance ²⁷ , Barnes Maze ²⁹	Intact HPC LTP up to 24 months, but reduced synaptic transmission at 12 months ³⁰ . Behavioural training induces a more rapid decay of LTP ³¹
TgCRND8 (Chishti et al., 2001)	APP Swedish, 695.K670N-M671L, and Indiana V717F, Syrian hamster PrP promoter ³²	Aβ deposits at 3 months, dense core plaques by 5 months ³² . Increased microglia activation focussed around Aβ plaques ³³	Spatial learning ³² , spatial reference memory ^{32,34} , spatial working memory ^{34,35} , contextual fear conditioning ³⁶	Reduced number of HPC neurons and dendritic spine loss ³⁷ . Diminished LTP ³⁸
J20 (Mucke et al., 2000)	APP Swedish, 770.K670N-M671L and Indiana V717F, PDGFβ promoter ³⁹	Early increase in Aβ-42 at 2 months of age and plaque deposition at 5-7 months ³⁹ . Increased Aβ*56 at 5-6 months of age ^{40,42} . Increased astrogliosis ⁴¹ and phospho-tau ⁴²	Spatial reference memory ^{40,41} , spatial working memory ⁴¹ , object recognition memory ⁴² , contextual fear conditioning ⁴³	Reduced neuronal c-fos in the DG ^{40,41} , HPC synapses ⁴¹ , impaired basal synaptic transmission and LTP ⁴⁴
APP/PS1 (Citron et al., 1997)	APP Swedish, 695.K670N-M671L, PS1, M146L, PDGFβ, PrP promoter ⁴⁵	Amyloid deposits by 3m, abundant plaques by 6-9m ⁴⁵ . Early increase of insoluble Aβ-42 and -40 relative to Tg2576 mice from 2 months of age ⁴⁶ .	Spatial reference memory ⁴⁶ , spatial learning ⁴⁷ and fear conditioned learning ⁴⁸	Impaired LTP from 3-4 months and basal transmission from 6 months ⁴⁷ .
5xFAD (Oakley et al., 2006)	APP Swedish 695.K670N-M671L, Florida 1716V, London V717L, PS1 M146L-L286V, Thy-1 promoter ⁴⁹ .	Aβ-42 accumulation and astrogliosis from 2-3 months ^{49,51} , reduced whole-brain synaptophysin at 4 months ⁴⁹	Spatial working memory ^{49,51} , spatial reference memory ⁵⁰ , context fear conditioning ^{50,52}	Impaired LTP at 6 months and reduced basal synaptic transmission ^{52,53}
3xTg (Oddo et al., 2003)	APP Swedish, 695.K670N-M671L, PS1 M146V, Tau P301L, Thy1.2 promoter ⁵⁴ .	Aβ deposition (6 months) precedes NFT pathology (15 months) ⁵⁴ . Increased phospho-tau at 6 months ⁵⁵ Elevated levels of Aβ*56 by 12 months ⁵⁶ . Soluble oligomeric Aβ originating intraneuronally at 6 months ⁵⁷	Spatial reference memory ^{55,56} , spatial working memory ⁵⁹ , object recognition memory ^{54,58} , passive avoidance ⁵⁴	Reduced levels of synaptophysin and PSD95 ⁶⁰ . Impaired LTP and reduced synaptic transmission ⁵⁴

Table 1.1: Overview of commonly used transgenic mouse models of AD. 1: (Games et al. 1995), 2: (Masliah et al. 1996), 3: (Johnson-Wood et al. 1997), 4: (Reilly et al. 2003), 5: (Redwine et al. 2003), 6: (Dodart et al. 1999), 7: (Chen et al. 2000), 8: (Hartmann et al. 2005), 9: (Gerlai et al. 2002), 10: (Larson et al. 1999), 11: (Bales et al. 2006), 12: (Hsiao et al. 1996), 13: (Kawarabayashi et al. 2001), 14: (Irizarry et al. 1997), 15: (Frautschy et al. 1998), 16: (Kotilinek et al. 2002b), 17: (Pedersen et al. 2006), 18: (Chapman et al. 1999), 19: (Barnes et al. 2004), 20: (Good & Hale 2007), 21: (Hale & Good 2005), 22: (Corcoran et al. 2002), 23: (Jacobsen et al. 2006), 24: (Sturchler-Pierrat et al. 1997), 25: (Calhoun et al. 1998), 25: (Vloeberghs et al. 2006), 27: (Kelly et al. 2003), 28: (Lefterov et al. 2009), 29: (Prut et al. 2007), 30: (Roder et al. 2003), 31: (Middei et al. 2010), 32: (Chishti et al. 2001), 33: (Chauhan et al. 2004), 34: (Janus 2004a), 35: (Lovasic et al. 2005), 36: (Hana et al. 2012), 37: (Steele et al. 2014), 38: (Kimura et al. 2012), 39: (Mucke et al. 2000), 40: (Meilandt et al. 2009), 41: (Galvan et al. 2007), 42: (Escribano et al. 2010), 43: (Saura et al. 2005), 44: (Saganich et al. 2006), 45: (Citron et al., 1997), 46: (Westerman et al., 2002), 47: (Trinchese et al., 2004), 48: (Dineley et al., 2002), 49: (Oakley et al. 2006), 50: (Ohno et al., 2006), 51: (Jawhar et al. 2012), 52: (Kimura & Ohno 2009), 53: (Crouzin et al. 2013), 54: (Oddo et al. 2003), 55: (Clinton et al. 2007), 56: (Billings et al. 2007), 57: (Oddo, Caccamo, et al. 2006), 58: (Filali et al. 2012), 59: (Carroll et al. 2007), 60: (Revilla et al. 2014)

Object recognition memory refers to an animals ability to discriminate previously encountered objects over novel objects that have not previously been encountered (Ennaceur & Delacour 1988; Ennaceur 2010). When carried out as originally described by Ennaceur and Delacour (animals are presented with two identical objects (A+A) for a short acquisition phase then allowed a delay period prior to testing. In the test phase one original object, A, will be presented with a new, novel object B) recognition memory has been reported to be sensitive to perirhinal cortex (PRC) function, independent of the HPC (Barker & Warburton 2011). However, manipulations of this task to involve spatial or temporal information (detailed in Chapter 4 and outlined in Table 4.1) are able to activate neural circuits that involve both the HPC and PRC (Barker & Warburton 2011; Warburton & Brown 2015b).

Many behavioural tasks used to assess cognition in mouse models of AD require intact functioning of specific neuroanatomical structures, including the HPC. They further rely on the ability of these structures to process and retrieve information dependent on the function of specific neuronal circuits. For example, in object recognition memory, the PRC has been observed to be responsible for encoding object information, but the HPC for the spatial associative information (Barker & Warburton 2011). Moreover, the ventral CA1/subiculum, prefrontal cortex and nucleus accumbens have been reported to play significant roles in processing information in the RAM in a delay-dependent manner (Floresco et al. 1997). The different anatomical structures and circuits involved in these behavioural tasks allows for the investigation of their sensitivity toward pathologies associated with Tg AD mouse models and potentially how these circuits may be affected in AD. Table 1.1 outlines the onset of amyloid pathology in multiple Tg models used to investigate AD. Table 1.2 displays the progressive cognitive deficits observed within individual memory systems determined by behavioural tasks that are able to assess these types of memory (i.e. RAM – SWM, novel object recognition – object recognition memory) and also allows for a comparison of these memory types and their decline with age in Tg mouse models. The data presented in Tables 1.1 and 1.2 suggest that certain neuroanatomical structures and/or circuits are more susceptible to amyloid pathology in Tg models based on a similar progressive pattern of deficits illustrated in Figure 1.4.

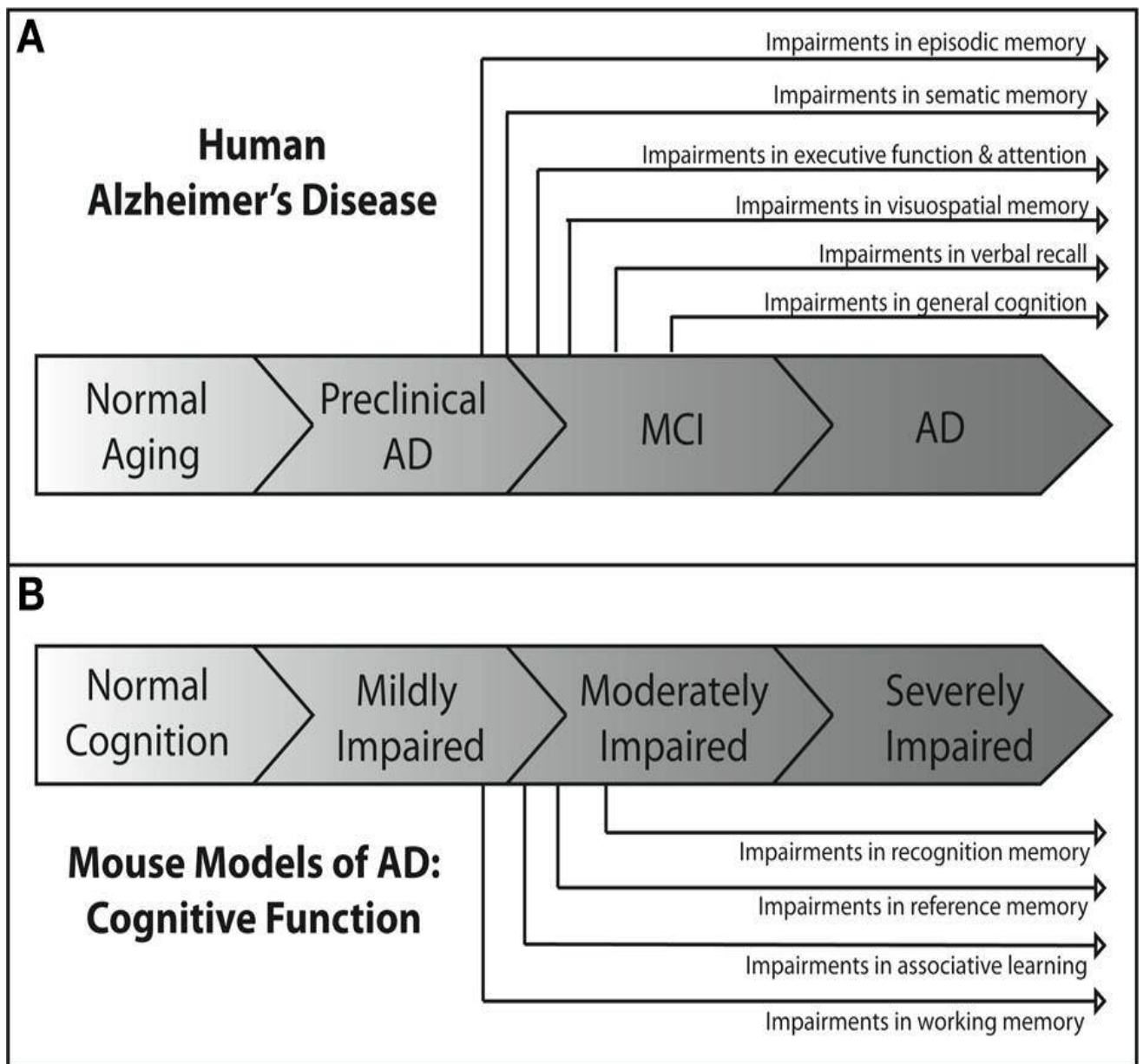


Figure 1.4: Overview of the progressive cognitive decline in AD. The pattern of cognitive deficits is illustrated in order of clinical AD disease severity (A) and cognitive impairment in murine models of AD (B). (Webster et al., 2014)

Model	Memory Type				Age
	Working Memory	Reference Memory	Fear Conditioned Memory	Object Recognition Memory	
PDAPP					≤ 2 months
	2, 3	2		2	3-5 months
	1* 2	2		1, 2	6-10 months
	1, 2, 3	2		1 2	11-15 months
	1, 3			1	≥ 16 months
Tg2576					≤ 2 months
	5	7	4*, 5		3-5 months
	5	6 7*	4, 5	6*	6-10 months
		7*			11-15 months
		6, 7		6*	≥ 16 months
APP23		8	8		≤ 2 months
		8 9*	8, 9		3-5 months
		8	8		6-10 months
					11-15 months
		9	9		≥ 16 months
TgCRND8		10			≤ 2 months
		10	11		3-5 months
		10	11		6-10 months
			11		11-15 months
					≥ 16 months
J20					≤ 2 months
	12	14	12	15	3-5 months
		13, 14	12	15	6-10 months
		13			11-15 months
	12				≥ 16 months
APP/PS1		16			≤ 2 months
		16	17*		3-5 months
		16	17		6-10 months
					11-15 months
					≥ 16 months
5xFAD	18				≤ 2 months
	18 20		19*		3-5 months
	20		19		6-10 months
	20				11-15 months
					≥ 16 months
3xTg		21, 22	21, 22	21	≤ 2 months
	23	22	22		3-5 months
	23	21 22*	21 22*	21	6-10 months
	23	21	21	21	11-15 months
					≥ 16 months

Table 1.2: Overview of the progressive cognitive decline observed in Tg models of AD from longitudinal and cross-sectional studies. Tg Models of AD show a pattern of progressive cognitive decline within individual tasks, but also across different memory tasks/systems. Earlier deficits are commonly observed in spatial working and reference memory tasks and later deficits in object recognition memory. All studies referred to in this table assess cognitive performance at two or more age points in either cross-sectional or longitudinal design protocols. Boxes in a light shade of grey represent a time point when Tg mice show no significant difference to age-matched WT littermates. * Represents Tg mice showing a deficit in any manipulation of the behavioural task being tested, e.g., increased retention period prior to test. Those in darker shades represent a deficit when compared to WT controls across all manipulations. Numbers in boxes refer to referenced studies reported below. All other deficits not reported here are reported in table 1.1, which were taken at one age point only. Working memory measures are taken from reported T/Y-maze (Y-M) and specific MWM protocols as detailed in (Chen et al. 2000). Reference memory deficits are taken from RAM, or probe trial results of RAWM or MWM following repeated acquisition. This measure from MWM has previously been defined as reference memory following the escape platform remaining in the same location during the repeated acquisition trials (Frick et al. 1995). Fear conditioned memory measures are reported from context association and conditioned stimulus (CFC) as well as passive avoidance (PA) of aversive stimulus experiments associating either a context of tone with a foot shock. Finally, object recognition memory measures an animal's ability to discriminate novel objects (or object novelty (ON)) from those previously encountered. Studies reported here: 1: MWM, ON (Chen, Chen, Knox, Inglis, Bernard, Martin, Justice, Mcconlogue, et al. 2000), 2: RAM, ON (Dodart et al. 1999), 3: MWM (Hartman et al. 2005), 4: CFC (Dineley et al. 2002), 5: Y-M, CFC (King et al. 1999), 6: Y-M, BM, ON, OL (Yassine et al. 2013), 7: MWM (Westerman et al. 2002), 8: MWM, PA (Van Dam et al. 2003), 9: MWM, PA (Kelly et al. 2003), 10: MWM (Hyde et al. 2005), 11: CFC (Hanna et al. 2012), 12: MWM, CFC (Saura et al. 2005), 13: RAWM (Du et al. 2008), 14: RAWM (Arancio et al. 2004), 15: ON (Escribano et al. 2009), 16: RAWM (Trinchese et al. 2004), 17: CFC (Dineley et al. (2002), 18: Y-M (Oakley et al. 2006), 19: CFC (Kimura & Ohno 2009), 20: Y-M (Shukla et al. 2013), 21: MWM, PA, ON (Clinton et al. 2007), 22: MWM, PA (Billings et al. 2005), 23: Y-M (Carroll et al. 2007).

It is intriguing that there is a lack of evidence to suggest a worsening of the cognitive deficits once they become apparent. As these deficits are thought to be caused by increasing deposition of A β , it would be logical that the severity of the deficit should increase with time. A numerical age-related worsening of SWM is observed in the PDAPP mouse model at 17-19 months of age following an initial deficit at 4-6 months of age (Hartman et al. 2005). However, Hartman and colleagues fail to show any increase in levels of A β at 4-6 months, but do report a small increase at 10-12 and much greater deposition by 17-19 months of age. One interpretation of this pattern is that the initial deficit is due to an effect of *APP* overexpression, whereas A β deposition may contribute to the later decline in memory at 17-19 months of age (Hartman et al. 2005). A further two studies in the Tg2576 and 5xFAD models also suggest an age related worsening of memory potentially related to accumulating levels of amyloid (Westerman et al. 2002; Shukla et al. 2013). Westerman and colleagues demonstrated an initial decline in spatial reference memory at 6-11 months of age. This deficit was ameliorated in mice up to the age of 12-18 months by reinforcement of spatial reference information (by increased training), however older cohorts (20-25 months) remained impaired. Further analysis revealed that these deficits in older mice were significantly associated with levels of insoluble A β (Westerman et al. 2002). Similar to this, other studies have also demonstrated that increased stimulus (e.g. increased number of foot shocks received in a fear conditioned response task), training to criterion protocols in the Morris Water Maze (MWM) or simplification of a task can change the age of which a cognitive deficit manifests (Chen et al. 2000; Dineley et al. 2002; Kelly et al. 2003; Dumas et al. 2008). However, no further studies present evidence that age-dependent increases in levels of amyloid lead to progressive cognitive changes.

The absence of evidence suggesting A β -mediated worsening of memory may be due a lack of sensitivity in behavioural tests. Alternatively, the absence of severe tau pathology in *hAPP* models may also restrict the severity of cognitive change. Indeed, in human studies, a much stronger correlation is reported between tau biomarkers and cognitive decline (Jack et al. 2010; Jack et al. 2013). Moreover, cognitive tasks more closely associated with memory deficits observed in AD may provide a closer parallel for AD-related cognitive deficits. For example, AD patients display episodic memory deficits; an inability to recall events in relation to their content and temporal-spatial information (Tulving 1972; Butters et al. 1987; Greene et al. 1996). Rodent cognitive tasks have been able to assess an analogue of episodic-like memory that determine an animals ability to exhibit a memory of “what” happened,

“where” and “when”. These tasks include adaptations of object-based and fear conditioned memory paradigms (Good et al. 2007; Iordanova et al. 2008; Iordanova et al. 2011). Tg2576 mice have been reported to express “episodic-like” deficits in an object-based memory task (Good et al. 2007). However, no study has yet assessed episodic, or episodic-like memory across a range of ages in Tg models of AD. Collectively, these data suggest that Tg models provide an important tool for understanding the neural circuits and anatomical structures sensitive to AD pathogenesis. The tasks commonly used to assess cognition in mouse models of AD have been extensively characterised and it is clear that although there is critical involvement of the HPC in these tasks (discussed in Chapter 3 and 4), other circuits and structures are also required for the processing of information. For example, fear conditioned memory tasks rely on an anxious response to a foot shock in order to form the required memory. This task has been shown to be sensitive to both HPC function and the amygdala (Phillips & LeDoux 1992; Nader et al. 2000). Increased fear response has been reported in PDAPP, J20 and 3xTg mice previously, which was associated with A β pathology in the amygdala (España et al. 2010). Therefore, when assessing memory in Tg models, appropriate control measures or prior assessment of emotionality is advised in order to carry out the most optimal cognitive task and provide more reliable conclusions to the structures and circuits effected by AD pathogenesis and possible pharmacological intervention.

1.4.2 The PDAPP Model

The PDAPP model was originally reported in 1995 by Games et al., and has since been used widely in AD research (Games et al. 1995). The transgene, otherwise known as the *hAPP*^{V717F} mutation, expresses a point mutation located around the γ -secretase cleavage site, leading to an altered amino acid structure of APP at Valine 717 (Murrell et al. 1991). The expression of this transgene is driven by the platelet-derived growth factor (PDGF) β -promoter, which targets the expression of this mutant transgene to neurons (Sasahara et al. 1991). The overexpression of *hAPP* generates a total APP protein level 10-fold higher than the amount of endogenous brain murine APP (Games et al. 1995).

The PDAPP model has traditionally been bred on a mixed background with Swiss-Webster, DBA/2 and C57Bl6 (Games et al. 1995). However, variations in behaviour have been reported to occur between different genetic backgrounds (Brooks et al. 2005; Kobayashi & Chen 2005). Brooks and colleagues assessed several mouse strains commonly used as Tg

background strains, including DBA/2 and C57Bl/6. Brooks (2005) reported differences in a range of behavioural tasks, including novel object recognition task (described and used in Chapter 4). One interesting observation was that the total exploration time of objects in the novel object recognition memory task was greatest in DBA/2 and BALB/c mice, which significantly differed from the 129S2/Sv strain. C57Bl/6 mice also appeared to show reduced contact time with objects relative to the DBA/2 strain, of which both of these strains are used in the mixed PDAPP background (Games et al. 1995; Brooks et al. 2005). Interestingly, when comparing the behavioural data between different labs using the PDAPP model differences in object recognition memory have been reported (Dodart et al. 1999; Chen et al. 2000). Dodart and colleagues (1999) reported an age-dependent deficit in object recognition memory, where as Chen et al (2000) showed no deficit in object recognition memory across all ages tested. These mice were generated from different colonies and no data were provided to determine if each colony had an equal contribution of each strains phenotype, which may have lead to altered behavioural phenotypes. This question of age-related changes in object recognition memory in the PDAPP model will be further evaluated in chapter 4. Gender-specific differences of behavioural performance have also been reported within background strains, including C57Bl/6 (Võikar et al. 2001; Frick & Gresack 2003; Gresack & Frick 2003). Studies by Frick and Gresack have revealed that male C57Bl/6 mice showed greater object recognition memory performance and lower SWM and reference memory errors in the radial arm maze when compared to female C57Bl/6 mice (Frick & Gresack 2003; Gresack & Frick 2003). For these reasons, in this study, we have bred the PDAPP model on a C57Bl/6 background and used only male mice to increase the potential of any alteration in behaviour between wild type and transgenic to be a phenotype of the *hAPP^{V717F}* mutation.

The neuropathology of this model has previously been characterised, both on the original mixed background, and C57Bl/6 background only. In summary PDAPP mice have shown increased soluble amyloid levels at ages as young as 4 months and plaque development from approximately 6-8 months; which significantly increase with age (Games et al. 1995; Johnson-Wood et al. 1997; Fryer et al. 2003; Redwine et al. 2003; Reilly et al. 2003; Basak & Holtzman 2011). These effects were not observed quite as early in PDAPP mice on a C57Bl/6 background (Hartman et al. 2005). Hartman and colleagues observed plaque pathology at 10-12 months of age in the HPC of PDAPP mice, which increased significantly by 17-19 months of age (Hartman et al. 2005). This age-related increase in soluble and aggregated plaque pathology appears similar to ages reported in Tg2576 mice (6 months soluble, 9 months

insoluble) and APP23 mice (6 months of age) (Struchler-Pierrat et al. 1997; Kawarabayashi et al. 2001). However, more rapid plaque pathology appears to be common in Tg APP mice expressing 2 or more FAD *APP* genes, including the TgCRND8 (plaque pathology at 3 months) and 5xFAD (amyloid deposits at 2 months of age; Chishti et al. 2001; Oakley et al. 2006). However, although these latter models offer a more rapid onset of pathology, multiple FAD mutations have not been reported in patient populations and therefore offer an unrealistic model compared to those expressing single FAD *APP* mutations. Thus, the more progressive onset of amyloid pathology in the PDAPP mouse model offers a more realistic parallel to model AD pathology.

The *hAPP*^{V717F} mutation causes a significant shift in the production of A β 42 over A β 40, most likely causing the increased propensity for A β aggregation in PDAPP mice (Suzuki et al. 1994; Zerbinatti et al. 2004). This differs in comparison to other models such as the Tg2576, which exhibit a greater level of A β 40 than A β 42 and may therefore offer a tool to investigate differences in amyloid pathology, aggregation and cognitive effects based on individual FAD mutations (Kim et al. 2007). Nonetheless, A β deposits appear initially in the cingulate cortex before accumulating in the molecular layer of the dentate gyrus (DG), CA1 region of the HPC, the EHC and further progressing into cortical structures in brains of PDAPP mice (Games et al. 1995; Irizarry et al. 1997; Johnson-Wood et al. 1997; Su & Ni 1998;). No deposition has been reported in the thalamus and cerebellum. The areas of greatest deposition are the DG and EHC suggesting the perforant pathway to be most susceptible to A β pathology (Irizarry et al. 1997; Johnson-Wood et al. 1997). This pathway has been reported to show plaque pathology in human AD and is most likely a cause of cognitive deficits in tasks sensitive to HPC function (Lippa et al. 1992; Hyman et al. 1986).

As reported in Tables 1.1 and 1.2, PDAPP mice exhibit age-related cognitive deficits. However, age-independent deficits in spatial reference memory have also been reported as early as 3 months of age, which precedes plaque pathology (Dodart et al. 1999; Hartman et al. 2005). Moreover synaptic changes have also been reported early on in PDAPP mice. Mice at 4-5 months of age show a rapid decay in LTP compared to WT controls (Larson et al. 1999). They also exhibit a reduced basal level of acetylcholine (ACh), and reduced ACh release following pharmacological stimulation. The latter is consistent with an early impairment in cholinergic signalling (Bales et al. 2006). This is most likely an effect of *hAPP* overexpression. It has been reported that an overall 12% reduction in total HPC volume of PDAPP mice can be observed at 3 months of age (Weiss et al. 2002; Redwine et al. 2003;

Reilly et al. 2003). This HPC atrophy is likely to contribute to early age-independent cognitive deficits in this model (Dodart et al. 1999; Hartman et al., 2005). Some studies have reported age-related changes in object recognition memory and SWM (Dodart et al. 1999; Chen et al. 2000; Hartman et al. 2005). These age-related cognitive deficits are associated with insoluble A β and plaque deposition. Furthermore, treatment with A β -immunotherapy has showed significant improvement in both object recognition memory and SWM suggesting these age-related cognitive deficits observed in PDAPP mice are caused by A β accumulation (Dodart et al. 2002; Hartman et al. 2005). A more thorough evaluation of SWM and object recognition memory will be provided in Chapters 3 and 4 respectively.

Further differences in PDAPP and WT controls have also been reported. PDAPP mice exhibit lower body temperatures with age, compared to WT controls (Huitrón-Reséndiz et al. 2002). These reduced body temperatures complicate behavioural paradigms using water maze protocols, such as the MWM, which would require set water temperatures to prevent hypothermia in mice, which has previously been reported to cause impaired learning and memory in the MWM (Rauch et al. 1989). PDAPP mice also exhibit increased locomotor activity in younger ages (3-5 months) during dark period (active period) of the 12hour light dark cycle, but not the light period (Huitrón-Reséndiz et al. 2002). A confounding observation was reported that this effect was no longer observed in aged PDAPP mice (20-26 months of age), to which the authors provided no explanation of how this effect was likely reversed (Huitrón-Reséndiz et al. 2002). Alternative Tg models have also been reported to exhibit increased locomotor activity, including 3xTg and Tg2576 mice (Ognibene et al. 2005; Knight et al. 2013). Hyperactivity has been associated with impaired spatial learning and memory in cognitive tasks including the MWM and RAM (Cain et al. 1996; D’Hooge & De Deyn 2001). Therefore considerations must be made when using cognitive tasks to assess memory in Tg models of AD, whether underlying behavioural phenotypes, such as hyperactivity, impact on impaired memory function reported in these models.

The data discussed above provide evidence that PDAPP mice model an age-related increase in amyloid levels, which are associated with progressive cognitive decline. Early cognitive deficits have been reported from 3 months of age, which precede amyloid pathology and are likely an effect of APP overexpression (Johnson-Wood et al., 1997; Dodart et al. 1999). These early changes in behavioural performance must be considered when using PDAPP mice to study pharmacological interventions for AD as well as amyloid pathology in

this model. However, the PDAPP model provides a useful tool for studying age-related cognitive decline associated with amyloid pathology.

Collectively, Tg models of AD, despite not recapitulating the full human AD pathology, have been invaluable in studying the neurotoxic properties of tau and amyloid in AD as well as other dementias. These models demonstrate age-related increases in soluble A β and plaque pathology, which have been correlated to the onset of cognitive deficits. They have also provided an *in vivo* system to test pharmacological compounds or antibody-based therapies as well as potential amyloid/tau based therapies. However, from the studies carried out thus far it is apparent that a number of considerations must be made before using Tg animals in these types of experiments. For example, if characterising the cognitive phenotype of a Tg model, it is ideal to have a starting age at which both Tg and WT mice perform at relatively equal levels in at least one behavioural task. As amyloid levels increase with age it allows the observation of these age-related effects instead of any early developmental effects of transgene overexpression. Moreover, it presents an age point to test whether pharmacological intervention may reverse or prevent this amyloid-induced deficit. Thus, for both cognitive phenotyping and pharmacological assessment of compounds *in vivo* considerations of precise model, pathologies reported, age of onset of cognitive deficits and sensitivity to relative difficulty of specific cognitive tasks must all be carefully considered for appropriate completion of these studies.

1.5 Current and Developing Treatment for Alzheimer's Disease

In this final introductory section, an overview of the current and developing treatments for AD will be discussed. The focus will be on therapies targeting amyloid production and A β . Given that one of the main aims of this thesis is to test the *in vivo* effects of 2B3, an anti-APP BACE cleavage site antibody, a more thorough description of BACE1 inhibitors and modulators will be provided in chapter 6. However, current therapy strategies including γ -secretase inhibitors, passive and active immunotherapies will be discussed below.

1.5.1 Current Alzheimer's Disease Treatment

Despite promising therapeutic results from *in vivo* data, currently only symptomatic treatments are approved for AD (NICE Guidelines 2011). There are currently two main types of pharmacological intervention for AD patients. The first major group of pharmacological compounds, and the first line of treatment available for AD, are anticholinesterase inhibitors; donepezil (Aricept; Pfizer), rivastigmine (Exelon; Novartis) and galantamine (Reminyl; Janssen), which act to enhance ACh levels by targeting acetyl cholinesterase, the enzyme involved in the breakdown of ACh. Despite all three compounds having similar mechanisms, all are reported to be variable in their pharmacology and pharmacokinetics (Scarpini et al. 2003).

Galantamine has been further reported to enhance cholinergic neurotransmission through postsynaptic mechanisms (Scott & Goa 2000). Rivastigmine is also reported to inhibit butyrylcholinesterase as well as acetyl cholinesterase. Butyrylcholinesterase is thought to contribute to cholinergic pathology in AD and this may therefore be a further beneficial effect of rivastigmine (Arendt et al. 1992; Perry et al. 1978). Memantine is a moderate-to-severe stage treatment (Ebixa; Eli Lilly), and is an NMDA receptor antagonist (Scarpini et al. 2003). Memantine disrupts neuronal death mediated by the deregulation of Ca²⁺ homeostasis, caused by excess extracellular glutamate via activation of NMDA receptors (Greenamyre & Young 1989; Danysz & Parsons 2012). Drug trials with memantine in advanced AD patients reported a significant reduction in deterioration in cognitive and functional measures (Tariot et al. 2003). However, all these treatments only target symptoms of AD and are thought to modify disease processes per se. For these reasons, scientific research has continued to

explore methods to promote clearance, modify processing and/or accumulation of amyloid, as well as tau-based interventions (for review please see Pedersen & Sigurdsson 2015)

1.5.2 Non-immunotherapy-based treatments

Secretase Inhibitors

Given the role of β - and γ -secretase in the metabolism of APP and production of A β they have both been attractive targets for therapeutic intervention. Both targets have undergone clinical trials in forms of secretase inhibitors, currently of which 4 clinical stage II/III trials are being carried out for BACE1 inhibitors (Qian et al. 2015). A more detailed discussion of β -secretase inhibition as a therapy for AD will be reserved until Chapter 6. The next section will consider γ -secretase based therapies.

Early studies indicated that selective mutation or deletion of PS1 (γ -secretase) complex prevented transmembrane APP cleavage and significantly reduced levels of A β (Wolfe et al. 1999; De Strooper et al. 1998). Soon after, pharmacological γ -secretase inhibition was reported to reduce A β *in vitro* as well as *in vivo*, including total A β in the brain (Dovey et al. 2001). However, the initial preclinical success of γ -secretase inhibitors was not reflected in clinical trials. Semagacestat (Eli Lilly) was discontinued following a phase III trial due to a lack of cognitive improvement in patients with probable AD, as well as high levels of adverse effects, including skin cancer (Doody et al. 2013). A similar failure of avagacestat (Bristol-Myers Squibb) was also reported following clinical stage II trials, with adverse reaction at higher doses that included skin cancers (Coric et al. 2012). These adverse reactions are most likely due to the fact that both γ - and β -secretases are involved in multiple physiological pathways (Haass 2004). Indeed, γ -secretase has been reported to have a role in Notch signalling, which when disrupted has been linked to oncogenic changes (De Strooper et al. 1999; Shih & Wang 2007).

The presence of adverse reactions with γ -secretase inhibitors have lead to the development of more selective γ -secretase inhibitors, specifically targeting γ -secretase cleavage of APP, while have no or limited impact on Notch or other substrates. γ -secretase modulation modifies PS1 conformation allowing for altered APP processing and can lead to reduced levels of A β 42 (Lleó et al. 2004; Crump et al. 2013). Second generation γ -secretase modulators with increased potency have recently been synthesized and have reduced A β 42

production and improved cognitive measures in Tg2576 mice, without any alteration in Notch signalling (Kounnas et al. 2010; Rogers et al. 2012). Whether this strategy will prevent the adverse reactions observed with older γ -secretase inhibitors as well as show cognitive benefit will be a key question for current and future clinical trials.

Anti-Aggregation Therapy

A β monomers secreted at physiological pico-nano molar ranges show no signs of neural toxicity. An alternative strategy developed for AD treatment prevents the toxic aggregation of monomeric A β into soluble oligomeric and aggregated forms of amyloid (Haass & Selkoe 2007; Selkoe 2013). Early reports showed that a naturally occurring glycolipid, scyllo-inositol was able to inhibit A β aggregation *in vitro* (McLaurin et al. 1998). Later *in vivo* studies with TgCRND8 mice showed that scyllo-inositol derivatives reduced A β plaques and improved spatial memory on the MWM (McLaurin et al. 2006). Scyllo-inositol also prevented A β -mediated inhibition of LTP in the hippocampus, and prevented cognitive deficits in rats receiving ICV administered of A β (Townsend et al. 2006). Following these positive animal studies, a clinical phase II trial assessed the beneficial effects of ELND005 (Elan/Transition Therapeutics), a stereoisomer of scyllo-inositol, in mild-moderate AD patients. Reports showed a significant reduction in CSF A β , however the end point targets of improved cognition and activity of daily living were not met (Salloway et al. 2011). This compound continued into a clinical phase 2/3 with investigation into secondary aggressive and aggitative symptoms in moderate AD patients. In October 2015 it was announced that results from this trial had shown significantly reduced aggressive/aggitative behaviours in severe AD patients (Transition Therapeutics Press Release, October 2015). This compound is now seeking clinical phase III assessment.

1.5.3 Immunotherapy in Alzheimer's Disease

In 1996 Beka Solomon's group suggested that anti-A β antibodies could prevent A β fibril formation *in vitro* (Solomon et al. 1996; Solomon et al. 1997). This work was later demonstrated *in vivo* following active immunisation against full length A β -42 in young, pre-plaque, and old PDAPP mice with A β plaque pathology (Schenk et al. 1999). This study demonstrated that immunisation prevented the build up of A β plaques in younger mice and significantly reduced A β -mediated pathology in older mice (Schenk et al. 1999). Soon after, it

was reported that systemic delivery of anti-A β monoclonal antibodies showed similar effects in PDAPP mice; crossing the BBB, binding A β plaques and leading to plaque clearance via Fc receptor mediated microglial phagocytosis (Bard et al. 2000). Following the publication of these two original studies, immunotherapy has been a popular therapeutic strategy.

β -Amyloid Passive Immunotherapy

Swiftly following the early success of active A β vaccination, Bard and colleagues were able to demonstrate significant reduction of amyloid pathology in the PDAPP model, a large amount of research has focussed on the removal of A β from the brain with the use of passive A β immunotherapy (Bard et al. 2000; Lemere 2013; Wisniewski & Goñi 2015). Passive immunotherapies targeting different A β epitopes have reported variable clearance of aggregated and soluble A β , but often show improved cognition (Solomon & Frenkel 2010; Lemere 2013). Peripheral administration of m266, a monoclonal antibody binding the central region of A β , in the PDAPP model showed improved cognition in object recognition memory and SWM (Dodart et al. 2002). Furthermore, following m266 treatment, PDAPP mice were reported to show increased serum A β , suggesting increased clearance from the brain. However, no effects on amyloid burden were observed in the brain (DeMattos et al. 2001; Dodart et al. 2002). Similar to this study, Kotilinek and colleagues treated Tg2576 mice with BAM-10, an antibody directed against the N-terminal region of A β , and reported improved spatial learning and memory, without showing a significant reduction in soluble or insoluble forms of A β (Kotilinek et al. 2002a). A further study utilising the PDAPP model, peripherally administered 10D5, an N-terminal directed anti-A β antibody (Hartman et al. 2005). Hartman et al reported that chronic treatment with 10D5 showed improved spatial learning in the MWM, but not on spatial reference memory performance. Mice also showed improved hippocampal LTP as well as increased plasma A β levels and overall reduced plaque and A β SAD in the HPC (Hartman et al. 2005).

Collectively the above summary shows that passive immunotherapy improved cognitive deficits in multiple transgenic models of amyloid pathology. However, the mechanism for the improvement in cognition and how A β is cleared from the brain remains unclear. Several hypotheses have been proposed for the mechanism by which A β is removed from the brain, including the peripheral sink, microglial-mediated phagocytosis, antibody-mediated alteration of A β aggregation and neutralization of A β toxicity (Fu et al. 2010). These mechanisms will be discussed in more detail in chapter 6. A further observation to note

is that different species of ADDLs and localisation of A β may be contribute to the impaired cognition in Tg models (Billings et al. 2007). Billings and colleagues observed that 3xTg mice, that received extensive behavioural training performed better on the MWM and showed reduced insoluble A β 42, but increased soluble A β 42 when compared to 3xTg mice naïve to any behavioural training (Billings et al. 2007). This study also reported that A β *56 was significantly reduced in 3xTg mice with extensive training, despite the overall increase in soluble A β 42. This pattern of results suggests that precise species of soluble A β may contribute to the onset of cognitive deficits in the 3xTg model. A study prior to this also reported that the accumulation of intraneuronal A β was responsible for the onset of cognitive deficits in the 3xTg model (Billings et al. 2005). Following ICV administration of anti-A β immunotherapy, spatial reference memory deficits were reversed and levels of intraneuronal A β were significantly reduced. A more recent study by Liu et al., (2015) showed that different models of AD show different levels of A β *56, which may be related to the extent of cognitive deficits in each models (Liu et al. 2015). The lack of changes in total soluble A β discussed above argues for caution when interpreting/analysing changes to A β in whole brain extracts following an immunotherapy. It may be conceptually more informative to investigate changes in different soluble A β species.

Although immunotherapies targeting A β directly have shown promising results in preclinical studies, early clinical trials provided little support for their use in humans (Winblad et al. 2014; Wisniewski & Goñi 2015). Bapineuzemab (Pfizer), the humanised 3D6 antibody, was one of the first passive immunotherapies to pass through clinical phase I, II and III. Despite showing a reduction in A β burden in the brain following PET imaging, little clinical benefit was observed in terms of neuropsychological assessment in patients with mild-moderate AD (Rinne et al. 2010; Lemere 2013). The Bapineuzemab clinical phase III trial was terminated in 2012, for reasons believed to be related to little clinical benefit (www.clinicaltrials.gov). The humanized m266, Solanezumab (Eli Lilly), is currently in an extended clinical phase III trial (www.clinicaltrials.gov). Initial results of Solanezumab clinical phase III trial failed to report improved cognition in mild-moderate AD patients. However, in 2012, promising results were shown when Lilly combined data of mild AD patients only across two separate phase III clinical trials and reported slowed cognitive decline (Lilly press release 2012). Clinical phase III trials are now continuing in mild AD patients only. Clinical data reported at the Alzheimer's Association International Conference (AAIC) 2015 revealed reduced disease progression and cognitive rating scores 34% better

than placebo treated patients (Qian et al. 2015; Reardon 2015). However, these are preliminary data of the 108-week time point and not the study end point, which will be available following study completion in October 2016. Improved cognitive measures and CSF biomarkers were also reported at the AAIC 2015 conference for clinical phase III trials of Crenezumab (Roche/Genetech/AC Immune) and Gantenerumab (Roche/Genetech) and clinical phase Ib trial data of Aducanumab (Phase Ib trial) (Qian et al. 2015; Reardon 2015). These current clinical A β immunotherapy trials focus on the prevention as well as treatment of AD patients in earlier disease stages. Further prevention trials are also currently commencing in individuals with FAD. These include a consortium of Lilly, Roche and the Alzheimer's Association, (The Dominantly Inherited Alzheimer's Network; DIAN) as well as the Alzheimer's Prevention Initiative partnered by Genetech, the Banner Institute and the National Institute of Health (www.nia.nih.gov/alzheimers/clinical-trials).

2B3, an Anti-Amyloid Precursor Protein Antibody

Despite the predominant target of immunotherapies being the A β peptide itself, other groups have focussed on targeting APP and its metabolism by antibody-induced steric hindrance of the BACE1 cleavage site of APP (Arbel et al. 2005; Thomas et al. 2006; Thomas et al. 2011). Thomas et al. developed a novel monoclonal antibody, 2B3, which binds to the BACE1 cleavage site of APP, and showed that it reduced the production of A β by steric hindrance (Thomas et al. 2011). Targeting APP processing has advantages over other immunotherapies that target A β directly. For example, by targeting the BACE1 cleavage site of APP, 2B3 avoids direct inhibition of BACE1. This feature of 2B3 avoids interference with BACE1 activity in its alternate processes and pathways, thus reducing the risk of adverse reactions (Vassar et al. 1999; Cole & Vassar 2007; Hunt & Turner 2009; Vassar et al. 2009). APP metabolic products other than A β (e.g., β -CTF) are also believed to express neurotoxic properties that may induce behavioural abnormalities (Griffin 2010; Pimplikar et al. 2010; Xu et al. 2015;). Moreover, proteolytic cleavage of A β has been reported to produce several isoforms with truncated N- and C-terminus, which exhibit different pathological properties (Pike et al. 1991; Pike et al. 1995; Tekirian et al. 1999; Cleary et al. 2005). Therefore, the 2B3 or steric hindrance approach avoids issues related to targeting specific forms of A β .

Thomas et al. (2011) showed that 2B3 reduced levels of A β in a concentration- and time-dependent manner in human astrocytoma (MOG-G-UVW) cells, which express

endogenous APP (Thomas et al. 2011). More recently, the reduction in levels of A β with 2B3 administration has been shown in primary cortical neurons derived from a transgenic model of AD expressing the *hAPP* London mutation (Thomas et al. 2013). These data indicate that 2B3 may also bind to APP *in vivo*, reduce levels of A β and potentially improve cognitive function in mouse models of amyloid pathology.

To date, only one other APP immunotherapy, using BBS1, has been reported *in vivo* (Rakover et al. 2007; Rabinovich-Nikitin et al. 2012). These studies were carried out in 2 different mouse models, Tg2576 and the 3xTg model, respectively. Both studies reported differing effects on levels of A β . Rakover et al do not report a reduction in A β , but Rabinovich-Nikitin et al did. This may be due to differences in BBS1 delivery. Rakover and colleagues administered treatment via peripheral administration, whereas Rabinovich-Nikitin and colleagues delivered BBS1 via ICV infusion direct into the brains. However, both studies reported improved object recognition memory following BBS1 treatment. However, it must be noted that the study using 3xTg mice used a very small number of mice in the treatment group (n=3). Given the variability in amyloid production shown by transgenic lines, these results should be confirmed in a larger sample of mice (Dodart et al. 1999; Chen et al. 2000; Dodart et al. 2002; Hale & Good 2005; Rabinovich-Nikitin et al. 2012). A further point of concern is that Rabinovich-Nikitin et al. (2012) did not report data from a WT control group to establish baseline levels for behaviour or normal physiological levels of protein. For this reason, data from this study must be considered with caution. Further assessment of anti-BACE1 cleavage site antibodies is still required to validate this strategy as a useful therapeutic tool. Assessment of 2B3 *in vivo* will provide further information of the effects of targeting APP metabolism as a treatment for AD and further show any alterations of brain biochemistry and cognitive performance regarding this approach.

β -Amyloid Active Immunotherapy

Following the successful preclinical results reported by Schenk and colleagues in 1999, subsequent studies have confirmed reduced amyloid pathology and improved cognition in APP transgenic mice following β -amyloid active immunotherapy (for review see Lemere & Masliah 2010). Studies also revealed differential binding epitopes of B and T cells. The B cell epitopes were located in the first 15 amino acid residues of the A β sequence and T cell epitopes were located in the mid- and C-terminal region of A β (Lemere et al. 2000; Cribbs et

al. 2003; Lee et al. 2005). The first clinical trial assessing active immunisation, AN1792, in moderate to severe AD patients was comprised of full length A β -42, a strong adjuvant (QS-21) and polysorbate 80, which increased the stability and solubility of the vaccine. This trial was ceased because 6% of the treatment group developed meningoencephalitis (Gilman et al. 2005). Whilst 19% of patients generated plaque-binding anti-A β antibodies, those that came to autopsy still showed severe cognitive impairment determined by MMSE (MMSE scores=0), despite reduced A β deposition in the cerebral cortex (Holmes et al. 2008). These results indicated that perhaps plaque removal in late stage AD was not an appropriate strategy given the level of established NFT pathology and neuronal loss. Although the precise reason for the meningoencephalitis is unknown, there was evidence that an overactive Th1 response was present surrounding a number of plaques. This suggested that immunization with the full A β 42 peptide may have induced an autotoxic T cell reaction (Boche & Nicoll 2008).

This initial problem in active immunisation triggered interest in passive immunotherapy, but also generated a surge in second generation active vaccines focussing on the B cell epitope, consisting of the first 15 amino acid residues of the A β peptide (Winblad et al. 2014). Currently, seven active immunotherapies are in development and under clinical trials (www.clinicaltrials.gov; Winblad et al. 2014; Wisniewski & Goñi 2015). Two of the most advanced in these trials are CAD106 (Novartis) and ACC-001 (Janssen/Pfizer). Both of these vaccines are currently being tested in clinical phase II trials (www.clinicaltrials.gov). Currently, no adverse reactions similar to those originally reported with AN1792 have been observed and high antibody titres have so far been reported over a chronic vaccination period (Hagen et al. 2011; Winblad et al. 2012; Winblad et al. 2014). Cognitive measures in these studies are yet to be reported.

While both active and passive immunotherapies demonstrated positive changes in preclinical AD studies, both methods have their limitations. Active immunotherapy engages the cellular and humoral immune system to generate and maintain the production of anti-A β antibodies. This immunisation process uses an antigen (either full length A β , or a small fragment) that can be delivered with an adjuvant to stimulate high antibody titres. Whilst this approach can induce a more chronic antibody production and offer a cost-effective method of treatment, the active vaccine can also induce T cell activation and stimulate a pro-inflammatory response. This adverse reaction can then take a long period of time to stop, leading to potentially extensive autoimmune damage. (Gilman et al. 2005; Winblad et al. 2014; Wisniewski & Goñi 2015). Passive immunotherapy on the other hand focuses on the

peripheral delivery of monoclonal antibodies designed to target specific epitopes. This approach has the advantage of prompt reversal, should any adverse reactions occur. In addition, it has the advantage of being highly specific in terms of targeting individual species or conformations of A β without disrupting other forms of the protein. However, this method of treatment requires more routine administration and is a much more costly method of treatment. Moreover, chronic treatment with humanized monoclonal antibodies may lead to a gradual development of anti-antibodies, neutralizing the anti-AD treatment effects (Brüggemann et al. 1989; Lemere 2013).

1.6 Thesis Summary, Aims and Hypotheses

This chapter has provided an overview of the clinical and pathological hallmarks of AD as well as providing a review of some of the systems adopted to model this neurodegenerative condition. The current therapies in clinical trials have also been discussed. To-date, no significant success has been translated from *in vivo* studies to clinical trials (Karran & Hardy 2014). For this reason, further efforts into developing effective treatments that may be translated to the clinical levels are still under investigation. Results so far using anti-APP β -secretase cleavage site antibodies 2B3 and BBS1 have shown promising results by reduction of A β levels *in vitro* and BBS1 has been reported to have shown this effect *in vivo* with further improved memory performance in Tg models (Arbel et al. 2005; Rakover et al. 2007; Arbel-Ornath et al. 2009; Thomas et al. 2011; Rabinovich-Nikitin et al. 2012; Thomas et al. 2013). However, this assessment of 2B3 *in vivo* has not yet been carried out.

Therefore, to assess the *in vivo* effects of 2B3 administration, PDAPP mice were characterised in terms of behavioural and biochemical phenotype across a range of ages in order to determine an optimal age to assess whether 2B3 would be able to improve memory performance *in vivo* and replicate reductions in A β as reported *in vitro* (Thomas et al. 2011; Thomas et al. 2013). PDAPP mice were tested on a foraging-based task, which assessed SWM, in Chapter 3, prior to object recognition memory and object-place associative memory assessment in Chapter 4. A β pathology in the HPC of PDAPP mice was also determined in Chapter 4. A hypothesis was determined that PDAPP mice would show an age-dependent decline in memory performance that would be associated with an increase in A β pathology. Once an age-dependent impairment was observed, PDAPP mice were administered 2B3 as reported in Chapter 5. Chapter 5 thus tests the main hypothesis of this thesis that inhibition of APP metabolism at the β -secretase cleavage site by 2B3 will inhibit A β production and improve memory performance in PDAPP mice.

Chapter 2: General Methods

2.1: Introduction

This chapter details the methods used to breed, maintain and characterise the behavioural phenotype and pathological hallmarks of the PDAPP colony, used throughout this thesis. It further describes the procedures and experimental design used to characterise behavioural phenotypes in PDAPP mice. The biochemical techniques used to analyse and quantify protein levels in brain tissue from PDAPP & WT mice are also described. Protocols that are specific to individual Experiments are described in the relevant Chapter.

2.2 Maintenance and breeding of the PDAPP colony

2.2.1 Housing conditions

All mice used were housed in standard conditions in cages measuring L 48cm x W 15 cm x H 13cm with an opaque plastic base and a wire top. The cage floors were covered in sawdust, approximately 1cm deep, and contained a cardboard tube, wooden gnawing block and approved nesting material. Holding rooms were maintained at a stable temperature and relative humidity levels at around $21^{\circ}\text{C} \pm 2^{\circ}\text{C}$ and $60 \pm 10\%$ respectively. Mice were given *ad libitum* access to food and water, unless otherwise stated as part of a behavioural test, and were kept on a 12hr light/dark cycle. All behavioural testing was carried out during the light hours. All animals were health-checked weekly and maintained according to UK Home Office and EU regulations and the Animal Scientific Procedures Act (1986).

2.2.2 PDAPP Breeding

PDAPP mice have been previously bred on a mixed triple background comprised of Swiss-Webster, DB2 and C57Bl/6 to maintain the *hAPP*^{V717F} genetic mutation (Games et al. 1995, Eriksen & Janus, 2007). However, the PDAPP colony used throughout this work was maintained on a C57Bl/6 (Harlan) background. Heterozygous male PDAPP mice were crossed with female C57Bl/6 (Harlan) mice. At approximately 5 weeks of age pups were weaned and males from the litter were group housed or individually housed depending on numbers of males in the litter. It was not possible to house two individual males from different litters due to aggressive behaviours. An ear-biopsy was then taken from each mouse for genotyping.

2.2.3 Genotyping using polymerase chain reaction

In order to identify the PDAPP mice, a polymerase chain reaction (PCR) was used to amplify the *hAPP V717F* transgene DNA (Figure 2.1). A tissue sample (ear clip) was collected from each mouse at 6-8 weeks of age and stored at -20°C. Tissue was digested and DNA extracted using DNeasy Blood and Tissue kits (Quiagen, UK). To carry out the PCR, 5µL of DNA was added to 20µL of Master Mix on ice in DNase, RNase-free aliquots. A 20µL measure of Master Mix contained 15.425µL nuclease free water (Fisher), 2.5µL 10x PCR Buffer (InVitrogen, Paisley, UK), 0.5µL 50mM MgCl₂ (InVitrogen, UK), 1.25µL deoxynucleotide tri-phosphates (dNTPs, GE Healthcare, Little Chalfont, UK), 0.05µL of each primer at a concentration of 100pmol, and 0.125µL of Taq polymerase (InVitrogen, UK). Two sets of primers were used in the APP (V717F) Master Mix to target and amplify *APP* and *Actin*. The primers 2010 (Eurofins MWG Operon; 5' - ATCTGGCCCTGGGGAAAAAAG- 3') and 2011 (5' -GATGTCCTTCCTCCTCTGTTC- 3') targeted and amplified the *hAPP V717F* mutation, whilst primers MusA-ActinF1 (Eurofins MWG Operon; 5' -CACCACACCTTCTACAATGAGCTG- 3') and MusA-ActinR1 (5' - TCATCAGGTAGTCAGTGAGGTCGC- 3') targeted *Actin*. Samples were immediately transferred from ice to a thermocycler (MJ Research, Massachusetts, USA) for amplification and run at the following conditions: 72°C for 2 minutes, 36 cycles at 94°C for 1 minute for DNA denaturing, 60°C for 1 minute for primer annealing, and 72°C for 2 minutes to allow for strand elongation. Following these cycles, samples were incubated at 4°C overnight.

DNA products were separated by gel electrophoresis on a 1% agarose gel in TAE buffer (Pierce) in an ethidium bromide-free docking system (Bio-Rad, Hertfordshire, UK). Prior to separation, 20µL of DNA product was loaded with a loading dye, "Novel Juice" (GeneDirex, Newmarket, UK) at 1 part novel juice to 5 parts sample. Samples were run at 100V for 120minutes and were run alongside a 100bp DNA ladder (GeneDirex), a water control, containing nuclease-free H₂O in place of DNA and a negative and a positive control from mice of a known genotype. Products were visualised using (Olympus X3 camera to capture the image and Alpha DigiDoc to process the image) and sized against the DNA ladder. The *hAPP^{V717F}* transgene DNA product is approximately 900bp and appears in transgenic (Tg) samples only, whilst the Actin DNA product appears as a band at approximately 500bp in each both wild type (WT) and Tg samples containing genomic DNA.

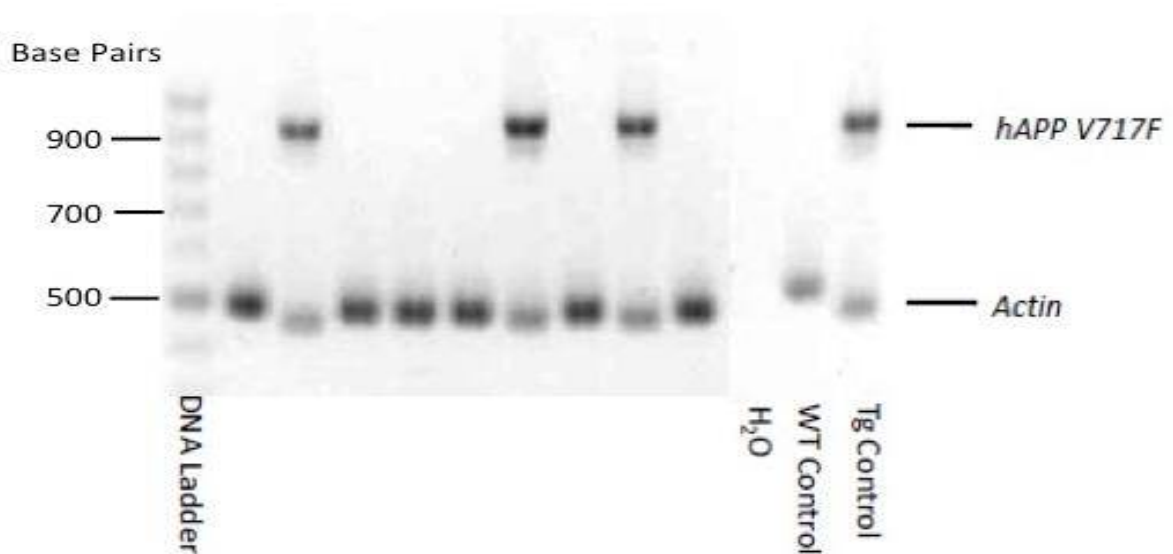


Figure 2.1: Example of visualised DNA bands following PCR and gel electrophoresis to identify wild type and PDAPP mice. Transgenic mice produce 2 bands of approximately 900 and 500 bp representing the *hAPP V717F* mutation and *Actin*, whilst wild-type mice produce only the band representing *Actin*.

2.3 Characterising the behavioural phenotype of male PDAPP mice

2.3.1 Design

Heterozygous male PDAPP mice were subjected to three separate tasks to assess memory across a range of ages. A full scientific justification for the use of these tasks will be reserved for the appropriate empirical chapters; here I describe the basic procedures. These tasks tested object-novelty memory, object-in-place (OiP) memory and spatial working memory (SWM) in a foraging-based task. All three behavioural tasks were run in a counterbalanced design at 6-8, 10-12 and 14-16 months of age (Figure 2.2). Mice were divided into 2 groups, A and B; counterbalanced for age, and genotype. Initially, both groups underwent 3 days of habituation. Group A was then subjected to object novelty memory assessment, followed by SWM assessment and finally OiP memory. Group B underwent this sequence of memory tasks counterbalanced to group A to prevent order effects (Figure 2.2). All mice were previously trained at 3-4 months of age as detailed in the tasks below to habituate them to handling, the behavioural room, test arena and task-specific details (objects and foraging apparatus).

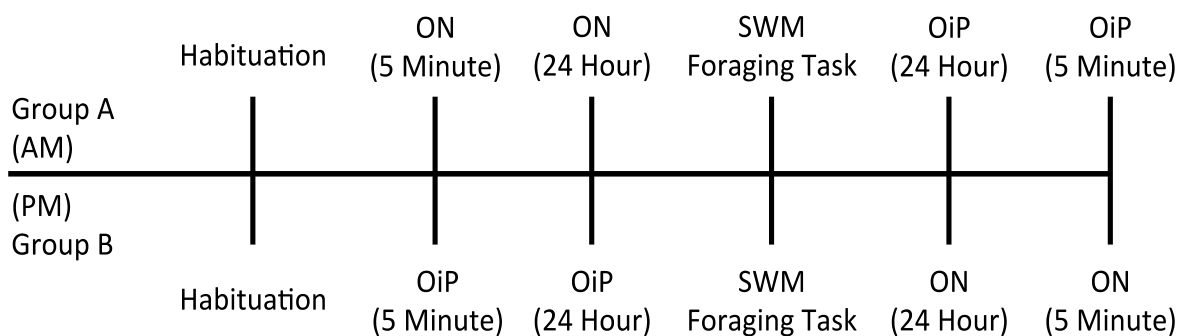


Figure 2.2: Schematic diagram illustrating the counterbalancing of the behavioural design to characterise memory in PDAPP mice across a range of ages. The same design was used at each age point (6-8, 10-12 and 14-16 months of age) in the experiment. ON – object novelty; OiP – object in place; SWM – spatial working memory.

Subjects:

Heterozygous male PDAPP mice expressing the *hAPP^{V717F}* genetic mutation and WT littermate control mice (all maintained on a C57Bl/6 genetic background (Harlan) as previously described (Hartman et al. 2005)) were used in the present study. There were a total of 16 Tg and 16 WT littermate controls at the start of this study. Therefore, 8 Tg and 8 WT mice were in group A and an equal proportion in group B. However, due to attrition, the final time point assessed cognitive function of 14 Tg mice and 15 WT mice. The same mice were used across all tests and ages examined. During this longitudinal study, the aim was to maintain mice in group housing conditions although, due to attrition, 3 mice were re-housed individually.

2.3.2 Object Recognition Memory

Apparatus:

A square arena measuring 60cm x 60cm with 40cm high walls was used for all tasks in this study. The walls were made of clear Perspex and covered externally with white card. The arena was placed on a stand that elevated it 50cm above floor level and was situated in the centre of a quiet testing room. The room contained a variety of extra-maze visual cues (e.g., wall posters, shelving, equipment etc.) around the walls of the test room at a height observable from inside the arena. The position of the extra-maze cues, the experimenter and

recording equipment remained constant throughout the study. The floor and walls of the arena were wiped clean with 70% ethanol wipes after each sample and test phase to remove odour cues. Each trial was recorded using a camera (VM-904K, Shiba Electrics Ltd, Hong Kong) suspended above the centre point of the arena connected to a DVD recorder (Panasonic), and interaction with the objects was recorded with an electronic stopwatch (Thermo Scientific, UK) by the experimenter.

Objects:

Objects were obtained from a variety of sources. They were matched in size and were made of materials such as ceramic, glass and plastic. Objects included garden gnome, vinegar bottle an empty salt/pepper grinder. They were weighted appropriately to withstand the investigative behaviour of mice. Objects were of a height and shape that made it difficult for mice to climb onto them. All objects were wiped clean with 70% ethanol wipes after each sample and test phase to reduce the use of differential odour cues.

Scoring:

Object exploration was defined according to the methods described by Ennaceur & Delacour, (1988). The time spent actively interacting with an object; this included sniffing, gnawing and pushing at a distance no greater than 2cm. Object exploration was not scored if the animal was using the object to explore extra-maze environment or was within the 2cm area of the object, but not facing it. Time spent exploring objects was recorded across all testing with an electronic timer. A discrimination ratio (DR) was used to index the animals' discriminative performance that was independent of individual differences in contact times; this was calculated as follows:

$$\frac{\text{Total Time Spent Exploring Novel Object (A)}}{\text{Total Time Spent Exploring Novel and Familiar Objects (A+B)}} = \frac{\text{Discrimination Ratio}}{\text{(DR)}}$$

As each trial was carried out twice, this score was averaged across both trials. DR scores above 0.5 indicate a preference to explore novel over familiar objects.

Procedures:

Object Recognition Task

Habituation: Mice were always transferred from a holding cage into the centre of the test arena. The start location remained constant throughout all testing in these procedures. Mice were allowed to explore freely for 10 minutes on Day 1 in an empty arena. Mice were then further habituated for 2 consecutive days to the arena containing 2 identical objects for 10 minutes each day. Objects were positioned approximately 30cm apart and were positioned in a different location on each day. A different pair of objects was used each day and across all ages tested.

Novel-object memory: To assess object novelty memory two identical objects were placed in the centre of the arena and mice were allowed to explore the objects for 10 minutes during the sample phase (see Figure 2.3A). Preliminary experiments revealed that 3 sample phases produced robust recognition across delays. Thus, following each sample phase, the mouse was removed from the arena and placed in a holding cage for a delay period of 5 minutes. Following the third sample phase, mice received either a 5 minute and 24 hour delay period in a counterbalanced order. Subsequently, one familiar and one novel object were then replaced in the arena (Figure 2.3A). The mouse was returned to the arena for 10 minutes during the test period. For both sample and test phases the animals' exploratory behaviour was assessed as described above. Time spent exploring objects in both sample and test phases was recorded by an experimenter out of view of the animal. Animals received 2 consecutive days of testing for each delay period, which occurred immediately following the 3 consecutive days of habituation. No sets of objects were re-used for an individual mouse.

Object-in-Place memory: Four different objects were placed in the centre of the arena in a square formation (see Figure 2.3B). Each object was approximately 15cm from the walls and 25cm apart from each other. Mice were placed in the centre of the arena and exposed to the four different objects for three separate 10 minute sample phases as described for object novelty memory. Time spent exploring these objects was recorded. Following the 10-minute sample phase, mice were removed from the arena and returned to their home cage for a 5-minute retention interval. Following the third sample phase, mice underwent either a 5-minute or 24-hour delay period before the test phase, whereby the position of one set of two objects positioned diagonally opposite each other were switched. Mice were then given a 10-minute

test phase and time spent exploring the familiar and novel location of objects was recorded. Animals received 2 consecutive days of testing for each delay period. Counterbalancing was conducted for the order of objects animals were exposed to and the novel spatial location of objects.

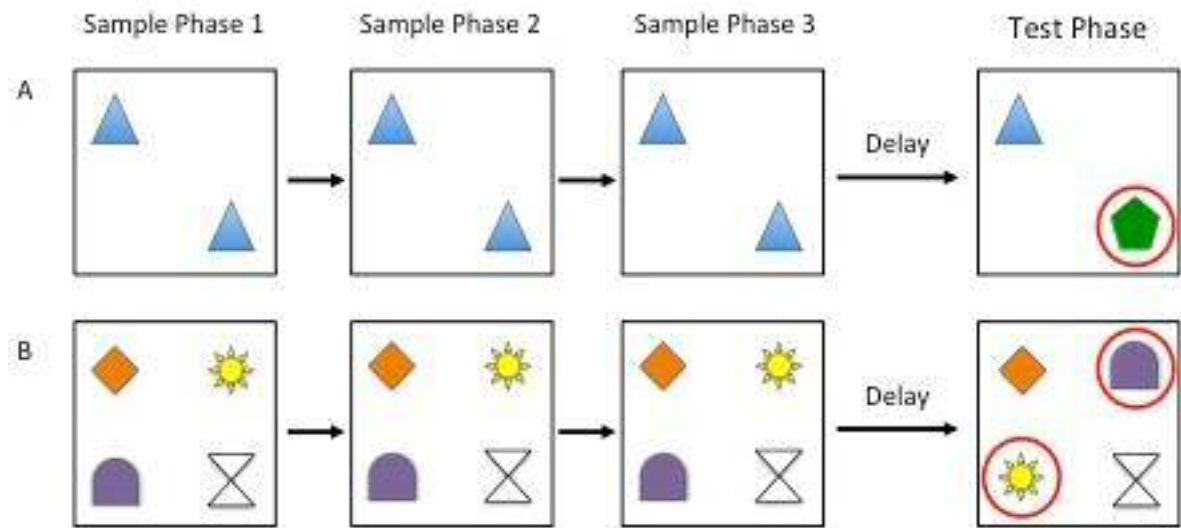


Figure 2.3: Illustration to demonstrate object recognition memory testing paradigms. A) Object novelty memory was assessed following 3 sample phases, each separated by a 5-minute retention delay indicated by the arrow. Following a delay of 5 minutes or 24 hours mice were subjected to a test phase. In the test phase mice were presented with one familiar object and one novel object for a period of 10 minutes. B) Object-in-Place memory was assessed in an identical manner as object novelty, however, animals were presented with 4 different objects during the sample phase. In the test phase the spatial orientation of 2 of these objects was changed.

2.3.3 Data Analysis

Data were analysed using Microsoft Excel for calculation of means, DR scores, standard deviations and standard error of the mean. IBM SPSS statistics was used for all statistical data analysis as described below.

Statistical Analysis

IBM SPSS Statistics software was used to statistically analyze all data. An α -level of 0.05 was used for all measures showing statistical significance. All data were checked for violations of normality by Shapiro-Wilk test and violations of equal variance by Levene's

test. Due to high levels of variability in contact times, violations of these tests were observed ($p < 0.05$). Therefore, data that violated these tests were subjected to transformation based on the level of positive/negative skew and reassessed. Data that showed no (further) violations of any tests of normality were analysed by mixed measures analysis of variance (ANOVA), One-Way ANOVAs and students' t-tests (one sample, independent samples and paired samples) where appropriate. All significant main effects and interactions were obtained following Bonferroni correction to adjust for multiple post hoc comparisons. Any data where transformation were either not possible or did not prevent violations were analysed by non-parametric equivalent tests; Mann-Whitney U (Independent Samples t-test), Kruskal-Wallis H Test (One-Way ANOVA), Wilcoxon-Signed Rank (Paired-Samples t-test), Friedman Test (Repeat Measures ANOVA). Any further statistical analysis carried out in experimental chapters will be described in the relevant chapter.

2.4 Biochemical Analysis of PDAPP and Wild-Type Brains

2.4.1 Preparation of Brain Samples for Biochemical Analysis

Brain Dissection

Mice were culled by cervical dislocation and brains were removed immediately. Brains were then dissected bilaterally and the hippocampus removed. Samples were snap frozen on liquid nitrogen. Dissected samples were stored at -80°C until further processing.

Protein Extraction

Brain samples of each mouse were homogenised in 2% sodium dodecyl sulphate (SDS) in dH_2O with 1% inhibitor cocktail (Millipore) at 75mg/ml of wet tissue weight. The samples were homogenised using a Precellys 24 Dual (Bertin technologies, Montigny le Bretonneux, France) at 6000rpm for 2*30 seconds with a 30 second delay. The homogenate was rotated at 4°C overnight. Homogenate was removed and centrifuged at 100 000Xg (28 300rpm) for 1 hour at 4°C . The supernatant was carefully removed and diluted either in 1:5 EC Sodium Buffer (All chemicals were purchased from Fischer Scientific, Loughborough, UK unless otherwise stated; 20mM $\text{Na}_2\text{HPO}_4/\text{NaH}_2\text{PO}_4$, 0.2mM EDTA, 0.4M NaCl, 0.2% (w/v) bovine serum albumin (BSA; Sigma Aldrich, UK), 0.05% (w/v)

CHAPS (Sigma Aldrich, UK), 0.05% (w/v) NaN_3 at pH 7) or 2:3 in 3 X sample buffer (SB) (6.3mM TrisBase, 0.8% (w/v) SDS (BioRad, UK) 20% (v/v) Glycerol, 10% (v/v) β -mercaptoethanol, 2% (v/v) bromophenol blue, dH_2O to 50ml). Samples were stored at -20°C .

The insoluble pellet was further dissolved in 70% formic acid (Sigma Aldrich, UK) at 150mg/ml original wet tissue weight. Samples were centrifuged again at 100 000xg (28 300rpm) for 1 hour at 4°C . The supernatant was carefully removed and added 1:20 to a neutralising buffer (1M Tris, 0.5M Na_2HPO_4 , pH 11) and stored at -20°C .

Bicinchonic Acid Protein Assay

A bicinchonic acid (BCA) protein assay kit (ThermoScientific, UK) was used to determine the protein concentration of soluble fractions. Diluted bovine serum albumin standards (Pierce) were prepared ranging from 2 - 0.003mg/ml in a serial dilution. All standards samples and blanks were analysed in duplicate on a 96 well plate. The standards and negative blank control (dH_2O) were loaded at a volume of 25 μL , and samples and sample blanks (2% SDS) at 1 μL to ensure protein concentrations could be determined by the standard curve. A volume of 200 μL BCA Working Reagent consisting of 50 parts Reagent A and 1 part Reagent B was further added to wells. The plate was mixed thoroughly for 30 seconds on a plate shaker and incubated at 37°C for 30 minutes. The plate was read at absorbance 540nm using a spectrophotometer. Protein concentration of each sample was then calculated using Microsoft Excel from the standard curve generated by the BSA standards.

2.4.2 Western blotting

Samples were diluted 1:3 with 3x Sample Buffer and heated at 70°C for 40 minutes to reduce samples prior to first use in Western blot analysis. Samples were then re-frozen for subsequent use when they were briefly thawed at 70°C for five minutes before loading. 10 μL of the molecular weight marker (Precision Plus Protein Standards marker, Bio-Rad Laboratories, Hercules, California, USA) were loaded and samples were loaded at 20 μg onto a 10% polyacrylamide gel (H_2O , 3.3% (v/v) acrylamide, 1.25% (v/v) (BioRad) Tris.HCl, 0.1% (v/v) SDS, 0.05% (BioRad) APS, 0.005% TEMED (Sigma Aldrich, UK)) and separated by sodium dodecyl sulphate-polyacrylamide gel electrophoresis (SDS-PAGE) in running buffer (25mM Tris base, 190mM glycine, 0.05% SDS, pH 8.3). The separated proteins were then blotted on to a 0.2 μm nitrocellulose membrane (Amersham Biosciences,

Little Chalfont, UK), before being washed in Tris-buffered saline with Tween 20 (TBST, 2 mM Tris, 15 mM NaCl, 0.1% Tween-20, pH 7.5) and blocked for 1 hour at RTP in 5% (w/v) blotto (non-fat milk powder; Tesco). Membranes were washed three times in TBST for five minutes and incubated in 1% blotto with primary antibody prepared as described in Table 2.1. Membranes were incubated overnight on a roller. The membranes were washed as above in TBST. Membranes were then incubated for 2 hours at RTP in secondary antibody, conjugated to horseradish peroxidase (HRP; according to primary antibody species, Table 2.2) prepared in 1% blotto. Membranes were washed again in the same fashion. Bands were visualised using enhanced chemiluminescent detection (Super Signal, West Dura, Perbio Science, UK) and exposed to high performance chemiluminescent X-ray film (Amersham Biosciences). Films were scanned and analysed using ImageJ software.

Primary Antibody	Species	Dilution	Source
APP (22C11)	Mouse	1:1000	Millipore
NMDAR1	Mouse	1:1000	BD Biosciences
NMDAR2B	Rabbit	1:500	Millipore
NMDAR2B Y1472	Rabbit	1:750	Millipore
PSD95	Rabbit	1:1000	AbCam
GAPDH	Pre-Conjugated	1:50,000	Sigma

Table 2.1: Primary antibodies used in this thesis for Western blot analysis. Species, dilution factor and antibody distributor are described.

Secondary Antibody	Species	Dilution Factor	Source
Anti-Mouse	Horse	1:15,000	Pierce
Anti-Rabbit	Goat	1:15,000	Pierce

Table 2.2: Secondary antibodies used in this thesis for Western blot analysis. Species, dilution used and distributor are also described.

2.4.3 Enzyme linked immunosorbent assay (ELISA)

Amyloid Precursor Protein (APP) ELISA

APP levels were determined using human APP DuoSet ELISA (R&D Systems, Abingdon, UK). A detailed protocol can be found at <https://www.rndsystems.com/>. In brief, a 96-well plate (Greiner Bio-One, Frickenhausen, Germany) was coated with the “Capture Antibody” at a concentration of 4µg/ml, prepared in phosphate-buffered saline (PBS) (137mM NaCl, 2.5mM KCl, 8mM Na₂HPO₄ and 1.5mM KH₂PO₄) and incubated overnight at RTP. Wells were then washed four times with 0.05% (v/v) PBS-Tween (PBST). Unbound sites were blocked by adding 200µL/well of “Reagent Diluent” (RD) (PBS with 1% w/v bovine serum albumin (BSA)) with 5% (w/v) sucrose for 60 minutes at RTP. Wells were washed and aspirated four times with PBST. Standards and samples were prepared in RD. Standards were prepared in two-fold serial dilutions ranging from 20-0.625ng/ml. Samples were diluted 1:50 in RD. Standards and samples were loaded at 100µL/well in duplicate and incubated at RTP for 2 hours. Wells were then washed four times in PBST. “Detection Antibody” was prepared at 300ng/ml and loaded at 100µL/well and incubated for 2 hours at RTP. Wells were washed and aspirated four times with PBST. Enzyme-labelled HRP Streptavidin was then loaded at 100µL/well and incubated for 20 minutes at RTP in the dark. Wells were washed and aspirated four times with PBST. Each well was then loaded with “Enzyme Substrate” (0.02M Citric Acid, 0.03M Phosphate, 20mg OPD (o-phenylenediamine dihydrochloride; Sigma Aldrich, UK), 0.012% (v/v) H₂O₂ and incubated at RTP for 30 minutes in the dark. “Stop Solution” (2.5M H₂SO₄) was loaded at 50µL/well to stop any further colour change. Wells were read at 492nm using a plate reader. Concentrations of APP were determined using GraphPad Prism 4.0 and Microsoft Excel and normalised to the total protein concentration of each sample.

Amyloid-β (Aβ) 40 (Non-Commercial)

The methods utilised to determine the levels of soluble and insoluble Aβ40 were as previously described by Thomas et al., (2006, 2011). A 96-well plate (Greiner Bio-One, Frickenhausen, Germany) was coated in the anti-N-terminal human Aβ monoclonal antibody (MAb) 6E10 (Covance, Princeton, USA) at a concentration of 0.167µg/ml, diluted in carbonate/bicarbonate buffer (15mM Na₂CO₃, 35mM NaHCO₃, pH 9.6) overnight at 4°C. The plate was aspirated and washed with PBST (137mM NaCl, 2.5mM KCL, 8mM Na₂HPO₄,

1.5mM KH₂PO₄, 0.05% Tween20) in between each stage. All incubations were at room temperature (RT). Unbound sites were blocked with 1% non-fat milk powder (Tesco) in PBS for 30 minutes. Standards and negative controls were prepared in an identical final buffer solution as samples (eg. Where samples were diluted 1:10, the PBST was 9 parts to 1 part sample preparation buffer; 1 part 2%SDS, 4 parts EC sodium buffer as described in 2.4.1). Samples were prepared in PBST. Samples and standards were loaded at 100µl per well in duplicate for 2 hours. Standards (Invitrogen) ranged from 10-0.019ng/ml in doubling dilutions. Samples of the soluble fraction were prepared at 1:10. Insoluble fraction samples were prepared 1:20. Negative controls included the final buffer used to prepare standards. The detection antibody, BAM401AP (affinity purified, Autogen Bioclear, Calne, UK), an affinity-purified antibody specific to the C-terminal of the Aβ₄₀ peptide was used as the detection antibody at a concentration of 0.45µg/ml in PBST for 1.5 hours. BAM401AP has been verified as specific through western blotting work within the laboratory group (Thomas, unpublished data). The secondary HRP-labeled anti-rabbit IgG (Pierce Thermo Scientific) was applied at 0.33µg/ml in PBST for 1 hour. The enzyme substrate, o- phenylenediamine (OPD), in 0.1M citrate-phosphate buffer (24mM citric acid, 51mM Na₂HPO₄, pH5) was applied and incubated for approximately 20 minutes in the dark. The reaction was stopped using 50µl 2.5M H₂SO₄ and read at 492nm using a spectrophotometer. The ELISA protocol provides a lower sensitivity limit of around 0.1ng/ml (Thomas et al., 2006). The concentration of Aβ₄₀ was then determined using GraphPad Prism 4.0 and Microsoft Excel and normalised to the total protein concentration of each sample.

Aβ₄₀ ELISA (IBL)

A commercial Aβ₄₀ ELISA kit (IBL International GmbH, Hamburg, Germany) was used to determine smaller changes in amyloid levels following 2B3 administration in PDAPP mice, Chapter 5. A detailed protocol may be found at <http://www.ibl-international.com/>. In brief, standards were prepared in “Assay Buffer” in 2 fold serial dilutions ranging from 100-1.56pg/ml. Samples were prepared at a 1:4 dilution in “Assay Buffer”. Samples and standards were loaded at 100µL/well onto a microtitre plate (pre-coated with Anti-Human Aβ₃₅₋₄₀ (1A10)) and incubated at 4°C overnight. Each well was then washed and aspirated thoroughly 7 times. “Enzyme Conjugate” (HRP conjugated Anti-Human Aβ NH₂ terminus (82E1)) was loaded at 100µL/well and incubated for 60 minutes at 4°C. Wells were washed again in an identical fashion. “TMB Substrate” was then loaded at 100µL/well and incubated at RTP for

30 minutes in the dark. “TMB Stop Solution” was then added at 100 μ L/well in order to stop any further colour change. Change in colour went from blue to yellow. Wells were read in a plate reader at 450nm and data analysed in an identical fashion as described above.

A β 42 ELISA (Invitrogen)

All assays to quantify levels of soluble and insoluble A β 42 were carried out using a human A β 42 ELISA kit (Invitrogen Corporation, California, USA). A detailed protocol for this kit can be found at www.invitrogen.com. In brief, standards and samples were prepared in *Standard Diluent Buffer*. Standards were prepared in serial two-fold dilutions with a range from 1000-15.63pg/ml. Soluble and insoluble samples were diluted at 1:10 in *Standard Diluent Buffer*. 50 μ L of standards and samples were loaded to the appropriate wells on the microtitre plate (*A β Antibody Coated Wells* (antibody targeted the NH₂ terminus region of A β)). 50 μ L of the *Human A β 42 Detection Antibody* was loaded and mixed on a plate shaker. The microtitre plate was incubated at 4°C overnight. Wells were washed and aspirated thoroughly four times. *Anti-Rabbit IgG HRP Working Solution* was then added at 100 μ L/well and incubated for 30 minutes at RTP. Wells were washed and aspirated thoroughly again before adding *Stabilized Chromogen* at 100 μ L/well. Plates were incubated at RTP for 30 minutes in the dark. 100 μ L *Stop Solution* was then added to cease any further colour change leading to a change from blue to yellow. Wells were read in a plate reader at 450nm. Data were analysed as described above.

β Carboxy Terminal Fragment ELISA (IBL)

A commercial β CTF ELISA kit (IBL International GmbH, Hamburg, Germany) was used to determine changes in β CTF levels following 2B3 administration in PDAPP mice, Chapter 5. A detailed protocol may be found at <http://www.ibl-international.com/>. In brief, standards were prepared in “EIA Buffer” in 2 fold serial dilutions ranging from 12-0.19pmol/L. Samples were prepared at a 1:10 dilution in “EIA Buffer”. Samples and standards were loaded at 100 μ L/well onto a microtitre plate (pre-coated with Anti-APP-C Rabbit IgG) and incubated at 4°C overnight. Each well was then washed and aspirated thoroughly 9 times. “Labelled Antibody Solution” (HRP conjugated Anti-Human A β NH₂ terminus (82E1)) Mouse IgG) was loaded at 100 μ L/well and incubated for 60 minutes at 4°C. Wells were washed again in an identical fashion. “Chromogen” was then loaded at 100 μ L/well and incubated at RTP for 30 minutes in the dark. “Stop Solution” was then added at 100 μ L/well in order to stop any further colour change. Change in colour went from blue to

yellow. Wells were read in a plate reader at 450nm and data analysed in an identical fashion as described above.

2.4.4 Data analysis

ImageJ software was used to quantify Western blot images. GraphPad Prism software was used to analyse all ELISA data presented in this Thesis. All data were further analysed in Microsoft Excel and SPSS statistics as described in Section 2.3.3.

Chapter 3: Characterising Foraging Behaviour in PDAPP Mice

Chapter Overview

Chapter 3 describes a foraging-based task that aimed to determine spatial working memory (SWM) performance in PDAPP mice across a range of ages. The task used was based on a design previously carried out to assess SWM in pigeons, which was shown to be sensitive to hippocampal function (Pearce et al. 2005). Pearce and colleagues presented pigeons with eight baited pots in different spatial locations in a training arena. To assess WM, pigeons had to forage the food reward from all eight pots and any return visits to pots during the trial was considered a WM error. In the task used in this chapter, six pots were placed in a radial formation, each containing a small liquid reward. Mice were trained to forage rewards and during testing were assessed on their ability to forage all six pots. Errors were determined as a mouse returning to a pot, which had already been foraged. However, to date, no published data have yet been presented using this task in mice in order to show sensitivity to hippocampal (HPC) function in the processing of spatial information.

The first two experiments in this chapter therefore aimed to assess if the successful completion of this foraging-based task required HPC function. Male C57Bl/6 mice received either bilateral HPC lesions or sham procedures and were assessed on this task in an environment enriched with extra-maze spatial stimuli (Experiment 1) and without (Experiment 2). The final experiment (Experiment 3) of this chapter determined the performance of PDAPP mice on this task across a range of ages to investigate how foraging behaviour was affected by age and amyloid pathology in this mouse model. Results from these experiments will be discussed with reference to the involvement of the HPC in processing spatial information in SWM tasks and other foraging behaviours.

3.1 Chapter Introduction

Working memory (WM) was first described by Werner Honig in 1978 as stimulus information that is used during one trial of an experiment, but not for subsequent trials thereafter (Honig 1978). One of the most common tasks used to assess WM is the radial arm maze (RAM), which was first described by David Olton and Robert Samuelson in 1976, (Olton & Samuelson 1976). In this task, eight arms radiate from a central platform. At the end of each arm is a small food (or liquid) reward, which is readily consumed by rodents. Olton

and Samuelson initially observed that rats would retrieve all eight rewards with minimal re-entries to previously baited arms. Subsequent experiments were carried out testing the theory that rats completed the task using WM, as opposed to exploiting kinaesthetic strategies (such as simply entering a series of adjacent arm or through the use of odour cues in previously visited arms) (Olton et al., 1979; Olton & Samuelson, 1976; Olton et al., 1977). These experiments provided evidence that rats would complete the task by remembering which arms had been visited in a single session. However, this information was not transferred between sessions when arms were re-baited. It was therefore concluded that rats used a type of WM to complete the RAM (Olton et al., 1979).

Animals use spatial navigation processes to manoeuvre quickly and safely through their environments when foraging and/or exploring, as described by Vorhees & Williams (2014). In order to reduce energy expenditure and predatorial risk whilst doing so, animals must form a memory or cognitive map. The capacity to navigate effectively relies on two main navigation systems. Allocentric navigation uses environmental, or distal, cues, whereas egocentric navigation relies more on the internal cues generated by the animal's movement and/or proximal cues. The use of allocentric navigation is believed to be supported by the hippocampal (HPC) formation (O'Keefe & Nadel 1978; O'Keefe & Conway 1978; Olton & Collison, 1979; O'Keefe & Kraemer et al., 1983; Morris et al., 1986; Speakman 1987; Morris et al., 1990). Since the early reports by O'Keefe and colleagues, more recent studies have revealed distinct contributions of HPC sub-regions, as well as specific receptors, in the processing of spatial WM (SWM) information (Steele & Morris 1999; Bannerman et al. 2004; van Strien et al. 2009; Sanderson et al. 2010; Murray et al. 2011; Sahay et al. 2011). For example, GluA1 receptor knock out mice have been observed to show impaired SWM, but not spatial reference memory in a modified version of the six-arm RAM, whilst HPC lesion mice showed impairment in both measures (Schmitt et al. 2003). Furthermore, HPC NMDA receptor NR2B subunit knockout mice showed impaired SWM performance as determined by reduced spontaneous alternation in the T-maze, but intact spatial reference memory performance on the MWM (von Engelhardt et al. 2008). Collectively, these observations showed that the HPC plays a key role in the processing of spatial information for these tasks, however different neuronal mechanisms within the HPC appear to support the processing of different types of information.

WM deficits are commonly observed in patients with AD and are clinically assessed with tests such as the Mini-Mental Status Examination (MMSE), the Montreal Cognitive

Assessment (MCoA; Folstein et al. 1975; Nasreddine et al. 2005; Snyderman & Rovner 2009). These tests lend themselves well to study the progressive cognitive decline associated with AD over a longitudinal period. Ideally, cognitive testing in rodents would assess identical cognitive functions in paradigms matching those mentioned above. Although not identical, SWM tasks provide a method to assess WM in rodent models of dementia.

Although no current AD model fully recapitulates the full pathology of AD, A β -induced HPC pathology is observed in models expressing FAD mutations in *APP* and/or *Presinilin* (Games et al. 1995; Hsiao et al. 1996; Sturchler-Pierrat et al. 1997; Holcomb et al. 1998). Studies have shown significant HPC involvement in WM and the processing of spatial information in these tasks and it is therefore not surprising that many of the rodent dementia models show age-related cognitive impairments in these types of tasks (Chapman et al. 1999; Chen et al. 2000; Minkeviciene et al. 2008; Wirths et al. 2008). Interestingly, the SWM deficits in AD models often manifest before the onset of other cognitive deficits, such as associative learning and recognition memory impairments, similar to the progressive decline of cognitive functions in clinical AD (Webster et al. 2013; Webster et al. 2014). For reasons such as these, SWM tasks provide a valuable tool to study the effects of AD-related pathologies and their effect on cognition.

Cognitive deficits related to AD-like pathology are sensitive to age, therefore, the nature of the tasks and the time it takes to run is an important consideration. Many SWM memory tasks require either multiple trials in one day, such as the T-maze and MWM (Steele & Morris 1999; Dudchenko 2001). This can be highly time consuming with larger cohorts of animals. Furthermore, tasks such as RAM require extensive training with long testing protocols lasting over 14 days (Olton et al., 1977; Hodges, 1996). In fact, it has been reported that mice have varying levels of performance on the RAM and require extensive training for successful performance (Foreman & Gillett 1998; Foreman & Ermakova 1998). In order to promote learning, a water-based version of the RAM (the radial arm water maze; RAWM) is often used to assess SWM (Alamed et al. 2006). In this version of the task, mice must swim to the end of each arm in order to find a submerged platform. Any re-visits to arms already explored is a measure of WM error.

Water-based tasks exert high levels of stress on animals as observed by increased levels of corticosterone and glucocorticoids (Francis et al. 1995; Harrison et al. 2009). The HPC has a dense population of glucocorticoid receptors, which have been associated with

altered cognitive performance following a stressful episode (Francis et al. 1995; Magarin & McEwen 1995; Lupien & McEwen 1997). The results of these tasks may therefore be confounded with stress effects on cognition and potential interaction with on-going pathological processes. Moreover, extended periods of stress in AD models has been associated with increased levels of A β production and accelerated learning and memory deficits (Green et al. 2006; Jeong et al. 2006; Srivareerat et al. 2009). For this reason the differences between control animals and AD models must be treated cautiously. Finally, specific tasks require equal performance in other behaviours influencing task performance to more thoroughly assess the memory systems involved in successful task completion. For example, motor performance as well as anxiety and motivation are non-cognitive based behaviours that are associated with these tasks (Kobayashi & Chen 2005; Webster et al. 2014). These behaviours are affected differentially across AD models. Therefore careful consideration must be made when choosing the precise behavioural task(s) for a given mouse model of AD.

With the above points taken into consideration, we have developed a foraging-based task that was designed to provide efficient and effective assessment of SWM. The original basis of this task was taken from an avian foraging task reported by Pearce and colleagues (Pearce et al. 2005). In this study, pigeons were presented with eight baited pots in different spatial locations in a training arena. To assess WM, pigeons had to forage the food reward from all eight pots and any return visits to pots during the trial was considered a WM error. I adapted this task for mice using an open arena containing six pots positioned in a similar formation as the reward locations in a RAM (Figure 3.1). Extra maze stimuli surrounding the test arena were available to assist spatial navigation. In each session, the mouse was placed in the centre of the arena and was allowed to freely explore and forage the six rewards available in the pots. Each pot was baited with a single liquid reward and was not replenished during the trial. Mice were required to consume all six rewards in order to complete the task. The most efficient behaviour was to visit each pot only once during the session. This required the animals to remember within a given trial which pots had been foraged in relation to their spatial location. Within a trial, the difficulty of task increased with each successful forage. The animals received 4 trials in total, 1/day. A WM error was scored within a trial when a mouse returned to a pot previously visited in that session. As well as WM errors, additional measures included total time to complete the task, and time taken to engage with the task (indices of motivation and motor performance).

In order to validate the task as one that requires a functionally intact HPC, the first experiment examined the effects of excitotoxic lesions of the HPC in male C57Bl/6 mice on the foraging task (Experiment 1). It was hypothesised that HPC lesioned mice would show a significant increase in the number of WM errors compared to control animals. Experiment 2 was designed to determine whether any disruption caused by HPC cell loss was restricted to conditions under which animals used extramaze (i.e., spatial) information. All distal extramaze cues were removed by drawing a black curtain around the arena and the foraging pots were each made visually distinctive by the addition of a unique pattern on the outside of each pot. The task was then carried out in an identical fashion. To the extent that the HPC contributes to processing spatial information but not to a visual discrimination, it was predicted that mice with HPC lesions would perform at a similar level to control mice. Experiment 3 examined foraging behaviour in PDAPP mice across different age ranges. Based on results from previous studies assessing SWM in PDAPP mice, it was hypothesised that PDAPP mice would show an age-related deficit in efficient performance of the foraging task.

3.2 Experiment 1: The effects of hippocampal cell loss of foraging behaviour

3.2.1 Introduction:

Assessment of the effect of HPC lesions on SWM was carried out on 6-month-old C57Bl/6 male mice. C57Bl/6 mice used were wild-type (WT) littermate controls taken from PDAPP breeding line to ensure that the mice used to assess HPC involvement in the foraging task were as similar as possible to the PDAPP background strain.

3.2.3 Methods:

Subjects:

A total of 26 male C57Bl/6 mice aged 6 months were used to assess HPC involvement in this foraging-based WM task. 13 mice received bilateral HPC excitotoxic lesion surgery and 13 received control (SHAM) surgery (as described) 3 weeks prior to behavioural assessment.

All mice in experiment 1 and 2 were maintained on a 12-hour light/dark cycle. Two days before training and throughout test days, all mice were water deprived to 85% of their

original body weight and allowed access to water for only 2 hours per day after testing, but maintained on *ad libitum* food throughout.

Surgery:

Mice were anaesthetised with Isoflurane [2-chloro-2-(difluoromethoxy)-1, 1, 1-trifluoro-(ethane)] in O₂ during stereotaxic surgery. The skull was exposed by a scalp incision. Two holes were drilled on opposite sides of the midline at the appropriate coordinates (see Table 3.1). Infusions of 0.09mM N-Methyl D-Aspartic Acid (NMDA, Sigma-Aldrich, UK) in sterile phosphate were delivered at a rate of 0.3µl per minute into each hemisphere using a 30G cannulae microinjection 2µl Hamilton #75 syringe (Hamilton Company, Reno, USA). Following each infusion, the needle was left in place for 2 minutes before being retracted slowly. Upon completion, the wound was sutured and the animal was given a subcutaneous injection of glucosaline to aid rehydration. In SHAM-operated mice, 2 holes were drilled in accordance to the stereotaxic coordinates in table 3.1 before being sutured. Each mouse was then placed in a 30°C temperature controlled recovery chamber with monitoring until the mouse was deemed alert and mobile. Following this mice were returned into a new home cage containing a sawdust bedding, covered in tissue paper to prevent any sawdust entering the wound. Mice were also provided with sweetened porridge (ReadyBrek) and *ad libitum* supply to food and water.

Perfusion:

Mice were given an intraperitoneal (IP) injection of 0.2ml 200mg/ml pentobarbitol (Euthetal, Merial, Harlow, UK) to induce terminal anaesthesia. A cannula was inserted into the left ventricle of the heart whereby approximately 50ml of 0.1M PBS (pH 7.4) was pumped through the circulatory system. Following this, approximately 100ml of 4% paraformaldehyde in 0.1M PBS (PFA) was further pumped through the circulatory system to initially fix brain tissue. The brain was then extracted and post-fixed in 4% PFA at room temperature (RTP) for 6 hours before being transferred to 30% reagent grade sucrose in dH₂O. The brain remained in sucrose until sinking, indicating it was fully saturated (approximately 48 hours). Brains were then sliced using a freezing microtome. 40µm coronal sections were mounted on gelatinised slides in 0.1M PBS. Slides were left to dry for 48 hours.

Site	Stereotaxic Coordinates			
	Anterior/Posterior	Lateral	Ventral	Volume
	(-)	()	(-)	(uL)
1	1.2	1.0	2.0	0.15
2	1.7	1.0	2.0	0.15
3	1.7	1.5	2.0	0.15
4	2.2	1.0	2.0	0.15
5	2.2	2.0	2.0	0.15
6	2.5	1.5	2.0	0.15
7	2.5	2.2	2.2	0.15
8	3.0	3.0	4.2, 3.0, 2.5	0.15
9	3.6	3.0	4.0, 3.0,	0.15

Table 3.1: The stereotaxic coordinates for bilateral HPC lesions outlined as mm from bregma (anterior posterior), from the midline (lateral) and from the dura (ventral).

Cresyl violet staining:

Staining of coronal sections was carried out by immersing slides in xylene for 4 minutes before immersion into descending concentrations of ethanol (100% → 90% → 70%) for 2 minutes per ethanol concentration. Slides were then immersed in dH₂O for 2 minutes before 0.005% Cresyl violet was applied for 3 minutes. Slides were then further immersed in dH₂O for 30 seconds before dehydrated in an ascending concentration of ethanol (70% → 90% → 100% → 100%) for 3 minutes per immersion. Slides were given two final exposures to xylene, each for 5 minutes. Finally, slides were cover-slipped with DPX Mounting media and allowed to dry for 48 hours. Sections were then imaged using a Leica DMRB microscope and images were captured using an Olympus DP70 camera and the programme analySIS-D.

Apparatus:

All training and testing was carried out in the same testing room as described in 2.3.3. Initial training of the task was carried out in identical homecages (L 48cm x W 15 cm x H 13cm) with a 1cm deep bed of sawdust covering the floor. White ceramic pots (Lakeland, UK) with a diameter of 6.5cm and a depth of 3.5cm were mounted on a wooden cube base measuring 3x3x6cm. Pots were secured to the floor of the cage/arena with blue-tac. Following initial training, mice were exposed to the same pots in the same arena used in 2.3.3. The floor

of the arena was also covered in sawdust, approximately 1cm in depth. In the arena pots were arranged approximately 20cm apart. Each trial was recorded using a camera (VM-904K, Shiba Electrics Ltd, Hong Kong) suspended above the centre point of the arena connected to a DVD recorder (Panasonic DMR E50EBS), and time taken to complete the task was measured with an electronic stopwatch (Fischer Scientific, UK) by the experimenter.

Procedure:

Training (homecage): Throughout the training and test phase mice were water-deprived to approximately 90% of their pre-training weight. Water was given for 2 hours immediately after training or testing each day. The first stage of training focussed on mice associating a reward with a ceramic pot. During this training the mice had to learn to forage the ceramic pots to gain a liquid reward of 1:3 sweetened condensed milk (Nestle) solution (prepared in water; H₂O). During initial training, mice were removed from their home cage and placed into an identical home cage with sawdust bedding together with one ceramic pot placed in the centre of the cage for three successive trials. The cage wire lid was removed to increase exploration and paper was taped around the edges of the cage to prevent climbing out as shown in Figure 3.1A. Between each mouse, pots were wiped clean with 70% ethanol wipes to remove any odour cues, and the milk solution replenished accordingly. On the first day, the ceramic pot was baited with lowering volumes of milk solution (50, 10 and 5ml) to initially engage mice and to encourage interaction with the pot. Once a mouse had foraged a small volume of the liquid reward it was removed immediately from the cage and returned to its home cage. Mice were given no more than 10 minutes per trial. When mice had successfully demonstrated foraging behaviour with the volumes used above, 30uL was pipetted into the centre of the pot, the volume used for the remainder of training and testing. This process was repeated until each mouse had consumed the 30uL reward in all trials for 2 consecutive days.

Training (Test Arena): Mice continued training in the test arena. Mice were initially exposed to an empty arena with sawdust covering the base for 10 minutes to allow free exploration. For the following consecutive days of training, 2 baited pots were placed diagonal across from one another in the arena, 40cm apart (Figure 3.1B). On each day, the location of the pots was moved to prevent the development of a spatial bias in the test phase. Mice were placed into the centre of the arena and allowed to explore until they had consumed both rewards or a 10-minute time limit was reached. After this the mouse was

returned to its home cage. This process was repeated until all mice foraged in both pots in less than 3 minutes.

Testing: Mice were then tested over the next four consecutive days with one session per day. During these sessions the arena was set up with six pots arranged in a circular shape, each 20cm apart (Figure 3.1C). Each pot contained 30uL of milk solution. Each mouse in turn was taken from their home cage and placed in the centre of the arena always facing away from the experimenter. The mouse was allowed to explore the arena and forage pots until they had consumed the reward in all 6 pots or until 10 minutes had elapsed from when the first pot was foraged. Following the trial, mice were returned to their home cage. The pots were then wiped clean with 70% ethanol wipes and the milk solution replenished before the next mouse. All test sessions were recorded onto a DVD player using an overhead camera.

Scoring

A score of foraging behaviour was defined as a mouse jumping onto the rim of a pot and directing its nose in toward the bottom to consume a reward. A number of error scores were taken from this task to assess SWM performance and foraging behaviour. They are detailed in Table 3.2 below. It was hypothesized that mice in this task would adopt a win-shift strategy whereby a pot that has been foraged from should not be returned to, as no further reward will be obtained. A win-shift strategy on the RAM implies that rats will search for food in different spatial locations (or maze arms) once foraging a reward from a given arm (Olton & Schlosberg 1978). Win-stay implies that rats will return to the same arm to obtain a further reward. Olton and Scholberg (1978) determined that rats adopted a win-shift over a win-stay strategy when being tested on the RAM (Olton & Schlosberg 1978). Mice have also been reported to exhibit win-shift foraging behaviour in both RAM and RAWM protocols (Hyde et al. 1998; Anagnostaras et al. 2003). This would suggest that mice would be likely to adopt a win-shift foraging strategy for successful task completion. Therefore, WM should prevent mice from returning to pots where a liquid reward has already been consumed.

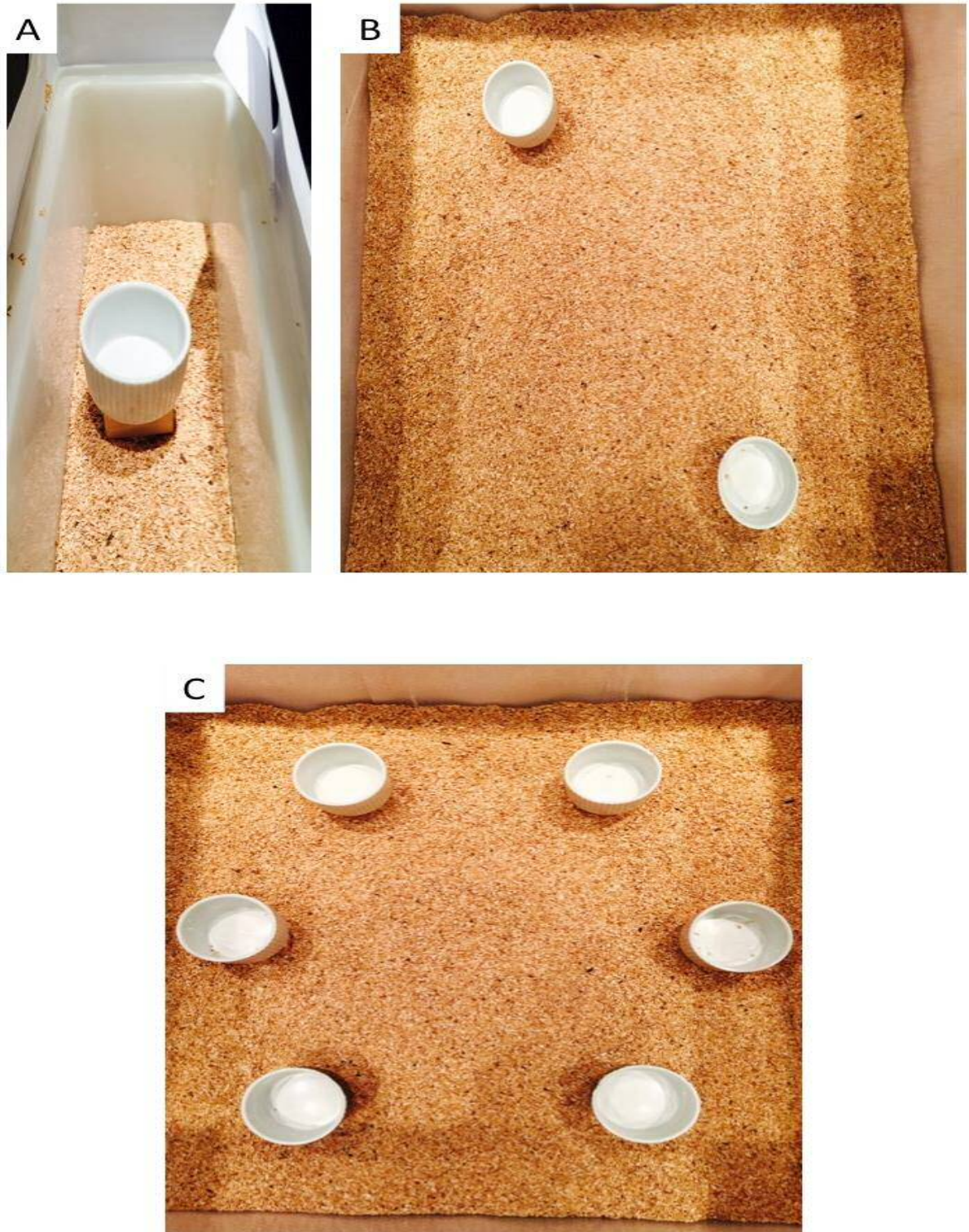


Figure 3.1: Figure to illustrate pots and the pot arrangement through training and testing. (A) Shows an individual pot in a home cage used for initial training. (B) Two pots placed opposite each other in the arena-training phase. (C) Six pots are placed in a radial formation for the test phase of the foraging task.

Error Measurement	Definition	Example of behaviour
Error	A mouse returning to a pot where the reward was previously consumed.	A mouse forages a reward from pot A and leaves pot A. The mouse then returns to pot A (Error).
Repeat Error	A mouse returning to a pot where an error was already made. Hence, repeating the error.	A mouse forages a reward from pot A, and leaves pot A. The mouse then returns to pot A (error). It leaves pot A again, forages in pot B before returning to pot A (repeat error).
Error in neighbouring pot	A mouse making an error immediately in the same pot or the neighbouring pot to which it has just foraged (if this pot has already been foraged in).	A mouse forages a reward from pot A. The mouse then forages in pot B before foraging in pot A
Error in distal pot	A mouse making an error in a pot one or more distant from a pot it has just foraged or made an error in.	A mouse forages in pot A. The mouse then forages in pot C before returning to pot A.
Chaining Response	When a mouse forages pots in a sequence of 3 or more pots immediately adjacent to one another	A mouse forages in pot A, B, and C etc. until the sequence is broken.
Perseverative Error	A mouse returning to a pot immediately after receiving a reward, or immediately after making an error.	A mouse forages in pot A. The mouse leaves pot A and immediately returns to pot A.

Table 3.2: Overview of the types of errors scored to assess SWM in a foraging-based task. Errors are defined and examples of when these errors are scored are described.

In this scoring procedure, “total error” acts as a baseline measure of SWM function. As described in Table 3.2, further measures were used to assess within-trial behaviours, such as foraging strategy, perseveration and factors representing more severe working memory deficits.

A repeat error was scored as a mouse returning to a pot where an error had already been made during the trial. This type of error was independent of the perseverative error described, as it was not an immediate return to a pot that had just been foraged. As total error incorporated all types of errors made within the trial, the repeat error was able to provide a more distinctive WM error measure.

A measure of chaining response was recorded to determine whether mice foraged in a random sequence or had a tendency to alternate pot choices within a given trial. This measure aimed to establish if animals adopted different foraging strategies to complete the task. The spatial distribution of errors was also assessed to compliment the measure of chaining response. Errors made in pots neighbouring a pot that had just been foraged or distal to those just foraged were recorded. This score was calculated as a ratio against total errors made by each mouse to give a measure that was unbiased by differences in total errors between groups.

Perseverative errors were also scored when a mouse returned immediately to a pot it had just successfully foraged in or made an error in. Perseverative errors were recorded as this behaviour has been observed in HPC lesioned animals and have further been reported in AD patients and mouse models (Lamar et al. 1997; Huitron-Resendiz et al. 2002; Wang & Cai 2006; Yoon et al. 2008).

Further measures were taken to look at motor performance as a measure of total time taken to complete the task from when the mouse was placed into the arena to when the final reward was consumed. Lastly, the time taken to observe engagement with the task (i.e. the time taken from when the mouse was placed into the arena to when it foraged the first pot) was recorded. This measure was thought to reflect the effect of anxiety or motivation on engagement with the task.

Statistical Analysis

Data were analysed using Microsoft Excel for calculation of mean number of errors, times and standard error of the mean. IBM SPSS Statistics software was used to

analyse all data statistically. An α -level of 0.05 was used for all measures showing statistical significance. All data were checked for violations of distribution and homogeneity of variance by Shapiro-Wilk test and Levene's test respectively. Due to high levels of variability in data sets, and a large number of zero scores in the error measures, violations of these tests were observed ($p < 0.05$). Therefore, data that violated these tests were subjected to transformation (i.e. Square root, log-10) based on the level of positive/negative skew and reassessed. Data that then showed no further violations of distribution were analysed by repeat measures ANOVA and independent samples t-test. In t-tests that reported violations of Levene's test for equality of variance, results reported were from a modified t-test, the Welch t-test, which accommodates for unequal variances. Data that could not be transformed due to the presence of zeros in the data were analysed using non-parametric statistics. Mann-Whitney U Tests were used to compare between group factors and Wilcoxon Signed-Rank Tests or Friedman's test with Bonferroni correction to adjust for multiple post hoc comparisons were used to compare within subject factors.

3.2.4 Experiment 1 – Results:

Histology:

An example of bilateral HPC lesions are presented in figure 3.3 and the maximum and minimum tissue damage obtained as a result of excitotoxic lesions are displayed in Figure 3.3 and 3.4 respectively. In this study 2 lesioned animals were removed from the study following histological analysis due to completely intact ventral hippocampal structure. Eight mice showed a complete lesion of the HPC with the exception of the most posterior ventral DG (mostly observed unilaterally) and small sparing of the ventral pyramidal cell layer of the HPC. Three mice showed complete removal of the dorsal HPC with further bilateral damage to the ventral HPC. As observed in Figure 3.4, the minimal lesion effect showed intact ventral HPC structure unilaterally at the most posterior reference. However damage was observed in the ventral DG. Cortical damage around the infusion site was observed in all lesioned animals, predominantly of the parietal association cortex and visual cortex. No HPC damage or other damage was present in the SHAM control mice except two mice that displayed a small amount of damage unilaterally to the visual cortex. Further damage observed was not focussed around the craniotomy site and was likely related to mechanical damage during tissue sectioning.

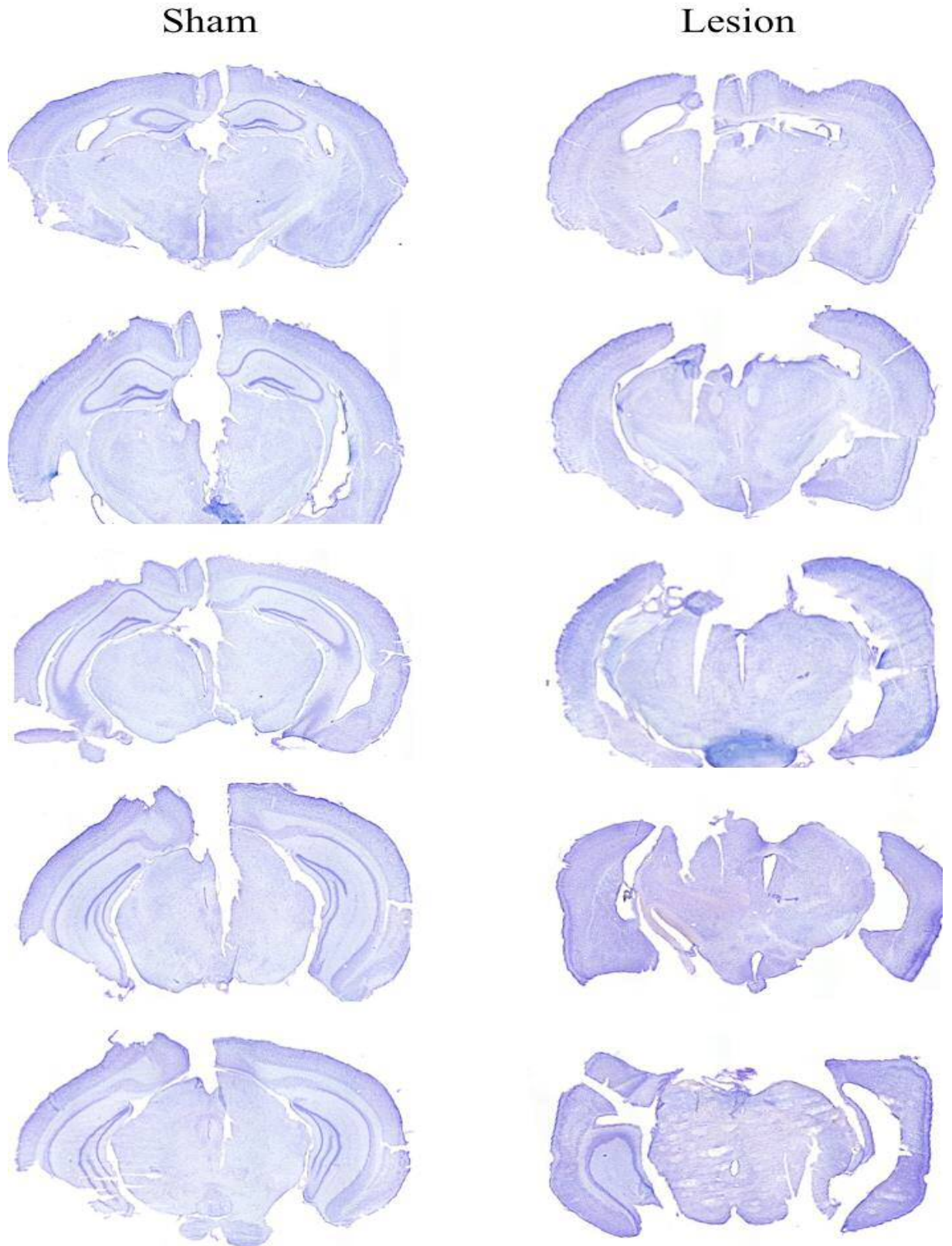


Figure 3.2: Cresyl stained example of hippocampal lesion and SHAM control mice. HPC lesions (right) show a significant loss of the HPC structure compared to intact HPC formation in the SHAM control mice (left).

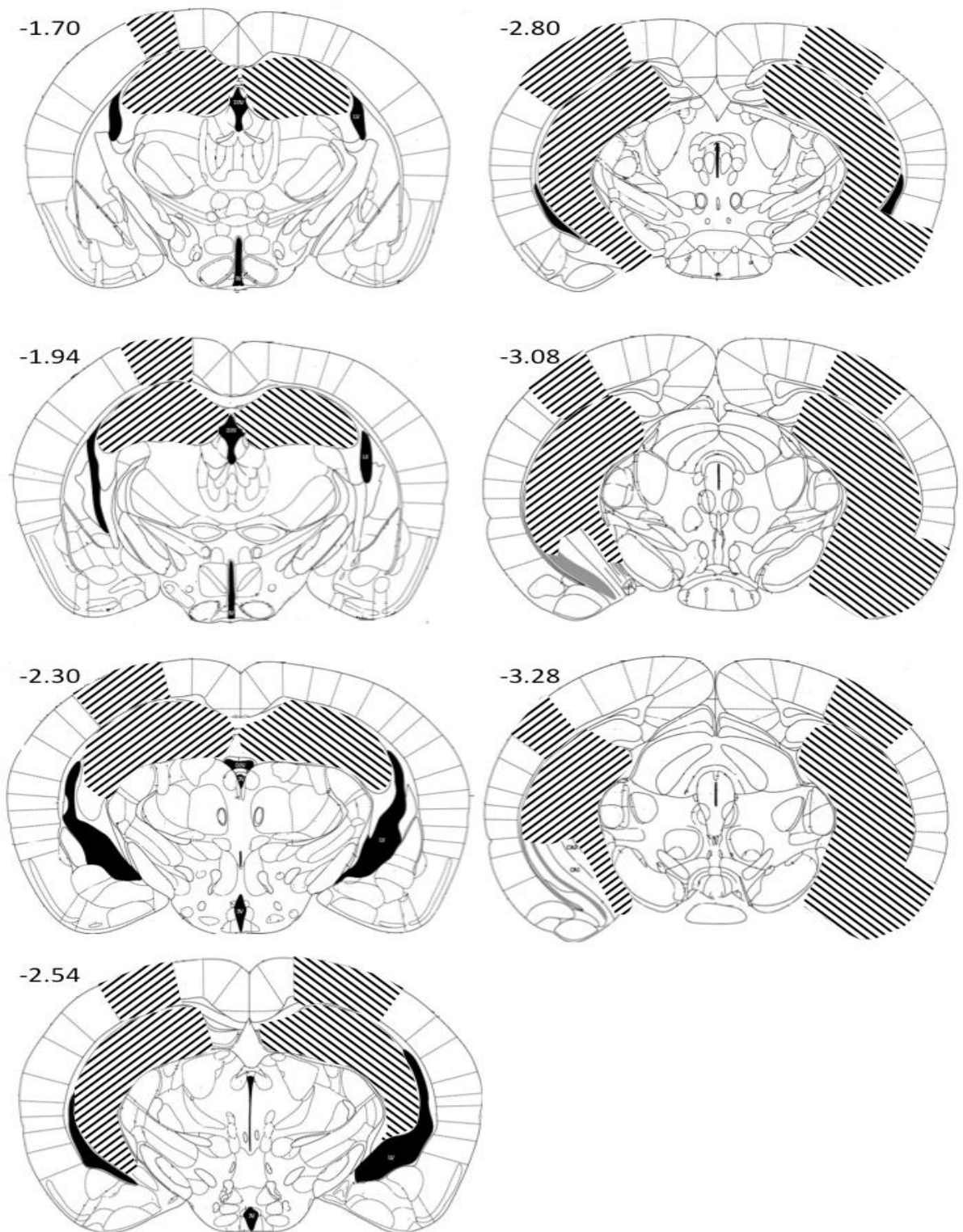


Figure 3.3: Schematic illustration of the maximum hippocampal lesion. The level of HPC (and cortical) damage is illustrated by the shaded areas. Each section is denoted from the distance posterior to bregma.

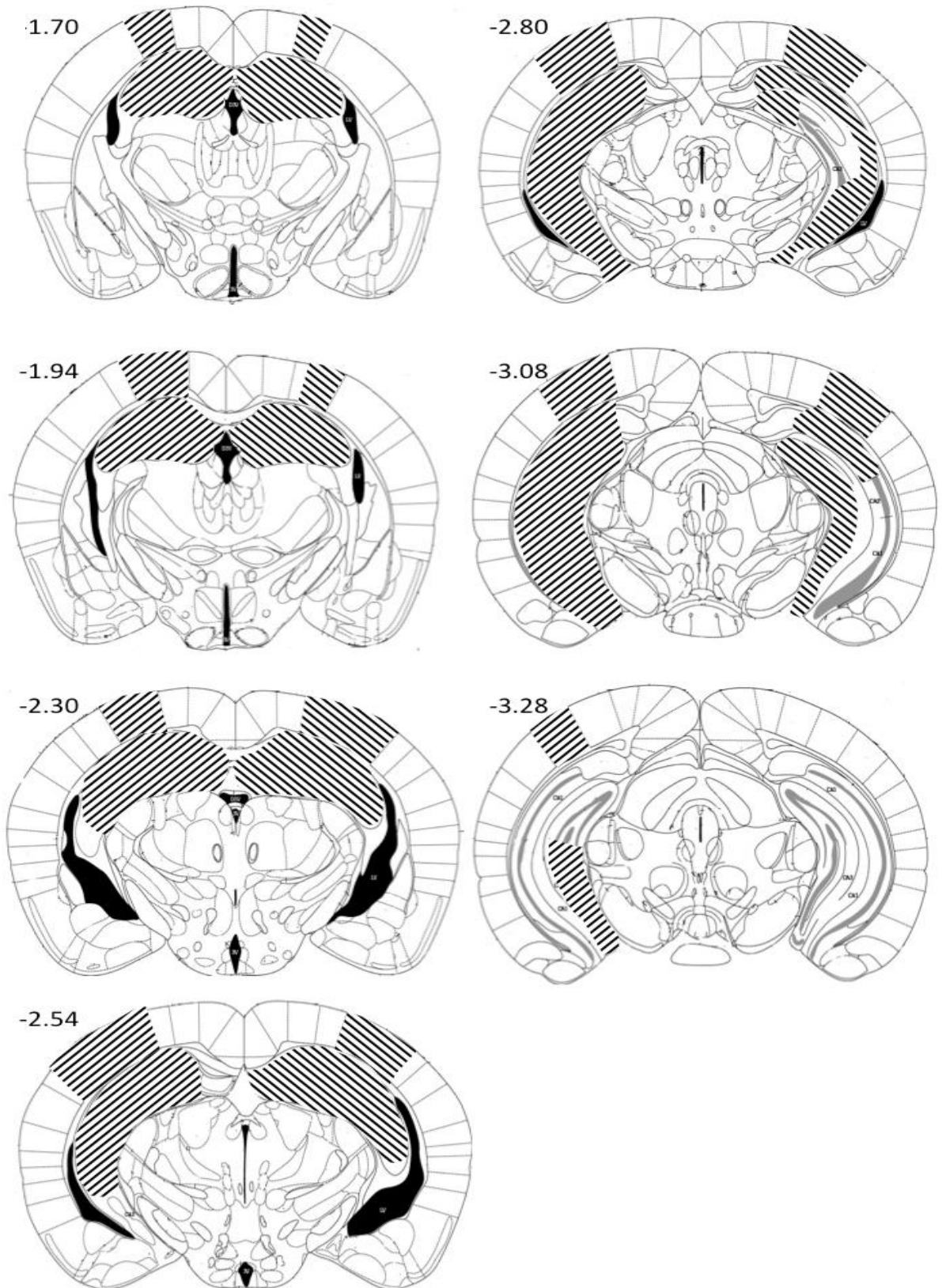


Figure 3.4: Schematic illustration of the maximum hippocampal lesion. The level of HPC (and cortical) damage is illustrated by the shaded areas. Each section is denoted from the distance posterior to bregma.

Time Taken:

The mean measurements of time taken across all 4 trials can be observed in Table 3.3. Lesion mice showed very similar times to SHAM controls for the total time taken to complete the task as well as the time taken to engage with the task. This was confirmed following independent samples t-tests. Total time taken showed no significant difference between groups, $t(22)=-0.15$, $p>0.5$. Time taken to engage with the task also showed no significant difference between groups, $t(22)=0.83$, $p>0.1$. These results indicate that any changes in memory performance between these two groups are not an effect of gross motor and/or motivational changes.

Perseverative Errors:

Lesion mice appear to show a greater number of perseverative errors as observed in Table 3.3. Data were analysed using Mann-Whitney U Test, which confirmed that HPC lesioned mice made a greater number of perseverative errors when compared to sham-control mice, $U=118.5$, $z=2.7$, $p<0.01$.

Chaining response:

To determine if HPC lesioned mice showed any difference in strategy to complete the task, chaining responses were determined (Table 3.3). HPC lesioned mice showed a greater number of chaining responses compared to SHAM controls as determined by Mann-Whitney U test, $U=113.0$, $z=0.1$, $p<0.05$.

Time Measure	Treatment			
	SHAM		Lesion	
	Mean	SD	Mean	SD
Total Time (s)	190.8	56.10	194.4	64.33
Engagement Time (s)	43.1	24.57	36.1	19.15
Perseverative Errors	0.73	0.61	2.80	3.53
Chaining Response	0.69	0.36	1.06	0.36

Table 3.3: Results table showing motor and foraging behaviours in the foraging task. Means and standard deviation (SD) in HPC lesion mice (n=11) and SHAM controls (n=13) are reported.

Total Errors:

To determine if there was any main effect of lesion on total errors and task acquisition, a repeated measures ANOVA with the between subject main effect of lesion and within-subject main effect of trial was used to assess the number of errors recorded across the 4 trials, as observed in Table 3.4 and Figure 3.5A. Results showed no significant main effect of trial, $F(3, 66)=0.48$, $p>0.5$ and no significant trial * group interaction, $F(3, 66)=0.03$, $p>0.5$ when assessing with-subjects factors. However, a main effect of treatment was reported, $F(1, 22)=154.2$, $p<0.05$.

Trial	Treatment			
	SHAM		Lesion	
	Mean	SD	Mean	SD
Trial 1	4.38	2.33	6.75	5.96
Trial 2	4.69	2.84	7.08	3.88
Trial 3	4.15	2.19	6.17	3.88
Trial 4	3.54	3.13	6.17	3.56

Table 3.4: Table showing the mean number of errors made in each trial by HPC lesion mice (n=11) and SHAM controls (n=13).

Repeat Errors:

Inspection of Figure 3.5B showed that HPC lesioned mice displayed a greater number of repeat errors. This was confirmed following analysis by independent samples t-test, $t(16.29)=-2.86$, $p<0.05$.

Ratio of Neighbouring and Distal errors to Total errors:

The number of errors in neighbouring and distal pots are presented as a ratio of total errors, corrected for perseverative errors (Figure 3.5C). Independent samples t-test revealed that HPC lesion mice have a significantly higher ratio of error scores in neighbouring pots than SHAM controls, $t(22)=2.14$, $p<0.05$. HPC lesion mice further made less errors in distal pots when compared to SHAM control mice, $t(22)=2.14$, $p<0.05$.

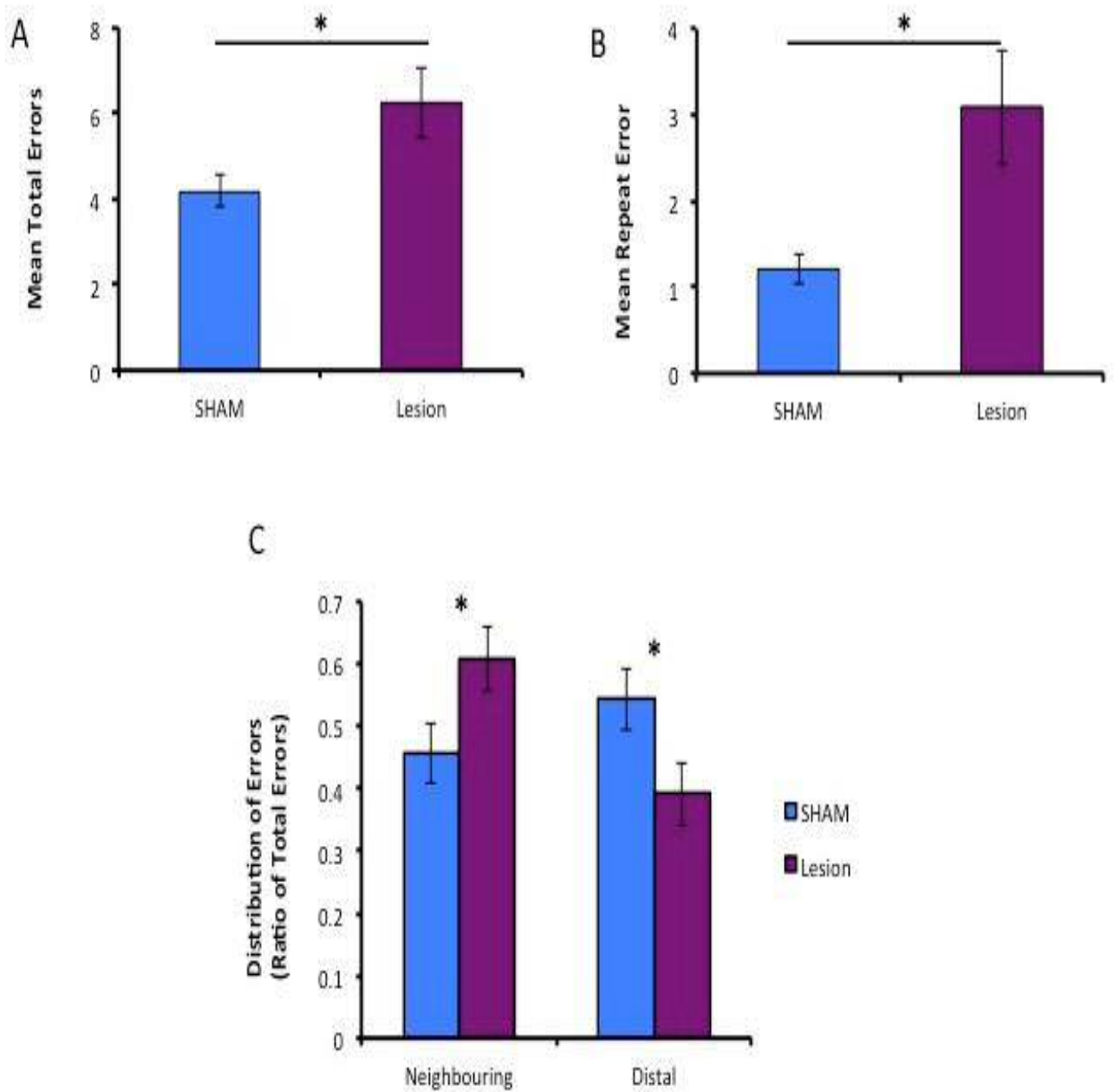


Figure 3.5: Foraging behaviour in HPC lesion mice. Measures of SWM in SHAM control (n=13) and HPC lesion mice (n=11). Data were averaged across four trials for each mouse and mean score for each group is reported. Error bars represent the S.E.M. A) Total number of errors. B) Total number of repeat errors. C) The ratio of neighbouring and distal errors to total errors made. *p<0.05.

3.2.5 Discussion

Results from Experiment 1 demonstrate that lesions of the HPC impair performance of the foraging task. HPC lesion mice made a greater number of total errors and repeat errors, which were used to determine WM performance in this study. This result agrees with previous HPC lesion experiments assessing SWM function in both rats and mice in WM tasks (Nadel & Moscovitch 1997; Cassel et al. 1998; Deacon et al. 2002; Winters et al. 2004). However, interestingly previous studies in SWM assessment have reported task acquisition over a period of trials or days on maze-based WM tasks (Cassel et al. 1998; Morgan et al. 2000; Richter et al. 2013; Wilson et al. 2015;). This was not observed in this task by either sham-controls or HPC lesioned mice. This indicates a validity to compare means of HPC lesion mice and sham-controls across all four trials, which are unbiased by any changes across trials.

The analysis of the distribution of errors showed that HPC lesioned mice made a greater portion of their errors in adjacent pots than in distal located pots. This result was consistent with the observed increase in chaining foraging responses in HPC lesioned mice whereby mice would forage three or more pots immediately adjacent to one another before breaking this response and foraging in a pot in a more distal location. Thus, HPC lesioned mice appeared to adopt a different foraging strategy in order to complete the task by foraging in a sequential pattern and in pots with adjacent locations, whereas SHAM control mice appeared to forage pots in neighbouring and distal locations in an equal ratio, likely using the extra-maze spatial stimuli to complete the task.

HPC lesioned mice showed no difference in total times and latency to engage with foraging compared to SHAM controls. This suggests that performance was not affected by gross motoric or motivational changes following the lesion. HPC lesioned mice showed a greater level of perseverative behaviours. This result is further in agreement with other reports observing this type of behaviour in HPC lesion animals (Olton & Werz, 1978; Johnson et al., 1996; Whishaw & Tomie, 1997; Pouzet et al., 2002).

Collectively, the data from the present experiment indicated that the HPC was required for effective foraging behaviour. Experiment 2 evaluated whether the changes in total errors, response perseveration and pattern separation were restricted to circumstances where performance did not rely on processing extra-maze cues.

3.2 - Experiment 2: Assessment of non-spatial WM in HPC lesion mice

3.2.1 Introduction:

To test that the deficits in the foraging task were due to impaired processing of spatial information, a non-spatial version of this task was carried out. Two distinct types of navigation have been reported, allocentric and egocentric. Egocentric navigation employs the use of more internal cues such as self-movement or internal markers of the environment and therefore is not considered as spatial information. Allocentric navigation relies strongly on the use of distal cues or landmarks in order to form a cognitive map and has been associated with HPC function (Morris et al. 1986; Morris et al. 1990; Vorhees & Williams 2014). It is hypothesized that mice used allocentric navigation in order to complete the foraging task in Experiment 1.

To test this hypothesis, in Experiment 2, extramaze cues were removed by drawing a black curtain around the arena and pots were each given a novel pattern. Mice therefore relied upon non-spatial cues in order to complete the foraging task. Studies have previously found conflicting results when assessing HPC involvement in non-spatial memory tasks (Olton & Feustle 1981; Aggleton & Road 1986; Morris et al. 1986; Raffaele & Olton 1988; Ennaceur & Meliani 1992). For instance, Olton and Feustle examined non-spatial WM through the use of an enclosed 8-arm RAM where each arm was given a distinctive discriminative stimuli. Rats with fimbria-fornix lesions showed working memory impairments relative to sham controls (Olton & Feustle 1981). However, Aggleton and Road used a three-arm Y-maze delayed non-matching-to-sample task, which revealed that rats with HPC lesions were able to learn and perform the task similar to sham controls (Aggleton & Road 1986). Precise reasons for these differences remain speculative and are likely influenced by factors including task difficulty, levels of proactive interference, maze type etc. Despite conflicts between studies implicating the HPC in non-spatial WM tasks, experiment 2 aims to test a hypothesis that the working memory deficits reported in experiment 1 were due to impaired processing of spatial information instead of a more total WM impairment.

3.2.2 Design:

The same mice used in experiment 1 were used in experiment 2. In this task each pot was given a novel design and all visual spatial extra-maze cues were obscured.

Apparatus:

All apparatus used was identical to that used in experiment 1. A black curtain was now drawn around the test arena to remove the distant spatial cues in the testing room. The pots were also changed. The size and shape remained identical, however, each pot was now individually designed and patterned distinctively from one another (Figure 3.6).



Figure 3.6: Novel pot designs used in experiment 2. All 6 pots were given a novel design (4 are shown in this figure). Position of the pots was changed each day, but the radial formation remained.

Procedure:

No pre-training was carried out and animals received training as follows:

Test Phase: Following testing in the spatial version of the task, mice were then subjected to a non-spatial WM assessment. An identical testing procedure was used as described above, however a black curtain was drawn around the test arena to remove all visual extra-maze cues. All pots were placed in the same arrangement as previously described, but each pot now had a unique design (Figure 3.6). To prevent any familiarity in the pattern of the pots occurring across the 4 days of testing, pots were swapped in their location each day so that no individual pot was neighbouring the same 2 pots on any test day.

3.2.3 Experiment 2 - Results:

Time Taken:

The mean measurements of time taken across all 4 trials can be observed in table 3.5. HPC lesion mice showed very similar times in both total and engagement times to SHAM control. This was confirmed following independent samples t-tests. There was no significant difference in total time taken to complete the task between groups, $t(22)=-0.28$, $p>0.5$, or for animals to engage with the task, $t(22)=0.20$, $p>0.5$.

Perseverative Errors:

Initial observation of Table 3.5 shows a greater number of perseverative errors made by HPC lesion animals. This observation was supported by independent samples t-test statistical analysis, which revealed a significant difference between SHAM controls and HPC lesioned mice, $t(22)=-0.97$, $p<0.05$.

Chaining strategy

HPC lesioned mice showed a greater chaining response when compared to SHAM control mice as determined by independent-samples t-test, $t(22)=-4.20$, $p<0.001$ (Table 3.5).

Time Measure	Treatment			
	SHAM		Lesion	
	Mean (s)	SD	Mean (s)	SD
Total Time	169.85	71.02	178.06	69.87
Engagement Time	40.12	16.51	38.77	15.99
Perseverative Errors	0.75	0.51	1.65	1.53
Chaining Response	0.62	0.47	1.44	0.45

Table 3.5: Results table showing non-WM measures made by HPC lesion mice (n=11) and SHAM controls (n=13).

Total Errors:

To determine if there was any overall mean difference in total errors and task acquisition, a repeated measures ANOVA with the between subject main effect of lesion and within-subject main effect of trial was used to assess the number of errors recorded across the 4 trials, as observed in Table 3.6 and the total mean in Figure 3.7A. Results showed a non-significant difference between lesion group, $F(1, 22)=131.4$, $p>0.1$, a non significant within-subjects main effect of trial, $F(3, 66)=2.44$, $p>0.05$, and a non-significant trial * treatment interaction, $F(3, 66)=2.42$, $p<0.05$.

Trial	Treatment			
	SHAM		Lesion	
	Mean	SD	Mean	SD
Trial 1	4.23	3.14	7.92	3.49
Trial 2	4.31	2.53	4.23	3.85
Trial 3	4.77	4.95	3.92	1.94
Trial 4	3.77	1.54	4.15	2.10

Table 3.6: Table showing the mean number of errors made in each trial by HPC lesion mice (n=11) and SHAM controls (n=13).

Repeat Errors:

No significant difference between groups was reported for mean repeat errors (Figure 3.7B), as determined by Mann-Whitney U Test, $U=89.0$, $z=1.02$, $p>0.1$.

Neighbouring/Distal Errors:

The ratio of neighbouring and distal errors are presented as a ratio to total errors made (figure 3.7C) to assess the pattern of errors in lesion and SHAM control mice. An independent samples t-test reported that HPC lesioned mice made a greater number of errors in neighbouring pots, $t(22)=-3.04$, $p<0.01$ and less in distal pots, $t(22)=3.58$, $p<0.01$ when compared to SHAM control mice.

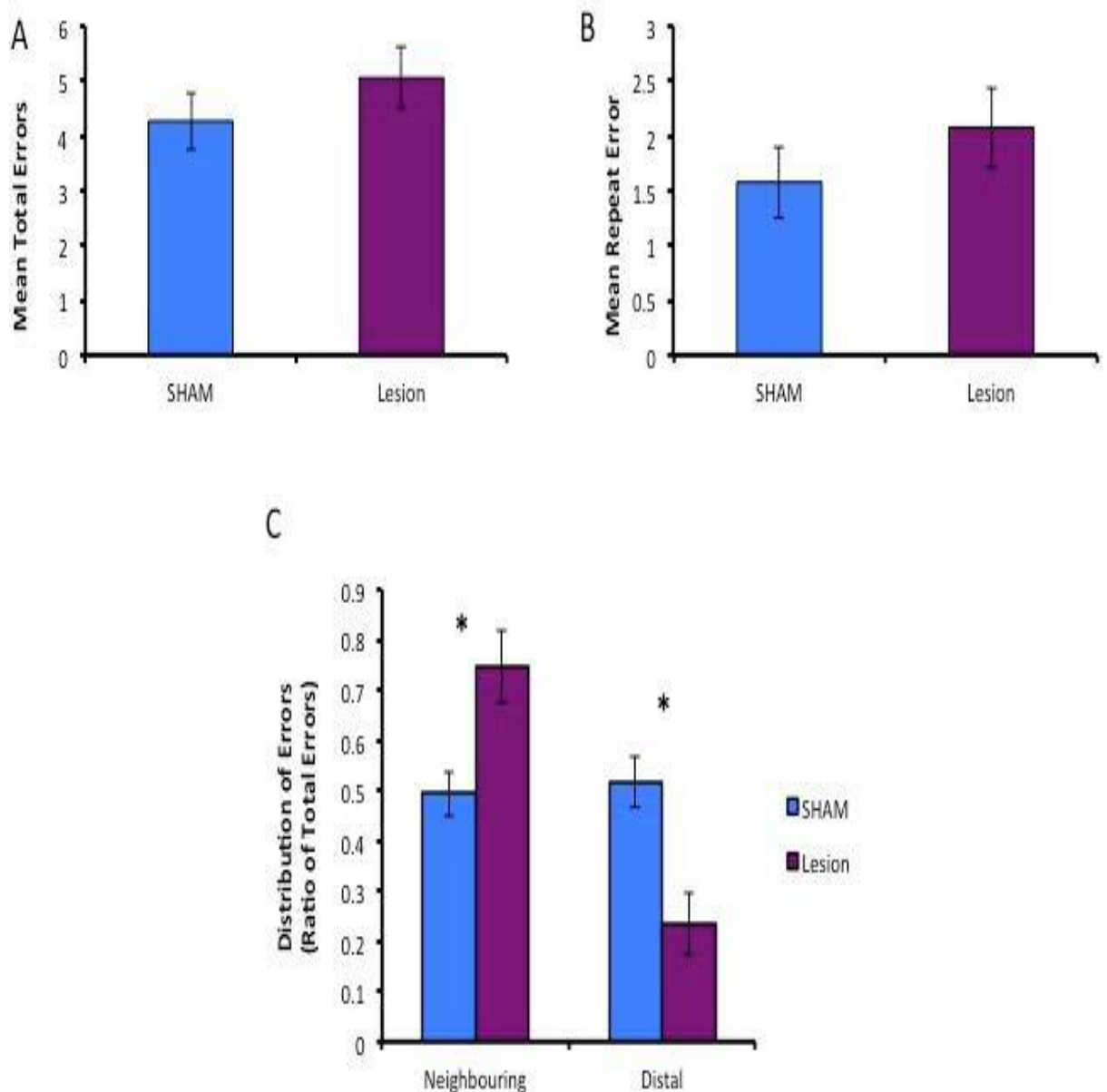


Figure 3.7: Foraging behaviour in HPC lesion mice. Measures of SWM in SHAM control (n=13) and HPC lesion mice (n=11). Data were averaged across four trials for each mouse and mean score for each group is reported. Error bars represent the S.E.M. A) Total number of errors. B) Total number of repeat errors. C) The ratio of neighbouring and distal errors to total errors made. * $p<0.05$.

3.2.4 Discussion:

Results from this experiment indicated that HPC lesion mice displayed a similar WM performance to SHAM control mice when spatial stimuli were removed. Similar to experiment 1, no differences were observed in the times taken to complete the task or engage suggesting the removal of spatial cues did not affect states of emotion in these mice or motor performance differentially. Moreover, perseverative behaviour was observed in HPC lesion mice across both spatial and non-spatial versions of the foraging task.

Two further group differences that were observed in experiment 1 continued to present in experiment 2; chaining response and the greater ratio of errors made around a previous search location in mice with HPC lesions. The former effect showed that HPC lesion mice continued to display a chaining response pattern, ie, animals would tend to simply forage in the adjacent pot (1, 2, 3) regardless of whether this pot had had previously been foraged in or not. Complimentary of this response, HPC lesioned mice also continued to show a greater level of errors made in pots adjacent to where they had just foraged. Collectively, as discussed in experiment 1, these differences imply that HPC lesion mice adopted a different strategy for task completion compared to SHAM control mice. Given a continued response across both experiments, this strategy is likely independent of spatial stimuli.

Despite HPC lesion and SHAM mice displaying apparent different strategies, mice performed at comparable levels in regards to total errors and repeat error measures. These results indicate that HPC lesion mice were more able to use local cues to guide overall performance in this version of the foraging task and performed at a comparable level to SHAM controls. Moreover, these results suggest that inhibition of processing of spatial information by HPC ablation was responsible for impaired performance in experiment 1.

The results of experiment 2 show that HPC lesion mice are able to perform the foraging task at levels that are similar to sham-control mice. This would suggest that HPC lesions have minimal involvement in non-spatial WM processes in the foraging task.

3.4 - Experiment 3: Assessing foraging behaviour in PDAPP mice

3.4.1 Introduction:

To date, little work has been carried out to assess SWM in the PDAPP model. The only existing data were reported by Dodart et al., who showed age-independent WM deficits in the 8-arm RAM from as early as 3 months of age, which appeared to worsen with age by 9-10 months of age (Dodart et al., 1999). Similar to reports by Dodart et al. (1999), PDAPP mice have also been observed to exhibit early spatial learning deficits on the circular Barnes maze at 3-5 months of age (Huitrón-Reséndiz et al. 2001). Evidence of perseverative behaviour and different search strategies were also reported. These deficits appeared to worsen with age and by 22-26 months of age PDAPP mice displayed a greater number of total trial errors, perseverative behaviour and showed impaired spatial search strategies with a greater tendency to display random search strategies (crossing the arena) compared to WT littermate controls (Huitrón-Reséndiz et al. 2001). Chen et al., reported an age-dependent deficit in spatial learning following a training to criterion protocol of the MWM (Chen et al., 2000). This study predominantly focussed on the PDAPP models ability to learn a spatial location following multiple trials in order to meet a performance criterion (3 successive trials with a mean escape latency of <20 seconds). Results of this procedure showed an age-dependent worsening in spatial learning from 6-9 months to 13-15 months of age (Chen et al., 2000). Further studies have since confirmed these observations of age-dependent effects in the processing of spatial information in the MWM and confirmed the significant involvement of A β in PDAPP mice (Hartman et al., 2005; Daumas et al., 2008). However, still no study to date has determined age-dependent effects of SWM in the PDAPP model.

Reports in alternate APP and APP + PS1 models have reported age-related worsening in SWM performance in tasks such as the T-Maze and RAWM (Chapman et al. 1999; Wirths et al. 2008; Webster et al. 2013). Age-dependent cognitive effects also appear to be relative to the distribution of A β in the HPC (Chapman et al., 1999; Westerman et al., 2002). Given that PDAPP mice are reported to show age-dependent increases in levels of A β , particularly in areas such as the HPC, it is likely that SWM performance of PDAPP mice will be sensitive to aging (Games et al. 1995; Reilly et al. 2003; Hartman et al. 2005). Following evidence that the foraging task is sensitive to HPC function in experiment 1 it was

hypothesised that PDAPP mice would show an age-dependent decline in SWM performance on the foraging task.

3.4.2 Design

Design and subjects are fully described in section 2.3. PDAPP mice were not tested on the non-spatial version of this task due to time restraints as described in section 2.3. For this reason, all PDAPP and WT littermate control mice were initially trained on the foraging task at 4 months of age and were re-trained at each age point starting in the test arena, not in the home cage.

3.4.3 Methods

The apparatus, procedure and scoring used in this experiment were as described in experiment 1 (3.3.3).

Statistical Analysis:

The statistical analysis and treatment of data (transformations etc.) carried out in this experiment were as described in 4.3.3. However, because PDAPP mice were assessed across a range of ages, a further factor of age was analysed in all subsequent analyses. When violations in data distribution were observed by Shapiro-Wilk test, that were not rectified by transformations, the non-parametric Friedmans test of multiple within-subject comparisons was used. Post-hoc comparisons were made with appropriate Bonferroni corrections for multiple comparisons. This method is a more conservative non-parametric statistical test than multiple within-subject comparisons using only Wilcoxon signed order rank tests.

3.4.4 Results

Time Taken:

Initial inspection of the time measures (Table 3.8) suggests that on average PDAPP mice took numerically longer to complete the foraging task than their WT littermate controls. A repeat measures ANOVA comparing the main between subject factor of genotype and within subject factor of age was used to analyse these data. Analysis of total time revealed a non-significant main effect of genotype, $F(1, 27)=3.48$, $p>0.05$, a non-

significant main effect of age, $F(1.56, 42.13)=2.62$, $p>0.05$ and no significant age * genotype interaction, $F(1.56, 42.13)=0.19$, $p>0.5$.

Engagement Time:

Repeated measures ANOVA of engagement times (Table 3.8) revealed no significant main effect of genotype, $F(1, 27) = 3.88$, $p>0.05$ when comparing engagement times with the first pot in the foraging task. There was a significant main effect of age, $F(1.64, 44.37) = 3.57$, $p<0.05$, but no significant age * genotype interaction, $F(2, 54) = 0.67$, $p>0.5$. This analysis revealed that with age, engagement time decreased, but this effect was not different between genotype.

Perseverative Errors:

Inspection of the number of perseverative errors in Table 3.8 across the age range reveals that while WT mice have varying levels of perseverative behaviour, PDAPP mice show an age-related increase. These measures were analysed with non-parametric Mann-Whitney U Tests for between-subject analysis and Friedman Test for within subject effects of age. Mann-Whitney U Tests revealed no significant main effect of genotype at 6-8 months, $U=104.5$, $z=-0.2$, $p>0.5$, 10-12 months, $U=129.5$, $z=1.09$, $p>0.1$, but a significant main effect of genotype at 14-16 months of age, $U=174.5$, $z=3.09$, $p<0.01$. A Friedman test reported that there was a significant within-subject effect of age in WT mice, $X^2(2)=6.70$, $p<0.05$. Pairwise comparisons were then performed with a Bonferroni correction for multiple comparisons and revealed no significant differences between any individual age range. A significant within-subject effect was also obtained in PDAPP mice, $X^2(2)=6.37$, $p<0.05$. Pairwise comparisons further revealed a significant difference between perseverative errors made at 6-8 months and 14-16 months of age, $p<0.05$, but no other age comparisons.

Chaining response:

Analysis of chaining response as observed in Table 3.8 in PDAPP mice was carried out using a repeated measures ANOVA. Analysis revealed a main effect of genotype, $F(1, 27) = 39.77$, $p<0.001$, a main effect of age, $F(2, 54) = 5.18$, $p<0.01$ and no significant age * genotype interaction, $F(2, 54) = 1.09$, $p>0.1$.

Measure	Genotype	Age					
		6-8 Months		10-12 Months		14-16 Months	
		Mean	SD	Mean	SD	Mean	SD
Total Time (s)	WT	135	11.9	114	17.7	100	10.9
	PDAPP	175	26.1	134	23.9	141	19.9
Engagement Time	WT	26.95	20.30	23.92	30.03	12.48	13.45
	PDAPP	38.40	29.14	40.31	40.10	32.09	36.98
Perseverative Error	WT	0.38	0.06	0.65	0.12	0.25	0.07
	PDAPP	0.39	0.09	0.91	0.17	1.25	0.32
Chaining Response	WT	0.67	0.36	0.83	0.43	0.82	0.52
	PDAPP	1.08	0.48	1.45	0.48	1.63	0.44

Table 3.7: Results table showing motor and foraging behaviours in WT (n=15) and PDAPP (n=14) mice across all ages tested.

Total Errors:

Initial observation of Table 3.8 and Figure 3.8A suggested a trend that PDAPP mice showed a greater number of total errors with age. A repeat measures ANOVA was used to ascertain if mice showed any overall changes in total errors made or acquisition to the foraging task, which may be affected by age and/or genotype (Mean values reported in Table 3.6). In this analysis, the between-subject factor remained as genotype and within-subject factors were age and trial. Results revealed a non significant main effect of genotype, $F(1, 27)=1.84$, $p>0.1$, a non significant main effect of age, $F(2, 54)=0.13$, $p>0.5$, a non significant age x genotype interaction, $F(2, 54)=2.50$, $p>0.05$, a non significant main effect of trial, $F(2.09, 56.52)=0.23$, $p>0.5$, a non significant trial x genotype, $F(3, 81)=0.71$, $p>0.5$, a non-significant age x trial interaction, $F(6, 162)=0.60$, $p>0.5$ and a non-significant age x trial x genotype interaction, $F(6, 162)=0.46$, $p>0.5$.

Genotype	Age	Trial							
		1		2		3		4	
		Mean	SD	Mean	SD	Mean	SD	Mean	SD
6-8	WT	4.27	2.49	4.73	2.22	5.20	3.53	4.47	2.29
	PDAPP	4.29	3.07	4.64	5.05	4.57	3.25	4.57	3.20
10-12	WT	5.53	2.75	3.40	2.59	5.00	2.70	4.73	3.06
	PDAPP	5.00	2.72	5.64	4.92	4.86	4.02	4.79	5.31
14-16	WT	3.67	2.16	3.07	2.12	3.20	2.91	4.67	3.96
	PDAPP	7.07	8.26	6.14	5.40	4.71	5.20	5.93	5.57

Table 3.8: Mean numbers and standard deviation of working memory errors across trials in the foraging task in wild type (n=15) and PDAPP mice (n=14).

Repeat Errors:

A similar observation can be made of figure 3.8B as with total errors. These data were assessed using non-parametric Mann-Whitney U test (between-subjects) and Friedman's test (multiple within-subjects comparison) due to violations of Shapiro-Wilk test, $p < 0.05$ and inability to transform data due to a number of zero scores in the data set. Results from Mann-Whitney U test revealed no significant differences between genotypes at 6-8 months of age, $U=104.5$, $z=-0.22$, $p > 0.5$, 10-12 months of age, $U=139.5$, $z=1.52$, $p > 0.1$, but a significant difference between WT and PDAPP mice at 14-16 months of age, $U=150.5$, $z=1.99$, $p < 0.05$. Within-subjects analysis revealed no significant effect of age in WT mice, $X^2(2)=1.2$, $p > 0.5$, or in PDAPP mice, $X^2(2)=2.33$, $p > 0.1$.

Neighbouring/Distal Errors:

The number of errors in neighbouring and distal pots were converted to a ratio of total errors (figure 3.8C) to assess group differences in the pattern of errors. These data were analysed with a repeated measures ANOVA. Analysis of errors in neighbouring pots revealed a significant main effect of genotype, $F(1, 27) = 20.51$, $p < 0.001$, a significant main effect of age, $F(2, 54) = 7.39$, $p < 0.001$ and no significant age * genotype interaction, $F(2, 54) = 0.41$, $p > 0.5$. Analysis of the ratio of distal errors revealed a main effect of genotype, $F(1, 27) = 18.54$, $p < 0.001$, a main effect of age, $F(2, 54) = 7.01$, $p < 0.01$, but no significant age * genotype interaction, $F(2, 54) = 0.33$, $p > 0.5$. Collectively this analysis revealed that PDAPP

mice make a greater portion of errors in neighbouring pots and less in pots in distal locations when compared to WT controls at each age tested.

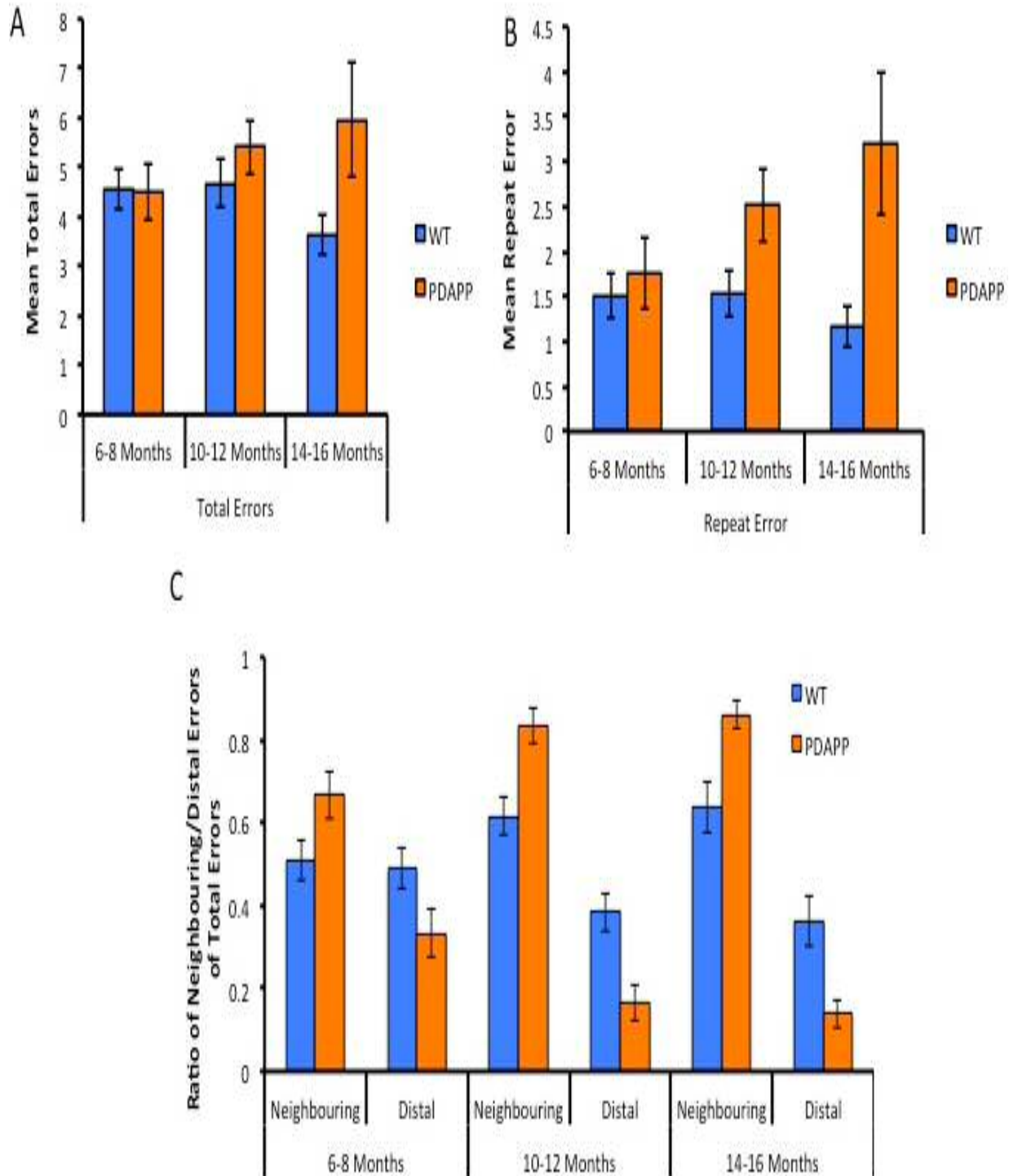


Figure 3.8: Foraging behaviour and SWM performance in PDAPP (n=14) and WT control mice (n=15). Data were averaged across four trials for each mouse and mean score for each group is

reported. Error bars represent the S.E.M. A) Total number of errors. B) Total number of repeat errors. C) The ratio of neighbouring and distal errors to total errors made.

3.3.5 Discussion

The results of experiment 3 demonstrate an overall general decline in SWM performance in PDAPP mice with age. Although numerically different, no significant differences were observed when comparing time taken to complete or engage with the task. The latter result suggests that gross changes in motor performance, motivation or anxiety did not influence the performance of PDAPP mice on this task. However, perseverative behaviour was observed by 14-16 months of age. This finding is similar to results observed with PDAPP mice in a holeboard maze and 3xTg mice using a touchscreen-based 5-choice serial reaction time-task (Huitrón-Reséndiz et al. 2002; Romberg et al. 2011a). Previous evidence showing that HPC lesions displayed similar behaviour, as well as observations from experiments 1 and 2, suggests that this pattern of deficit may reflect an age-dependent impairment in HPC function in PDAPP mice (Wang & Cai 2006; Yoon et al. 2008). The differences observed in the mean total number of errors, although by eye appearing to worsen with age, showed no significant difference in PDAPP mice at any age compared to WT mice. Nevertheless, PDAPP mice made a greater number of repeat errors compared to WT mice at 14-16 months of age.

PDAPP mice were also observed to use a chaining response during the foraging task. This was complimented by an overall increase in the number of errors made in pots adjacent to those that had just been foraged in. PDAPP mice have shown altered strategies from a young age (3-5 months) in a circular holeboard maze (Huitrón-Reséndiz et al. 2002). Huitrón-Reséndiz (2002) observed an age-related change in escape strategy in the holeboard maze in PDAPP mice at 20-26 months of age. Altered escape patterns were also observed in PDAPP mice in the MWM up to 18-21 months of age (Chen et al. 2000). This different pattern of response appears to worsen with age in PDAPP mice in the foraging task by 14-16 months of age, although no age * genotype interaction was observed and a main effect of age appears to effect foraging behaviour similarly between both PDAPP and WT control mice. This suggests that overexpression of APP, prior to the significant onset of amyloid pathology observed at 15 months (chapter 4) leads to altered foraging strategies in PDAPP mice from 6-8 months of age.

Collectively, these data were consistent with age-related impairments in the processing of SWM previously reported in PDAPP mice (Dodart et al. 1999; Chen et al. 2000; Hartman et al. 2005; Daumas et al. 2008). Levels of amyloid have been reported to increase from as early as 6 months and continue to rise with age (Dodart et al. 2002; Dodart et al. 2000; Games et al. 1995; Hartman et al. 2005; Reilly et al. 2003). Data reported in Chapter 4 showed that PDAPP mice showed a significant increase in the levels of soluble and insoluble A β 42 in the HPC at 15 months of age. This age-dependent increase in levels of A β in the HPC is likely to impair the processing of spatial information required for the successful completion of the foraging task and influence the behaviour of mice reported in experiment 3.

3.4 Chapter Discussion

The main aim of this chapter was to determine an age-dependent profile of SWM performance in the PDAPP model. To do this, a foraging based task was used that was less aversive than other water or fear motivated tests, and promoted rapid acquisition suitable for within-subject longitudinal designs. In order to evaluate the role of the HPC to this form of spatial working memory, Experiments 1 and 2 tested the hypothesis that mice with excitotoxic lesion of the HPC would show a selective deficit in the foraging task when extramaze cues guided performance compared to a similar task in which intramaze cues guided successful foraging.

The results from experiments 1 determined that HPC ablation caused impaired foraging behaviour, most likely because of a deficit in processing extramaze spatial information. This was further confirmed by a non-spatial manipulation of the foraging task (experiment 2) whereby all distal spatial cues were removed to prevent allocentric navigation. Despite evidence from experiments 1 and 2 suggesting a role for the HPC in this foraging-based task, alternative factors may influence task performance, such as the use of odour cues, which was not controlled for in this task. Rodents have been shown to use odour trails to aid navigation in water-escape and other WM tasks previously (Means et al. 1992; Hughes 2004). However, Olton and Collison (1979) reported that in the RAM, intramaze cues including odour trails were insufficient to govern accurate choice behaviour (Olton & Collison, 1979). Olton and Collison determined this by rotating the maze after each choice and food was either

kept in the same arm to determine if intramaze cues were used or food was kept in the same location to determine if extramaze cues were used to govern behaviour. Results from the study by Olton and Collison concluded that the use of extramaze stimuli governed accurate choice behaviour in rats (Olton & Collison, 1979). Thus, a further manipulation of the task described in this chapter, similar to that described by Olton and Collison, could be used in order to confirm whether mice used odour trails to navigate foraging behaviour, whereby the spatial locations of foraged pots could be changed half way through the trial (Olton & Collison, 1979).

Across both experiment 1 and 2 HPC lesion mice were observed to show a greater number of errors in pots adjacent to those just foraged in, which was complimented by a significantly greater chaining response. This reported behaviour to alternate in a preferred direction has previously been reported in foraging tasks such as the RAM (Olton & Werz 1978; Timberlake & White 1990). Contradicting to the results reported in experiment 1, Olton and Werz reported that HPC lesioned rats showed a more random response pattern and showed a preference for foraging in arms far away from the arm where they had just received a reward, whereas control rats showed a preference in foraging adjacent baited arms (Olton and Werz, 1978). This difference in behaviour may be influenced by the open arena design of the foraging task reported in this chapter compared to the radial arm design of the RAM whereby rodents must always return to a central platform prior to making their next choice. Interestingly, HPC lesioned rats have been reported to exhibit circling search strategies in the MWM in order to find the hidden platform (Pouzet et al. 2002). These results indicate that different types of maze may cause altered search strategies in rodents in order to successfully complete the given task. The differences in foraging strategy observed in this chapter and in HPC lesioned rats in the RAM and other spatial tasks may thus be an effect of the differences in maze type and/or the stimulus driving the goal-response (ie. food-reward/escape from aversive stimulus). This observation further adds to the caution that must be taken when comparing results of spatial memory and foraging behaviours across a range of tasks.

Collectively, evidence from experiments 1 and 2 suggest 3 main conclusions. First, the HPC plays a significant role in the processing of spatial-based allocentric information in the foraging task. Secondly, the processing of extra-maze information is likely sensitive to proactive interference as determined by the increase in number of total errors and repeated error choice made by HPC lesion mice. Thirdly, impaired HPC function can lead to altered

foraging behaviours and strategies in both the spatial and non-spatial versions of the foraging task.

The findings from experiment 1 and 2 provided a task with rapid acquisition and testing periods on which to assess SWM in PDAPP mice across a range of ages. To date, no study has used a within-subject longitudinal design to assess SWM performance in the PDAPP model; other studies have used cross-sectional designs (Dodart et al. 1999). Due to the evidence of age-dependent increases in A β production and deposition, particularly in the HPC, and the evidence of age- and A β -related cognitive deficits, it was hypothesised that PDAPP mice would display an age-related deficit in the foraging task (Games et al. 1995; Chapman et al. 1999; Dodart et al. 2002; Hartman et al. 2005). In experiment 3 no significant difference was reported when observing mean total errors only as a measure of SWM performance. However, differences were observed with age in regard to repeated errors. This identified a SWM deficit in 14-16 month old PDAPP mice only, relative to WT littermate controls. As total errors take into account all forms of “error” across the foraging task, repeat errors allow for the identification of a more severe WM deficit as mice repeat an error already made. Although speculative, one possible reason for increased repeat errors is an increased sensitivity to proactive interference. PDAPP mice have been reported to show age-dependent deficits in spatial learning at 13-15 months of age in a manipulation of the MWM, which could be reversed following A β immunotherapy (Chen et al. 2000; Hartman et al. 2005; Daumas et al. 2008). This spatial learning deficit was further shown to be sensitive to interference (Daumas et al. 2008). Daumas and colleagues showed that as the number of spatial locations learned in the MWM increased, the ability of PDAPP mice to recall them reduced in mice at 5-6 months of age and thus concluded that PDAPP mice were sensitive to spatial interference (Daumas et al. 2008). It was hypothesised that earlier deficits would most likely be an effect of soluble oligomeric forms of A β that had been implicated in disrupted neuronal function and preceded overt plaque deposition (Walsh et al. 2005; Lesné et al. 2006; Daumas et al. 2008). The sensitivity to interference observed by Daumas and colleagues presents an interesting comparison to the observations of patients with AD who show faster forgetting on recall tasks and remote memory and hence, examining memory interference in AD may be sensitive to earlier diagnosis (Kopelman, 1985; Christensen et al., 1998). A similar approach to Daumas and colleagues may better test the sensitivity of proactive interference in PDAPP mice in the foraging task by increasing the number of pots placed in the open arena.

This would require a greater level of spatial information to be processed within-trial in order to remember the spatial locations of pots already foraged and further confirm this observation.

Across all experiments in this chapter HPC lesion mice and PDAPP mice displayed a greater tendency to show a chaining response in foraging behaviour. This was further complimented by a significant increase in the ratio of errors made in pots adjacent to those just foraged in. Altered foraging responses and escape strategies have previously been reported in HPC lesioned mice and Tg models of amyloid pathology, including PDAPP mice (Olton & Werz 1978; Chen et al. 2000; Huitrón-Reséndiz et al. 2002; Janus 2004). In PDAPP and TgCRND8 models of amyloid pathology altered search strategies in the Barnes maze and MWM have been associated with age and with age-related increases in amyloid pathology (Johnson-Wood et al. 1997; Chishti et al. 2001; Huitrón-Reséndiz et al. 2002; Janus 2004). However, PDAPP mice also displayed age-independent, non-spatial search strategies in the Barnes maze from 3-5 months of age (Huitrón-Reséndiz et al. 2002). Similar to this, chaining strategies were observed in the foraging tagging task in PDAPP mice from 6-8 months of age. This preceded the significant increase in levels of A β in the HPC of PDAPP mice (Chapter 4, experiment 6). It has previously been observed that 100-day old PDAPP mice have a reduced HPC volume, an effect likely caused by APP overexpression (Redwine et al. 2003). It is probable that these early detrimental effects of the HPC play a role in spatial search strategies in spatial memory tasks and may be a reason for the early differences in foraging behaviours observed in PDAPP mice at 6-8 months of age in experiment 3.

The significant increase in errors made in adjacent pots may not purely be an effect of chaining response. It is difficult to distinguish the extent to which the reported increase in errors made in the adjacent pots is a direct effect of this chaining strategy used by HPC lesioned and PDAPP mice. It may reflect a deficit in pattern separation ability. Spatial pattern separation is the process in which memory components containing similar or overlapping spatial information are separated to form independent, distinguished memories (Rolls 2013). This process is believed to occur through inputs to the HPC and subsequent processing of information in the DG and CA3 (Gold & Kesner 2005; Yassa & Stark 2011). Pattern separation is reportedly effected by age, but more significantly by the pathological effects of AD (Stark et al. 2010; Holden et al. 2012; Ally et al. 2013; Stark et al. 2013). However, to date, no study has reported any specific deficits in pattern separation in any transgenic model of AD. Interestingly, one report has predicted aberrant processing of information within

DG/CA3 networks based on differential c-fos expression in Tg2576 mice following exposure to novel spatial stimuli in a familiar arena setting (Palmer & Good 2011). Palmer and Good further predicted that, based on these results, APP overexpression would likely impact on pattern separation processes supported by the DG/CA3 region. In this study, PDAPP mice made a significantly greater proportion of errors in pots adjacent to one another in comparison to WT littermate controls; an effect that was also observed in mice with HPC cell loss. This overall distribution of errors appeared to be age-independent, however, numerically a greater proportion of errors were made in adjacent pots with age. It has previously been reported that 100-day old PDAPP mice have a 12.3% reduction in total HPC volume as well as a localized 28% volume reduction in the DG compared to age-matched WT controls (Redwine et al. 2003). Thus, APP overexpression and reports of HPC morphological abnormalities may contribute to the overall increase in errors made in adjacent pots as reported in experiment 3. Furthermore, evidence from fMRI studies have reported hyperactive signals in the CA3 and DG and hypoactive signals in the EHC in patients with MCI (a preclinical marker of AD) undertaking a pattern separation task (Petersen et al. 1999; Yassa et al. 2010). Although speculative, a significant increase in levels of insoluble A β 40 and a numerical increase in A β 42 were observed in the HPC of 7-month old PDAPP mice (Chapter 4, experiment 6), which may have also contributed to this early change in error distribution. None-the-less, this measure and speculative hypothesis of pattern separation deficits requires further examination, independent of the reported chaining response. Therefore, more specific task manipulation that may inhibit chaining responses, or more precise lesions or pharmacological intervention of the HPC sub regions would be required to confirm this pattern separation hypothesis in this task.

In summary, the aims of this experimental chapter were to validate a new behavioural assay that was sensitive to HPC function to assess SWM performance in PDAPP mice. The main features of this task was that it would act to be less aversive than tasks such as the MWM and RAWM, and require less repeated training and extensive testing protocols, as is necessary for example, in the RAM. The results from this study demonstrate that the HPC played a significant role in forging behaviour when animals were able to use extramaze information. PDAPP mice showed altered foraging behaviour and strategies as well as an age-related WM deficit. Due to the age-dependent increase in levels of A β in the PDAPP model (Chapter 4), it would appear that the foraging task acts as a unique tool for testing SWM performance that may be sensitive to amyloid burden. However, further characterisation and

evaluation of the task is required in order to provide a more conclusive understanding of the deficits and foraging behaviours observed in mice during this task. This task therefore presents itself as a rapid and unique assay in which to test age-related effects of SWM performance and foraging behaviours in animal models of progressive neurological disorders, such as AD.

Chapter 4: Characterising object recognition memory and age-related amyloid pathology in PDAPP mice

Chapter Overview

This chapter describes experiments that evaluate object recognition memory in the PDAPP model across a range of ages. The main aim of these experiments was to identify any age-dependent deficit that could be used as a behavioural target for *in vivo* administration of the anti-APP antibody, 2B3. Two versions of the object recognition procedure were used. The first was the object novelty recognition memory task. The second task was the object-in-place (OiP) procedure. The former task was used to assess the encoding and memory for object information, the latter to assess encoding of object-place associations. An age-related profile of soluble and insoluble levels of A β 40 and A β 42 was also carried out by ELISA in order to establish the relationship between age-related behavioural phenotypes and pathological hallmarks of excess amyloid production in the hippocampus (HPC) of the PDAPP model. The first section of the chapter will provide an overview and rationale for the use of object recognition memory paradigms. Subsequently, a succinct review of the current literature regarding age related changes in recognition memory in the PDAPP mouse model and other transgenic lines will be provided. In summary this chapter reports that PDAPP mice showed intact memory for object novelty/familiarity across age and delay intervals, but impaired OiP memory that manifested at 14-16 months of age. The latter appeared to be related to a significant increase in levels of A β in the hippocampus (HPC). The results are discussed with reference to previous findings and how they contribute to our understanding of recognition memory processes in PDAPP mice.

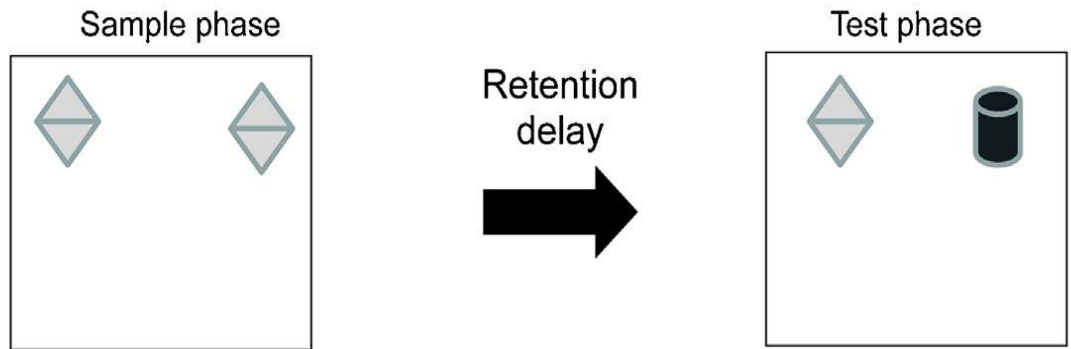
4.1 Chapter Introduction

The novel object recognition procedure was originally developed in 1988 by Ennaceur and Delacour as a one-trial task to examine recognition memory in rats. The task exploited the natural tendency of rodents to explore objects (Ennaceur & Delacour 1988). This task removed the need for explicit training and food deprivation (Aggleton 1985; Rothblat & Hayes 1987). In the basic procedure, rats are first placed in an arena with two identical objects. This sample trial (T1) lasted for 3 or 5 minutes before varying delays of up to 24 hours were introduced prior to the test trial. In the test trial (T2), rats were presented

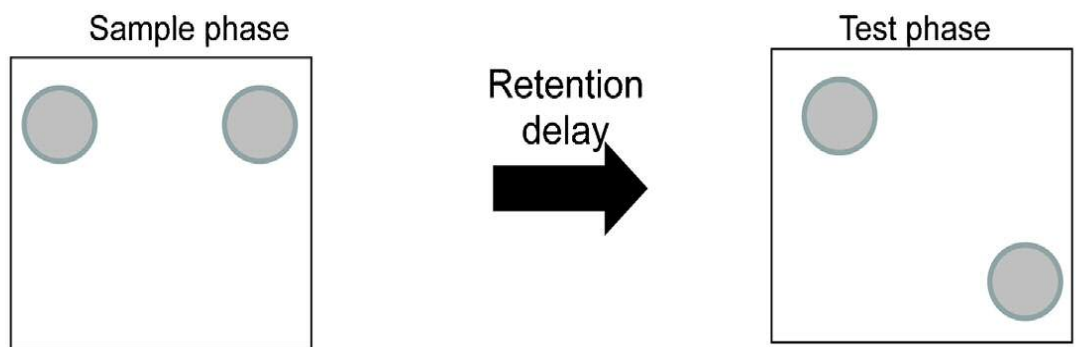
with one identical object that had been previously encountered in T1 and one novel object that had never been seen before. The total time spent exploring/interacting with the novel and familiar objects were recorded. Exploration was defined as directing the nose at a distance of ≤ 2 cm to the object and/or touching the object with the nose. Any further interaction with the object that was not directly exploring the object, ie, sitting on the object, was not considered exploring the object and was not scored. Findings from this study reported that rats showed a preference for exploring novel objects, which was highly influenced by the total time given in T1 to explore the sample objects and the interval between T1 and T2 (Ennaceur & Delacour 1988). This task therefore offered itself as a novel, more rapid one-trial memory testing protocol without the necessity for explicit training or positive/negative reinforcement.

Since the original report, the novel object recognition procedure has been used in many studies to assess recognition memory in a range of rodent models of neurological disorders, pharmacological studies, as well as studies designed to understand the neuroanatomical substrates of recognition memory (Antunes & Biala 2012; Warburton & Brown 2015a). The basic procedure has been extended to test memory for other features of objects, such as their spatial location (Figure 4.1 and Table 4.1). Results of this work are a comprehensive literature that has described major roles for three interconnected brain systems, the perirhinal cortex (PRC), HPC and medial prefrontal cortex (mPFC). Given that the experiments carried out in this chapter focus on object novelty memory and object-in-place (OiP) memory, the neural systems supporting information processing relative to these tasks will be the main focus. The object-location task will also be considered due to the HPC sensitivity in the processing of spatial information in this task (Barker et al., 2011). A more detailed review of the neural substrates of the temporal order memory can be found in Warburton et al. 2013 and Warburton & Brown 2015.

A. Object Recognition



B. Object Location



C. Object-in-place

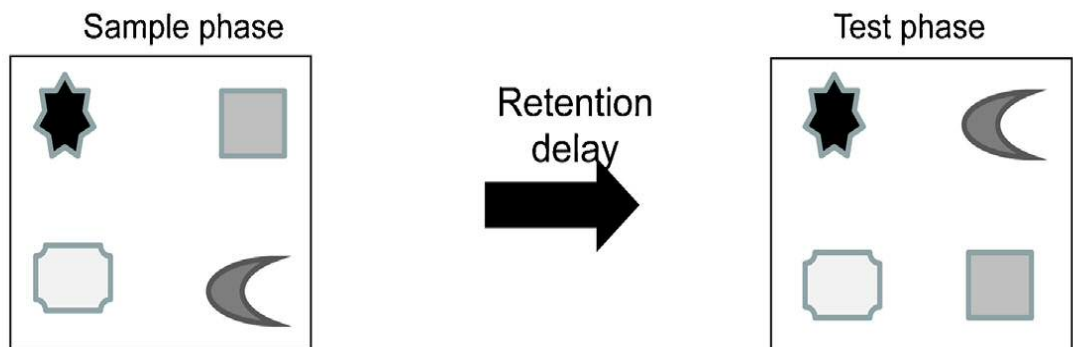


Figure 4.1: Illustration to show the varying object recognition memory tests used to assess object recognition memory in rodents. A. Object novelty memory. B. Object location memory. C. Object-in-Place memory. (Warburton & Brown 2015)

Task	Task Description	Successful Memory Performance	Anatomical Structures Involved
Object Novelty	Animals are exposed to two identical objects in a sample phase for a given period of time before a retention period. In the test phase one familiar object from the sample phase and one novel object is presented to the animal. These objects are presented in the same spatial locations as the objects presented in the sample phase.	Animals will explore the novel object in preference to the familiar object	Perirhinal Cortex <i>(Object-based information)</i>
Object Location	Two identical objects are presented to animals for a given period of time in the sample phase. Following a retention interval, animals are re-exposed to the same two objects, however, one is now in a novel spatial location.	Animals show preference to the object in the novel spatial location.	Hippocampus <i>(Spatial-based information)</i>
Object-in-Place	Animals are exposed to four different objects in the sample phase. Following a retention interval, animals are re-exposed to the same four objects. However, two objects remain in the same place as in the sample phase and two are switched in place.	The animal will explore the two objects that have switched from their original place.	Perirhinal Cortex <i>(Object-based information)</i> Hippocampus <i>(Spatial/contextual-based information)</i> Medial Prefrontal Cortex <i>(Spatial/contextual-based information)</i>

Table 4.1: Table describing the variations of object recognition memory tasks. These tasks are used in order to test object recognition memory and the functioning of specific neuroanatomical structures and/or pathways. Anatomical structures and neuronal circuits reviewed in Warburton et al. 2013 and Warburton & Brown 2015.

In animals, novel object recognition memory has been proposed to be dissociated from HPC function (Brown & Aggleton 2001). Brown and Aggleton proposed that the PRC supported object recognition memory and the HPC processed more complex information and stimuli, including spatial and environmental aspects (Brown & Aggleton 2001). Evidence from lesion studies showed that HPC ablation did not prevent rodents from discriminating novel and familiar objects. In contrast, lesions of the PRC resulted in an inability of animals to dissociate novel and familiar objects with delays of up to 24 hours (Bussey et al. 2000; Winters et al. 2004; Winters & Bussey 2005; Barker et al. 2007). However, other reports have identified a role for the HPC in object novelty memory (Gaskin et al. 2003; Hammond et al. 2004).

Gaskin (2003) reported that in rats with HPC lesions object novelty deficits were observed when familiar objects were presented prior to surgery, but not after. To determine this effect, rats were presented with sample objects for 5 minutes/day for 5 consecutive days, 1 or 5 weeks prior to surgery. 15-20 days after surgery object novelty memory was tested. Rats with HPC lesions showed impaired object novelty memory, however, sham controls showed a preference to explore novel objects over familiar. Object novelty memory was further tested in HPC lesioned rats after surgery with a new pair of familiar objects. Object memory was tested in all rats using a 15-minute and 24-hour delay period. In these trials, both HPC lesioned and sham control rats performed at similar levels. The authors concluded that extrahippocampal circuitry is involved in object recognition memory when the HPC is not involved in object encoding (Gaskin et al. 2003). However, an alternative or further observation could propose that the HPC plays a role in recognition memory over much longer delay periods than 24-hours. Unfortunately, Gaskin and colleagues did not repeat the primary experiment whereby rats were exposed to sample objects prior to a delay period of up to 7 weeks to observe if HPC lesioned rats were able to display novelty preference independent of the HPC over such a long-term delay period. Hammond and colleagues (2004) also reported that C57Bl/6 mice with HPC lesions showed object novelty deficits when recognition memory was tested 24-hours following sample phase, but not after a 5-minute delay. However, although less than sham controls, HPC lesioned mice still showed a significant preference to novel objects following a 24-hour delay and were therefore able to show memory towards the familiar object (Hammond et al. 2004).

These conflicting reports to the independent role of the PRC in object-novelty memory appear most likely an effect of delays ≥ 24 -hours. However, many studies report in-tact recognition memory using delays of ≤ 24 -hours (Clark et al. 2000; Broadbent et al. 2010;

Barker & Warburton 2011; Warburton & Brown 2015a). Thus, evidence has suggested that successful completion of the object novelty memory task is sensitive to PRC function, and is independent of the HPC and mPFC across short term delay periods, however delays ≥ 24 -hours require further investigation to better conclude the function of the HPC in long-term object recognition memory. More recently, studies have identified receptors involved in the processing of object recognition memory within the brain structures involved within object recognition memory tasks (Warburton et al. 2013). These precise receptor based mechanisms will be discussed in Chapter 5 and in more detail in the thesis General Discussion.

OiP memory refers to an animals' ability to associate object information with a place or location (see Figure 4.1 and Table 4.1). Lesion data has revealed that the mPFC, HPC and PRC are essential for successful memory performance in this task, in both rodents and monkeys (Bussey et al. 2000; Barker et al. 2007; Bachevalier & Nemanic 2008; Wilson et al. 2008; Barker & Warburton 2011). The interaction between these three brain regions plays a major role in the formation of object and place associations (Barker et al. 2007; Barker & Warburton 2011). Barker and colleagues (2007) reported that rats with bilateral lesions of the mPFC, PRC or unilateral lesions of the PRC and mPFC in contralateral hemispheres, showed a significant impairment in the OiP memory task compared to rats with unilateral PRC and mPFC lesions within the same hemisphere and SHAM controls (Barker et al. 2007). Barker et al., (ibid) also showed that all lesion groups were unimpaired in the object-location task and object novelty memory tasks following a 5 minute and 2 hour delay period, except rats with bilateral lesions of the PRC (Barker et al. 2007). These data provided evidence that an interaction between the mPFC and the PRC is essential for successful object and place associations required for the OiP task. In contrast, no lesions group was sensitive to the object-location task. These studies also confirmed the crucial role of the PRC in object-novelty memory.

A later study by Barker & Warburton (2011) examined the role of the HPC in recognition memory. In this study, rats initially received bilateral lesions of either the PRC, mPFC or HPC and were tested on object-novelty memory and spatial recognition (OiP and object-location) tasks (Barker & Warburton 2011). This study reported that HPC lesioned animals showed impairments in the OiP and object-location task, but no impairment in object-novelty detection with delays of up to 24 hours. PRC lesioned animals, however, showed impairments in the OiP task and object-novelty memory at all delays tested (5 minutes, 3 and 24 hours), whereas no impairment was observed in the object-location task. Therefore, the HPC appeared crucial in processing spatial information, while the PRC was essential for

encoding information regarding familiar objects. Collectively, both the PRC and HPC were essential for object recognition memory and spatial-associations (Barker & Warburton 2011). Similar to Barker and colleagues (2007), the interactions between the HPC, mPFC and PRC were assessed. Rats received unilateral lesions to the HPC combined with a further ipsilateral or contralateral lesion to either the PRC or the mPFC (Barker & Warburton 2011). These results showed that contralateral HPC-PRC and HPC-mPFC lesioned rats, but not ipsilateral lesioned groups were significantly impaired in the OiP task following a 5 minute delay, but not in the object-location or object-novelty task (Barker & Warburton 2011). This observation, confirmed a dual role of the PRC and HPC in the encoding of object and place associations and collectively with the dissociation study reported by Barker (2007), further suggested an intact PRC-HPC-mPFC circuit was essential for successful memory performance in the OiP task. Thus, disruption to this circuit by lesion or disease pathology is likely to impair the processing of object and place associative information.

Tg mice overexpressing mutated hAPP have elevated levels of A β that develop with age (Johnson-Wood et al. 1997; Hartman et al. 2005). In PDAPP mice, dense A β deposits appear in the molecular layer of the DG and the lateral entorhinal cortex (EHC) suggesting that the lateral perforant pathway may be particularly sensitive to amyloid pathology and may underpin some of the cognitive deficits in this mouse line (Games et al. 1995; Chen et al. 2000; Reilly et al. 2003). Consistent with this pattern of pathology, PDAPP mice have also shown age-dependent deficits in spatial learning and memory that correlated with levels of amyloid (Chen et al. 2000; Hartman et al. 2005). Other Tg models of amyloid pathology, such as Tg2576 mice display age-related increased levels of A β in regions that include the HPC and the mPFC (Hsiao et al. 1996; Kawarabayashi et al. 2001; Zhuo et al. 2008). Tg2576 mice also showed age-related deficits in spatial-based memory tasks, including the OiP task, while object-novelty memory remained intact (Hsiao et al. 1996; Hale & Good 2005; Good & Hale 2007). One interpretation of this pattern of results is that the PRC remained unaffected by amyloid pathology in aged Tg2576 mice. In contrast, object-place associative memories are clearly impaired. Collectively these data would suggest that impaired OiP memory in Tg2576 mice is likely due to amyloid-related pathology within the PRC-HPC-mPFC circuit previously described by Barker and Warburton (Barker & Warburton 2011; Warburton & Brown 2015). Given that similar age-related pathology is observed in the cortex and HPC of PDAPP mice, it is likely that the PDAPP model will be sensitive to spatial recognition memory in the OiP task.

To date, no studies have assessed object recognition memory in male PDAPP mice bred on a C57Bl/6 background. The dissociation between the HPC and PRC in processing object and spatial information permits assessment of these systems across age in relation to the *hAPP^{V717F}* mutation. Previous studies with PDAPP mice bred on a mixed background strain have reported an age-related deficit in object recognition memory (Dodart et al. 1999). However, this result has been inconsistent across laboratories (Chen, Chen, Knox, Inglis, Bernard, Martin, Justice, Mcconlogue, et al. 2000). There are a number of discrepancies between studies that must be considered. Differences in acquisition/familiarisation to the objects in the sample phase differed between both studies. Dodart (1999) allowed mice a 10 minute sample phase, whilst Chen (2000) allowed mice to accumulate a 30 second total inspection time of objects (or a maximum of 20 minutes sample phase). Previous reports have observed that an increased time for acquisition in the sample phase can significantly improve object recognition memory (Ennaceur & Delacour 1988; Antunes & Biala 2012). However, neither study reported contact times with objects for WT and PDAPP mice. The delay period used in both studies prior to testing also differed. Chen (2000) reported 10 seconds, 1 and 10 minutes, 1 and 4 hour delays, whereas Dodart (1999) used only a single 3-hour delay prior to testing. Dodart (1999) reported a significant difference at 9-10 months of age following a 3-hour delay. Chen (2000) reported no significant differences between PDAPP and WT mice up to latest age point tested (18-21 months) with a 4-hour delay. It therefore appears unlikely that this difference was an effect of delay, or age, and is tempting to speculate that contact times with objects may have contributed to the differences between studies.

One further experimental procedure differed across sample and test phase in these two studies that likely contributed to the differences in behavioural results reported. During the sample phase, Chen et al., (2000) exposed mice to two identical objects in fixed locations before replacing one of the sample objects with a novel object in the test phase. In contrast, Dodart and colleagues (1999) exposed mice to a single object in the sample phase and presented the familiar and a novel object in the test phase. The task used by Dodart et al., confounds object novelty with novel location information (of the novel object) and thus, the contribution of the spatial component to the recognition deficit in PDAPP mice remains unclear. Importantly, no study has yet directly assessed OiP memory in PDAPP mice. This analysis further highlights the need for careful and considered assessment of behavioural changes in Tg mice. Furthermore, mice from these studies were generated from different colonies and it is unclear if each study had an equal representation of each background strains phenotype.

The aim of the present experiment was to characterise object and object-in-place recognition memory in male PDAPP mice across an age range. Based on evidence for an age-related deficit in spatial memory in PDAPP mice and intact object novelty memory as reported by Chen (2000), the hypothesis for this experiment was that transgenic mice would show a task specific and age-related deficit in visuo-spatial memory.

4.2 - Experiment 4: Object Novelty Memory in PDAPP Mice

4.2.1 Experiment Introduction

This chapter is composed of 3 experiments; 4, 5 and 6. Experiment 4 assessed object novelty memory in PDAPP mice across a range of ages, 6-8, 10-12 and 14-16 months of age in order to determine any age-dependent changes. The protocol used to assess object recognition memory in this experiment was similar to the original protocol reported by Ennaceur and Delacour (1988) and that used by Chen and colleagues (2000). Experiment 5 assessed spatial and object associations using procedures similar to those adopted by Barker & Warburton (2011). Experiment 6 assayed brain A β level across an age range, similar to previous studies (Games et al. 1995; Johnson-Wood et al. 1997; Dodart et al. 2000; Hartman et al. 2005). This experiment used ELISA assays to quantify levels of soluble and insoluble A β 40 and A β 42 changed at 3, 7, 11 and 15 months of age in the HPC of PDAPP mice.

4.2.2 Design

Subjects, Apparatus, Method:

All mice used in the behavioural protocols to assess object novelty and OiP memory were identical to those described in Chapter 2 (section 2.3)

Mice used to quantify A β were obtained from separate cohorts. A total of 26 male PDAPP mice were used to determine the levels of A β across ages. 5 PDAPP mice were culled by cervical dislocation at 3 months of age and a further 7 at 7, 11 and 15 months of age. The HPC was dissected and snap frozen and stored at -80°C. All extraction and ELISA protocols are described in Chapter 2, (section 2.4).

Statistics

Data were analysed as described in Chapter 2 (section 2.3 and 2.4). Due to high levels of variability in data sets, violations of Shapiro Wilk's test and/or Levene's test were observed ($p < 0.05$). Therefore, data that violated these tests were subjected to transformation (ie. Square root, log-10) based on the level of positive/negative skew and reassessed. Data that no longer violated these assumptions were analysed by mixed measures ANOVA to determine age and genotype-related changes. Any further violations of Mauchly's Test of Sphericity were reported according to Greenhouse-Geisser analysis. One sample t-tests were used to determine if the performance of each group of mice was above chance (0.5) level. Where data remained in violation of these tests, despite transformations, non-parametric tests were used. This was only apparent in data assessing levels of A β 42. As these measures were compared as a between-subject analysis a Kruskal-Wallis test was performed with Dunn's test with a Bonferroni correction for multiple comparisons. The adjusted p-values are reported.

4.2.3 Experiment 4 - Results:

PDAPP mice showed intact object-novelty memory at 6-8, 10-12 and 14-16 months of age:

Sample Phase Contact Times

Table 4.2 shows the mean contact time with objects across sample phase of PDAPP mice and WT littermate controls at 6-8, 10-12 and 14-16 months of age. Inspection of these data suggests that PDAPP mice explored the two identical objects less in the initial sample phase, however both PDAPP and WT mice showed a reduced exploration of object contact times as the sample phase progressed. Exploration of the data and tests for normality revealed that distribution was not normal in specific data sets as assessed by Shapiro-Wilk's test, $p < 0.05$. For this reason, the data were transformed by square rooting which avoided further violations, $p > 0.05$. Results of repeat measures ANOVA revealed a significant main effect of genotype, $F(1, 27) = 8.6$, $p < 0.01$, a main effect of age, $F(2, 54) = 3.2$, $p < 0.05$, a main effect of sample phase, $F(1.6, 43.6) = 271.8$, $p < 0.001$, a significant genotype x sample phase interaction, $F(1.6, 43.6) = 16.8$, $p < 0.001$. No other main effects or interactions were significant (maximum $F(4, 108) = 2.1$, $p > 0.05$: sample phase x age x genotype).

Tests for simple main effects (between-subject comparison) revealed a main effect of genotype in terms of contact time at sample phase 1, $F(1, 27) = 21.3$, $p < 0.001$, and sample

phase 2, $F(1, 27) = 5.8$, $p < 0.05$, but not at sample phase 3, $F(1, 27) = 1.9$, $p > 0.05$. A further within-subjects main effect of sample phase in both PDAPP, $F(2, 26) = 56.2$, $p < 0.001$, and WT mice, $F(2, 26) = 161.8$, $p < 0.001$ was also reported. Thus, WT mice explored the objects more during sample phase 1 and 2 than PDAPP mice, however both groups performed at similar levels by sample phase 3. Indeed, both PDAPP and WT mice show habituation of object exploration across sample phase, indicating successful processing of objects information prior to test phase.

		WT			PDAPP		
		6-8 Months	10-12 Months	14-16 Months	6-8 Months	10-12 Months	14-16 Months
Sample	Mean	25.69	17.15	11.86	18.48	12.21	8.87
Phase 1	SD	6.39	3.91	3.10	7.01	3.63	3.71
Sample	Mean	21.40	14.10	9.38	13.51	9.90	8.01
Phase 2	SD	8.16	7.74	5.73	6.58	5.96	3.92
Sample	Mean	25.97	13.64	9.81	14.60	11.01	7.81
Phase 3	SD	9.76	7.69	6.78	9.62	10.10	6.55

Table 4.2: Mean contact times (in seconds) of WT mice (n=15) and PDAPP mice (n=14) across all 3 sample phases and ages tested. Standard deviations of the mean are also reported.

Test Phase Contact Times

Table 4.3 shows the mean contact time with objects during test phase for PDAPP mice and WT littermate controls across both delay periods (5 minutes and 24 hours) at 6-8, 10-12 and 14-16 months of age. Inspection of this table suggests that across both delay periods and all ages, WT and PDAPP mice explored novel objects more than familiar. It further suggests that WT mice explored objects more than PDAPP mice. Tests for normality revealed that distribution of data were not normal in specific data sets as assessed by Shapiro-Wilk's test, $p < 0.05$. Data were therefore transformed by square root to prevent further violations in distribution $p > 0.05$.

Transformed data were assessed by repeat measures ANOVA with genotype, object, delay and age as factors. Results revealed a significant main effect of genotype, $F(1, 27) = 22.1$, $p < 0.001$, a main effect of object, $F(1, 27) = 351.1$, $p < 0.001$, a significant object x genotype interaction, $F(1, 27) = 18.0$, $p < 0.001$, age x delay interaction, $F(2, 54) = 7.0$, $p < 0.001$, age x object interaction, $F(2, 54) = 13.8$, $p < 0.001$ and delay x object interaction,

$F(1, 27) = 121.8, p < 0.001$. No further main effects or interactions were reported; maximum effect, $F(2, 54) = 2.7, p > 0.05$; age x delay x genotype interaction.

Tests for simple main revealed that following a significant object x genotype interaction WT mice explored both the novel object, $F(1, 27) = 22.5, p < 0.001$ and familiar object, $F(1, 27) = 19.7, p < 0.001$, more than PDAPP mice. However, both WT mice, $F(1, 27) = 273.6, p < 0.001$ and PDAPP mice, $F(1, 27) = 101.5, p < 0.001$ explored the novel object in preference to the familiar object in the test phase when data were collapsed across age and delay.

An age x delay interaction revealed that mice explored objects more at 14-16 month of age following a 5-minute delay than mice at 6-8 months of age, $F(2, 26) = 4.1, p < 0.05$. No further main effects of age were reported. The main effect of delay reported that mice explored objects more following a 24-hour delay at 6-8 months of age, $F(1, 27) = 12.6, p < 0.001$. However, at 14-16 months of age, mice explored objects more following a 5-minute delay, $F(1, 27) = 4.5, p < 0.05$. No effect of delay was observed at 10-12 months of age, $p > 0.1$.

The age x object interaction revealed that mice explored the novel object more at 14-16 months of age when compared to mice at 10-12 months of age only, $F(2, 26) = 3.5, p < 0.05$. No further effect of age was observed in this interaction. A main effect of object was observed across all ages, whereby all mice explored the novel object more than the familiar; minimal effect, $F(1, 27) = 290.5, p < 0.001$.

A delay x object interaction revealed a main effect of delay on object exploration. Mice explored the novel object less following a 24-hour delay compared to novel object exploration following a 5-minute contact time, $F(1, 27) = 11.6, p < 0.01$. An opposite effect is observed for the familiar object whereby mice explored the familiar object more following a 24-hour delay than familiar object exploration following a 5-minute delay, $F(1, 27) = 60.8, p < 0.001$. Despite these differences a main effect of object was observed across both delay periods, whereby mice explored the novel object more than the familiar following a 5-minute delay, $F(1, 27) = 302.6, p < 0.001$ and a 24-hour delay. $F(1, 27) = 234.5, p < 0.001$.

Collectively these data suggest that PDAPP mice explored objects less in the test phase than WT mice. However, both WT and PDAPP mice still showed a preference to explore the novel object over the familiar object. An effect of delay appeared to increase forgetting of the familiar object as determined by increased exploration of this object

following a 24-hour delay period when compared to the 5-minute delay exploration time. However, this effect was the same across genotype and age.

		5 minutes				24 hours			
		Wild Type		PDAPP		Wild Type		PDAPP	
Age	Object	Mean	SD	Mean	SD	Mean	SD	Mean	SD
6-8 months	Novel	18.97	5.96	10.79	5.84	20.26	8.23	10.62	5.42
	Familiar	5.37	2.02	3.55	2.06	10.57	4.01	7.33	3.54
10-12 months	Novel	19.52	9.70	11.39	9.57	19.27	10.77	7.03	5.20
	Familiar	6.55	3.07	4.10	3.51	12.80	8.09	5.09	4.38
14-16 months	Novel	33.81	18.98	18.01	18.68	21.29	9.58	11.41	2.60
	Familiar	8.13	6.00	5.52	5.98	10.55	3.27	6.45	1.73

Table 4.3: Mean contact times (s) with novel and familiar objects of WT mice (n=15) and PDAPP mice (n=14) during the test phase following a 5-minute and 24-hour delay. Standard deviations (SD) of the mean are also reported.

Test Phase Discrimination Ratios

To ensure sensitivity towards the differences between groups, the data were converted into a discrimination ratio (DR) (time spent exploring the novel object/ time spent exploring the novel and familiar objects). Figure 5C shows the DR scores of both PDAPP and WT mice across all ages and delays. A repeat measures ANOVA was carried out on the ratio scores with factors of genotype, age and delay to confirm the absence of impairment between PDAPP mice and WT littermate controls. Results revealed no main effect of genotype, $F(1, 27) = 2.5$, $p > 0.1$, a significant main effect of age, $F(2, 54) = 7.7$, $p < 0.001$, and a main effect of delay, $F(1, 27) = 248.7$, $p < 0.001$. No further main effects or interactions were reported (maximum effect observed, genotype x delay interaction, $F(1, 27) = 2.8$, $p > 0.1$).

One sample t-tests showed that both WT and PDAPP mice differed from 0.5 (no discrimination) at each age and delay: WT mice at 6-8 months, 5 minutes and 24 hours delay, $t(14) = 22.2$ and 12.4 , $p < 0.001$, and PDAPP mice, $t(14) = 13.1$ and 5.5 , $p < 0.001$, WT mice at 10-12 months, 5 minutes and 24 hours delay, $t(14) = 18.7$ and 7.1 , $p < 0.001$ and PDAPP mice, $t(13) = 12.9$ and 8.6 , $p < 0.001$ and WT mice at 14-16 months, 5 minutes and 24 hours delay, $t(13) = 10.4$ and 11.6 , $p < 0.001$ and PDAPP mice, $t(13) = 16.1$ and 14.5 , $p < 0.001$.

These results confirm that both PDAPP and WT mice show an ability to discriminate novelty at a comparable level across all ages and delays tested in this study. Moreover, all DR

scores are significantly above chance level (0.5) indicating successful memory performance at each delay and age tested.

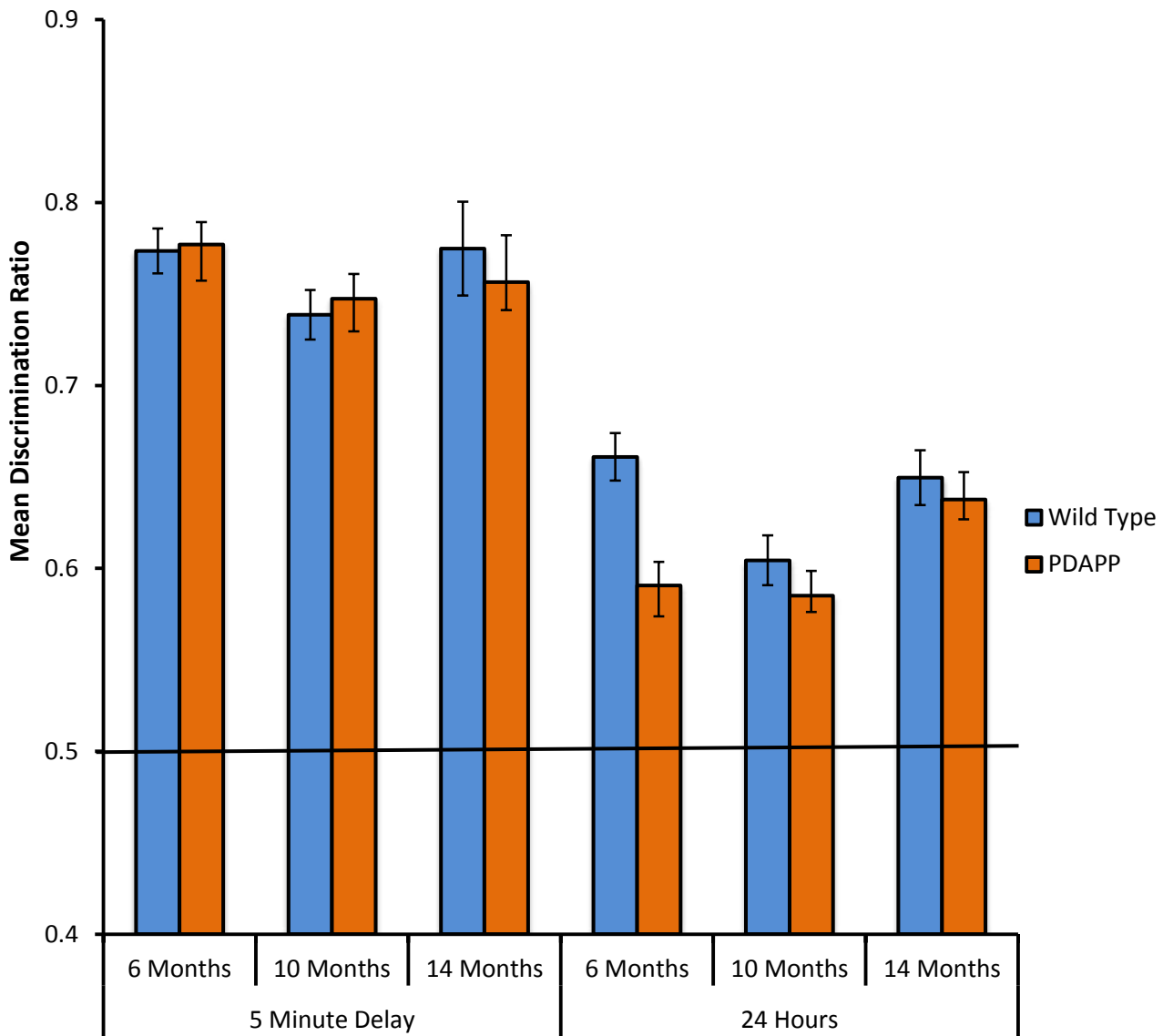


Figure 4.2 PDAPP mice show comparable novel object recognition memory to WT littermate controls across all ages and delays tested. Mean discrimination ratio (DR) calculated from test phase data for PDAPP (n=14) and WT (n=15) control mice. Chance level (0.5) is represented as a solid black line on the graph. Error bars show the S.E.M.

4.3 Experiment 5: Object-in-Place Memory in PDAPP mice

PDAPP mice show intact object location memory at 6-8 and 10-12 months of age, but impaired object-location memory at 14-16 months of age:

Sample Phase Contact Times

Table 4.4 shows the mean contact time with objects across sample phase of PDAPP mice and WT littermate controls at 6-8, 10-12 and 14-16 months of age. Inspection of these data suggests that PDAPP mice explored four different objects less in the initial sample phase, however both PDAPP and WT mice showed a reduced exploration of objects as the sample phase progressed. Exploration of data and tests for normality revealed that distribution of data were not normal as assessed by Shapiro-Wilk's test, $p < 0.05$. For this reason, the data were transformed by square root. Further exploration of transformed data revealed normal distribution across all WT and PDAPP exploration times, as assessed by Shapiro-Wilk's test, $p > 0.05$.

Transformed data were assessed by repeat measures ANOVA with genotype, sample phase and age as factors. Results revealed a significant main effect of genotype, $F(1, 27) = 22.9$, $p < 0.001$, a main effect of age, $F(2, 54) = 4.3$, $p < 0.05$, a main effect of sample phase, $F(2, 54) = 277.8$, $p < 0.001$, a significant genotype x age interaction, $F(2, 54) = 3.8$, $p < 0.05$, and a significant genotype x sample phase interaction, $F(2, 54) = 19.9$, $p < 0.001$. No other main effects or interactions were significant (maximum effect (Greenhouse-Geisser corrections), $F(2.4, 63.4) = 1.7$, $p > 0.05$: sample phase x age x genotype).

Tests for simple main effects carried out on the significant genotype x age interaction revealed WT mice explored objects more at 10-12 months of age, $F(1, 27) = 16.0$, $p < 0.001$ and 14-16 months of age, $F(1, 27) = 14.5$, $p < 0.001$, but not at 6-8 months of age, $F(1, 27) = 3.3$, $p > 0.05$. A further simple main effect of age showed that WT mice displayed greater contact time with objects at 14-16 months of age, $F(1, 27) = 6.0$, $p < 0.01$ when compared to contact times of WT animals at 6-8 and 10-12 months of age. This effect was not observed in PDAPP mice, which appeared to exhibit similar contact times across all ages examined, $F(2, 26) = 0.2$, $p > 0.05$.

Tests for simple main effects on the genotype x sample phase interaction revealed that WT mice explored objects more at sample phase 1, $F(1, 27) = 56.3$, $p < 0.001$, and sample phase 2, $F(1, 27) = 14.6$, $p < 0.01$, and sample phase 3, $F(1, 27) = 8.0$, $p < 0.05$ than PDAPP mice when

analysis was collapsed across age. Analysis revealed a main effect of sample phase in both PDAPP $F(2, 26) = 57.6$, $p < 0.001$, and WT mice $F(2, 26) = 189.5$, $p < 0.001$. These data indicate that WT mice showed greater contact with objects across sample phases than PDAPP mice. However, both PDAPP and WT mice showed reduced object exploration across sample phase, indicating both WT and PDAPP mice habituated to the four objects prior to test phase.

		WT			PDAPP		
		6-8	10-12	14-16	6-8	10-12	14-16
		Months	Months	Months	Months	Months	Months
Sample Phase 1	Mean	27.16	36.77	46.53	20.70	19.40	21.42
	SD	9.48	8.06	17.03	7.64	6.31	12.21
Sample Phase 2	Mean	18.26	21.57	29.80	14.59	11.99	16.01
	SD	5.95	10.19	14.55	5.70	4.67	11.52
Sample Phase 3	Mean	13.64	14.53	22.08	11.60	10.62	11.67
	SD	3.88	7.52	10.59	4.57	3.35	6.45

Table 4.4: Mean contact times (s) of WT mice (n=15) and PDAPP mice (n=14) across all 3 sample phases and ages tested. Contact time measures are taken from animals exploring four different objects. Standard deviations of the mean are also reported.

Test phase Contact Times

Table 4.5 shows the mean contact time with objects during test phase of PDAPP mice and WT littermate controls across both delay periods (5 minutes and 24 hours) at 6-8, 10-12 and 14-16 months of age. Data suggested that across both delay periods and all ages, WT and PDAPP mice explored objects in a novel spatial arrangement more than those in a familiar spatial location. However, WT mice explored novel arrangements more than PDAPP mice overall. It further suggests that WT mice explored objects more than PDAPP mice, as previously observed in object-novelty task. Similar to exploration times assessed in sample phase, exploration of data and tests for normality revealed that distribution of data were not normal as assessed by Sahpiro-Wilk's test, $p < 0.05$. Data were transformed by square root. Further exploration of transformed data revealed normal distribution across all WT and PDAPP exploration times, $p > 0.05$.

Repeated measures ANOVA with genotype, place, delay and age as factors. revealed a significant main effect of genotype, $F(1, 27) = 25.8$, $p < 0.001$, a main effect of place, $F(1, 27)$

= 276.6, $p < 0.001$, a main effect of delay, $F(1, 27) = 12.1$, $p < 0.001$, a significant place x genotype interaction, $F(1, 27) = 45.2$, $p < 0.001$, a significant place x delay interaction, $F(1, 27) = 14.1$, $p < 0.001$, a significant age x place x genotype interaction, $F(2, 54) = 4.6$, $p < 0.05$. No further main effects or interactions were reported (maximum effect; age x delay x genotype interaction, $F(2, 54) = 2.4$, $p > 0.05$).

Tests for simple main effects following a place x genotype interaction reported WT showed greater contact times with objects in novel locations, $F(1, 27) = 36.2$, $p < 0.001$, and familiar locations, $F(1, 27) = 22.4$, $p < 0.001$ than PDAPP mice. However, both WT, $F(1, 27) = 287.9$, $p < 0.001$, and PDAPP mice, $F(1, 27) = 44.6$, $p < 0.001$ explored objects in novel locations in preference to objects in familiar locations.

A place x delay interaction revealed that animals explored objects in familiar locations more following a 24 hour delay, $F(1, 27) = 33.0$, $p < 0.001$, compared to contact times with objects in familiar locations following a 5-minute delay. No difference was observed when comparing contact times with objects in novel locations, $F(1, 27) = 3.6$, $p > 0.05$. Despite this increased exploration of objects in familiar locations following a 24 hour delay, animals continued to explore objects in novel spatial locations more than objects in familiar locations following a 5 minute delay period, $F(1, 27) = 204.4$, $p < 0.001$ and a 24 hour delay, $F(1, 27) = 118.3$, $p < 0.001$.

A three-way interaction of age x location x genotype revealed that WT mice explored both novel and familiar object arrangements more than PDAPP mice across all ages (minimal effect = $F(1, 27) = 8.3$, $p < 0.01$, familiar exploration at 14-16 months of age). A main effect of place revealed that both WT and PDAPP mice explored objects in novel locations more than familiar locations at 6-8 and 10-12 months of age, however, only WT mice showed this preference at 4 -16 months of age (minimal effect; PDAPP mice at 10-12 months of age, $F(1, 27) = 23.6$, $p < 0.001$). PDAPP mice at 14-16 months of age showed no preference to objects in novel locations, $F(1, 27) = 3.2$, $p > 0.05$. No overall main effect of age was reported when comparing overall changes in total contact times with objects in familiar or novel locations (maximal effect; novel place exploration of WT mice, $F(2, 26) = 2.3$, $p > 0.1$).

Collectively this analysis showed that WT mice explore objects more than PDAPP mice. However, despite increased contact time of WT mice, both WT and PDAPP mice were able to discriminate objects in novel spatial locations at 6-8 and 10-12 months of age. However at 14-16 months of age WT mice maintained this ability, whereas PDAPP mice no

longer showed a preference to explore objects in novel spatial locations over familiar spatial locations.

		5 minutes				24 hours			
		Wild Type		PDAPP		Wild Type		PDAPP	
Age	Object	Mean	SD	Mean	SD	Mean	SD	Mean	SD
6-8 months	Novel	18.93	12.80	9.69	5.24	16.64	6.18	11.81	5.37
	Familiar	8.59	3.83	5.02	2.49	11.92	4.29	9.56	4.95
10-12 months	Novel	20.44	14.62	10.25	8.14	26.82	10.99	10.71	8.95
	Familiar	10.08	6.26	6.20	5.32	16.36	6.32	7.37	5.97
14-16 months	Novel	24.57	17.04	8.81	7.88	27.52	16.41	9.82	6.89
	Familiar	11.08	7.33	6.69	5.68	15.92	6.01	8.42	5.60

Table 4.5: Mean contact times (s) with objects in novel and familiar spatial locations of WT mice (n=15) and PDAPP mice (n=14) during the test phase following a 5-minute and 24-hour delay. Standard deviations (SD) of the mean are also reported.

Test Phase Discrimination Ratios

Figure 4.3 shows the DR scores of both PDAPP and WT mice across all ages and delays. A repeat measures ANOVA was carried out on the DR scores with factors of genotype, age and delay to confirm differences between groups observed in Table 4.5. Results revealed a significant main effect of genotype, $F(1, 27) = 54.9$, $p < 0.001$, a main effect of delay, $F(1, 27) = 25.9$, $p < 0.001$, a significant age x genotype interaction, $F(2, 54) = 9.2$, $p < 0.05$. No further main effects or interactions were reported (maximum effect; delay x age interaction, $F(2, 54) = 2.4$, $p > 0.1$).

Tests for simple main effects following a significant age x genotype interaction revealed that WT mice showed no change in OiP memory performance across all ages tested (maximal effect, 6-8 months vs 14-16 months, $F(2, 26) = 2.3$, $p > 0.1$). However, PDAPP mice showed a significant reduction in OiP memory performance when comparing PDAPP DR scores at 14-16 months of age with 6-8 and 10-12 months of age, $F(2, 26) = 9.8$, $p < 0.001$. Analysis further revealed a main effect of age in genotype. WT mice showed no difference in OiP memory performance compared to PDAPP mice at 6-8 months of age, $F(1, 27) = 1.9$, $p > 0.1$, or 10-12 months of age, $F(1, 27) = 2.4$, $p > 0.05$. However, PDAPP mice showed reduced memory performance compared to WT mice at 14-16 months of age, $F(1, 27) = 49.9$, $p < 0.001$.

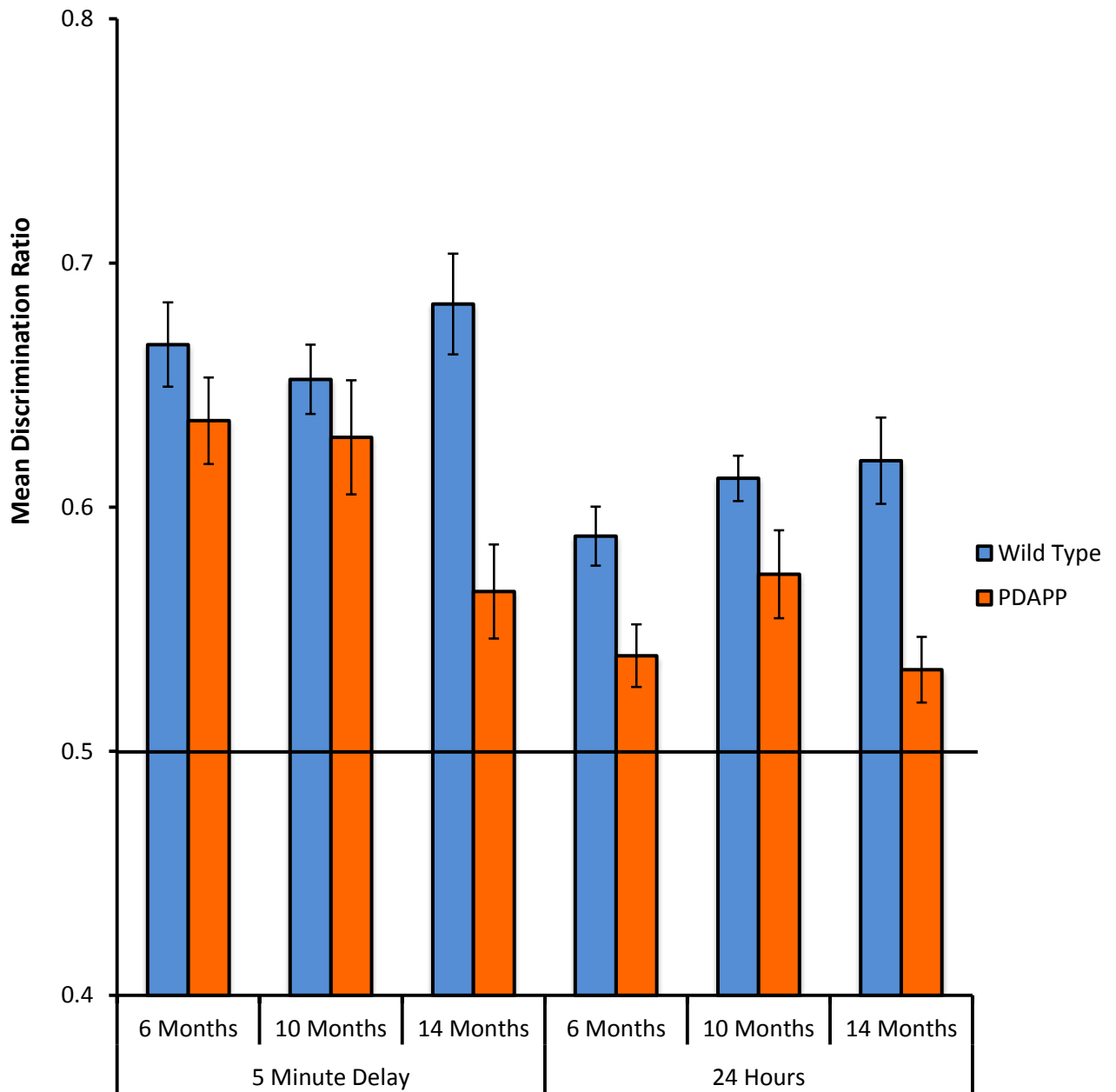


Figure 4.3 PDAPP mice show an age-dependent deficit in object-in-place memory. Mean discrimination ratio (DR) scores of WT (n=15) and PDAPP (n=14) mice with objects of novel object-place associations. Chance level (0.5) is marked with a solid black line. Error bars show the S.E.M.

One sample t-tests showed that both WT and PDAPP mice differed from 0.5 (no discrimination) at each age and delay: WT mice at 6-8 months, 5 minutes and 24 hours delay, $t(14) = 9.5$ and 8.7 , $p < 0.001$, and PDAPP mice, $t(13) = 8.8$ and 6.1 , $p < 0.001$, WT mice at 10-12 months, 5 minutes and 24 hours delay, $t(14) = 9.4$ and 12.8 , $p < 0.001$ and PDAPP mice, $t(13) = 6.4$ and 6.5 , $p < 0.01$ and WT mice at 14-16 months, 5 minutes and 24 hours delay, $t(14) = 6.0$ and 6.8 , $p < 0.001$ and PDAPP mice, $t(13) = 3.4$ and 3.9 , $p < 0.05$.

Collectively, these analyses of the DR scores revealed that both PDAPP and WT mice remained significantly above chance at all ages and delays tested. Therefore mice remained able to successfully complete the OiP memory task. However, PDAPP mice showed an age-dependent deficit in performance.

4.4 Experiment 6: Amyloid Pathology in PDAPP Mice

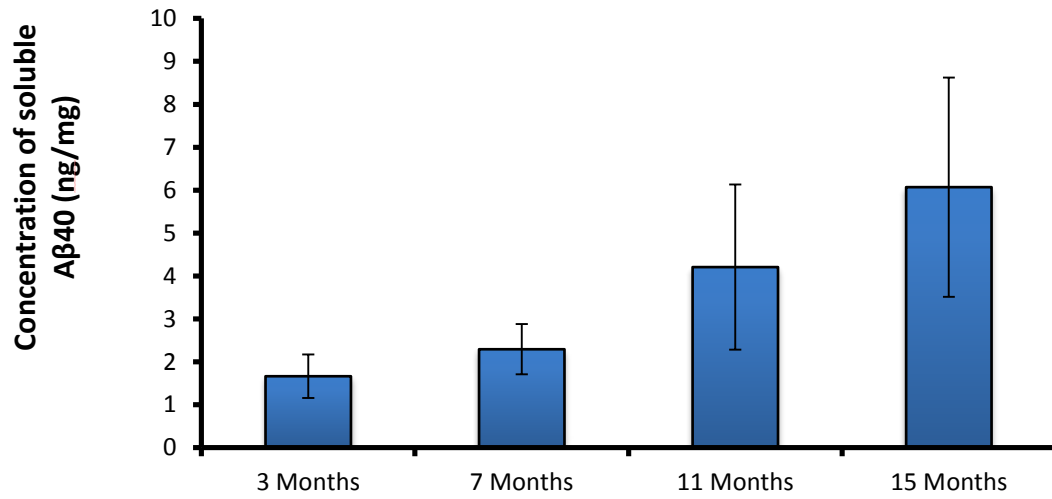
PDAPP mice showed an age-related increase in $A\beta$

Figure 4.4 shows an age-related profile of amyloid pathology in the HPC of ageing PDAPP mice. Inspection of Figure 4A shows an age-related increase in levels of soluble $A\beta_{40}$. However, despite levels of soluble $A\beta_{40}$ showing a general trend to increase with age, this observation was not confirmed statistically following analysis by Kruskal-Wallis test, $X^2(3) = 2.7$, $p > 0.1$. Nevertheless, a significant change in the levels of insoluble $A\beta_{40}$ was observed following analysis with Kruskal-Wallis test, $X^2(3) = 14.5$, $p < 0.01$. Dunn's test revealed that mice at 7 months of age ($p < 0.01$) and 11 months of age ($p < 0.01$) had a greater level of insoluble $A\beta_{40}$ when compared to mice at 3 months of age. No differences were observed with any age when compared to 15 months of age, $p > 0.1$.

However levels of both soluble and insoluble $A\beta_{42}$ (Figure 4.4 C, D) increased with age in the HPC of PDAPP mice. These age-related changes were confirmed by Kruskal-Wallis test in soluble $A\beta_{42}$, $X^2(3) = 10.5$, $p < 0.05$. Dunn's test for multiple comparisons showed a significant increase in the levels of soluble $A\beta_{42}$ when comparing mice at 3 months and 15 months of age, $p < 0.05$. A similar statistical report was observed for levels of insoluble $A\beta_{42}$, $X^2(3) = 9.9$, $p < 0.05$. Dunn's test confirmed a significant increase in levels of insoluble $A\beta_{42}$ from 3 months of 15 months of age in the HPC of PDAPP mice.

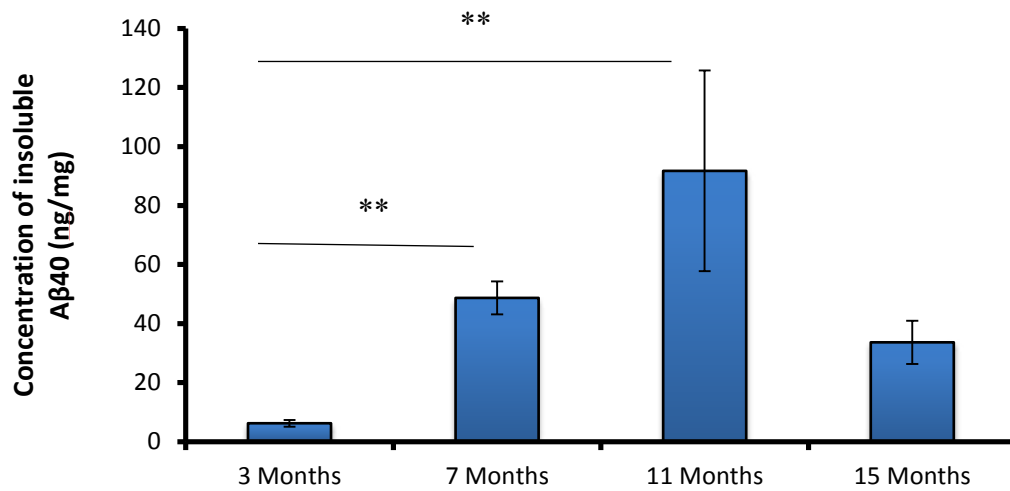
A

Soluble A β 40

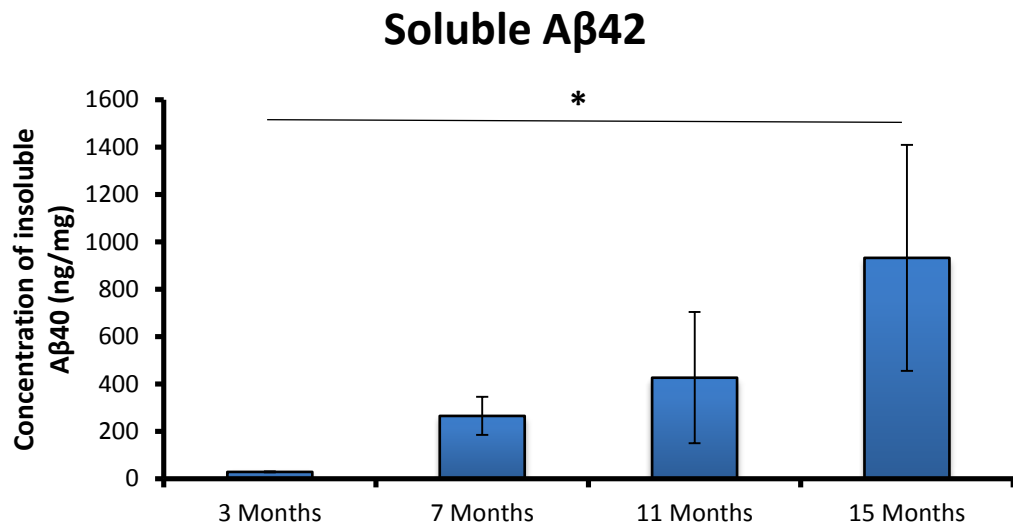


B

Insoluble A β 40



C



D

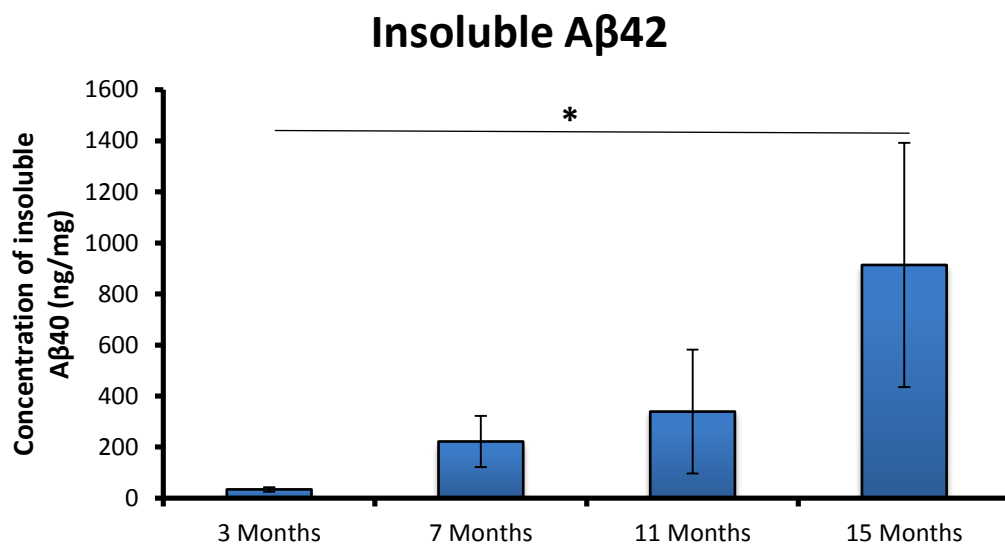


Figure 4.4: Levels of A β increase with age in the HPC of PDAPP mice. Soluble and insoluble levels of A β 40 (A and B) and A β 42 (C and D) were measured by ELISA. Amyloid levels were determined at 3 (n=5), 7 (n=7), 11 (n=7) and 15 (n=7) months of age. Error bars represent s.e.m. *p<0.05, **, p<0.01.

4.5 Chapter Discussion

The main aim of the present study was to examine the effect of the *hAPP*^{V717F} mutation on object recognition memory processes in PDAPP mice. The primary rationale for this was to identify any age-related change(s) in recognition memory that could be targeted for treatment with 2B3 (see Chapter 5). An additional rationale for this study was the conflicting evidence concerning an age-related deficit in object novelty detection reported in the literature (Dodart et al., 1999; Chen et al., 2000). Furthermore, despite some evidence for spatial memory impairment in PDAPP mice no study has established the effects of the mutation on detecting mismatches in object-in-place (OiP) associations. WT and PDAPP mice displayed OiP memory and showed a preference to explore objects in novel locations between 6-12 months of age. However, in contrast to their performance in object novelty detection, PDAPP mice showed a decline in OiP performance at 14-16 months of age. Concurrent with this decline in memory performance, soluble and insoluble forms of A β showed an age-related increase in the level of A β 42 in the HPC of PDAPP mice at 15 months of age. The absence of a deficit in object novelty discrimination in PDAPP mice in this study indicates that the representational processes and neural systems involved in novelty detection and object identity remained intact. Furthermore, it would argue for a specific age-dependent deficit in processing object-place information, which may be associated with an age-related increase in A β 42.

It is important to note that the sample phase data from both tasks revealed that PDAPP mice explored the objects less than WT mice at all ages. This suggests that *hAPP* overexpression may influence either locomotor activity, or engagement with objects. Spontaneous locomotor activity has been reported to be altered in PDAPP mice when compared to WT controls, however there is conflicting evidence. For example, Dodart and colleagues (1999) reported that PDAPP mice showed increased locomotor activity compared to WT control mice in ages up to 10 months (Dodart et al. 1999). However, Hartman and colleagues reported no significant difference in locomotor activity between PDAPP and WT mice in young and aged mice (exact ages not reported; Hartman et al. 2005). A notable difference between these studies is that Dodart and colleagues used male PDAPP mice bred on a mixed background, whereas Hartman and colleagues used male and female PDAPP mice bred on just a C57Bl/6 background (Dodart et al. 1999; Hartman et al. 2005). It has previously been observed that different background strains and gender show altered behavioural

phenotypes likely to be responsible for such differences between these two studies (Võikar et al. 2001; Şık et al. 2003). Due to the differences influenced by gender and background strain, it may be plausible that reduced contact times with objects reported in this chapter may be an effect of using male PDAPP mice bred on a C57Bl/6 background. Nevertheless, it is important to note both WT and PDAPP showed a significant reduction in object contact time across the sample phases. This suggests that short-term habituation remained intact in PDAPP mice and object information was encoded during the sample phase. This would further indicate that the deficit observed in OiP memory is unlikely to be explained by gross visual or motor impairments.

As discussed in the chapter introduction, the PRC is crucial in the processing of object information, while the HPC is essential for processing associative context/spatial information related to the object (Winters et al. 2004; Good et al. 2007; Barker & Warburton 2011). Given the involvement of the PRC in object novelty memory, and the HPC in processing spatial associative information, it is unclear whether this deficit in PDAPP mice reported by Dodart and colleagues reflected an impairment in object novelty detection *per se* or impaired processing of object position information. The data reported by Chen (2000) and that in this chapter showed intact object novelty memory in PDAPP mice (Chen, Chen, Knox, Inglis, Bernard, Martin, Justice, Mcconlogue, et al. 2000). It is therefore likely that PRC function in PDAPP mice is relatively unaffected by age and the *hAPP^{V717F}* mutation. However, the impaired OiP memory observed in PDAPP mice at 14-16 months of age and increased levels of A β in the HPC of 15 month PDAPP mice suggests impaired functioning of the HPC and processing of spatial information required for successful OiP memory performance. Moreover, the significant age-dependent impairment in OiP memory and increased levels of A β in the HPC at 14-16 months of age in PDAPP mice compliments previous findings of amyloid and age-related deficits in OiP memory in Tg2576 mice (Hale & Good 2005; Good & Hale 2007).

Interestingly, other Tg models of AD have also showed mixed recognition memory profiles. The TgCRND8, J20, APP/PS1 and 3xTg models have been reported to display object recognition deficits following amyloid deposition (Mucke et al. 2000; Chishti et al. 2001; Oddo et al. 2003; Clinton et al. 2007; Escribano et al. 2009; Francis et al. 2012; Heneka et al. 2013; McClean & Hölscher 2014). In contrast, PDAPP, Tg2576 and APP23 mice showed no deficits in object recognition memory (Chen et al. 2000; Hale & Good 2005; Heneka et al. 2006; Good & Hale 2007). Interestingly, the Tg models reported to display object recognition memory deficits all express multiple transgenes related to AD pathology, including more than

one APP mutation. PDAPP, Tg2576 and APP23 mice however only express single mutant *hAPP* transgenes. These deficits may therefore be sensitive to the overall level of mutant APP and other transgene expression. Moreover, there is evidence for PRC plaque pathology in TgCRND8 and APP/PS1 mice and hypoperfusion in the PRC of J20 mice from a young age (Minkeviciene et al. 2009; Romberg et al. 2012; Hébert et al. 2013). To date, no study has determined pathology in the PRC of APP23 mice, whilst almost no amyloid burden has been reported in the PRC of PDAPP mice by 9-10 months of age (Dodart et al. 2000). Plaque pathology in the PRC of Tg2576 mice has been reported at 22.5 months of age. However this age is much greater than the age (16 months) at which object recognition memory has been assessed in Tg2576 mice (Lim et al. 2005; Good & Hale 2007; Yassine et al. 2013). Collectively these data indicate that whereas some Tg models may show intact object recognition memory at ages where increased levels of amyloid are present in the HPC and cortical regions, others show impaired recognition memory, which may be related to altered PRC function. These differences appear to be based on the level of transgene expression and differences in regional amyloid pathology. Therefore, caution is required when comparing object recognition memory profiles in different Tg models of AD, as well as when considering object memory assessment of spatial/contextual associative information such as in this experimental chapter.

In conclusion, this study is the first to characterise object recognition memory in male PDAPP mice on a C57Bl/6 background. Following repeated exposure to objects, PDAPP showed comparable discrimination of familiar and novel objects over 5 minute and 24 hour delays at 6-8, 10-12 and 14-16 months of age. In contrast, PDAPP mice showed a deficit in OiP memory only at 14-16 months of age. Collectively these data reveal an age-dependent deficit in OiP memory that is unlikely to be a reflection of impairments in novelty detection *per se*. Furthermore, the deficit coincides with an elevation in A β levels in the HPC. These observations provide a sufficient rationale to evaluate the hypothesis that an antibody directed to the β -secretase cleavage site may have impact on A β production and cognition in aged PDAPP mice.

Chapter 5: 2B3 reverses an age-dependent cognitive deficit in PDAPP mice

Chapter Overview

This experimental chapter examines the hypothesis that inhibition of APP metabolism and A β production by administration of 2B3, an anti-APP antibody, is able to improve memory in PDAPP mice. To investigate this, chapter 6 has been divided into two main experiments. Experiment 7 assessed the *in vivo* effects of 2B3 in PDAPP mice following a 14-day intracerebroventricular (ICV) administration. Experiment 8 assessed *ex vivo* tissue of PDAPP mice treated with 2B3 or PBS for metabolites of BACE1 cleavage of APP and NMDAR-related synaptic plasticity mechanisms thought to underpin object-in-place (OiP) memory .

5.1 Chapter Introduction

β -Secretase as a therapeutic target for Alzheimer's disease

Despite promising early findings of anti-A β immunotherapy in preclinical AD models, little translational benefits has been observed in clinical trials, as discussed in Chapter 1 (section 1.5.3). Nevertheless, many current therapeutic strategies still focus on the role of amyloid and its proteogenesis in AD pathology. One specific target is BACE1, or the BACE1 cleavage site of APP. Many studies have reported BACE1 to play a significant role in the generation of A β . Inhibition of BACE1 activity should, therefore, prevent the production of A β . Consistent with the view, *BACE1* knock-out (KO) mice crossed with Tg2576 or PDAPP mice have almost undetectable levels of A β and β CTF (Luo et al. 2001; McConlogue et al. 2007). Furthermore, *BACE1* deficiency in Tg2576 and 5xFAD models is reported to rescue spatial working and reference memory deficits to comparable levels of WT controls (Ohno et al. 2004; Ohno et al. 2007). More recently, a human *BACE1* knock-in model has been reported (Plucińska et al. 2014). This model showed progressive AD-like pathology, including increased levels of β CTF and soluble A β *56 as well as cognitive abnormalities at 6 months of age. Evidence has also revealed A β -independent contributions to pathology specifically focusing on β CTF (Pimplikar et al. 2010; Tamayev et al. 2012; Kim et al. 2015). It has been reported *in vitro* that increased β CTF stimulated the overactivation of rab5, a regulator of early endosomes. This overactivation lead to endosomal swelling, accelerated endocytosis and impaired axonal transport of rab5 positive endosomes (Kim et al. 2015).

Moreover, *in vivo* inhibition of BACE1, but not γ -secretase cleavage of APP lead to improved LTP and novel object memory in a model of familial Danish dementia (Tamayev et al. 2012). This study suggested that β CTF and/or sAPP β may act as neurotoxic metabolites, independent of A β . Collectively, these studies provide evidence implicating BACE1 cleavage of APP in AD pathogenesis and identify BACE1 as a prominent target for AD therapy.

Since the discovery of BACE1 and its role in amyloidogenic processing, there has been considerable research into developing small molecule BACE1 inhibitors. First generation BACE1 inhibitors consisted of non-cleavable peptidomimetic analogues of the APP β -secretase cleavage site, which successfully reduced soluble A β both *in vitro* and *in vivo* (Kimura et al. 2005; Asai et al. 2006). However, these first generation peptide-based drugs faced early complications and could not deliver appropriate pharmacokinetic properties, including poor oral bioavailability, BBB penetrability and long serum half-life (De Strooper et al. 2010; Yan & Vassar 2014). Continued development of BACE1 inhibitors has led to small molecule inhibitors that exhibit significantly improved pharmacokinetics, display robust A β reduction and improved cognition in Tg models (Hussain et al. 2007; Fukumoto et al. 2010). As a result, several BACE1 inhibitors are currently in clinical trials (www.clinicaltrials.gov). One of the most promising of these, MK-8931 (Merck & Co.), is currently in a phase III clinical trial with a total of 1500 prodromal and mild-moderate AD patients. This compound showed much promise in earlier clinical phase 1b trials in mild-moderate AD patients, which reported a robust dose-dependent reduction of CSF A β concentrations without any serious adverse reactions (Forman et al. 2013).

However, one major concern about BACE1 inhibition is the potential side effects caused by chronic BACE1 inhibition in non-APP processing pathways. Early reports in BACE1 null mice suggested a lack of negative phenotypes, however subsequent studies have reported more than a dozen abnormalities (as reviewed in Yan & Vassar 2014). BACE1 is now reported to have multiple substrates and is a regulator of physiological pathways including neuron myelination, axon guidance and neurogenesis (von Arnim et al. 2005; Hu et al. 2008; De Strooper et al. 2010; Hitt et al. 2012; Hu et al. 2013; Yan & Vassar 2014). However, the effects of BACE1 knockout are present from conception and it is therefore unclear to what extent the phenotypes described previously may reflect BACE1 inhibitor side effects in later stages of life. For this reason, the risk of BACE1 inhibition-related toxicity will depend on the extent of therapeutic efficacy. The results of on going clinical trials will, no doubt, provide answers to these questions.

To overcome these challenges an alternative strategy has been developed using antibodies targeting the β -secretase cleavage site of APP (Arbel et al. 2005; Thomas et al. 2006). Arbel and colleagues (*ibid*) designed a monoclonal antibody (mAb) called “blocking β -site 1” (BBS1), which was raised against multiple antigenic peptides for the β -secretase cleavage site of APP (Arbel et al. 2005). These multiple antigenic peptides consisted of eight copies of the amino acid sequence representing the β -secretase cleavage site of healthy human APP (ISEVKMDA), as well as half of the Swedish APP mutation (ISEVKLDA). This approach was taken to overcome poor immunogenicity to short peptides as well as tolerance to self-antigens (Arbel et al. 2005). *In vitro* analysis of BBS1 treatment of CHO cells, transfected with the human APP 751 isoform, revealed that BBS1 reduced intracellular and secreted A β when compared to non-treated CHO-APP cells. Furthermore, Arbel and colleagues were able to visualize BBS1 internalisation and co-localisation with EEA1, a marker of early endosomes, where BACE1 cleavage of APP is believed to occur (Kinoshita et al. 2003; Arbel et al. 2005).

To determine if BBS1 had a similar effect *in vivo*, Tg2576 mice and mice harbouring the *hAPP* London mutation were subjected to chronic systemic BBS1 treatment (Moechars et al. 1999; Rakover et al. 2007; Arbel-Ornath et al. 2009). Results showed improved object recognition memory in Tg2576 mice receiving a dose of 16mg/kg. However, no changes in levels of soluble or insoluble A β or β CTF were reported, although a reduction in neuroinflammation was observed (Rakover et al. 2007). Mice expressing the *hAPP* London mutation, however, did show reduced A β plaque burden and reduced intracellular A β accumulation following BBS1 administration at 16mg/kg (Arbel-Ornath et al. 2009). These mice were further assessed on the Morris water maze (MWM), however no significant improvement was observed following BBS1 administration. Further studies by this group used 3xTg mice administered with BBS1 by ICV administration at 7.5 mg/kg/week for a period of 1 month at 17 months of age (Rabinovich-Nikitin et al. 2012; Rabinovich-Nikitin & Solomon 2014). Rabinovich-Nikitin and colleagues revealed BBS1 was able to improve object recognition memory performance in 3xTg mice to a level comparable to WT controls. *Ex vivo* tissue analysis also revealed that BBS1 treatment lead to reduced plaque size, total A β load and a reduction in phospho-tau and total GSK3 β levels (Rabinovich-Nikitin et al. 2012). It was later reported in these mice that BBS1 treatment reduced phospho-GSK3 β , the active form of GSK3 β , as well as p53, a signalling molecule associated with neuronal apoptosis (Jordán et al. 1997; Rabinovich-Nikitin & Solomon 2014). Collectively, these data suggest

that targeting the β -secretase cleavage site of APP may have therapeutic value for the treatment of AD-related pathology.

Thomas and colleagues (2006) reported that 2B12, a similar mAb directed against the β -secretase cleavage site of APP, inhibited BACE1 cleavage of APP and reduced levels of A β 40 in MOG-G-UVW and SH-SY5Y, an astrocytoma and neuroblastoma cell line (Thomas et al. 2006). It was later observed that 2B3 was also effective at blocking BACE cleavage of APP and showed similar effects to 2B12 (Thomas et al. 2011) Both 2B3 and 2B12 were raised against a 15 amino acid sequence spanning the human β -secretase cleavage site of APP (EEISEVKMDAEFRHD) (Thomas et al. 2011). However, both were observed to have different epitopes, but 2B3 showed a greater recognition of the β -secretase cleavage site of APP, as well as full length APP. Thomas et al., (2011) also showed that 2B3 was able to maintain a strong interaction with a secondary APP epitope containing the β -secretase cleavage site at pH4. This indicated that 2B3 should maintain an ability to inhibit BACE1 cleavage of APP in an equivalent acidic environment found in early endosomes, which provides optimal conditions for BACE1 activity (Vassar & Citron 2000). When determining BACE1 activity in a cell free assay containing only culture media, BACE1 and sAPP α , 2B3 and 2B12 showed little reduction in levels of sAPP α compared to media treated with a control N-terminal APP antibody. In fact, 2B3 virtually abolished BACE1 metabolism of sAPP α and it was determined that 2B3 inhibited BACE1 cleavage of the APP β -secretase cleavage site by “steric hindrance” (Thomas et al. 2011).

To further determine if both 2B3 and 2B12 were able to reduce levels of A β 40 or A β 42, Thomas et al. (2011) treated MOG cells with either 2B3 or 2B12 for 48 hours. Results indicated that 2B3 was more effective at reducing A β 40 and A β 42 as well as levels of β CTF when compared to 2B12 treated MOG cells. A more recent study by Thomas et al., (2013) showed that 2B3 was able to significantly reduce soluble A β 40 in mouse C57Bl/6 primary cortical neurons.

Given the evidence from Rabinovich-Nikitin et al., (2012) for a positive impact of mAb-mediated blockade of BACE1 processing on cognition in transgenic APP mice, the present study evaluated the hypothesis that inhibition of BACE1 cleavage of APP by 2B3 administration *in vivo* would ameliorate the cognitive deficit in visuo-spatial memory in PDAPP mice.

5.2 Experiment 7: *In vivo* assessment of 2B3

5.2.1 Introduction

As reported in Chapter 4, PDAPP mice displayed an age-dependent deficit in object-in-place memory at 14-16 months of age. Given the extensive work carried out to determine HPC involvement in the object-in-place task (as discussed in Chapter 4 and reviewed in Barker & Warburton 2013), this task was chosen over the foraging task to test the hypothesis that 2B3 would attenuate the cognitive deficits in PDAPP mice.

In this experiment, the same mice reported in Chapters 3 and 4 mice were administered 2B3 by ICV administration at 17-18 months of age. This age point provides an appropriate time at which to test 2B3 *in vivo*. Numerous studies have previously reported increased amyloid levels with age and further age-dependent cognitive deficits, sensitive to increased levels of A β pathology in the HPC (Chapter 3 and 4; Johnson-Wood et al. 1997; Chen et al. 2000; Hartman et al. 2005). This age point therefore allows an assessment of the abilities of 2B3 to reduce amyloid production and potentially alleviate cognitive dysfunction.

A concern regarding immunotherapy targeting the CNS is access to the brain via the BBB. The BBB is a highly regulated protective membrane separating the CNS from the periphery. Despite previous immunotherapy studies delivering mAbs via peripheral administration in animals, very few have reported positive antibody presence in the brain (Wilcock, Rojiani, Rosenthal, Levkowitz, et al. 2004; Yamada et al. 2009). Moreover, it has been estimated that approximately 0.1% of an antibody dose delivered peripherally will cross the BBB and spread into the brain (Banks et al. 2002). Therefore, to optimally assess the ability of 2B3 to inhibit β -secretase cleavage of APP and improve memory in PDAPP mice, 2B3 was delivered directly into the left lateral ventricle of the brain using osmotic minipumps (Alzet, Cupertino, USA). A pilot study had previously been carried out to show 2B3 was successfully delivered into the brain using this method and was able to spread into HPC and cortical structures (PhD Thesis: Hvoslef-Eide, 2013).

5.2.2 Method:

Design

To assess the effect of 2B3 on OiP memory, PDAPP and WT control mice used in Chapters 3 and 4 were assessed on the OiP task with a five-minute delay between the sample and test phase. The experimental protocol was identical to that described in Chapter 2. All mice used in this experiment were tested at 14-16 months of age prior to surgical implantation of osmotic minipumps in order to allow a pre-treatment as well as post-treatment measure to be taken. This allowed for both within-subjects and between subjects comparisons to be carried out.

Transgenic mice were administered with 2B3 or PBS vehicle control. A group of WT mice were also administered PBS vehicle control and a further WT group received no treatment. The latter group was included to assess whether osmotic minipump implants altered the performance of mice in the OiP task. Treatment was continuous for a 14-day period. On days 13 and 14, OiP memory was assessed and mice were culled following the final test on day 14 for *ex vivo* tissue analysis, discussed in Experiment 8 of this chapter. It was hypothesised that PDAPP mice receiving 2B3 treatment would show improved memory performance relative to PDAPP vehicle treated mice.

Subjects

A total of 21 PDAPP mice and 21 WT controls were used in this experiment. The same 14 PDAPP and 15 WT mice used in Chapters 3 and 4 were used in this study. A second cohort of animals were also used to replicate the age-related changes in PDAPP mice, as discussed in Chapter 3 and 4, and were also administered 2B3 in an identical fashion. These mice were used in order to increase the sample size of treatment groups in this study and improve the statistical power of the analysis used in this study (Baguley 2004; Cohen 1992). Therefore, a further 7 PDAPP and 6 WT mice were also used. These additional mice had undergone the same behavioural tasks in an identical fashion as described in Chapters 3 and 4, however only at 6-8 and 14-16 months of age. These mice therefore received similar levels of exposure to behavioural assays as the initial group of mice. At 17-18 months of age 21 PDAPP mice underwent surgical osmotic minipump fitting. Of these, 10 PDAPP mice received 2B3 (2.1mg/ml) treatment and 11 received PBS vehicle control. A further 10 age-matched WT mice underwent identical surgical procedures and received PBS vehicle only and 11 WT mice received no treatment.

Production of 2B3

2B3 producing hybridoma cells, stored in liquid nitrogen, were thawed on ice. Cells were resuspended in 1.5ml of cell culture medium [RPMI1640 (Sigma-Aldrich, Dorset, UK), 2mM Glutamine, 10% Foetal Bovine Serum, 1% Penicillin, 1% Streptomycin] before being added to a further 30ml of media. The solution was centrifuged at 1000rpm for 5 minutes at room temperature (RTP) and the supernatant removed. Pelleted hybridomas were resuspended in 1ml of media, pre-heated in an incubator (Pierce, Rockford, USA) at 37°C. Cells were transferred to a single well of a 24 well cell culture plate (Corning Incorporated, NY, USA) and grown at 37°C in 5% CO₂. Cells were split appropriately when confluent by resuspension into fresh, pre-heated media, and further grown in 25 and 75cm² flasks (Corning Incorporated). When cells were grown to confluence, the media containing 2B3 was collected at approximately 50% cell viability. The media was centrifuged at 1000rpm for 5 minutes at RTP and the supernatant was collected and stored at 20°C.

Concentration

2B3 cell media was concentrated using Amicon Ultra centrifugal filter units (Millipore, Billerica, USA) with a 100kDa molecular weight cut off. 10ml of media was centrifuged in a JS7.5 swing bucket rotor (Beckman Coulter, High Wycombe, UK) at 3000g at 4°C for 1 hour. Following centrifugation, media filtrate was discarded, and 10ml of fresh media was added. This pattern continued until approximately 70ml had passed through one centrifugal filter unit. When multiple centrifugal units were used, the concentrated antibody was pooled before the concentration of 2B3 was determined.

Quantification of 2B3 using ELISA

The methods utilised to determine the concentration of concentrated 2B3 were based on the procedure used by Thomas et al., (2006, 2011). A 96-well plate was coated in a sheep anti mouse IgG (Greiner Bio One, Frickenhausen, Germany) at a concentration of 1:4000, diluted in a carbonate/bicarbonate buffer (15mM Na₂CO₃, 35mM NaHCO₃, pH 9.6) and left overnight at 4°C. The plate was then washed 3 times with PBST (137mM NaCl, 2.5mM KCl, 8mM Na₂HPO₄, 1.5mM KH₂PO₄, 0.05% Tween20) between each stage, and all incubations were carried out at RTP. Following washing, the plate was then aspirated and blocked with 0.1% (w/v) milk powder in PBST for 1 hour. Standards, samples and negative controls were then added in duplicate at 100uL/well and were incubated for 2 hours at RT. Standards ranged from 200 0.3ng/ml in doubling dilutions. Doubling dilutions of the 2B3 sample were

applied, from 1/1000 to 1/2,048,000. 2B3 was detected following a 1-hour incubation with 100uL/well secondary goat anti-mouse antibody conjugated to HRP, 1:6000 (Pierce). The enzyme substrate, o-phenylenediamine (OPD) (Sigma-Aldrich), in 0.1M citrate phosphate buffer (24mM citric acid, 51mM Na₂HPO₄, pH5) was applied at 100uL/well and incubated for approximately 20 minutes in the dark. The reaction was stopped using 50µl 2.5M H₂SO₄ and read at 492nm using a spectrophotometer. The concentration of 2B3 was then determined using GraphPad Prism 4.0 and Microsoft Excel.

Purification

Concentrated media containing 2B3 was purified using an affinity chromatography MAb Trap™ Kit (GE Healthcare, Buckinghamshire, UK) with the aim of both purifying and further concentrating the IgG solution. Binding and elution buffers, as well as the antibody sample were passed through a HiTrap Protein G column containing recombinant protein G, genetically altered to lack the ability to bind albumin, while maintaining a high affinity for IgG. Binding and elution buffers within the kit were diluted 1:10 with dH₂O prior to use, and all flow through was collected in 1.5ml Eppendorf tubes containing 60uL neutralising buffer to maintain IgG activity. The column was washed with dH₂O at approximately 1 drop per second, to clear ethanol residues following storage. The column was equilibrated with 3ml of binding buffer before 2B3 was applied. 10mls of binding buffer was passed through the column to remove molecules other than the 2B3, before 5ml of elution buffer was passed to release 2B3.

Dialysis

The purified antibody was dialysed to remove MAb Trap buffers using PBS (137mM NaCl, 2.5mM KCL, 8mM Na₂HPO₄, 1.5mM KH₂PO₄, pH7.2) to ensure compatibility with the Tris and Glycine based buffers of the MAb Trap™ Kit. Slide-A Lyzer Dialysis Cassettes (Pierce) of 0.5 – 3ml sample volume with a 10kDa molecular weight cut off were utilised. Cassettes were rotated in 2 litres of PBS at 4°C overnight before 2B3 was collected. The PBS used for 2B3 dialysis was used as the vehicle control in the minipump study. Following dialysis, one last quantification measure was carried out in order to determine the final concentration of purified 2B3. This was performed using the NanoVue spectrophotometer (GE Healthcare Ltd, Buckinghamshire, UK), which is able to quantify IgG concentrations. A final concentration of 2.1mg/ml was determined.

Sterilisation

Once the final concentration was determined, both 2B3 and PBS vehicle were sterilised. This was carried out by passing 2B3 and vehicle PBS through a 5µm sterile filter into sterile collection tubes. Following this, treatment samples were frozen at -20°C until required.

Surgical Insertion of Osmotic Minipumps

The purified and sterilised 2B3 was administered to PDAPP mice by intracerebroventricular (ICV) infusion via osmotic minipumps. Sterile PBS was administered in an identical manner as a vehicle control.

Osmotic minipumps (Alzet, 1002) administered both solutions at a constant flow rate of 0.25µl/hour for a period of 14 days. Minipumps were filled with 200µl of either 2B3 or vehicle and back-filled through a 2.5cm catheter attached to a 28G cannula (Alzet, 0004760). Minipumps were then inserted into the mice as follows: Mice were anaesthetised by isoflurane carried by O₂ for the duration of stereotaxic surgery. Once the mouse was under anaesthesia, one small hole was drilled through the skull of the animal 0.5mm posterior and 1.2mm lateral to bregma where the 28G cannula was then inserted upto 3.0mm ventral into the left lateral ventricle of the brain. The cannula was fixed to the skull initially with four screws and secured in place using dental cement. A small subcutaneous cut was made at the lower neck of the mouse and the minipump was carefully inserted below the skin between the scapulae, spanning the lower back of the animal. Mice were sutured and allowed to recover in an incubator. All mice were then housed individually to prevent any chance of interference with the sutures, minipumps or mounts.

Behavioural Procedure

The OiP behavioural procedure was carried out using an identical method to that described in Chapter 2. However, only a 5-minute delay interval was interpolated between the sample and test phase.

Scoring and Data Analysis

Scoring and data analysis were carried out in an identical manner to that described in Chapter 2.

5.2.3 Experiment 7: Results

Pre-treatment analysis

Prior to minipump implantation, WT and PDAPP mice were divided into 4 groups; WT untreated (WT UT), WT vehicle (WT V), PDAPP vehicle (PDAPP V) and PDAPP 2B3. To ensure that the groups were matched in terms of their surgical assignments two separate 2x2 repeat measures ANOVAs were carried out on sample phase and test phase contact time data and a one-way ANOVA was performed with post-hoc Tukey analysis on DR data previously reported in Chapter 4, Experiment 6.

Data displaying contact times in sample phases 1-3 can be observed in Table 5.1. Contact times, violated Levene's test of equality of error variances, $p < 0.05$. Therefore, the data were transformed by square root transformation. Despite transformation no longer violating this test, Mauchly's test of Sphericity remained violated, $p < 0.05$. Therefore, Greenhouse-Geiser comparisons were reported where appropriate. Repeated measures ANOVA revealed a significant main effect of sample phase, $F(1.7, 63.5) = 50.2$, $p < 0.001$, no significant sample phase x treatment group interaction, $F(5.0, 63.5) = 0.6$, $p > 0.5$ and a significant main effect of treatment group, $F(3, 38) = 5.6$, $p < 0.01$. Post-hoc Tukey analysis of the significant main effect of treatment group revealed that only WT UT mice explored objects (when collapsed across sample phase) more than PDAPP V mice, $p < 0.01$. No further significant differences in total contact times were reported (WT V vs PDAPP V, $p = 0.052$).

A repeat measures ANOVA analysed the pre-treatment contact times. Times displayed in Table 5.2 were transformed by square root due to violations in Levene's Test of Equality of Error Variance. The analysis reported a significant main effect of object location, $F(1, 38) = 70.4$, $p < 0.001$, a significant object location x treatment group interaction, $F(3, 38) = 10.3$, $p < 0.001$ and a significant main effect of treatment group, $F(3, 38) = 9.1$, $p < 0.001$. Post-hoc Tukey analysis of the between-subject main effect collapsed across object location revealed no significant difference between WT UT and WT V mice, $p > 0.1$. WT UT mice showed a greater contact time with objects than PDAPP V, $p < 0.001$ and PDAPP 2B3, $p < 0.01$. No further significant differences between treatment groups were reported. Because there was a significant object location x treatment group interaction, tests for simple main effects were performed. Between-subjects comparisons revealed that WT UT mice explored objects in novel locations more than both PDAPP groups, $p < 0.001$. WT V mice explored objects in novel locations more than PDAPP V mice only. No further significant effects were reported

when the novel location data. WT UT mice showed a greater contact time with objects in familiar locations than PDAPP V mice only, $p < 0.05$. No further differences in contact times with objects in familiar locations were reported. Within-subjects analysis to determine if objects in novel locations were explored significantly more than familiar locations revealed that both WT UT and WT V mice explored objects in novel locations significantly more than objects in familiar locations, $p < 0.001$. Neither PDAPP V or PDAPP 2B3 mice explored objects in novel locations more than objects in familiar locations, both p 's > 0.05 .

One-way ANOVA analysis of DR scores revealed a significant main effect of group, $F(3, 41) = 5.8$, $p < 0.01$. Post-hoc analysis revealed no significant differences between either WT group, $p > 0.5$, or PDAPP group, $p > 0.5$. The only significant differences were reported when comparing WT groups to PDAPP groups respectively, p 's < 0.05 , which was previously reported in Chapter 5, Experiment 6. Taken together, this pre-treatment analysis showed that mice habituated to objects across sample phases without differential effects across treatment group as determined by a lack of sample phase x treatment group interaction. Test phase contact times revealed that both WT groups showed a discrimination toward objects in novel locations over objects in familiar locations, whereas both treatment groups of PDAPP mice did not. This was further observed when contact times were converted to DRs, both WT groups showed significantly greater DR scores than either PDAPP group. Collectively, dividing WT and PDAPP mice into 4 separate treatment groups showed no significant differences within genotypes or novel differences between groups previously unreported in Chapter 4. Therefore, any changes in behaviour reported post surgical treatment cannot be attributed to pre-treatment differences in performance.

Control groups analysis

The initial analysis following pre- and post-treatment determined if any changes were observed by the implantation of osmotic minipumps in WT mice. This analysis was performed with the intention to collapse across both WT control groups and prevent unnecessary multiple comparisons in the mixed measures ANOVA used to determine the effects of 2B3 *in vivo*. Both contact times with objects and DR scores were analysed using repeated measures ANOVA. Two main factors, treatment group (between-subject) and time (pre- and post-treatment intervention; within-subject), were analysed. One further within-subject analysis of object location was analysed for the contact time data as well as the effect

of sample phase was assessed prior to test phase. Due to violation of Levene's test of equality of error variances, all contact time data were transformed by square root.

Sample phase contact times were analysed in a 2x3x2 repeat measures ANOVA. Analysis revealed a significant main effect of sample phase, $F(2, 38) = 53.7$, $p < 0.001$, no significant sample phase x treatment group interaction, $F(2, 38) = 2.0$, $p > 0.1$, no significant main effect of time (pre-treatment and post-treatment), $F(1, 19) = 0.9$, $p > 0.1$, no significant time x treatment group interaction, $F(1, 19) = 0.04$, $p > 0.5$, no significant sample phase x time interaction, $F(2, 38) = 0.9$, $p > 0.1$ and no significant sample phase x time x treatment group interaction, $F(2, 38) = 1.7$, $p > 0.1$. No significant main effect of treatment group was reported, $F(1, 19) = 2.9$, $p > 0.1$. Therefore the effect of sample phase remained equal across both WT groups. No effect of surgical implantation of osmotic minipumps and vehicle administration in WT mice was apparent compared to mice that received no treatment.

Contact times with objects in novel and familiar locations were analysed with a 2x2x2 repeat measures ANOVA. This analysis reported a significant main effect of object location, $F(1, 19) = 89.4$, $p < 0.001$, no significant object location x treatment group interaction, $F(1, 19) = 1.8$, $p > 0.1$, no significant main effect of time, $F(1, 19) = 0.7$, $p > 0.1$, no significant time x treatment group interaction, $F(1, 19) = 1.7$, $p > 0.1$, no significant object location x time interaction, $F(1, 19) = 0.6$, $p > 0.1$, no significant object location x time x treatment group interaction, $F(1, 19) = 1.7$, $p > 0.1$. No significant main effect of treatment group was reported, $F(1, 19) = 2.5$, $p > 0.1$. These results showed no effect of minipumps implantation in WT mice.

DR scores were analysed using a 2x2 repeat measures ANOVA. No significant main effect of time, $F(1, 19) = 0$, $p > 0.5$ and no significant group x treatment time interaction, $F(1, 19) = 0.1$, $p > 0.5$ was reported. There was no significant main effect of group, $F(1, 19) = 0.13$, $p > 0.5$. As no changes were observed following within- and between-subject comparisons the data from both WT groups were collapsed for all subsequent analyses.

2B3 treatment and habituation to objects

Sample phase data (Table 5.1) obtained following 2B3 treatment was analysed using a 3x2x3 repeat measures ANOVA. These violated Levene's test of equality of error variances and was therefore transformed using square root. Despite this transformation, sample phase data violated the Mauchly's Test of Sphericity and analysis of this factor was performed with Greenhouse-Geisser corrections. This analysis revealed a significant main effect of sample

phase, $F(1.6, 63.2) = 88.4$, $p < 0.001$, no significant sample phase x treatment group interaction, $F(3.2, 63.2) = 0.5$, $p > 0.1$, no significant main effect of time, $F(1, 39) = 1.3$, $p > 0.1$, no significant time x treatment group interaction, $F(2, 39) = 0.1$, $p > 0.5$, no significant sample phase x time interaction, $F(2, 78) = 1.2$, $p > 0.1$ and no significant sample phase x time x treatment group interaction, $F(4, 78) = 0.9$, $p > 0.1$. A significant main effect of treatment group was reported, $F(1, 39) = 16.9$, $p < 0.001$. A post-hoc Tukey analysis revealed that WT mice explored objects significantly more than PDAPP V mice, $p < 0.001$ and PDAPP 2B3 mice, $p < 0.01$. No significant difference in contact times was reported between either PDAPP treatment group, $p > 0.1$. These results indicate that 2B3 treatment did not effect habituation of object contact times in PDAPP mice.

Sample Phase		Treatment Group							
		WT Untreated		WT Vehicle		PDAPP Vehicle		PDAPP 2B3	
		Pre	Post	Pre	Post	Pre	Post	Pre	Post
Sample	Mean	43.60	43.52	34.53	27.16	17.10	17.60	24.23	23.10
Phase 1	SD	20.90	13.45	20.56	10.87	6.28	10.62	15.86	10.24
Sample	Mean	28.84	24.32	25.17	19.47	9.95	9.06	15.95	15.71
Phase 2	SD	14.82	11.71	12.61	13.49	4.14	7.28	10.49	8.81
Sample	Mean	23.40	17.56	15.67	16.35	8.22	4.80	12.46	10.30
Phase 3	SD	15.71	7.75	8.68	8.90	3.66	3.01	8.28	7.95

Table 5.1: Mean contact time scores with objects of WT untreated (n=11), WT V (n=10), PDAPP V (n=11) and PDAPP 2B3 (n=10) mice across sample phase 1-3 and standard deviations (SD). Both pre- and post-treatment scores are reported in seconds.

2B3 treatment and object-in-place memory in PDAPP mice

Table 5.2 shows the mean contact times with objects in novel and familiar locations across treatment groups and pre- and post-treatment intervention. A 2x2x3 repeat measures ANOVA analysed the main effects of object location, time and treatment group. This analysis revealed a significant main effect of object location, $F(1, 39) = 84.1$, $p < 0.001$, a significant object location x treatment group interaction, $F(2, 39) = 15.5$, $p < 0.001$, no significant main effect of time, $F(1, 39) = 0.002$, $p > 0.5$, no significant time x treatment group interaction, $F(2, 39) = 0.8$, $p > 0.1$, no significant object location x time interaction, $F(1, 39) = 1.2$, $p > 0.1$, no significant object location x time x treatment group interaction, $F(2, 39) = 2.8$, $p > 0.05$. A

significant main effect of treatment group, $F(2, 39) = 10.1$, $p < 0.001$ was also reported. Post-hoc Tukey analysis of the significant main effect of treatment group revealed that WT mice had higher contact times with objects than either PDAPP V mice, $p < 0.01$ and PDAPP 2B3 treated mice, $p < 0.05$. No significant difference in contact times were observed between either PDAPP treatment group, $p > 0.1$. The significant object location x treatment group interaction was further analysed with tests for simple main effects. Within-subjects comparisons reported that all groups showed an ability to discriminate objects in novel locations as determined by a significant difference in exploration times between objects in novel vs familiar locations, p 's < 0.05 . Between-subjects analysis revealed that WT mice explored objects in novel locations more than PDAPP V mice, $p < 0.001$, and PDAPP 2B3 mice, $p < 0.01$. WT mice also showed greater contact times with objects in familiar locations than PDAPP V mice, $p < 0.01$, but not PDAPP 2B3 mice, $p > 0.1$. No significant difference was reported between PDAPP mice for objects in novel or familiar locations, both p 's > 0.1 . This analysis suggests that 2B3 treatment in PDAPP mice did not increase overall contact time with objects. 2

Figure 5.1 displays the DR scores of mice before and following treatment with 2B3. These data were analysed using a 3 x 2 repeat measures ANOVA to determine if 2B3 treatment had any effect on OiP memory in PDAPP mice. The two main factors analysed were treatment (PDAPP Vehicle, PDAPP 2B3 etc.) and Time (pre- vs post-treatment). The analysis revealed a significant main effect of time, $F(1, 39) = 4.12$, $p < 0.05$ and a significant treatment x time interaction $F(2, 39) = 3.27$, $p < 0.05$ and a significant main effect of treatment, $F(1, 39) = 16.59$, $p < 0.001$. A post-hoc Tukey analysis of the main effect of treatment revealed that overall WT mice showed higher DR scores than PDAPP vehicle treated mice, $p < 0.001$ and PDAPP 2B3 treated mice, $p < 0.05$. It was also revealed that PDAPP 2B3 treated mice showed an overall improvement in DR scores compared to PDAPP vehicle treated mice, $p < 0.05$. Tests for simple main effects were performed following the significant treatment x time interaction. Within-subjects analysis revealed no change in pre- vs. post-treatment DR scores for WT mice or PDAPP vehicle mice, $p > 0.5$. However, 2B3 treated mice showed a significant improvement in post-treatment OiP memory performance, $p < 0.01$. The between-subjects analysis revealed that PDAPP 2B3 treated mice showed significantly lower DR scores in the pre-treatment stage when compared to WT mice, $p < 0.01$, but were not significantly different compared to PDAPP vehicle mice, $p = 1.0$. However, following 2B3 treatment PDAPP mice showed no difference in DR scores compared to WT mice, $p = 1.0$, but did show significantly better DR scores than PDAPP vehicle control mice, $p < 0.001$. WT mice

showed a significantly greater DR score than PDAPP vehicle mice across both pre- and post-time periods, $p < 0.001$.

Treatment Group	Pre-Treatment				Post-Treatment			
	Novel		Familiar		Novel		Familiar	
	Mean	SD	Mean	SD	Mean	SD	Mean	SD
WT Untreated	30.51	16.90	13.51	6.77	23.82	19.22	11.40	6.87
WT Vehicle	16.01	5.48	8.77	5.33	18.32	11.32	9.98	8.81
PDAPP Vehicle	6.51	3.54	4.85	1.69	6.53	3.56	4.87	2.91
PDAPP 2B3	12.78	9.17	9.02	6.72	13.19	7.16	7.14	4.65

Table 5.2: Mean contact time scores with objects in novel and familiar locations of WT untreated (n=11), WT V (n=10), PDAPP V (n=11) and PDAPP 2B3 (n=10) and standard deviations (SD). Both pre- and post-treatment scores are reported in seconds.

One sample t-tests were also run to determine if WT and PDAPP mice DR scores were significantly above chance (0.5). The analysis showed that all treatment groups at both pre- and post-treatment time points were significantly above chance level: WT UT mice pre-treatment, $t(10) = 7.9$, $p < 0.001$ and post-treatment, $t(10) = 10.8$, $p < 0.001$, WT V mice pre-treatment, $t(9) = 7.4$, $p < 0.001$ and post-treatment, $t(9) = 5.8$, $p < 0.001$. PDAPP vehicle treated mice, $t(10) = 3.1$, $p < 0.05$ and post-treatment, $t(10) = 4.8$, $p < 0.01$. PDAPP 2B3 treated mice, $t(9) = 2.9$, $p < 0.05$ and post-treatment, $t(9) = 11.2$, $p < 0.001$.

Despite a non significant difference in total contact times between PDAPP treatment groups, there was an observed bias of increased overall contact time with objects in 2B3 administered PDAPP mice (both in pre- and post-treatment conditions). For this reason, the 3 mice with the highest contact times in the 2B3 administered group and the 3 mice with the lowest contact times in the vehicle administered PDAPP group were removed to observe if this effect in any way biased the overall DR scores. Following removal of these mice the mean contact time with objects can be observed in table 5.3. An identical analysis of DR scores was then carried out as described above, revealing the same overall results. Thus, this difference in contact times initially observed did not show any bias in the ability of 2B3 administered PDAPP mice to discriminate objects in novel locations when compared to

vehicle treated PDAPP mice. Collectively these results show that 2B3 treatment improved OiP memory performance in PDAPP mice.

Treatment Group	Pre-Treatment				Post-Treatment			
	Novel		Familiar		Novel		Familiar	
	Mean	SD	Mean	SD	Mean	SD	Mean	SD
WT Untreated	30.51	16.90	13.51	6.77	23.82	19.22	11.40	6.87
WT Vehicle	16.01	5.48	8.77	5.33	18.32	11.32	9.98	8.81
PDAPP Vehicle	7.77	3.32	5.78	0.57	5.85	3.44	4.36	3.08
PDAPP 2B3	5.14	3.48	3.95	2.63	9.39	5.66	4.66	3.12

Table 5.3: Adjusted mean contact time scores with objects in novel and familiar locations of WT untreated (n=11), WT V (n=10), PDAPP V (n=8) and PDAPP 2B3 (n=7) and standard deviations (SD). Both pre- and post-treatment scores are reported in seconds.

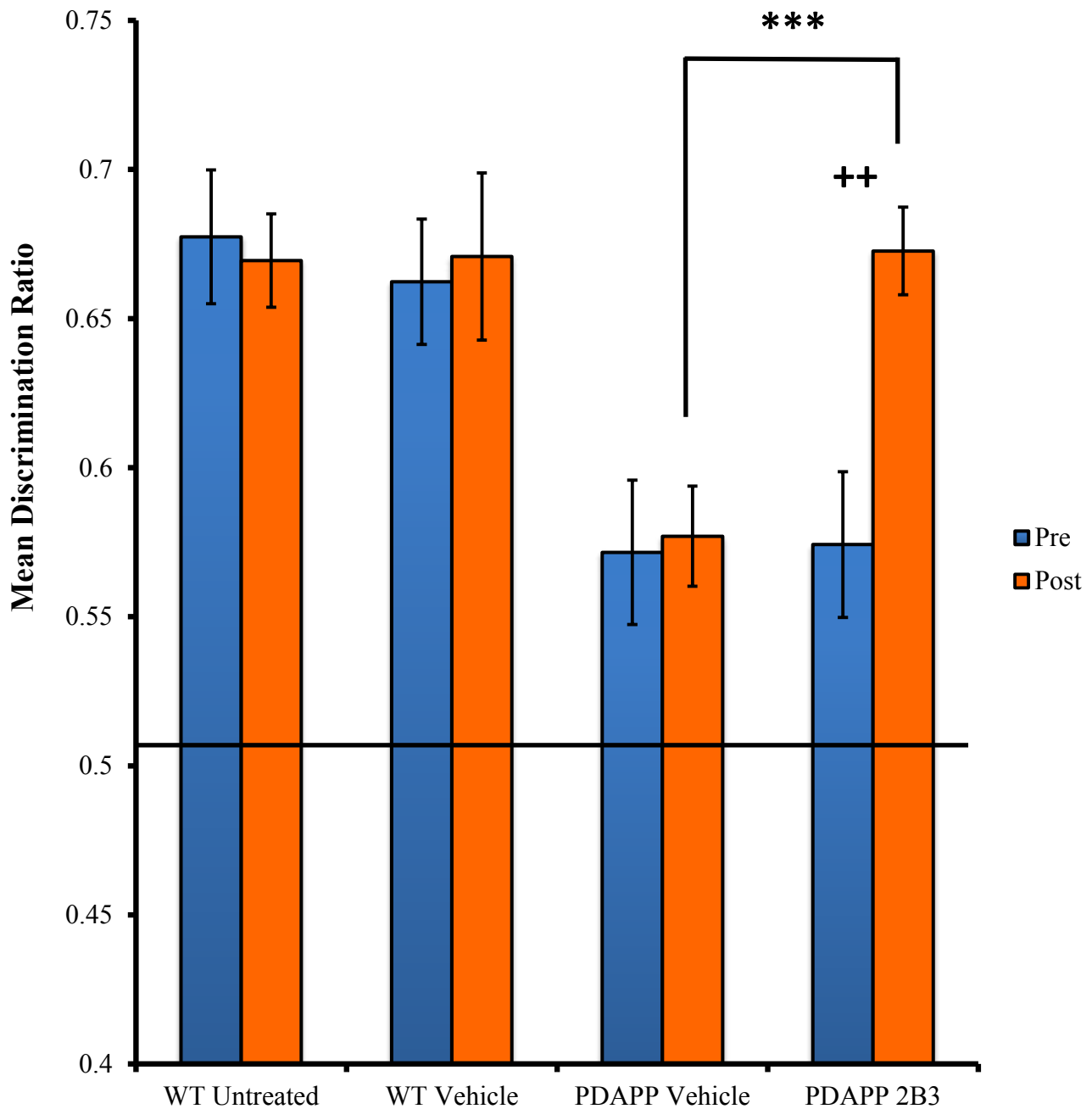


Figure 5.1: 2B3 treatment improved OiP memory in PDAPP mice. Graph shows mean DR scores of WT untreated (n=11), WT V (n=10), PDAPP V (n=11) and PDAPP 2B3 (n=10) mice. 2B3 treatment showed a significant improvement in memory performance in PDAPP mice when compared to pre-treatment performance and when compared to PDAPP vehicle treated mice. Graph shows the mean DR scores of pre- and post-treatment times for all groups tested. Error bars indicate S.E.M. A solid black line indicates chance level at 0.5. *** $p < 0.001$ between-subjects difference between post-treated PDAPP vehicle mice and post-treated PDAPP 2B3 mice. ++ $p < 0.01$ within-subject difference between pre-treated and post-treated PDAPP 2B3 mice.

5.2.4 Discussion

Results from this experiment have shown that ICV 2B3 administration to PDAPP mice significantly improved OiP recognition memory performance. To date, two previous reports have assessed the cognitive benefits of passive immunotherapy in PDAPP mice following the onset of an age-related cognitive deficit (Dodart et al. 2002; Hartman et al. 2005). For example, Dodart and colleagues reported significant improvements in object recognition memory performance following peripheral administration of m266, an anti-A β antibody, in a dose-dependent manner (Dodart et al. 2002). The results reported in Experiment 7 compliment these findings and, in addition, show that interfering with A β production by steric hindrance of APP β -secretase cleavage site activity can improve visuo-spatial object recognition memory in PDAPP mice.

No overall changes in contact time with objects were observed in any treatment group following vehicle or 2B3 treatment in this experiment, suggesting that 2B3 did not interact with motor performance or a tendency to engage with novel or familiar objects. Moreover, this suggests that overall reduced contact times with objects, also reported in Chapter 4, was an effect of APP overexpression and unlikely to be related to age-related A β production. Observation of test phase contact times in 2B3 administered PDAPP mice suggested a shift in the distribution of contact times. PDAPP mice spent more time exploring objects in novel locations and less time exploring objects in familiar locations. However, this effect was subtle and no significant location x time x treatment group interaction was observed. However, when contact times were converted to DR scores a difference in the discriminability of the novel and familiar locations within and between groups was clearly observed. Therefore, the results reported in this experiment provide evidence that *in vivo* administration of 2B3 significantly improved OiP memory in aged PDAPP mice.

These results also compliment other studies using a similar antibody approach. BBS1 improved non-spatial object recognition memory in both Tg2576 and 3xTg mice following chronic intraperitoneal or 4-week ICV administration respectively (Rakover et al. 2007; Rabinovich-Nikitin et al. 2012). In contrast to the present study, neither of these earlier reports assessed pre-drug performance scores. The partially within-subject design used in the present study allowed the severity of memory impairment to be established prior to and after 2B3 administration. Following 2B3 administration, no significant difference in DR scores was observed when comparing 2B3 administered PDAPP mice and WT vehicle mice. Rabinovich-Nikitin et al. (2012) reported a similar result in 3xTg mice testing the BBS1 antibody. However, the comparison to WT controls was not reported in the Rakover et al., (2007) study

using Tg2576 mice. A more thorough comparison of the designs used in these studies will be reserved until the chapter discussion.

Collectively, the behavioural analysis reported in Experiment 7 showed significant improvements in OiP memory. This task is exquisitely sensitive to manipulations involving the hippocampus. These results support the hypothesis that antibodies targeting the β -secretase cleavage site of APP can improve memory performance in aged Tg models of amyloid pathology and may provide an exciting therapeutic strategy for the treatment of early stage AD.

5.3 Experiment 8: *Ex vivo* tissue analysis of 2B3 treated mice

5.3.1 Introduction

The aim of this experiment was to determine if 2B3 administration changed APP metabolism in *ex vivo* tissue of PDAPP mice. As discussed in Chapter 1 and Chapter 6 introduction, 2B3 binds at the β -secretase cleavage site of APP, preventing the processing of A β by steric hindrance *in vitro* (Thomas et al. 2011; Thomas et al. 2013). It was therefore hypothesised that 2B3 administration in PDAPP mice would reduce the levels of APP metabolites, including β CTF, A β 40 and A β 42.

The second aim of this experiment was to investigate if 2B3 inhibition of APP processing by beta-secretase would have downstream consequences on NMDARs activity. The mechanism under investigation has previously been described in Chapter 1. Briefly, NMDARs in the hippocampus contribute to OiP memory performance (Barker & Warburton 2008; Barker & Warburton 2013). Previous reports using hAPP Tg mice have reported increased phosphorylation of the NMDAR subunit NR2B (Ittner et al. 2010). This increase in NR2B phosphorylation led to impaired spatial working memory, as determined by T-maze alternation task (Ittner et al. 2010). It was therefore hypothesised that inhibition of A β production by steric hindrance of β -secretase cleavage of APP reduced NR2B phosphorylation. The administration of 2B3 to PDAPP mice may thereby have improved NMDAR-dependent activity required for the OiP memory task.

5.3.2 Methods

All methods used in this experiment have previously been detailed in Chapter 2.

Samples

All samples used in this experiment were prepared as described in Chapter 2. WT vehicle (n=10), PDAPP vehicle (n=11) and PDAPP 2B3 administered (n=10) mice were used for analysis in this experiment. All Western blot analysis used all 3 groups. ELISA analysis used PDAPP mice only. Due to violations in data normality and distribution (described below), one PDAPP 2B3-treated mouse was removed from all ELISA analysis.

Statistics

All data in this experiment were analysed using one-way ANOVA with post-hoc Tukey analysis or independent samples t-tests. Prior to these analyses, data were explored for normality of distribution using the Shapiro-Wilk test. Extreme outliers were also observed using Tukey's box plots in SPSS. If violations of normality occurred and outliers were reported, data were transformed appropriately. If transformations showed no effect it was determined if the violations were caused by individual outliers. As it has been reported that Tukey's box plots (used in SPSS) may not be appropriate for detecting outliers in smaller sample sizes, more robust models for labelling outliers were used (Iglewicz & Hoaglin 1993). Methods for labelling outliers were adopted as according to Hoaglin & Iglewicz for normally distributed data and Carling for non-normally distributed data (Hoaglin & Iglewicz 1987; Carling 1998). These methods were chosen due to similar mathematical protocols for identifying outliers; the method reported by Carling is an adaptation using the "Median Rule" as opposed to the adapted "Tukey Rule" proposed by Hoaglin & Iglewicz. If any data points labelled as outliers were reported from non-normally distributed data these data points were removed and normality was re-analyzed. If the removal of this datum or data generated a normal distribution as determined by Shapiro-Wilk test the excluded values were referred to as "extreme outliers" and were removed from the study. In this analysis, one mouse from the PDAPP 2B3 administered group met the criteria for an extreme outlier in APP, A β 40 and β CTF ELISA analyses and was hence removed from all ELISA analyses.

5.3.3 Experiment 8 – Results:

2B3 treatment alters APP processing ex vivo without affecting levels of APP expression

APP

To establish that 2B3 administration did not alter levels of total APP, left HPC homogenates of 2B3 treated PDAPP mice were compared to vehicle treated PDAPP mice. Western blot analysis (Fig 6.2A) showed a small reduction in total levels of APP in 2B3 treated mice. However, this trend was not observed following ELISA quantification of APP (Fig 6.2B). Independent samples t-test reported no difference in APP levels in either Western blot, $t(19) = 1.02$, $p > 0.1$, or ELISA, $t(18) = 1.33$, $p > 0.1$, measurements.

APP Metabolites

To determine if 2B3 altered APP processing in PDAPP mice levels of soluble A β 40 and A β 42 and β CTF were analysed by ELISA (Fig 6.2 A-C). A significant reduction in A β 40 was observed in 2B3 treated PDAPP mice (Fig 6.2A), $t(18) = 2.28$, $p < 0.05$, however this was not observed with A β 42, $t(18) = 1.01$, $p > 0.1$. Consistent with the finding that levels of soluble A β 40 were reduced following 2B3 treatment, there was a significant reduction in β CTF was in 2B3 treated PDAPP mice, $t(18) = 2.22$, $p < 0.05$. Collectively, these results show that 2B3 treatment of PDAPP mice altered APP processing in the HPC most likely by steric hindrance of β -secretase cleavage of APP.

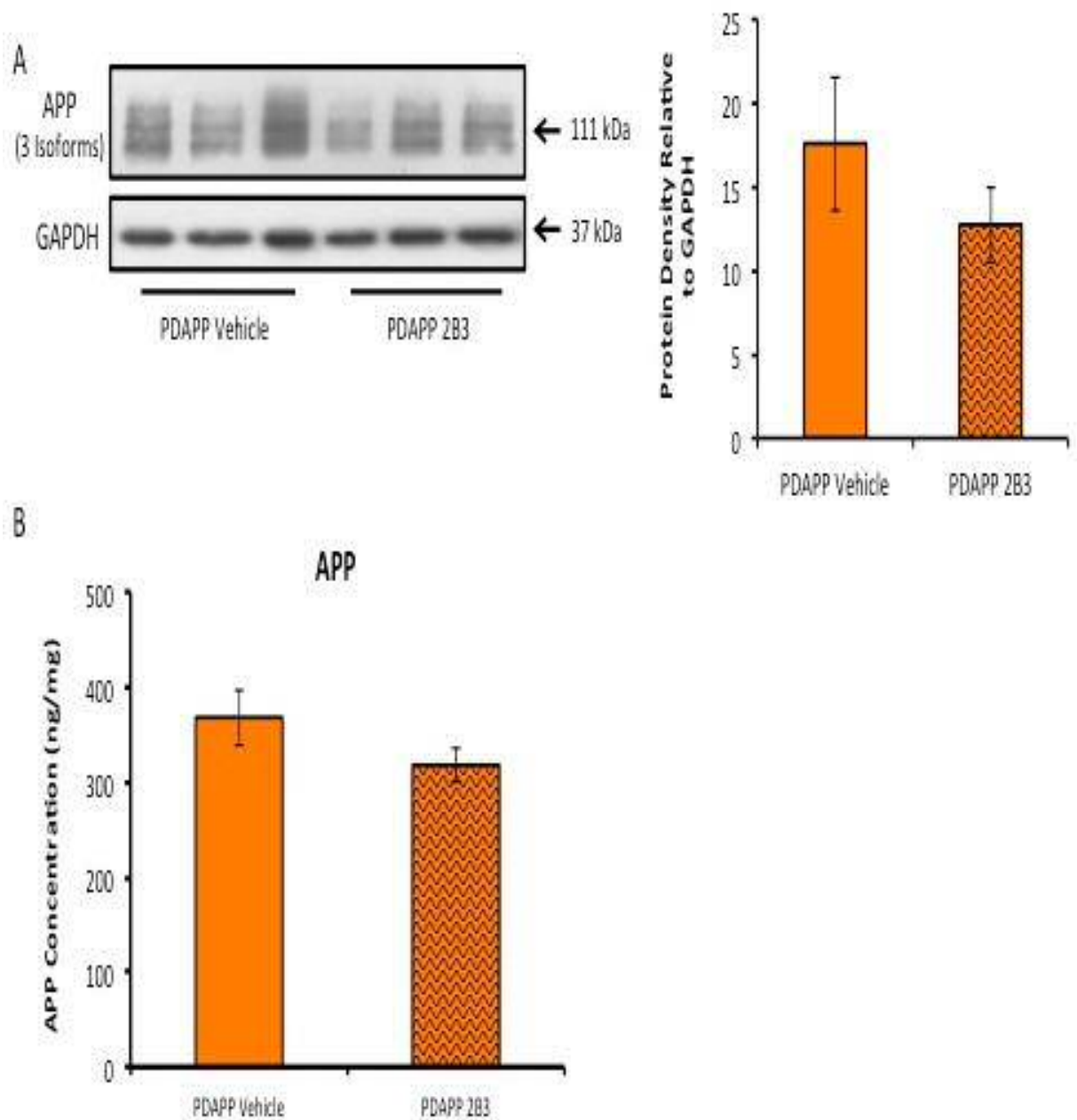


Figure 5.2: Levels of total APP in vehicle and 2B3-treated PDAPP mice. No significant differences in total levels of APP were observed in Western blot analysis. (A) shows a representative example of three PDAPP mice/treatment group. (B) shows quantified levels of APP in PDAPP vehicle (n=11) and PDAPP 2B3 (n=10) determined by Western blot. (C) displays ELISA quantification of APP for PDAPP vehicle (n=11) and PDAPP 2B3 mice (n=9). Error bars represent S.E.M.

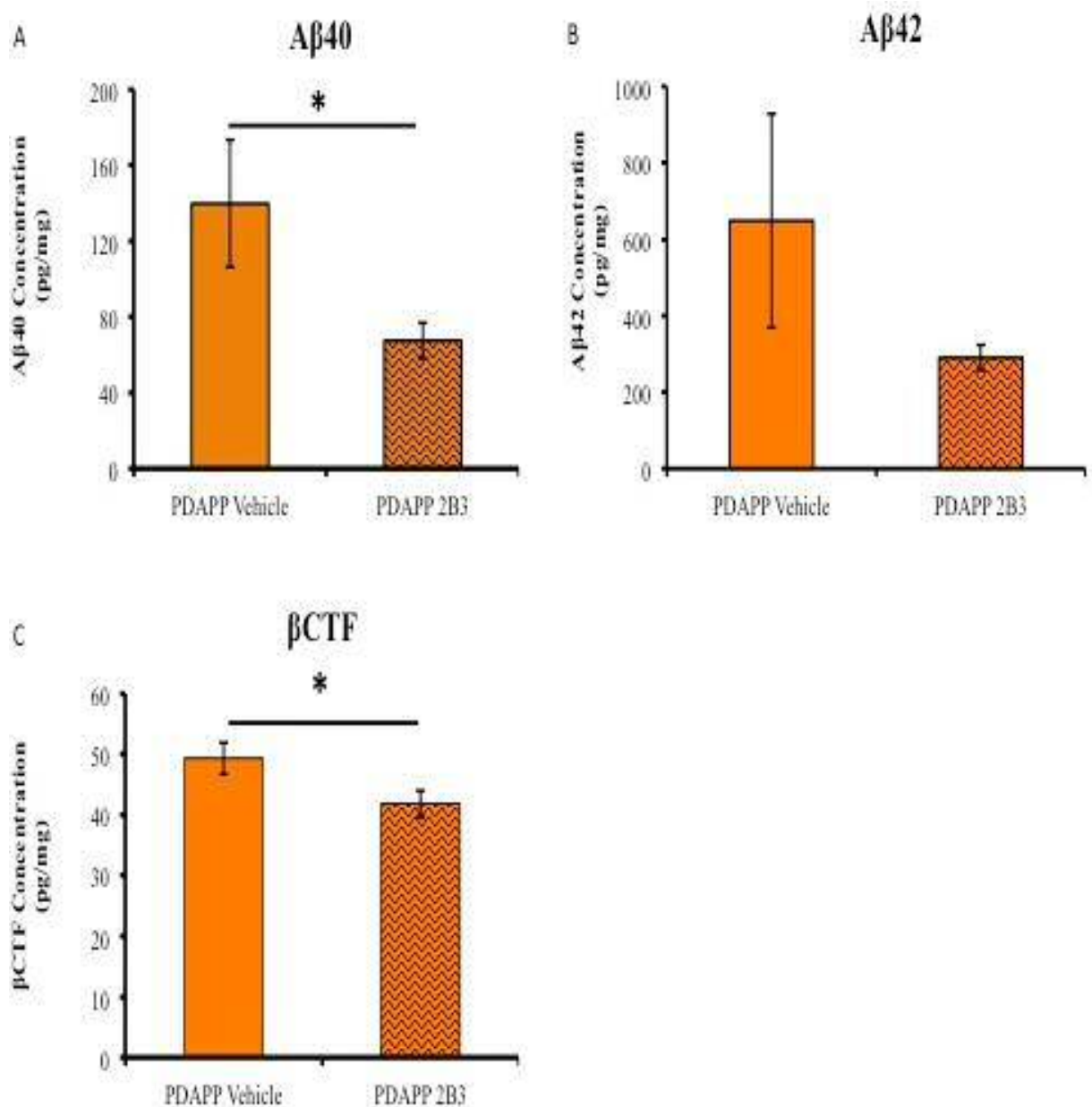


Figure 5.3: Quantification of $A\beta_{40}$, $A\beta_{42}$ and β CTF by ELISA in hippocampal homogenates of 2B3 treated PDAPP mice. 2B3 treatment showed a significant reduction in the total levels of soluble $A\beta_{40}$ (A), but not $A\beta_{42}$ (B). A significant reduction in β CTF levels was also observed following 2B3 treatment (C). Error bars represent S.E.M. All measures were determined by ELISA. * $p < 0.05$ represents a significant reduction in protein levels in PDAPP 2B3 mice (n=9) compared to PDAPP vehicle mice (n=11).

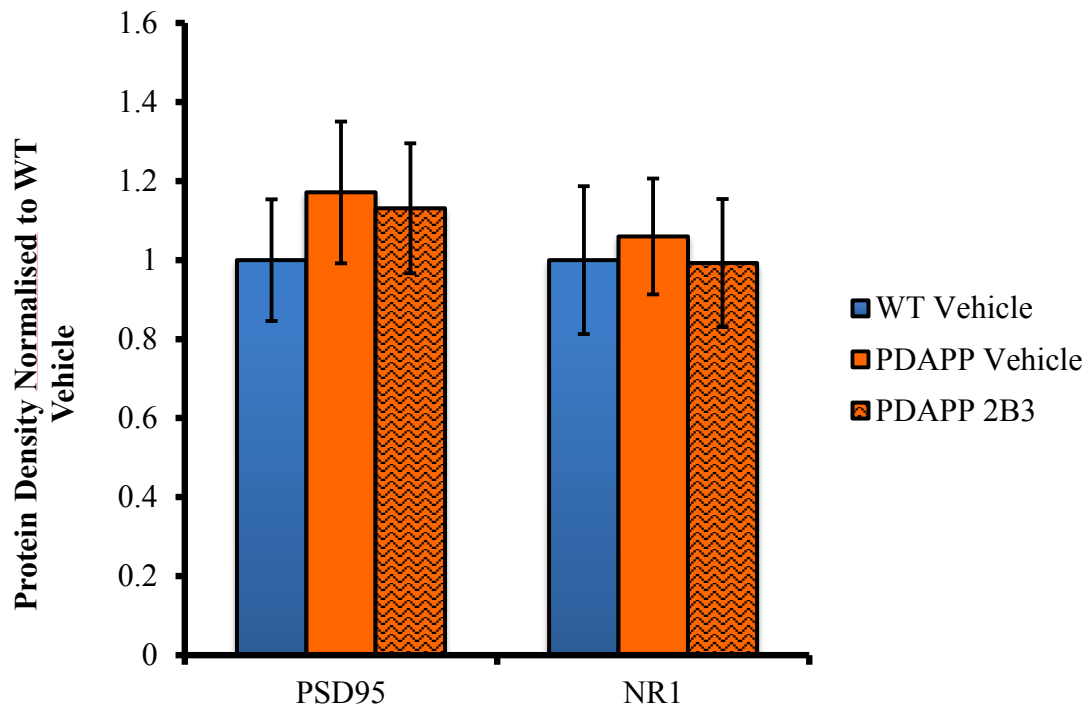
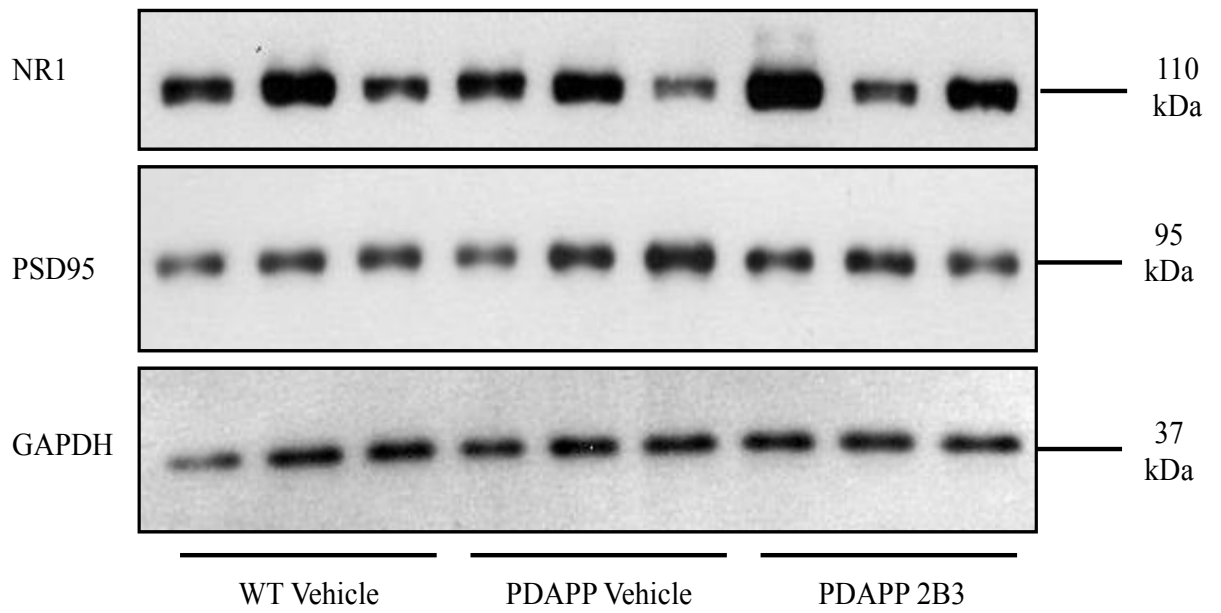
Treatment with 2B3 alters NMDA receptor phosphorylation

Western blot analysis was used to determine if 2B3 caused any changes in total PSD95, a synaptic marker, total NMDAR (NR1) expression and the level of NR2B and the phosphorylated state of the regulatory tyrosine residue 1472 (pY1472).

No significant changes in total levels of NR1 (a measure of total NMDAR) was observed, $F(2, 28) = 0.05$, $p > 0.5$, nor were any differences in total levels of PSD95 reported, $F(2, 28) = 0.3$, $p > 0.5$ as determined by one way ANOVA (Fig 6.4A). Following this result, any changes observed in NR2B and pY1472 cannot be attributed to changes in total levels of NMDARs or total synaptic density.

Figure 6.4B shows levels of NR2B and pY1472. Analysis by one-way ANOVA revealed no significant difference of total NR2B, $F(2, 30) = 1.3$, $p > 0.1$. Despite a small numerical increase in pY1472 being observed in PDAPP vehicle mice, this was not significant, $F(2, 30) = 1.7$, $p > 0.1$. A ratio of total NR2B to pY1472 was calculated to determine if levels of NR2B pY1472 were altered relative to the total levels of NR2B. A significant difference was reported when analysing the NR2B:pY1472 ratio, $F(2, 30) = 8.9$, $p < 0.001$. Post-hoc Tukey analysis revealed that PDAPP vehicle mice showed a significantly greater level pY1472 as a ratio of NR2B than WT vehicle mice, $p < 0.01$ as well as PDAPP 2B3 administered mice, $p < 0.001$. PDAPP 2B3 mice showed no significant difference when compared to WT vehicle administered mice, $p > 0.5$. These results provide evidence that NR2B phosphorylation as a ratio of total NR2B is reduced in PDAPP mouse HPC following 2B3 treatment.

A



B

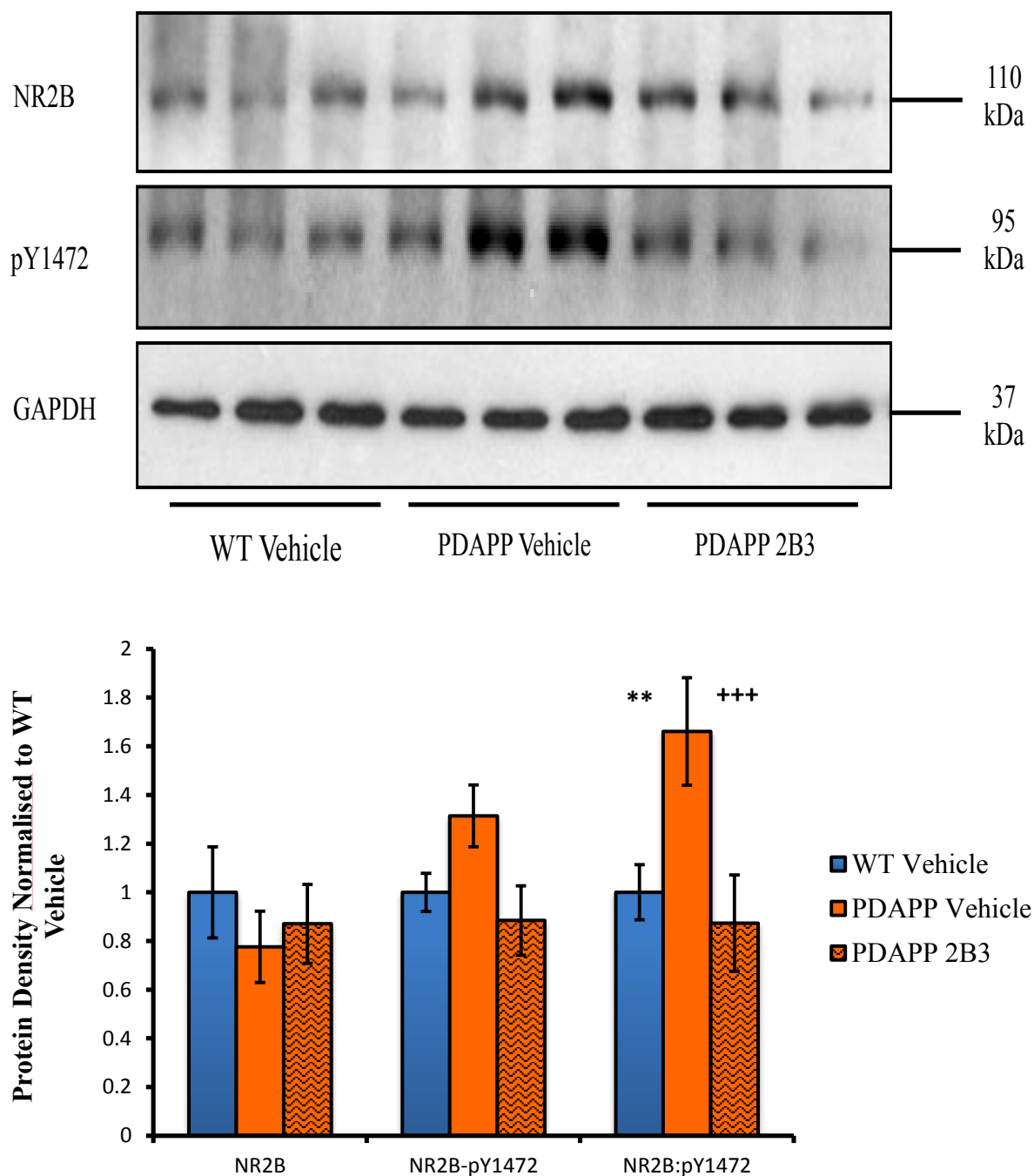


Figure 5.4: 2B3 reduced NR2B phosphorylation in PDAPP mice. Quantification by Western blot of synaptic proteins in PDAPP mice following 2B3 treatment. (A) Mice showed no overall changes in total levels of PSD95, NR1. (B) Numerical reductions in NR2B were observed and small increase in total pY1472 can also be observed in PDAPP V mice, however significant changes are observed when total levels of pY1472 are expressed as a ratio of total NR2B. Error bars represent S.E.M. ** $p < 0.01$ significant difference between WT vehicle (n=10) and PDAPP vehicle (n=11) groups. +++ $p < 0.001$ significant difference between PDAPP vehicle and PDAPP 2B3 (n=10).

5.3.4 Experimental Discussion

In this experiment, 2B3 administration showed significant reductions of soluble A β 40 and β CTF without affecting total levels of APP. No change in the level of A β 42 was reported. A significant reduction in total levels of β CTF was observed in the HPC of PDAPP mice following 2B3 administration. No change in A β 42 was reported following BBS1 treatment in 3xTg and Tg2576 mice (Rakover et al. 2007; Rabinovich-Nikitin et al. 2012). In contrast to the present study, there was no evidence that BBS1 treatment reduced the levels of CTFs (Rakover et al. 2007; Rabinovich-Nikitin et al. 2012). This novel finding in the present study is consistent with the hypothesis that the 2B3 monoclonal antibody targeted the APP β -secretase cleavage site.

To date, no study assessing the effects of amyloid-based immunotherapies have identified changes in a receptor-based mechanism linked to amyloid pathology. This study has shown for the first time that the 2B3-induced inhibition of APP processing *in vivo* reduced the phosphorylation of the NR2B subunit. The increased phosphorylation of NR2B has previously been linked with working memory impairments in APP23 mice (Ittner et al. 2010). There is also compelling evidence for the involvement of NMDAR-dependent synaptic processes in the object-in-place memory task used in Experiment 7 (Barker & Warburton 2008; Barker & Warburton 2013). Taken together the present study suggests that 2B3 improved memory function in PDAPP mice by reducing the amyloid-related increase in NMDAR phosphorylation. A more in-depth analysis of these results will be provided in the Chapter Discussion.

5.4 Chapter Discussion

Early studies using monoclonal anti-A β antibodies as a passive immunotherapy in PDAPP mice showed a reduction in amyloid load in the brains of 16 month old mice (Bard et al. 2000). Subsequent work showed that passive immunisation of PDAPP and Tg2576 mice was able to improve age-related cognitive deficits (Dodart et al. 1999; Dodart et al. 2002; Kotilinek et al. 2002a; Westerman et al. 2002). These early studies suggested that the reduction and clearance of A β from the brain by immunotherapy was a promising therapeutic

strategy for the treatment of AD. However, clinical trials using passive immunotherapies have yet to deliver successful reductions in levels of amyloid and improved cognition.

Other strategies to reduce A β levels in the brain have also been investigated, including the use of β -secretase inhibitors to prevent amyloidogenic metabolism of APP. These studies have revealed positive effects of with BACE1 inhibitors as well as BACE1 KO mice crossed with Tg models of amyloid pathology (Luo et al. 2001; Asai et al. 2006; Hussain et al. 2007; Vassar et al. 2009). However, targeting BACE1 directly has led to concerns about the potential negative impact of inhibiting various other roles of BACE1 (Vassar et al. 2009; De Strooper et al. 2010a). In order to overcome these challenges, anti-APP antibodies targeting the β -secretase cleavage site, such as 2B3 and BBS1, have been generated to selectively inhibit amyloidogenic processing of APP (Arbel et al., 2005; Thomas et al. 2011; Thomas et al. 2013).

Previous results assessing the effects of 2B3 *in vitro* have reported significant reductions of A β levels in MOG-G-UVW astrocytoma cells, as well as mouse primary cortical neurons (Thomas et al. 2011; Thomas et al. 2013). Based on these results, 2B3 was hypothesised to reduce amyloid processing and improve behavioural deficits in PDAPP mice (reported in Chapters 3 and 4). Experiment 7 showed that following 2B3 administration PDAPP mice exhibited a significant improvement in object-in-place memory. Rakover et al. (2007); Rabinovich-Nikitin et al. (2012) used a similar antibody to 2B3 (BBS1) which also targeted the β -secretase cleavage site of APP, and reported improved recognition memory following its administration in Tg2576 and 3xTg mice. A number of differences exist between these studies and that reported in Experiment 7, including age of mice, the transgene(s) expressed and route of antibody administration and the behavioural design.

The behavioural protocols assessing *in vivo* effects of BBS1 differ significantly. As discussed in detail in Chapter 4, alterations in behavioural methodology can lead to different results and performance in recognition memory (Dodart et al. 1999; Chen et al. 2000). The protocol used by Rakover and colleagues tests object novelty detection (A+B \rightarrow A+C) and has been reported to rely on perirhinal cortex (PRC) function (Warburton & Brown 2010; Barker & Warburton 2011; Warburton & Brown 2015). Rabinovich-Nikitin and colleagues exposed animals to one object during the sample phase followed by a test phase in which the familiar object and a novel object were presented (A \rightarrow A+B), therefore the novel object was also presented in a novel spatial location. This type of procedure is likely to involve the PRC to dissociate novel and familiar object information, but also the HPC in relation to processing

changes in the spatial organisation of the object array (Winters et al. 2004; Barker & Warburton 2011; Barker & Warburton 2013). The behavioural phenotype exhibited between models is also reported to be different. 3xTg mice have previously been reported to show object-novelty memory deficits at 9 and 15 months of age, which was also observed by Rabinovich-Nikitin and colleagues at the 18 month age in the control 3xTg mice tested (Clinton et al. 2007; Rabinovich-Nikitin et al. 2012). However, Tg2576 mice have shown intact object novelty memory at 14 and 16 months of age, which was not observed by Rakover and colleagues (Hale & Good 2005; Good & Hale 2007; Rakover et al. 2007).

Although both studies using recognition memory to assess *in vivo* effects of BBS1 report improved performance, it is unclear given the differences in behavioural methodology and Tg model phenotype whether the antibody improved overall HPC function and processing of information in the HPC in either Tg2576 or 3xTg mice. No study to date using BBS1 has observed a significant improvement in a cognitive task sensitive to HPC function. Therefore the improvement in memory function reported in 3xTg mice following BBS1 administration may be due to improved PRC function and/or HPC function, but can not be concluded given the behavioural protocol used (Rabinovich-Nikitin et al. 2012). The improved memory performance in Tg2576 mice following chronic BBS1 treatment is likely to be a consequence of improved PRC function (Rakover et al. 2007). However, the PBS administered Tg2576 control mice showed a preference for the familiar object over the novel object (Rakover et al. 2007). This suggests a neophobic response (anxiety of novel objects) in the Tg2576 mice used in this study and thus any improvement in performance may not have been an overall measure of improved memory function, but reduced anxiety. Finally, Arbel-Ornath and colleagues assessed the London mutation model following chronic BBS1 administration of the MWM (Arbel-Ornath et al. 2009). No significant improvement in spatial reference memory was observed in the probe trial of the MWM following BBS1 administration, however a numerical improvement was observed (Arbel-Ornath et al. 2009). Collectively, although *in vivo* assessment of BBS1 has reported improvements in behaviour following BBS1 administration, it is unclear whether these effects are specific to HPC function or altered emotionality and require further investigation.

In Experiment 7, PDAPP mice showed a significant improvement in OiP memory following 2B3 administration. As reported in Chapter 4, PDAPP mice showed no deficit in object recognition across all ages tested. A large body of work suggests that the OiP task involves an interaction between the PRC and HPC for successful memory performance (Warburton & Brown 2015b). Given the evidence of intact novelty recognition in aged

PDAPP mice it is likely that changes the OiP deficit reflected impaired spatial processing and not a failure to discriminate between objects. Therefore, the 2B3-induced improvement in OiP memory is likely caused by improvements in HPC function or improved connectivity in the neural circuit connecting the PRC and HPC in PDAPP mice. This observation is further supported by 2B3-induced the changes in hippocampal A β and β CTF levels in PDAPP mice. Therefore, this study has presented evidence that inhibition of APP cleavage at the β -secretase cleavage site improved memory performance in an object-in-place recognition task sensitive to HPC dysfunction.

To compliment the findings that 2B3 improved object-in-place performance in PDAPP mice, there were significant changes in markers of APP processing, specifically hippocampal A β and β CTF levels, without changes in total levels of APP. These neurotoxic peptides have been implicated in the cognitive deficits observed in Tg and experimental models of AD (Nalbantoglu et al. 1997; Choi et al. 2001; Chishti et al. 2001; Cleary et al. 2005). In Experiment 8, levels of A β 40 were reduced by 51.7% in PDAPP mice by 2B3 administration. However levels of A β 42 remained unaffected. Published evidence indicates that the A β 42 peptide is significantly more neurotoxic than the A β 40 peptide (Klein et al. 1999; Walsh & Selkoe 2004). Indeed, it has also been shown in PDAPP mice that there is a much greater ratio of A β 42 to A β 40 (Johnson-Wood et al. 1997; Fryer et al. 2005; Hartman et al. 2005). These data are consistent with the view that increasing A β 42 levels is more likely to be the cause of cognitive deficits in PDAPP mice than A β 40. However, rat models of AD in which A β 40 is infused into the ventricles display cognitive deficits, including impaired spatial memory (Nitta et al. 1994; Özdemir et al. 2013; Xu et al. 2015). These models showed that A β 40 pathology is sufficient to drive cognitive deficits and potentially impair HPC function, independent of A β 42. The result that 2B3 reduced levels of A β 40 in the HPC of PDAPP mice and improved memory is consistent with the view A β 40 peptide contributes to neuronal changes that underpin cognitive deficits in APP transgenic mice. This result may imply that soluble A β 40 also contributes to memory deficits in PDAPP mice as well as A β 42.

2B3 also caused a 23.9% reduction in total levels of β CTF in the HPC of PDAPP mice. Despite the fact that most research has focussed on the role of A β and tau pathology in AD, increased levels of β CTF have been observed in AD patients. Furthermore, β CTF have been implicated in the disruption of neuronal physiology and cognitive deficits in rodents (Nalbantoglu et al. 1997; Choi et al. 2001; Holsinger et al. 2002; Liu et al. 2009; Tamayev et al. 2012; Kim et al. 2015). Indeed, recent research into the role of β CTF has revealed an A β -independent mechanism causing dysregulated endocytosis (Pimplikar et al. 2010; Kim et al.

2015). Thus, increased levels of β CTF can cause pathologically accelerated endocytosis and up-regulation of rab5, a marker of early endosomes (Grbovic et al. 2003; Kim et al. 2015). Enlarged endosomes and endosome related genes, including rab5, are up-regulated in early AD (Cataldo et al. 2000; Ginsberg et al. 2010). β CTF-induced acceleration of endocytosis caused endosome swelling and impaired axonal transport of endosomes in mouse primary cortical neurons (Kim et al. 2015). Endocytosis is involved in multiple signalling pathways and trafficking of neuronal receptors, including NMDARs (Washbourne et al. 2004; Nixon 2005; Lau & Zukin 2007). A disruption of endosomal processing is therefore likely to contribute to impaired neurotransmission and thus cognitive deficits. It remains possible that this mechanism is improved by the 2B3-induced reduction in β CTF in PDAPP mice and this may also contribute to enhanced memory function. However, further work is required to test this.

Similar changes in APP metabolites following *in vivo* administration of the anti-APP antibody BBS1 have also been reported (Arbel-Ornath et al. 2009; Rabinovich-Nikitin et al. 2012). However, inconsistencies exist between studies. Tg2576 mice administered BBS1 showed no change in levels of soluble or insoluble A β 40 and A β 42 (Rakover et al. 2007). 3xTg mice administered BBS1 also showed no significant reduction in soluble A β 42, but significant reductions in total A β load, plaque size and reduced tau pathology (Rabinovich-Nikitin et al. 2012). These results were similar to the BBS1-mediated reduction in plaque size, intracellular A β and A β oligomers reported in London mutation APP mice (Arbel-Ornath et al. 2009). However, to date, no study assessing BBS1 or any anti-A β antibodies *ex vivo* has reported any changes in levels of β CTF.

Despite *in vivo* assessment of a number of anti-A β antibodies and BBS1 showing improved cognition and reduced A β pathology, no study has yet reported the impact of the antibody on a receptor-based mechanism linked A β toxicity. Hippocampal NMDARs contribute to successful performance on the OiP memory task (Barker & Warburton 2008). Experiment 8 showed that there was no overall change in total levels of NMDARs in 2B3 treated PDAPP mice. However, A β has been observed to reduce NMDAR surface expression in primary cortical neurons and in primary neurons of APP_{Swe} mice, without affecting total levels of NMDARs (Snyder et al. 2005). A reduced surface expression of total NMDARs has also been reported in 12 month old Tg2576 mice (Kurup et al. 2010). In this study, the precise localisation of NMDARs was not assessed due to differences in protein extraction protocols used here and by Kurup and colleagues. However, it is possible that surface NMDARs may not have been reduced to the same extent in the present study as that reported by Kurup et al.,

(2010). In Experiment 8, PBS control PDAPP mice showed increased phosphorylation of the tyrosine 1472 (Y1472) residue of the NR2B subunit. This phosphorylation has been reported to increase the interaction of PSD95 with NMDA-NR2B containing complexes and prevent receptor internalisation (Lin et al. 2004; Prybylowski et al. 2005). Tg2576 mice show a reduction in phosphorylated Y1472 (pY1472) when compared to age-matched WT controls (Zhang et al. 2010). This may explain why Tg2576 mice showed reduced NMDAR surface expression. However, to date, no study has reported NMDAR surface expression of PDAPP mice. It is tempting to speculate that it may be increased relative to Tg2576 mice or WT control mice because of the increased NR2B pY1472. However, further analysis is required to test this hypothesis.

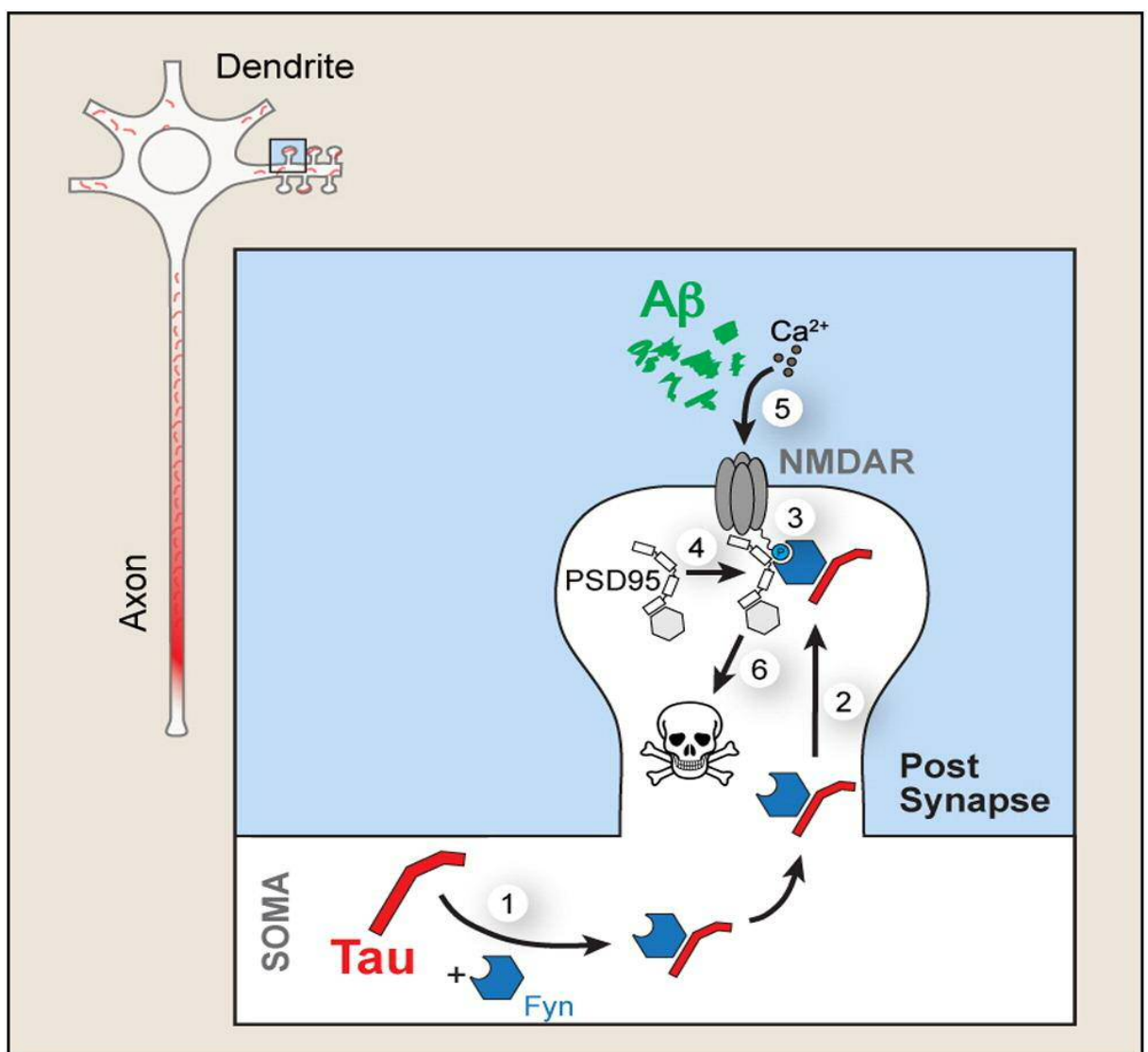


Figure 5.5: Schematic illustration demonstrating the interactions between Aβ, tau and Fyn leading to NMDAR-mediated neuronal excitotoxicity. Src kinase Fyn interacts with phosphorylated tau protein leading to the translocation of both proteins to the post synapse (1-2). Fyn at the synapse

phosphorylates the NR2B subunit of the NMDAR complex, stabilizing its interaction with PSD95 and expression at the synapse (3-4). Increased A β and enhanced expression of NR2B containing NMDARs at the synapse causes disproportionate influx of Ca²⁺ leading to downstream neurotoxicity.

No change in levels of PSD95 was observed in either WT or PDAPP treatment group in this study. This may indicate that there was no overall neuronal or synaptic loss. However, previous research has shown in PDAPP mice that significant reductions in numbers of dendritic spines occurs with age and overall synaptic loss has also been reported (Games et al. 1995; Lanz et al. 2003). These data were obtained using more optimal protocols (confocal microscopy and photomicrographs of Golgi-stained neurons) to determine synaptic quantification. It may therefore be likely that the Western blot quantification of HPC homogenate used in this study was not sensitive enough to quantify synaptic changes caused by A β -induced neurotoxicity in aged PDAPP mice.

Phosphorylation of the NMDAR NR2B subunit has been found to be altered in mouse models of AD (Ittner et al. 2010; Zhang et al. 2010) It must be noted however, that while Tg2576 and 3xTg mice have been reported to show reduced NR2B phosphorylation, APP23 mice have shown increased NR2B phosphorylation (further discussion of these conflicting studies is provided in Chapter 6, section 6.3). This increased NR2B phosphorylation was observed in 18-month control PDAPP mice reported in Experiment 5B. The reasons for these differences between Tg models remain undetermined. The increased ratio of total NR2B to NR2B pY1472 observed in PBS administered PDAPP mice was reduced by 2B3 without affecting total levels of NR2B or total NMDARs. The phosphorylation of NR2B is reported to increase NMDAR-PSD95 interaction (Figure 5.5), NMDAR surface expression and has been shown to be regulated by SRC kinase Fyn (Prybylowski et al. 2005; Ittner et al. 2010). This enhanced NMDAR surface expression is thought to lead to increased NMDAR activation and Ca²⁺ influx leading to excitotoxicity in neurons (Figure 5.5; Ittner et al. 2010) In AD brains increased levels of Fyn have been observed (Ho et al. 2005). Indeed, overexpression of Fyn in the J9 and J20 mouse model of AD caused more severe cognitive deficits than control Fyn overexpression and hAPP overexpression alone, as well as an increased loss of synapses (Chin et al. 2004; Chin et al. 2005). The increased loss of synapses and increased cognitive impairment is a likely an effect of A β -induced and fyn-mediated increased phosphorylation of Y1472 of the NR2B subunit as proposed by Ittner and colleagues (Figure 5.5; Ittner et al. 2010; Ittner & Götz 2011). This mechanism may further be implicated in the synaptic loss reported in PDAPP and APP23 mice, both of which have shown increased pY1472 (Games et al. 1995; Calhoun et al. 1998). Given the reduced level of A β 40 in 2B3-administered mice, it

may be possible that fyn activity is also reduced leading to the reduction of the phosphorylated NR2B Y1472 residue. However, further research is required to confirm this mechanism.

Finally, the phosphorylation state of the NR2B Y1472 subunit has been observed to play a significant role in memory performance. APP23 mice exhibited significant impairments of a T-maze working memory task and increased pY1472 (Ittner et al. 2010). However, following administration with a peptide compound, Tat-NR2B9c, which has been shown to prevent NMDA-induced excitotoxicity and perturb the NR2B containing NMDAR-PSD95 interaction, APP23 mice showed significant improvement in T-maze performance (Aarts et al. 2002; Ittner et al. 2010). More recently a mouse model expressing the Arctic APP mutation and WT human tau (*ArcTau*) crossed onto a heterozygous *BACE* KO line to produce *ArcTau/BACE*^{+/-} and *ArcTau/BACE*^{+/+} mice has been reported (Chabrier et al. 2012). *ArcTau/BACE*^{+/-} mice showed improved spatial learning and reference memory when compared to the *ArcTau/BACE*^{+/+} mice. Moreover a significant reduction in soluble A β 40 and phospho-tau S396/404 were also observed in *ArcTau/BACE*^{+/-}. Interestingly, a reduction of PSD95-associated NR2B was also reported as a result of partial BACE KO (Chabrier et al. 2012). These data are supportive of those reported in Chapter 5 suggesting altered APP processing by BACE can improve learning and memory in mice, which is associated with NMDAR function.

Given the above evidence it is tempting to conclude that improved performance in the OiP task may be related to 2B3-induced changes in NR2B phosphorylation. Further research is required to confirm the involvement of NR2B-containing NMDAR complexes in the OiP recognition memory task. Collectively, results reported Experiment 7 and 8 show that 2B3 administration reversed an age-dependent OiP recognition memory deficit in PDAPP mice. 2B3 also reduced total levels of soluble A β 40 and β CTF without affecting total levels of APP. Furthermore, the results have highlighted a receptor-based mechanism linked to amyloid-induced excitotoxicity. More specifically, the normalisation of NR2B phosphorylation may play a role in the improved cognition observed in PDAPP mice administered 2B3. This is a novel finding and provides important new evidence that the inhibition of APP processing at the β -secretase cleavage site by steric hindrance can improve both memory and synaptic pathology in the PDAPP mice.

Chapter 6: Thesis Discussion

6.1 Thesis Overview

The main aims of this thesis were three-fold. Firstly, to characterise the behavioural phenotype of the PDAPP model on a C57Bl/6 background and identify any age-dependent cognitive deficits and age-associated changes in A β pathology. The second was to administer 2B3, an anti-APP antibody that binds at the β -secretase cleavage site of APP and evaluate its impact on cognition in PDAPP mice. The third was to evaluate a possible mechanism by which 2B3 improved synaptic and thereby cognitive function. In this chapter, a summary of the findings are reported, followed by a more detailed discussion of how these data contribute to our current understanding of amyloid pathology, potential therapies associated with this target and cognitive decline in AD.

6.2 Summaries and Discussion of Findings

Currently, clinically available treatments for AD target the symptomatology of AD and not the underlying mechanisms of the disease (i.e. progressive amyloid and tau pathology). Transgenic mouse models of AD have provided insight and theories regarding the mechanisms underpinning neurodegeneration and provided tools to investigate therapies targeting amyloid and/or tau-based mechanisms of AD (Götz & Ittner 2008; Solomon & Frenkel 2010; C. a Lemere 2013; Herrmann & Spires-Jones 2015). Although positive effects are often reported in current mouse models there has been little success in translating this to the clinical condition. While several factors may contribute to this lack of translation one common concern is that there is a marked mismatch between mouse models and patients in terms of the severity and stage of the disease (Qian et al. 2015; Reardon 2015). The use of therapies derived from mouse models may be beneficial if used at the earliest possible stage of disease pathogenesis in humans. In this regard there is still on-going research into the safe and effective modulation of APP processing, a mechanism that remains a corner stone of the amyloid cascade hypothesis of AD.

The main aim of this thesis was to evaluate the hypothesis that an antibody-mediated inhibition of β -secretase activity would reduce amyloid production and improve memory performance in a transgenic mouse overexpressing mutant human APP. Before addressing this issue it was first necessary to establish the profile of amyloid pathology and cognitive

function in PDAPP mice. Although PDAPP mice have been available for some time, they have recently been switched to a pure C57Bl/6 background strain (for reasons as discussed in Chapter 1, section 1.4.2). Previous studies have reported age-related memory impairment and amyloid pathology in PDAPP mice bred on a mixed genetic background (Swiss-Webster, DB2 and C57Bl/6) (Games et al. 1995; Johnson-Wood et al. 1997; Dodart et al. 1999; Chen et al. 2000). To-date, only one study has characterised behaviour in PDAPP mice bred on a C57Bl/6 background (Hartman et al. 2005). Hartman and colleagues reported age-independent deficits in spatial learning and spatial reference memory as determined by the Morris water maze (MWM), which nevertheless worsened with age. Moreover the age-related deterioration in spatial reference memory was correlated with a significant increase in levels of A β in the HPC (Hartman et al. 2005). This supported the initial aim and hypothesis of this thesis that PDAPP mice would show an age-dependent (and task-specific) memory impairment, together with increased levels of A β production (see Chapters 3 and 4).

The extensive evidence that human APP mutations cause deficits in spatial navigation and spatial working memory (SWM) in several mouse lines led to the decision to evaluate SWM in PDAPP using a novel foraging task (based on the Olton radial arm maze procedure and prior studies of navigation in pigeons; Pearce et al. 2005). Mice with excitotoxic HPC lesions performed poorly on this task relative sham control mice. Moreover when the reliance upon spatial cues was removed and each pot was given a unique design, the performance of sham and lesioned mice was similar. These data indicated a role for the hippocampus in processing spatial information and complimented findings published by Pearce and colleagues (2005).

Given extensive evidence that HPC neuronal function is compromised by excess amyloid production, the foraging task was used to examine SWM performance in PDAPP mice across a range of ages. In addition, object recognition memory and object-place associations were also analysed in Chapter 4 in order to assess the distinct components of recognition memory and the integrity of circuits thought to underpin them. Previous studies have reported task specific impairments in the PDAPP model and other APP mouse lines, including the Tg2576 mouse model (Dodart et al. 1999; Hale & Good 2005; Good & Hale 2007). Chapters 3 and 4 reported age-dependent deficits in SWM and OiP memory at 14-16 months of age, but intact object recognition memory across all ages tested. These deficits were paralleled by a significant increase in levels of soluble and insoluble A β 42 in the HPC of 15-month old PDAPP male mice (Chapter 4, Experiment 6). Data obtained from Chapters 3 and 4 provide evidence that different tasks that require processing of spatial information are

sensitive to amyloid pathology. Collectively, these data further validated the use of the PDAPP model of amyloid pathology to assess the *in vivo* effects of 2B3.

The main aim of this thesis was to assess a monoclonal antibody, 2B3, in a mouse model of amyloid pathology. 2B3 had been shown to bind to APP at the β -secretase cleavage site and prevented the production of A β in multiple cell lines, including mouse primary cortical cultures (Thomas et al. 2011; Thomas et al. 2013). It was hypothesised that *in vivo* administration in APP transgenic mice would inhibit β -secretase mediated APP metabolism and thus A β production. Given a putative reduction in amyloid it was also hypothesised that 2B3 would improve memory function in transgenic APP mice. Following a 14-day ICV administration of 2B3 by osmotic minipumps, PDAPP mice were tested on the OiP task. 2B3 administration showed a significant improvement in OiP memory, as well as reduced levels of soluble A β 40, β CTF and reduced phosphorylation of the NMDAR NR2B subunit. These data support the hypothesis that administration of 2B3 *in vivo* will improve memory function by inhibiting APP cleavage at the β -secretase cleavage site. However, the overall levels of soluble A β 42 were not significantly reduced by 2B3 administration. The absence of a significant reduction in A β 42 may simple reflect the high levels variability in this measure and the need for greater statistical power. A similar observation was made with 3xTg mice following four-week ICV BBS1 administration. Despite significant reductions in total A β load and plaque size (Rabinovich-Nikitin et al. 2012), there was no significant change in soluble A β 42. A longer duration of treatment may arguably have a greater impact on A β production. Nevertheless, the changes in levels of β CTF and soluble A β 40 provide compelling evidence that 2B3 administration in PDAPP mice inhibited APP metabolism via the β -secretase cleavage site.

More recent studies with the antibody BBS1 have assessed its therapeutic values in a number of mouse models including Tg2576, the London APP mutation, as well as the 3xTg model (Rakover et al. 2007; Arbel-Ornath et al. 2009; Rabinovich-Nikitin et al. 2012). Data obtained between these studies however are often variable. For example, chronic intraperitoneal administration of BBS1 to Tg2576 mice showed reduced neuroinflammation (a reduction in active microglia). However, this effect was not observed in mice expressing the APP London mutation or 3xTg mice, which observed no change in either microglia or astrocyte activation and a reduction in astroglial activity only, respectively (Rakover et al. 2007; Arbel-Ornath et al. 2009; Rabinovich-Nikitin et al. 2012). Moreover, improved recognition memory performance was reported by Rakover (2007) and Rabinovich-Nikitin (2012) in Tg2576 and 3xTg mice, but no improvement in spatial learning and memory was

reported in the APP London mutation mice (Rakover et al. 2007; Arbel-Ornath et al. 2009; Rabinovich-Nikitin et al. 2012). Changes in amyloid pathology are also inconsistent following BBS1 treatment. BBS1 in the London APP mouse model showed significant reduction in insoluble A β 40 and A β 42, but not total levels of soluble A β . However, intraneuronal A β was significantly reduced (Arbel-Ornath et al. 2009). In the 3xTg mice BBS1 caused a significant reduction in plaque size and overall amyloid load (Rabinovich-Nikitin et al. 2012). However, no change in soluble or insoluble levels of A β 40 or A β 42 was observed in Tg2576 mice following chronic IP administration of BBS1 (Rakover et al. 2007). Variability in the impact of BBS1 on amyloid pathology may be due to (1) transgene or background differences in the Tg model, (2) route of administration, (3) duration of treatment and methodology used to assess protein levels *ex vivo*. Collectively, however, the BBS1 studies suggests that inhibition of APP metabolism via the β -secretase site provides a beneficial effect at both the cognitive and pathological level in transgenic mice.

Similar to 2B3 and BBS1, a non-antibody peptide treatment, S1, has been reported by Yang et al. (2012). S1 reportedly interacts and binds to the APP β -secretase cleavage site to inhibit BACE1 cleavage of APP. APP/PS1 mice received 5 weekly bilateral ICV infusions of S1 by Hamilton micro syringe prior to behavioural testing and *ex vivo* tissue analysis. S1 administration showed significant reductions in levels of soluble and insoluble A β 40, A β 42 and total levels of β CTF in *ex vivo* tissue of APP/PS1 mice (Yang et al. 2012). These mice also showed improved spatial learning and memory as determined by the MWM. Collectively, these data show that multiple compounds targeting the β -secretase cleavage site of APP can significantly improve memory performance and reduce amyloid pathology in multiple models of AD. It is therefore likely that the beneficial effects reported in Chapter 5 are therefore not specific to the PDAPP mouse model. Moreover, the data reported in Chapter 5 contributes to the growing evidence that inhibition of APP metabolism by β -secretase is a potential therapeutic target site for the treatment of early stage AD.

6.3 Does 2B3 Improve Synaptic Function underpinning memory in PDAPP Mice?

NMDA Receptors and Recognition Memory

As discussed in Chapter 4 (Section 4.1 and 4.4), successful memory performance in the OiP memory task is sensitive to HPC, mPFC and PRC dysfunction (Barker & Warburton 2011; Warburton & Brown 2015b). The receptors involved in processing object-based and

spatial information in these structures have also been investigated. Bilateral infusion of AP5, an NMDA receptor antagonist, into the PRC impaired novel object memory only in delays greater than 1 hour, but not less than (Barker et al., 2006; Winters & Bussey, 2005b). However, following infusion of kainite and muscarinic antagonists into the PRC, novel object memory impairments were observed following delays of less than 1 hour (Barker et al., 2006; Tinsley et al., 2011). Collectively these data indicate that object novelty memory is sensitive to different receptor mechanisms in a delay-dependent manner. Data reported in Chapter 4 showed no change in object recognition memory performance in PDAPP mice compared to WT controls across all delays and ages tested. As “short-term” delay periods have been defined as ≤ 5 -minutes and “long-term” as ≥ 1 -hour in the studies discussed above, this would suggest that all receptor mechanisms involved in processing object-based information remain intact in the PRC with age in PDAPP mice.

The roles of the HPC and mPFC in the OiP task have been reported to involve NMDAR-dependent processes, as the infusion of AP5 into each region independently impaired performance (Barker & Warburton, 2008, 2009). The neural circuit involved in processing object and place information was further determined following contralateral unilateral infusions of AP5 into the mPFC and PRC or HPC and PRC. AP5 infusion caused impairment following long delay periods, while short term object-in-place memory remained unaffected in rats (Barker & Warburton, 2009; Barker & Warburton, 2013). It has further been reported that OiP memory is impaired in both short- and long-term delays after subsequent crossed unilateral AP5 and CNQX infusion in mPFC and HPC (Barker & Warburton 2009; Barker et al., 2013). Thus, the processing of spatial-based information in the OiP memory task is sensitive to NMDA and glutamate receptor manipulations across both short and long-term delays. In contrast, object-based information is only NMDA-sensitive with long delays. Based on this analysis one can conclude that as PDAPP mice showed intact object recognition memory (Chapter 4, Experiment 4), but impaired OiP memory at 14-16 months of age (at both delays tested; Chapter 4, Experiment 5), it is likely that the behavioural impairment is a result of glutamate receptor, and more specifically, NMDAR function.

Chapter 4 (Experiment 6) reported an age-related increase in levels of soluble and insoluble A β 42 in the HPC of PDAPP mice at 15 months of age, it is likely that A β 42 played a significant role in the impaired processing of spatial information required for successful memory performance in the OiP task in PDAPP mice. Elevated levels of A β reduced synaptic NMDAR expression in cortical neuronal cultures (Kelly et al., 1996; Snyder et al., 2005;

Shankar et al., 2007). This reduced NMDAR expression has also been reported in synaptosomal membranes of 3xTg and Tg2576 mice (Zhang et al. 2010). Therefore it is likely that increased levels of A β in the HPC of PDAPP mice impacted upon the NMDAR-sensitive mechanisms involved in processing spatial information.

Although conflicting to findings *in vitro* and in Tg2576 and 3xTg mice, a further synaptic mechanism suggesting enhanced synaptic NMDAR expression has also been reported (Ittner et al. 2010). A more detailed discussion of these conflicting mechanisms can be found in the following section “*A β and NR2B – An enzymatic imbalance*”. The synaptic mechanism described by Ittner and colleagues reported an NR2B-associated mechanism stimulating NMDA activity and A β -mediated hyper-excitotoxicity, which has already been discussed in this thesis (Chapter 1, section 1.3.5). More specifically, the phosphorylation of the NR2B subunit at the tyrosine 1472 (Y1472) residue by the Src kinase, Fyn. Increased phosphorylation of the NR2B Y1472 subunit increases NR2B interaction with PSD95, inhibits AP2 clathrin-mediated endocytosis and stabilizes post-synaptic NMDARs (Prybylowski et al. 2005). A β activates NMDARs causing increased Ca²⁺ influx and neuronal excitotoxicity (Ittner et al. 2010). APP23 Tg mice have been reported to show increased levels of phosphorylated NR2B Y1472, leading to increased neuronal hyper excitability and SWM deficits in the T-maze. This deficit was reversed following ICV administration of Tat-NR2B9c, a peptide reported to protect from NMDAR-induced excitotoxicity (Ittner et al. 2010). APP23 mice have also been reported to show improved spatial learning and reference memory in the MWM following administration of memantine, a non-competitive NMDAR antagonist (Van Dam & De Deyn 2006) Results in Chapter 5 (Experiment 5B) revealed that vehicle-treated PDAPP mice showed an increase in NR2B phosphorylation at the Y1472 residue as a ratio to total NR2B levels. It is possible that this effect prevented NMDAR internalisation at the synapse in PDAPP mice and further caused neuronal excitotoxicity. However, to date, no study has determined NMDAR expression at the synapse in comparison to internalised NMDARs in order to confirm this in PDAPP mice.

The NR2B subunit in the HPC and forebrain of mice has been implicated in spatial learning and memory (von Engelhardt et al. 2008). Mice lacking the NR2B receptor specifically in the HPC showed intact spatial reference memory in the MWM. However, the same mice showed an impairment in reversal learning in the MWM and SWM in a spontaneous alternation protocol of the T-maze (von Engelhardt et al. 2008). Similarly, PDAPP mice show impaired reversal learning on the MWM and SWM deficits reported in Chapter 3 (Chen, Chen, Knox, Inglis, Bernard, Martin, Justice, Mcconlogue, et al. 2000;

Daumas et al. 2008). Following A β active immunotherapy in PDAPP mice, Chen et al., (2007) reported reductions in total levels of A β that negatively correlated with improved learning capacity on a serial reversal learning protocol in the MWM (Chen et al. 2007). In Chapter 5 (Experiment 5B) 17-18 month old PDAPP mice showed increased phosphorylation of the NR2B Y1472 subunit, which was reversed along following 2B3 administration. This reversal of NR2B phosphorylation is likely to have contributed to 2B3 mediated improvement in OiP memory in PDAPP mice. This finding parallels that reported by Chen et al., 2007 who demonstrated lower overall Ab load and improved learning capacity in PDAPP mice following an immunotherapy. Interestingly NR2B has been observed to facilitate both LTD and LTP in the CA1 region of the HPC (von Engelhardt et al. 2008; Dong et al. 2013). Interestingly, novel object and place associations stimulate the induction of LTD in the rat HPC CA1 sub region (Kemp & Manahan-Vaughan 2012). It is therefore tempting to suggest that the effects observed following 2B3 administration may be linked to improved LTD facilitation in PDAPP mice. However, further investigation is required in order to confirm this theory.

A β and NR2B – An enzymatic imbalance

Although increased NR2B phosphorylation at tyrosine 1472 in PDAPP mice was reported in Chapter 5, and in APP23 mice by Ittner and colleagues (2010), contradictory findings have been reported in other Tg models of AD (Zhang et al. 2010). Zhang and colleagues reported that Tg2576 and 3xTg mice showed an age-related *decrease* in levels of NR2B phosphorylated at the Y1472 residue. Ittner and colleagues reported the phosphorylation of the NR2B subunit was regulated by Fyn in a tau-dependent manner (Ittner et al 2010). However, Ittner and colleagues (2010) gave no consideration to the regulatory STriatal Enriched protein tyrosine Phosphatase (STEP).

STEP has been reported to act as a regulatory tyrosine phosphatase, which dephosphorylates the NR2B Y1472 residue as well as Fyn in order to inhibit Fyn kinase activity (Figure 6.1) (Nguyen et al. 2002; Snyder et al. 2005; Zhang et al. 2008). Increased levels of STEP have been reported in the brains of AD patients and in Tg models of AD (Chin et al. 2005; Kurup et al. 2010; Zhang et al. 2010). As well as being associated with increasing Fyn activity, A β has been reported to indirectly increase STEP activation and increase its translation via interaction with the α 7-nicotinic acetylcholine receptor (α 7nAChR) and metabotropic glutamate receptor 5 (mGluR5) respectively through downstream signalling

mechanisms (Snyder et al. 2005; Zhang et al. 2008). Interestingly, oligomeric A β coupled to the cellular prion protein activates Fyn via a physical interaction with mGluR5 leading to an increase in intracellular Ca²⁺ (Um et al. 2013). Thus, it is plausible that A β -mediated increased Fyn activation could be counteracted by increased STEP activity. Indeed, *in vitro* data have demonstrated this effect in a time-dependent manner (Um et al. 2012). WT cortical neurons treated with oligomeric A β for 15-minutes showed a significant increase in NR2B pY1472 and active Fyn. However, following 3 hours oligomeric A β treatment a significant increase in levels of STEP was observed compared to baseline conditions. This result was paralleled by a reduction in NR2B pY1472 and active Fyn relative to the 15-minute treatment group (Um et al. 2012). This result was further complimented by a time-dependent reduction in surface NR2B expression and suppressed NMDA-induced calcium signals (Figure 6.1). Given that STEP normalises NR2B pY1472 and active Fyn *in vitro*, it is paradoxical that data reported in the literature have observed reduced NR2B pY1472 in Tg2576 and 3xTg mice, but increased in APP23 and PDAPP mice (Ittner et al. 2010; Zhang et al. 2010; Chapter 5, Experiment 8).

Behavioural studies focusing on this mechanism have shown evidence for Fyn and STEP in the deregulation of neuronal activity and cognitive performance. A study using J9 and J20 mice crossed with mice overexpressing Fyn (double transgenic) reported more severe spatial reference memory deficits following MWM assessment than J9 or J20 mice with physiological levels of Fyn (Chin et al. 2005). Moreover, when these double transgenic mice were further crossed onto a tau knockout background they showed similar spatial learning and reference memory to non-Tg controls, whilst double transgenic mice expressing endogenous tau remained impaired (Roberson et al. 2011). These data are consistent with the mechanism proposed by Ittner and colleagues (2010) that fyn-tau interactions at the synapse in the APP23 mouse model of AD are responsible for neuronal excitotoxicity (Ittner et al. 2010).

Despite this evidence focussing on A β , tau and Fyn, STEP knock out (KO) models have also been reported (Zhang et al. 2010; Venkitaramani et al. 2011). Zhang and colleagues (2010) investigated the role of STEP by crossing STEP KO mice with either 3xTg mice or Tg2576 (Zhang et al. 2010). In this study, double mutant 3xTg mice/STEP^{-/-} showed improved spatial learning and reference memory in the MWM and SWM in the spontaneous alternation Y maze. No behavioural analysis was performed on Tg2576 mice. However, biochemical analysis of synaptosomal preparations showed increased membrane NR1, NR2B and NR2B pY1472 levels in both Tg2576/STEP^{-/-} and 3xTg/STEP^{-/-}. (see also Zhang et al. 2010; Venkitaramani et al. 2011 for STEP KO mouse). STEP KO effects were further

paralleled to increased Fyn activity as well as active ERK, also involved in synaptic strengthening and memory performance (Sato et al. 2007; Zhang et al. 2010).

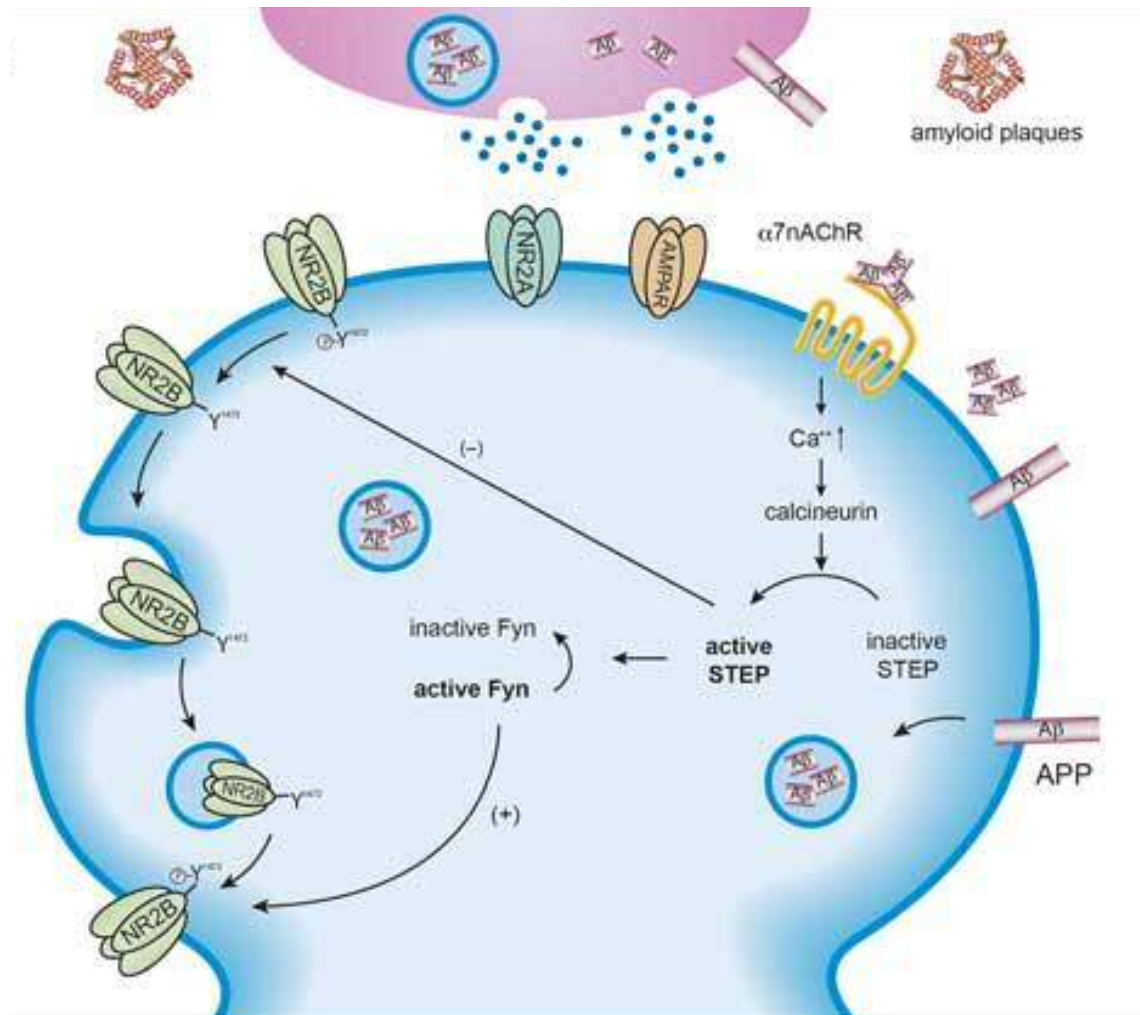


Figure 6.1: Increased activation of STEP reduces NR2B phosphorylation and increases NMDAR endocytosis. Aβ interaction with the α7nAChR results to an increase in Ca²⁺ influx and downstream signalling leading to an increase in STEP activity. Active STEP dephosphorylates Fyn kinase causing its deactivation and prevents further Fyn-mediated phosphorylation of the NR2B Y1472 residue. STEP also dephosphorylates the NR2B Y1472, which leads to an increase in NMDAR endocytosis and reduced NMDAR Ca²⁺ influx and excitotoxicity. Figure from (Venkitaramani et al. 2007)

The data considered above suggests that enzymatic activity of Fyn and STEP play significant roles in cognitive function and neuronal signalling pathways, particularly those involving NMDARs and the NR2B subunit. These pathways appear to be modulated by both

extracellular A β and intracellular tau protein. The physiological balance of the activity of Fyn and STEP is clearly of importance in memory performance in Tg AD models. However, it appears that discrepancies exist between specific mouse models such as the PDAPP and APP23 mouse model and the Tg2576 and 3xTg. Precise reasons why these differences exist remain elusive.

6.4 Are Transgenic Mouse Models of AD a useful tool for preclinical investigations?

Tg APP models of amyloid pathology often only exhibit increased amyloid production and deposition without developing NFTs. It has been argued that these models of AD only model pre-clinical AD at best (Zahs & Ashe, 2010). Therefore, how useful a tool are they to examine immunotherapy or indeed any therapy for AD? Despite a lack of NFT pathology in Tg models (except the 3xTg), APP mice show the majority of early stage AD pathologies; elevated A β , plaque pathology and neuroinflammation (Games et al. 1995; Hsiao et al. 1996; Mucke et al. 2000; Oddo et al. 2003; Oakley et al. 2006). Abnormal tau phosphorylation has been observed in a number of Tg mouse models, including the Tg2576, TgCRND8, APP/PS1 and APP23 (Kawarabayashi et al. 2004; Chauhan et al. 2005; Kurt et al. 2003; Bellucci et al. 2007; Maia et al. 2013). More recently, evidence has suggested that, similar to A β , hyperphosphorylated tau is likely to be neurotoxic, particularly at the synapse (Tai et al. 2012; Perez-Nievas et al. 2013; Pooler et al. 2013; Pooler et al. 2014). Indeed, fibrillar amyloid and associated oligomeric amyloid and increased phosphorylated tau protein at the synapse were correlated with dementia, whilst NFTs were not when compared to high-pathology controls (Perez-Nievas et al. 2013).

Currently, no anti-A β immunotherapy study using Tg APP mice has reported reduced tau phosphorylation as an effect of therapy, except when using the 3xTg mouse model (Oddo et al. 2004; Oddo, Vasilevko, et al. 2006; Rasool et al. 2013). However, although promising, it is unclear whether changes in tau phosphorylation in 3xTg mice are a true reflection of tau hyperphosphorylation induced by A β , independent of the P301L mutation, which, of course, is not a mutation associated with AD. Tg models such as Tg2576 and APP/PS1 mice have been observed to show hyperphosphorylated tau at 11 and 12 months of age respectively (Shi et al. 2011; G.-P. Liu et al. 2013). To date, very few studies have investigated the benefits of

pharmacological intervention in these models and changes in tau phosphorylation. However, it has been reported that reduced tau phosphorylation is observed in Tg2576 and APP/PS1 mice coupled with reduced total A β load following silencing of inhibitor-2 of protein phosphatase-2A and anti-TNF- α ICV infusion respectively (Shi et al. 2011; Liu et al. 2013). These results show that tau hyperphosphorylation in Tg APP models is sensitive to pharmacological intervention. However, these effects are yet to be investigated by anti-A β or anti-APP immunotherapy. Moreover, it would be interesting to investigate if this hyperphosphorylation in Tg APP models contributed to overall pathology or impaired cognitive function in these mouse models through the use of tau-directed therapies, including tau immunotherapy.

A missing parallel when comparing preclinical immunotherapy assessment with clinical trials is a matching stage of pathology between AD patients and AD mouse models. Clinical evidence has shown that immunotherapy treatment in late stages of the disease is unable to show clinical benefits, whilst preclinical trials in AD mouse models showed significant reversals in cognitive deficits and reduced pathology (Karran & Hardy 2014). These preclinical data strongly suggest that early intervention prior to NFT pathology may have significant benefit. However, no study has yet been able to investigate this in APP mouse models or human AD. Therefore, current models of AD are certainly not without limitation. Despite showing increased soluble A β and plaque pathology and increased tau phosphorylation, Tg APP models do not recapitulate the full extent of human AD pathophysiology, including NFT development and brain atrophy. Despite the generation of the 3xTg, a more representational model of AD that is able to develop the full AD pathology is required. At the same time, improved diagnostic protocols, which are not limited to research purpose only are required in order to detect the onset of AD at much earlier ages in order to optimise chances for significant clinical benefit from immunotherapy and other pharmacological trials to prevent/delay the onset of AD.

6.5 Is there still hope for immunotherapy and Alzheimer's disease?

Numerous pre-clinical studies assessing AD immunotherapies have shown both improved cognition as well as reduced pathology in Tg models (Solomon & Frenkel 2010; Karran & Hardy 2014). However, as discussed in Chapter 1 (Section 1.5), limited success has been observed at the clinical level using anti-A β immunotherapy. Despite this, the most recent data from clinical immunotherapy trials is beginning to show more promising results

(Reardon 2015; Qian et al. 2015). Despite these marginal improvements emerging from ongoing clinical trials, certain risk factors associated with immunotherapy have emerged which must be considered for chronic treatment periods that are likely required for AD treatment. One major risk factor is an increased incidence of amyloid-related imaging abnormalities (ARIA) and micro-haemorrhage. Increased micro-haemorrhage associated with cerebral amyloid angiopathy (CAA) has been reported in a number of preclinical investigations (Wilcock et al. 2004; Racke et al. 2005; Wilcock et al. 2006; Karlinski et al. 2008). These effects were associated with duration of treatment (Wilcock et al. 2006). This preclinical change was also observed following clinical Phase II trials with Bapinezumab (humanized 3D6), whereby ARIA-related complications, including abnormalities associated with parenchymal vasogenic oedema and micro-haemorrhages were reported (Sperling et al. 2012). A likely mechanism for these observations was the removal of A β from cerebral vasculature associated with increased BBB penetrability and the onset of micro-haemorrhage (Sperling et al. 2012; Farlow & Brosch 2013).

One interesting observation was reported following comparative immunotherapy of 3D6 (Bapinezumab, an N-terminal directed anti-A β antibody) and m266 (Solanezumab, targeting residues 16-24 of A β), in PDAPP mice over a period of six weeks. Following 3D6 treatment, PDAPP mice exhibited an increase in CAA-related micro-hemorrhage, also reported to be dose-dependent (Racke et al. 2005; Schroeter et al. 2008). However, this effect was not observed following treatment with m266, which showed no effect on CAA-associated micro-hemorrhages (Racke et al. 2005; Schroeter et al. 2008). Moreover, no ARIA-related complications were reported following clinical evaluation of Solanezumab trials. The mechanisms reported for A β clearance mediated by either 3D6 or m266 also differ significantly. 3D6 has been observed to bind A β plaques and induce Fc-mediated microglial phagocytosis, whilst m266 is believed to sequester peripheral A β , shifting the equilibrium of A β movement and increasing its removal from the brain as proposed by the “peripheral sink” hypothesis (DeMattos et al. 2002; Bard et al. 2003). These data indicate that targeting A β differentially can have significantly different clinical side effects, despite both antibodies providing preclinical benefit at the cognitive level. Understanding individual antibody mechanisms for A β clearance is therefore important in order to best monitor, limit or prevent side-effects discussed above.

The data obtained in this thesis on 2B3, alongside data obtained from BBS1 suggests that targeting APP at the β -secretase cleavage site provides a promising alternative/additional approach to anti-A β immunotherapy. Indeed, the added reduction in β CTF observed in

PDAPP mice following 2B3 administration may provide further clinical benefit where anti-A β immunotherapy is unable. However, further evaluation of 2B3 is still required as discussed below (section 6.6). It is tempting to suggest that effects such as micro-hemorrhage are unlikely using 2B3 immunotherapy as A β production is inhibited by binding to APP, not A β for subsequent removal from the brain as with 3D6 and m266. Moreover, a significant reduction in brain micro-hemorrhage was observed following BBS1 treatment in Tg2576 mice (Rakover et al. 2007). However, inconsistencies between studies assessing BBS1 (as discussed in Chapter 5, Section 5.4) exist and therefore these tests should be performed following 2B3.

Despite the lack of translational success from preclinical to clinical evaluation, multiple factors complicate such a transition between levels of research. These include the obvious differences that mice themselves do not develop (or do not naturally live long enough to develop) all AD symptoms. Tg models exhibit symptoms more closely associated with pre-clinical AD, not the mild-moderate AD that has been used to evaluate immunotherapies. Testing memory function in AD mice often relies on visual, non-verbal memory tasks, whereas those used in patients with AD often require both verbal communication and visual memory. Therefore, the precise memory systems being used in order to complete or show successful memory performance likely differ significantly. Despite this, Tg models of AD remain a focus for research into the pathological mechanisms of AD and associated cognitive deficits. It is arguable that for successful translational research from preclinical to clinical, lessons must be learnt from oversights of past research. Thus, future preclinical evaluation must be more thorough whilst reducing the clinical gap in terms of the model-based systems available to optimise the chance of successful translation of putative AD immunotherapies.

6.6 Future directions

Despite the exciting data obtained in Chapter 5 (Experiments 4 and 5), these results merely indicate a proof-of-principle that direct application of 2B3 into the brain and inhibition of APP metabolism at the β -secretase cleavage site can improve memory function in PDAPP mice. A number of further studies are still required in order to better understand how 2B3 improves memory, receptor activity and amyloid pathology in the PDAPP model.

Following altered NR2B phosphorylation, it is likely that surface NMDAR expression may be altered following 2B3 administration. Thus, it would be worthwhile examining altered neuronal activity through use of techniques such as *in vivo* 2-photon imaging or slice electrophysiology. Previous anti-A β immunotherapies have recently reported increased neuronal hyper-excitability in PDAPP and Tg2576 mice (Busche et al. 2015). However, Busche and colleagues determined this effect using 3D6 and β 1, both anti-A β N-terminal antibodies. Therefore, it remains unclear if this is an effect limited to antibodies directed at the N-terminus of A β . However, it has previously been reported that PDAPP mice administered 10D5 (anti-A β antibody targeting A β epitopes 3-6) showed improved spatial learning and LTP in the hippocampal CA1 region compared to control PDAPP mice (Hartman et al. 2005). Busche and colleagues (2015) determined cortical neuronal activity in PDAPP mice, whereas Hartman and colleagues (2005) assessed HPC activity in the CA1 region. It would be of interest therefore to assess the effects of immunotherapy, such as 2B3, on neuronal activity in multiple regions of the brain, the HPC as well as specific cortical regions such as the entorhinal cortex and prefrontal cortex.

Further biochemical assays should also be carried out to provide a clearer understanding of how 2B3 affects amyloid pathology and NMDAR physiology *ex vivo*. Despite measures of PSD95 being reported in Experiment 5B, analysis was performed on whole HPC soluble extracts. A more reliable measure of synaptic density might be obtained in Western blot analysis using synaptosomal preparations. Moreover, it would be interesting to observe whether altered NR2B phosphorylation changes NMDAR surface expression and whether this change in phosphorylation state is an effect of altered Fyn or STEP levels/activity in synaptosomal preparations (Ittner et al. 2010; Zhang et al. 2010). Following a significant reduction in levels of β CTF, an interesting study would be to examine changes in endocytosis, such as those described by Kim and colleagues (2015). Here, persistent rab5 over activation caused by increased levels of β CTF led to pathologically accelerated endocytosis and impaired axonal transport in AD brain (Kim et al. 2015). It is tempting to postulate that investigating this mechanism with 2B3 treatment may reveal that inhibiting APP metabolism at the β -secretase cleavage site might improve AD-related pathologies through more than one physiological process.

Experiment 7 only measured OiP memory following 2B3 administration. However, other cognitive deficits associated with age related changes in A β pathology have been reported and indeed reported in Chapter 3 (Experiment 2) (Dodart et al. 1999; Chen, Chen, Knox, Inglis, Bernard, Martin, Justice, Mcconlogue, et al. 2000; Hartman et al. 2005; Dumas

et al. 2008). Further investigation into whether 2B3 administration is able to improve memory across a range of memory tasks, sensitive to AD pathology would be beneficial to examine the generality of cognitive changes across different performance parameters. Moreover, cognitive tasks more closely associated with memory deficits observed in AD may provide a closer parallel for AD-related cognitive deficits. For example, AD patients display episodic memory deficits, an inability to recall events in relation to their content and temporal-spatial information (Tulving 1972; Butters et al. 1987; Greene et al. 1996). Rodent cognitive tasks have been able to assess an analogue of episodic-like memory that interrogate an animals ability to exhibit an integrated memory for “what” happened, “where” and “when”. These tasks include adaptations of object-based and fear conditioned memory paradigms (M. A. Good et al. 2007; Iordanova et al. 2008; Iordanova et al. 2011). These types of tasks offer a potentially more suitable cognitive platform in which to evaluate immunotherapies such as 2B3 prior to clinical investigation.

A final further investigation for 2B3 focuses on a more clinical application. In Chapter 5, 2B3 was administered directly into the brain of PDAPP mice. However, clinical application requires peripheral administration. The effects observed in Experiments 4 and 5 therefore need repeating following a peripheral route of administration, such as delivery into the intraperitoneal space, as with previous preclinical immunotherapy investigation of anti-A β and anti-APP antibodies (Bard et al. 2000; Dodart et al. 2002; Hartman et al. 2005; Rakover et al. 2007; Arbel-Ornath et al. 2009). Given that approximately 0.1% of antibody dose crosses the BBB, it may be possible that the effects of 2B3 observed following ICV administration occur due to the relatively high concentration that might have been present in the HPC. Moreover, a more chronic treatment period is also required for investigation, in order to assess the long-term affects of inhibiting APP metabolism at the β -secretase cleavage site. Indeed such an analysis could be extended to WT mice to explore the normal function of beta-secretase cleavage of APP

6.7 Thesis Summary and Conclusions

Over 15 years has passed since the initial report using antibody directed therapy to treat AD in Tg mouse models was presented (Bard et al. 2000). This strategy appears to still exist as one of the most promising forms of preventative treatment targeting the amyloid cascade hypothesis and AD pathogenesis. The success and advance of this potential treatment approach for AD owes a great deal to the use of Tg mouse models of AD and their contribution to our understanding today of AD mechanisms. It is with much excitement and anticipation that the results of on-going clinical trials using immunotherapy (and other forms of treatment) are awaited for.

The data presented in this thesis extends the current understanding of the behavioural phenotype of the PDAPP mouse model in relation to age-related amyloid pathology. The preclinical evaluation of 2B3 showed a significant improvement in OiP memory and significant reductions in A β 40 and β CTF. These analyses also revealed changes in NMDAR phosphorylation; a receptor class inextricably linked visuo-spatial memory. Collectively, these data offer novel *in vivo* and *ex vivo* findings following immunotherapy targeting the β -secretase cleavage site of APP. More extensive work to assess, confirm and extend these findings is still required. However, the data presented in this thesis are novel and important and provide support for the hypothesis that inhibition of A β production by steric hindrance can improve memory and amyloid-related pathology.

Bibliography

- Aarts, M. et al., 2002. Treatment of ischemic brain damage by perturbing NMDA receptor-PSD-95 protein interactions. *Science (New York, N.Y.)*, 298(5594), pp.846–50.
- Aggleton, J.P., 1985. One-trial object recognition by rats. *The Quarterly Journal of Experimental Psychology Section B*, 37(4), pp.279–294.
- Aggleton, J.P., Hunt, P.R. & Rawlins, J.N.P., 1986. The effects of hippocampal lesions upon spatial and non-spatial tests of working memory. *Behavioural Brain Research*, 19(2), pp.133–146.
- Aggleton, J.P. & Road, S., 1986. The effects of hippocampal lesions upon spatial and non-spatial tests of working memory. *Behavioural brain research*, 19, pp.133–146.
- Alamed, J. et al., 2006. Two-day radial-arm water maze learning and memory task; robust resolution of amyloid-related memory deficits in transgenic mice. *Nature protocols*, 1(4), pp.1671–1679.
- Albert, M.S. et al., 2011. The diagnosis of mild cognitive impairment due to Alzheimer's disease: Recommendations from the National Institute on Aging-Alzheimer's Association workgroups on diagnostic guidelines for Alzheimer's disease. *Alzheimer's & Dementia*, 7(3), pp.270–279.
- Ally, B.A. et al., 2013. Pattern separation and pattern completion in Alzheimer's disease: Evidence of rapid forgetting in amnesic mild cognitive impairment. *Hippocampus*, 23(12), pp.1246–1258.
- Alvarez, A., Muñoz, J.P. & Maccioni, R.B., 2001. A Cdk5–p35 Stable Complex Is Involved in the β -Amyloid-Induced Deregulation of Cdk5 Activity in Hippocampal Neurons. *Experimental Cell Research*, 264(2), pp.266–274.
- Anagnostaras, S.G. et al., 2003. Selective cognitive dysfunction in acetylcholine M1 muscarinic receptor mutant mice. *Nature neuroscience*, 6(1), pp.51–58.
- Antunes, M. & Biala, G., 2012. The novel object recognition memory: neurobiology, test procedure, and its modifications. *Cognitive processing*, 13(2), pp.93–110.
- Arancio, O. et al., 2004. RAGE potentiates A β -induced perturbation of neuronal function in transgenic mice. *The EMBO journal*, 23(20), pp.4096–105.
- Arbel, M., Yacoby, I. & Solomon, B., 2005. Inhibition of amyloid precursor protein processing by β -secretase through site-directed antibodies. *Proceedings of the National Academy of Sciences of the United States of America*, 102 (21), pp.7718–7723.
- Arbel-Ornath, M. et al., 2009. Immunomodulation of A β PP processing alleviates amyloid- β -related pathology in Alzheimer's disease transgenic mice. *Journal of Alzheimer's disease: JAD*, 22(2), pp.469–482.
- Arendt, T., Brockner, M.K. & Lange, M., 1992. CHANGES IN ACETYLCHOLINESTERASE AND BUTYRYLCHOLINESTERASE IN

ALZHEIMER ' S DISEASE RESEMBLE EMBRYONIC D E V E L O P M E N T - - A
S T U D Y O F M O L E C U L A R F O R M S * . , 21(3), pp.381–396.

- Von Arnim, C.A.F. et al., 2005. The low density lipoprotein receptor-related protein (LRP) is a novel β -secretase (BACE1) substrate. *Journal of Biological Chemistry*, 280(18), pp.17777–17785.
- Arriagada, P. V, Growdon, J.H., et al., 1992. Neurofibrillary tangles but not senile plaques parallel duration and severity of Alzheimer's disease. *Neurology*, 42(3), p.631.
- Arriagada, P. V, Marzloff, K. & Hyman, B.T., 1992. Distribution of Alzheimer type pathologic changes in nondemented elderly individuals matches the pattern in Alzheimer's disease. *Neurology*, 42(9), p.1681.
- Asai, M. et al., 2003. Putative function of ADAM9, ADAM10, and ADAM17 as APP α -secretase. *Biochemical and biophysical research communications*, 301(1), pp.231–235.
- Asai, M. et al., 2006. The novel beta-secretase inhibitor KMI-429 reduces amyloid beta peptide production in amyloid precursor protein transgenic and wild-type mice. *Journal of neurochemistry*, 96(2), pp.533–40.
- Association, A., 2014. 2014 Alzheimer ' s Disease Facts and Figures. *Alzheimer's & Dementia*, 10(2).
- Association, A.P., 1994. Diagnostic and statistical manual of mental disorders (DSM). *Washington, DC: American psychiatric association*, pp.143–147.
- Association, A.P., 2000. *diagnostic criteria from dsM-iV-tr*, American Psychiatric Pub.
- Bachevalier, J. & Nemanic, S., 2008. Memory for spatial location and object-place associations are differently processed by the hippocampal formation, parahippocampal areas TH/TF and perirhinal cortex. *Hippocampus*, 18(1), pp.64–80.
- Bäckman, L., Small, B.J. & Fratiglioni, L., 2001. Stability of the preclinical episodic memory deficit in Alzheimer's disease. *Brain*, 124(1), pp.96–102.
- Baguley, T., 2004. Understanding statistical power in the context of applied research. *Applied ergonomics*, 35(2), pp.73–80.
- Bales, K.R. et al., 2006. Cholinergic dysfunction in a mouse model of Alzheimer disease is reversed by an anti-A β antibody. *Journal of Clinical Investigation*, 116(3), p.825.
- Ballatore, C., Lee, V.M.-Y. & Trojanowski, J.Q., 2007. Tau-mediated neurodegeneration in Alzheimer's disease and related disorders. *Nature reviews. Neuroscience*, 8(9), pp.663–72.
- Banks, W. a. et al., 2002. Passage of amyloid β protein antibody across the blood–brain barrier in a mouse model of Alzheimer's disease. *Peptides*, 23(12), pp.2223–2226.
- Bannerman, D.M. et al., 2004. Regional dissociations within the hippocampus--memory and anxiety. *Neuroscience and biobehavioral reviews*, 28(3), pp.273–83.

- Bard, F. et al., 2003. Epitope and isotype specificities of antibodies to β -amyloid peptide for protection against Alzheimer's disease-like neuropathology. *Proceedings of the National Academy of Sciences*, 100(4), pp.2023–2028.
- Bard, F. et al., 2000. Peripherally administered antibodies against amyloid beta-peptide enter the central nervous system and reduce pathology in a mouse model of Alzheimer disease. *Nature medicine*, 6(8), pp.916–9.
- Barker, G.R.I. et al., 2007. Recognition memory for objects, place, and temporal order: a disconnection analysis of the role of the medial prefrontal cortex and perirhinal cortex. *The Journal of neuroscience : the official journal of the Society for Neuroscience*, 27(11), pp.2948–57.
- Barker, G.R.I. et al., 2006. The Different Effects on Recognition Memory of Perirhinal Kainate and NMDA Glutamate Receptor Antagonism: Implications for Underlying Plasticity Mechanisms. *The Journal of Neuroscience*, 26 (13), pp.3561–3566.
- Barker, G.R.I. & Warburton, E.C., 2009. Critical role of the cholinergic system for object-in-place associative recognition memory. *Learning & Memory*, 16 (1), pp.8–11.
- Barker, G.R.I. & Warburton, E.C., 2008. NMDA Receptor Plasticity in the Perirhinal and Prefrontal Cortices Is Crucial for the Acquisition of Long-Term Object-in-Place Associative Memory. *The Journal of Neuroscience*, 28 (11), pp.2837–2844.
- Barker, G.R.I. & Warburton, E.C., 2013. Object-in-Place Associative Recognition Memory Depends on Glutamate Receptor Neurotransmission Within Two Defined Hippocampal-Cortical Circuits: A Critical Role for AMPA and NMDA Receptors in the Hippocampus, Perirhinal, and Prefrontal Cortices. *Cerebral cortex (New York, N.Y. : 1991)*, pp.1–10.
- Barker, G.R.I. & Warburton, E.C., 2011. When is the hippocampus involved in recognition memory? *The Journal of neuroscience : the official journal of the Society for Neuroscience*, 31(29), pp.10721–31.
- Barnes, P., Hale, G. & Good, M., 2004. Intramaze and Extramaze Cue Processing in Adult APP SWE Tg2576 Transgenic Mice. *Behavioral neuroscience*, 118(6), p.1184.
- Baumann, K. et al., 1993. Abnormal Alzheimer-like phosphorylation of tau-protein by cyclin-dependent kinases cdk2 and cdk5. *FEBS letters*, 336(3), pp.417–24.
- Beach, T.G. et al., 2012. Accuracy of the Clinical Diagnosis of Alzheimer Disease at National Institute on Aging Alzheimer's Disease Centers, 2005–2010. *Journal of Neuropathology and Experimental Neurology*, 71(4), pp.266–273.
- Beatty, W.W. et al., 1988. Retrograde amnesia in patients with Alzheimer's disease or Huntington's disease. *Neurobiology of aging*, 9, pp.181–186.
- Bellucci, A. et al., 2007. Abnormal processing of tau in the brain of aged TgCRND8 mice. *Neurobiology of Disease*, 27(3), pp.328–338.
- Benilova, I., Karran, E. & De Strooper, B., 2012. The toxic A β oligomer and Alzheimer's disease: an emperor in need of clothes. *Nature neuroscience*, 15(3), pp.349–57.

- Berger, Z. et al., 2007. Accumulation of pathological tau species and memory loss in a conditional model of tauopathy. *The Journal of neuroscience*, 27(14), pp.3650–3662.
- Bettens, K., Sleegers, K. & Van Broeckhoven, C., 2013a. Genetic insights in Alzheimer's disease. *The Lancet Neurology*, 12(1), pp.92–104.
- Bettens, K., Sleegers, K. & Van Broeckhoven, C., 2013b. Genetic insights in Alzheimer's disease. *The Lancet. Neurology*, 12(1), pp.92–104.
- Bezprozvanny, I., 2009. Amyloid Goes Global. *Science Signaling*, (March 2009), pp.1–7.
- Bhaskar, K., Yen, S.-H. & Lee, G., 2005. Disease-related modifications in tau affect the interaction between Fyn and Tau. *The Journal of biological chemistry*, 280(42), pp.35119–25.
- Bierer, L.M. et al., 1995. Neocortical neurofibrillary tangles correlate with dementia severity in Alzheimer's disease. *Archives of neurology*, 52(1), pp.81–88.
- Billings, L.M. et al., 2005. Intraneuronal Aβ causes the onset of early Alzheimer's disease-related cognitive deficits in transgenic mice. *Neuron*, 45(5), pp.675–88.
- Billings, L.M. et al., 2007. Learning decreases Aβ*56 and tau pathology and ameliorates behavioral decline in 3xTg-AD mice. *The Journal of neuroscience : the official journal of the Society for Neuroscience*, 27(4), pp.751–61.
- Bliss, T.V.P. & Collingridge, G.L., 1993. A Synaptic model of memory: long-term potentiation in the hippocampus. *Nature*, 361, pp.31–39.
- Boche, D. & Nicoll, J.A.R., 2008. SYMPOSIUM: Clearance of Aβ from the Brain in Alzheimer's Disease: The Role of the Immune System in Clearance of Aβ from the Brain. *Brain Pathology*, 18(2), pp.267–278.
- Bondi, M.W. et al., 2008. Neuropsychological contributions to the early identification of Alzheimer's disease. *Neuropsychology review*, 18(1), pp.73–90.
- Braak, H. & Braak, E., 1991. Neuropathological staging of Alzheimer-related changes. *Acta Neuropathologica*, 82, pp.239 – 259.
- Braak, H. & Braak, E., 1995. Staging of Alzheimer's Disease-Related Neurofibrillary Changes. *Neurobiology of aging*, 16(3), pp.271–278.
- Braak, H. & Del Tredici, K., 2011. The pathological process underlying Alzheimer's disease in individuals under thirty. *Acta neuropathologica*, 121(2), pp.171–181.
- Broadbent, N.J. et al., 2010. Object recognition memory and the rodent hippocampus. *Learning & Memory*, 17(1), pp.5–11.
- Brooks, S.P. et al., 2005. Behavioural profiles of inbred mouse strains used as transgenic backgrounds. II: cognitive tests. *Genes, brain, and behavior*, 4(5), pp.307–17.

- Brown, M.W. & Aggleton, J.P., 2001. Recognition memory: what are the roles of the perirhinal cortex and hippocampus? *Nature reviews. Neuroscience*, 2(1), pp.51–61.
- Brüggemann, M. et al., 1989. The immunogenicity of chimeric antibodies. *The Journal of experimental medicine*, 170(6), pp.2153–2157.
- Burnham, S.C. et al., 2014. A blood-based predictor for neocortical A[β] burden in Alzheimer's disease: results from the AIBL study. *Mol Psychiatry*, 19(4), pp.519–526.
- Busche, M.A. et al., 2015. Decreased amyloid-[β] and increased neuronal hyperactivity by immunotherapy in Alzheimer's models. *Nature neuroscience*.
- Busciglio, J. et al., 1995. β -Amyloid fibrils induce tau phosphorylation and loss of microtubule binding. *Neuron*, 14(4), pp.879–888.
- Bussey, T.J. et al., 2000. Distinct patterns of behavioural impairments resulting from fornix transection or neurotoxic lesions of the perirhinal and postrhinal cortices in the rat. *Behavioural Brain Research*, 111(1–2), pp.187–202.
- Butters, N. et al., 1987. Episodic and semantic memory: A comparison of amnesic and demented patients. *Journal of Clinical and Experimental Neuropsychology*, 9(5), pp.479–497.
- Buttini, M. et al., 2005. β -Amyloid immunotherapy prevents synaptic degeneration in a mouse model of Alzheimer's disease. *The Journal of neuroscience*, 25(40), pp.9096–9101.
- Cain, D.P. et al., 1996. Detailed behavioral analysis of water maze acquisition under APV or CNQX: contribution of sensorimotor disturbances to drug-induced acquisition deficits. *Behavioral neuroscience*, 110(1), p.86.
- Calhoun, M.E. et al., 1998. Neuron loss in APP transgenic mice. *Nature*, 395(6704), pp.755–756.
- De Calignon, A. et al., 2012. Propagation of tau pathology in a model of early Alzheimer's disease. *Neuron*, 73(4), pp.685–97.
- Capecchi, M.R., 1989. The new mouse genetics: Altering the genome by gene targeting. *Trends in Genetics*, 5(0), pp.70–76.
- Carlesimo, G.A. et al., 1994. Verbal and spatial memory spans in Alzheimer's and multi-infarct dementia. *Acta Neurologica Scandinavica*, 89(2), pp.132–138.
- Carling, K., 1998. Resistant outlier rules and the non-Gaussian case *. *Computational Statistics and Data Analysis*, 33, pp.249–258.
- Carlson, M.C. et al., 2008. Midlife activity predicts risk of dementia in older male twin pairs. *Alzheimer's & Dementia*, 4(5), pp.324–331.

- Carroll, J.C. et al., 2007. Progesterone and estrogen regulate Alzheimer-like neuropathology in female 3xTg-AD mice. *The Journal of neuroscience : the official journal of the Society for Neuroscience*, 27(48), pp.13357–65.
- Cassel, J.C. et al., 1998. Fimbria-fornix vs selective hippocampal lesions in rats: effects on locomotor activity and spatial learning and memory. *Neurobiology of learning and memory*, 69(1), pp.22–45.
- Cataldo, A.M. et al., 2000. Endocytic pathway abnormalities precede amyloid β deposition in sporadic Alzheimer's disease and Down syndrome: differential effects of APOE genotype and presenilin mutations. *The American journal of pathology*, 157(1), pp.277–286.
- Cataldo, A.M. et al., 1997. Increased neuronal endocytosis and protease delivery to early endosomes in sporadic Alzheimer's disease: neuropathologic evidence for a mechanism of increased β -amyloidogenesis. *The Journal of neuroscience*, 17(16), pp.6142–6151.
- Chabrier, M.A. et al., 2012. Soluble A β promotes wild-type tau pathology in vivo. *The Journal of neuroscience*, 32(48), pp.17345–17350.
- Chapman, P.F. et al., 1999. Impaired synaptic plasticity and learning in aged amyloid precursor protein transgenic mice. *Nature neuroscience*, 2(3), pp.271–276.
- Chauhan, N.B., Siegel, G.J. & Feinstein, D.L., 2005. Propentofylline attenuates tau hyperphosphorylation in Alzheimer's Swedish mutant model Tg2576. *Neuropharmacology*, 48(1), pp.93–104.
- Chauhan, N.B., Siegel, G.J. & Lichtor, T., 2004. Effect of age on the duration and extent of amyloid plaque reduction and microglial activation after injection of anti-A β antibody into the third ventricle of TgCRND8 mice. *Journal of neuroscience research*, 78(5), pp.732–41.
- Chávez-Gutiérrez, L. et al., 2012. The mechanism of γ -Secretase dysfunction in familial Alzheimer disease. *The EMBO journal*, 31(10), pp.2261–74.
- Chen, G., Chen, K.S., Knox, J., Inglis, J., Bernard, A., Martin, S.J., Justice, A., McConlogue, L., et al., 2000. A learning deficit related to age and [beta]-amyloid plaques in a mouse model of Alzheimer's disease. *Nature*, 408(6815), pp.975–979.
- Chen, G., Chen, K.S., Knox, J., Inglis, J., Bernard, A., Martin, S.J., Justice, A., McConlogue, L., et al., 2000. A learning deficit related to age and β -amyloid plaques in a mouse model of Alzheimer's disease. *Nature*, 2940(1998), pp.975–979.
- Chen, G. et al., 2007. Active β -amyloid immunization restores spatial learning in PDAPP mice displaying very low levels of β -amyloid. *The Journal of neuroscience*, 27(10), pp.2654–2662.
- Chételat, G. et al., 2012. Accelerated cortical atrophy in cognitively normal elderly with high β -amyloid deposition. *Neurology*, 78(7), pp.477–484.

- Chin, J. et al., 2005. Fyn kinase induces synaptic and cognitive impairments in a transgenic mouse model of Alzheimer's disease. *The Journal of neuroscience*, 25(42), pp.9694–703.
- Chin, J. et al., 2004. Fyn kinase modulates synaptotoxicity, but not aberrant sprouting, in human amyloid precursor protein transgenic mice. *The Journal of neuroscience*, 24(19), pp.4692–7.
- Chishti, M.A. et al., 2001. Early-onset amyloid deposition and cognitive deficits in transgenic mice expressing a double mutant form of amyloid precursor protein 695. *Journal of Biological Chemistry*, 276(24), pp.21562–21570.
- Choi, S.H. et al., 2014. A three-dimensional human neural cell culture model of Alzheimer's disease. *Nature*, 515(7526), pp.274–278.
- Choi, S.H. et al., 2001. Memory impairment and cholinergic dysfunction by centrally administered A β and carboxyl-terminal fragment of Alzheimer's APP in mice. *The FASEB Journal*, 15(10), pp.1816–1818.
- Christensen, H. et al., 1998. Rates of forgetting in Alzheimer dementia. *Neuropsychologia*, 36(6), pp.547–557.
- Chromy, B.A. et al., 2003. Self-assembly of A β 1-42 into globular neurotoxins. *Biochemistry*, 42(44), pp.12749–12760.
- Clark, R.E., Zola, S.M. & Squire, L.R., 2000. Impaired recognition memory in rats after damage to the hippocampus. *The Journal of Neuroscience*, 20(23), pp.8853–8860.
- Cleary, J.P. et al., 2005. Natural oligomers of the amyloid-beta protein specifically disrupt cognitive function. *Nature neuroscience*, 8(1), pp.79–84.
- Clinton, L.K. et al., 2007. Age-dependent sexual dimorphism in cognition and stress response in the 3xTg-AD mice. *Neurobiology of disease*, 28(1), pp.76–82.
- Cockrell, J.R. & Folstein, M.F., 1988. Mini-Mental State Examination (MMSE). *Psychopharmacology bulletin*, 24(4), p.689.
- Cohen, J., 1992. A power primer. *Psychological bulletin*, 112(1), p.155.
- Cole, S.L. & Vassar, R., 2007. The Alzheimer's disease beta-secretase enzyme, BACE1. *Molecular neurodegeneration*, 2, p.22.
- Corcoran, K.A. et al., 2002. Overexpression of hAPPswe impairs rewarded alternation and contextual fear conditioning in a transgenic mouse model of Alzheimer's disease. *Learning & Memory*, 9(5), pp.243–252.
- Coric, V. et al., 2012. Safety and tolerability of the γ -secretase inhibitor avagacestat in a phase 2 study of mild to moderate Alzheimer disease. *Archives of neurology*, 69(11), pp.1430–1440.

- Cribbs, D.H. et al., 2003. Adjuvant dependent modulation of Th1 and Th2 responses to immunization with β amyloid. *International Immunology*, 15 (4), pp.505–514.
- Crouzin, N. et al., 2013. Area-specific alterations of synaptic plasticity in the 5XFAD mouse model of Alzheimer's disease: dissociation between somatosensory cortex and hippocampus. *PloS one*, 8(9), p.e74667.
- Crump, C.J., Johnson, D.S. & Li, Y.-M., 2013. Development and mechanism of γ -secretase modulators for Alzheimer's disease. *Biochemistry*, 52(19), pp.3197–3216.
- D'Hooge, R. & De Deyn, P.P., 2001. Applications of the Morris water maze in the study of learning and memory. *Brain research reviews*, 36(1), pp.60–90.
- Van Dam, D. et al., 2003. Age-dependent cognitive decline in the APP23 model precedes amyloid deposition. *European Journal of Neuroscience*, 17(2), pp.388–396.
- Van Dam, D. & De Deyn, P.P., 2006. Cognitive evaluation of disease-modifying efficacy of galantamine and memantine in the APP23 model. *European neuropsychopharmacology*, 16(1), pp.59–69.
- Danysz, W. & Parsons, C.G., 2012. Alzheimer's disease, β amyloid, glutamate, NMDA receptors and memantine—searching for the connections. *British journal of pharmacology*, 167(2), pp.324–352.
- Daumas, S. et al., 2008. Faster forgetting contributes to impaired spatial memory in the PDAPP mouse : Deficit in memory retrieval associated with increased sensitivity to interference ? *Learning & Memory*, pp.625–632.
- Deacon, R.M.J. et al., 2002. Effects of cytotoxic hippocampal lesions in mice on a cognitive test battery. *Behavioural Brain Research*, 133(1), pp.57–68.
- DeMattos, R.B. et al., 2002. Brain to plasma amyloid- β efflux: a measure of brain amyloid burden in a mouse model of Alzheimer's disease. *Science*, 295(5563), pp.2264–2267.
- DeMattos, R.B. et al., 2001. Peripheral anti-A beta antibody alters CNS and plasma A beta clearance and decreases brain A beta burden in a mouse model of Alzheimer's disease. *Proceedings of the National Academy of Sciences of the United States of America*, 98(15), pp.8850–5.
- Dineley, K.T. et al., 2002. Accelerated plaque accumulation, associative learning deficits, and up-regulation of $\alpha 7$ nicotinic receptor protein in transgenic mice co-expressing mutant human presenilin 1 and amyloid precursor proteins. *Journal of Biological Chemistry*, 277(25), pp.22768–22780.
- Dodart, J.-C. et al., 2002. Immunization reverses memory deficits without reducing brain Abeta burden in Alzheimer's disease model. *Nature neuroscience*, 5(5), pp.452–7.
- Dodart, J.-C. et al., 2000. Neuroanatomical Abnormalities in Behaviorally Characterized APPV717F Transgenic Mice. *Neurobiology of Disease*, 7(2), pp.71–85.

- Dodart, J.C. et al., 1999. Behavioral disturbances in transgenic mice overexpressing the V717F beta-amyloid precursor protein. *Behavioral neuroscience*, 113(5), pp.982–90.
- Dodart, J.C. et al., 2000. Neuroanatomical abnormalities in behaviorally characterized APP(V717F) transgenic mice. *Neurobiology of disease*, 7(2), pp.71–85.
- Dong, Z. et al., 2013. Hippocampal long-term depression mediates spatial reversal learning in the Morris water maze. *Neuropharmacology*, 64, pp.65–73.
- Donohue, M.C. et al., 2014. The preclinical Alzheimer cognitive composite: measuring amyloid-related decline. *JAMA neurology*, 71(8), pp.961–970.
- Doody, R.S. et al., 2013. A phase 3 trial of semagacestat for treatment of Alzheimer’s disease. *New England Journal of Medicine*, 369(4), pp.341–350.
- Dovey, H.F. et al., 2001. Functional gamma-secretase inhibitors reduce beta-amyloid peptide levels in brain. *Journal of Neurochemistry*, 76(1), pp.173–181.
- Du, H. et al., 2008. Cyclophilin D deficiency attenuates mitochondrial and neuronal perturbation and ameliorates learning and memory in Alzheimer’s disease. *Nat Med*, 14(10), pp.1097–1105.
- Dubois, B. et al., 2007. Research criteria for the diagnosis of Alzheimer’s disease: revising the NINCDS–ADRDA criteria. *The Lancet Neurology*, 6(8), pp.734–746.
- Dudchenko, P., 2004. An overview of the tasks used to test working memory in rodents. *Neuroscience and biobehavioral reviews*, 28(7), pp.699–709.
- Dudchenko, P.A., 2001. How do animals actually solve the T maze? *Behavioral neuroscience*, 115(4), p.850.
- Von Engelhardt, J. et al., 2008. Contribution of hippocampal and extra-hippocampal NR2B-containing NMDA receptors to performance on spatial learning tasks. *Neuron*, 60(5), pp.846–860.
- Ennaceur, a & Delacour, J., 1988. A new one-trial test for neurobiological studies of memory in rats. 1: Behavioral data. *Behavioural brain research*, 31(1), pp.47–59.
- Ennaceur, A., 2010. One-trial object recognition in rats and mice: methodological and theoretical issues. *Behavioural brain research*, 215(2), pp.244–254.
- Ennaceur, A. & Meliani, K., 1992. A new one-trial test for neurobiological studies of memory in rats. III. Spatial vs. non-spatial working memory. *Behavioural Brain Research*, 51(1), pp.83–92.
- Erickson, M. a & Banks, W. a, 2013. Blood-brain barrier dysfunction as a cause and consequence of Alzheimer’s disease. *Journal of cerebral blood flow and metabolism : official journal of the International Society of Cerebral Blood Flow and Metabolism*, 33(10), pp.1500–13.

- Escribano, L. et al., 2010. Rosiglitazone rescues memory impairment in Alzheimer's transgenic mice: mechanisms involving a reduced amyloid and tau pathology. *Neuropsychopharmacology : official publication of the American College of Neuropsychopharmacology*, 35(7), pp.1593–604.
- Escribano, L. et al., 2009. Rosiglitazone reverses memory decline and hippocampal glucocorticoid receptor down-regulation in an Alzheimer's disease mouse model. *Biochemical and Biophysical Research Communications*, 379(2), pp.406–410.
- España, J. et al., 2010. Intraneuronal β -Amyloid Accumulation in the Amygdala Enhances Fear and Anxiety in Alzheimer's Disease Transgenic Mice. *Biological Psychiatry*, 67(6), pp.513–521.
- Farlow, M.R. & Brosch, J.R., 2013. Immunotherapy for Alzheimer's Disease. *Neurologic Clinics*, 31(3), pp.869–878.
- Farrer, L.A. et al., 1997. Effects of age, sex, and ethnicity on the association between apolipoprotein E genotype and Alzheimer disease: a meta-analysis. *Jama*, 278(16), pp.1349–1356.
- Fernández-Tomé, P. et al., 2004. β -Amyloid 25-35 inhibits glutamate uptake in cultured neurons and astrocytes: modulation of uptake as a survival mechanism. *Neurobiology of disease*, 15(3), pp.580–589.
- Ferrara, M. et al., 2008. Prevalence of stress, anxiety and depression in with Alzheimer caregivers. *Health and quality of life outcomes*, 6, p.93.
- Filali, M. et al., 2012. Cognitive and non-cognitive behaviors in the triple transgenic mouse model of Alzheimer's disease expressing mutated APP, PS1, and Mapt (3xTg-AD). *Behavioural brain research*, 234(2), pp.334–42.
- Floresco, S.B., Seamans, J.K. & Phillips, A.G., 1997. Selective Roles for Hippocampal, Prefrontal Cortical, and Ventral Striatal Circuits in Radial-Arm Maze Tasks With or Without a Delay. *The Journal of Neuroscience*, 17 (5), pp.1880–1890.
- Folstein, M.F., Folstein, S.E. & McHugh, P.R., 1975. "Mini-mental state": a practical method for grading the cognitive state of patients for the clinician. *Journal of psychiatric research*, 12(3), pp.189–198.
- Foreman, N. & Ermakova, I., 1998. The radial arm maze: twenty years on. *Handbook of spatial research paradigms and methodologies*, 2, pp.87–143.
- Foreman, N. & Gillett, R., 1998. *A handbook of spatial research paradigms and methodologies*, Psychology Press.
- Forman, M. et al., 2013. The novel BACE inhibitor MK-8931 dramatically lowers CSF beta-amyloid in patients with mild-to-moderate Alzheimer's disease. *Alzheimer's & Dementia: The Journal of the Alzheimer's Association*, 9(4), p.P139.
- Förstl, H. & Kurz, a., 1999. Clinical features of Alzheimer's disease. *European Archives of Psychiatry and Clinical Neuroscience*, 249(6), pp.288–290.

- Francis, B.M. et al., 2012. Object recognition memory and BDNF expression are reduced in young TgCRND8 mice. *Neurobiology of Aging*, 33(3), pp.555–563.
- Francis, D.D. et al., 1995. Stress-induced disturbances in Morris water-maze performance: interstrain variability. *Physiology & behavior*, 58(1), pp.57–65.
- Francis, R. et al., 2002. *aph-1* and *pen-2* are required for Notch pathway signaling, γ -secretase cleavage of β APP, and presenilin protein accumulation. *Developmental cell*, 3(1), pp.85–97.
- Fratiglioni, L., Paillard-Borg, S. & Winblad, B., 2004. An active and socially integrated lifestyle in late life might protect against dementia. *The Lancet Neurology*, 3(6), pp.343–353.
- Frautschy, S.A. et al., 1998. Microglial response to amyloid plaques in APPsw transgenic mice. *The American journal of pathology*, 152(1), p.307.
- Fray, P.J. & Robbins, T.W., 1996. CANTAB battery: proposed utility in neurotoxicology. *Neurotoxicology and teratology*, 18(4), pp.499–504.
- Fray, P.J., Robbins, T.W. & Sahakian, B.J., 1996. Neuropsychiatric applications of CANTAB. *International Journal of Geriatric Psychiatry*.
- Frick, K.M. et al., 1995. Age-related spatial reference and working memory deficits assessed in the water maze. *Neurobiology of Aging*, 16(2), pp.149–160.
- Frick, K.M. & Gresack, J.E., 2003. Sex differences in the behavioral response to spatial and object novelty in adult C57BL/6 mice. *Behavioral neuroscience*, 117(6), pp.1283–91.
- Fryer, J.D. et al., 2005. The Low Density Lipoprotein Receptor Regulates the Level of Central Nervous System Human and Murine Apolipoprotein E but Does Not Modify Amyloid Plaque Pathology in PDAPP Mice. *Journal of Biological Chemistry*, 280 (27), pp.25754–25759.
- Fu, H. et al., 2010. Amyloid- β Immunotherapy for Alzheimer's Disease. *CNS Neurol Disord Drug Targets*, 9(2), pp.197–206.
- Fukumoto, H. et al., 2010. A noncompetitive BACE1 inhibitor TAK-070 ameliorates A β pathology and behavioral deficits in a mouse model of Alzheimer's disease. *The Journal of neuroscience : the official journal of the Society for Neuroscience*, 30(33), pp.11157–66.
- Galvan, V. et al., 2007. Reversal of Alzheimer's-like pathology and behavior in human APP transgenic mice by mutation of Asp664. *Proceedings of the National Academy of Sciences*, 104(16), pp.7130–7135.
- Games, D. et al., 1995. Alzheimer-type neuropathology in transgenic mice overexpressing V717F APP. *Letters to Nature*, 373(9), pp.523–527.
- Gaskin, S., Tremblay, A. & Mumby, D.G., 2003. Retrograde and anterograde object recognition in rats with hippocampal lesions. *Hippocampus*, 13(8), pp.962–969.

- Gaspar, R.C. et al., 2010. Oligomers of β -amyloid are sequestered into and seed new plaques in the brains of an AD mouse model. *Experimental Neurology*, 223(2), pp.394–400.
- Gatz, M. et al., 2006. Role of genes and environments for explaining Alzheimer disease. *Archives of general psychiatry*, 63(2), pp.168–174.
- Genin, E. et al., 2011. APOE and Alzheimer disease: a major gene with semi-dominant inheritance. *Molecular psychiatry*, 16(9), pp.903–907.
- Gerlai, R. et al., 2002. Behavioral impairment of APP V717F mice in fear conditioning : is it only cognition ? *Behavioural Brain*, 136, pp.503–509.
- Giacobini, E. & Gold, G., 2013. Alzheimer disease therapy--moving from amyloid- β to tau. *Nature reviews. Neurology*, 9(12), pp.677–86.
- Gilman, S. et al., 2005. Clinical effects of A β immunization (AN1792) in patients with AD in an interrupted trial. *Neurology*, 64(9), pp.1553–1562.
- Ginsberg, S.D. et al., 2010. Microarray analysis of hippocampal CA1 neurons implicates early endosomal dysfunction during Alzheimer's disease progression. *Biological psychiatry*, 68(10), pp.885–893.
- Glennner, G.G. & Wong, C.W., 1984. Alzheimer's disease and Down's syndrome: sharing of a unique cerebrovascular amyloid fibril protein. *Biochemical and biophysical research communications*, 122(3), pp.1131–1135.
- Goate, A. et al., 1991. Segregation of a missense mutation in the amyloid precursor protein gene with familial Alzheimer's disease. *Nature*, 349, pp.704–706.
- Gold, A.E. & Kesner, R.P., 2005. The role of the CA3 subregion of the dorsal hippocampus in spatial pattern completion in the rat. *Hippocampus*, 15(6), pp.808–814.
- Goldgaber, D. et al., 1987. Characterization and chromosomal localization of a cDNA encoding brain amyloid of Alzheimer's disease. *Science*, 235(4791), pp.877–880.
- Gómez-Isla, T. et al., 1996. Profound loss of layer II entorhinal cortex neurons occurs in very mild Alzheimer's disease. *The Journal of neuroscience*, 16(14), pp.4491–4500.
- Gómez Isla, T. et al., 1997. Neuronal loss correlates with but exceeds neurofibrillary tangles in Alzheimer's disease. *Annals of neurology*, 41(1), pp.17–24.
- Gong, C.-X., Grundke-Iqbal, I. & Iqbal, K., 1994. Dephosphorylation of Alzheimer's disease abnormally phosphorylated tau by protein phosphatase-2A. *Neuroscience*, 61(4), pp.765–772.
- Good, M. a et al., 2007. Context- but not familiarity-dependent forms of object recognition are impaired following excitotoxic hippocampal lesions in rats. *Behavioral neuroscience*, 121(1), pp.218–23.

- Good, M. a & Hale, G., 2007. The “Swedish” mutation of the amyloid precursor protein (APP^{swe}) dissociates components of object-location memory in aged Tg2576 mice. *Behavioral neuroscience*, 121(6), pp.1180–91.
- Good, M.A., Hale, G. & Staal, V., 2007. Impaired“ episodic-like” object memory in adult APP swe transgenic mice. *Behavioral neuroscience*, 121(2), p.443.
- Götz, J. et al., 2007. A Decade of Tau Transgenic Animal Models and Beyond. *Brain Pathology*, 17(1), pp.91–103.
- Götz, J. et al., 1995. Somatodendritic localization and hyperphosphorylation of tau protein in transgenic mice expressing the longest human brain tau isoform. *The EMBO journal*, 14(7), p.1304.
- Götz, J. & Ittner, L.M., 2008. Animal models of Alzheimer’s disease and frontotemporal dementia. *Nature reviews. Neuroscience*, 9(7), pp.532–44.
- Grbovic, O.M. et al., 2003. Rab5-stimulated Up-regulation of the Endocytic Pathway Increases Intracellular β -Cleaved Amyloid Precursor Protein Carboxyl-terminal Fragment Levels and A β Production. *Journal of Biological Chemistry* , 278 (33), pp.31261–31268.
- Green, K.N. et al., 2006. Glucocorticoids increase amyloid-beta and tau pathology in a mouse model of Alzheimer’s disease. *The Journal of neuroscience : the official journal of the Society for Neuroscience*, 26(35), pp.9047–56.
- Greenamyre, T. & Young, A., 1989. Excitatory Amino Acids and Alzheimer ’ s Disease. *Neurobiology of Aging*, 10, pp.593–602.
- Greenberg, S.M. et al., 1994. Secreted beta-amyloid precursor protein stimulates mitogen-activated protein kinase and enhances tau phosphorylation. *Proceedings of the National Academy of Sciences*, 91(15), pp.7104–7108.
- Greene, J.D.W., Baddeley, A.D. & Hodges, J.R., 1996. Analysis of the episodic memory deficit in early Alzheimer’s disease: evidence from the doors and people test. *Neuropsychologia*, 34(6), pp.537–551.
- Gresack, J.E. & Frick, K.M., 2003. Male mice exhibit better spatial working and reference memory than females in a water-escape radial arm maze task. *Brain Research*, 982(1), pp.98–107.
- Griffin, W.S.T., 2010. Excess betaCTF, not Abeta: the culprit in Alzheimer-related endocytic dysfunction. *Proceedings of the National Academy of Sciences of the United States of America*, 107(4), pp.1263–4.
- Gu, Y. et al., 2001. Distinct intramembrane cleavage of the β -amyloid precursor protein family resembling γ -secretase-like cleavage of Notch. *Journal of Biological Chemistry*, 276(38), pp.35235–35238.
- Gu, Y. et al., 2010. Food combination and Alzheimer disease risk: a protective diet. *Archives of neurology*, 67(6), pp.699–706.

- Haass, C. et al., 1993. beta-Amyloid peptide and a 3-kDa fragment are derived by distinct cellular mechanisms. *J Biol Chem*, 268, pp.3021–3024.
- Haass, C., 2004. Take five—BACE and the γ secretase quartet conduct Alzheimer's amyloid β peptide generation. *The EMBO journal*, 23(3), pp.483–488.
- Haass, C. et al., 1992. Targeting of cell-surface β -amyloid precursor protein to lysosomes: alternative processing into amyloid-bearing fragments. *Letters to Nature*, pp.500–503.
- Haass, C., Hung, A.Y. & Selkoe, D.J., 1991. Processing of beta-amyloid precursor protein in microglia and astrocytes favors an internal localization over constitutive secretion. *The Journal of neuroscience*, 11(12), pp.3783–3793.
- Haass, C. & Selkoe, D.J., 2007. Soluble protein oligomers in neurodegeneration: lessons from the Alzheimer's amyloid beta-peptide. *Nature reviews. Molecular cell biology*, 8(2), pp.101–112.
- Hagen, M. et al., 2011. The A β peptide conjugate vaccine, ACC-001, generates N-terminal anti-A β antibodies in the absence of A β directed T-cell responses. *Alzheimer's & Dementia*, 7(4), pp.S460–S461.
- Hale, G. & Good, M., 2005. Impaired visuospatial recognition memory but normal object novelty detection and relative familiarity judgments in adult mice expressing the APP^{swe} Alzheimer's disease mutation. *Behavioral neuroscience*, 119(4), pp.884–91.
- Hammond, R.S., Tull, L.E. & Stackman, R.W., 2004. On the delay-dependent involvement of the hippocampus in object recognition memory. *Neurobiology of Learning and Memory*, 82(1), pp.26–34.
- Handoko, M. et al., 2013. Correlation of specific amyloid- β oligomers with tau in cerebrospinal fluid from cognitively normal older adults. *JAMA neurology*, 70(5), pp.594–599.
- Hanna, A. et al., 2012. Age-related increase in amyloid plaque burden is associated with impairment in conditioned fear memory in CRND8 mouse model of amyloidosis. *Alzheimer's Research & Therapy*, 4(3), p.21.
- Hardy, J. & Allsop, D., 1991. Amyloid deposition as the central event in the aetiology of Alzheimer's disease. *Trends in Pharmacological Sciences*, 12, pp.383–388.
- Hardy, J. & Selkoe, D.J., 2002. The amyloid hypothesis of Alzheimer's disease: progress and problems on the road to therapeutics. *Science (New York, N.Y.)*, 297(5580), pp.353–6.
- Hardy, J.A. & Higgins, G.A., 1992. Alzheimer's disease: the amyloid cascade hypothesis. *Science*, 256 (5054), pp.184–185.
- Harold, D. et al., 2009. Genome-wide association study identifies variants at CLU and PICALM associated with Alzheimer's disease. *Nature genetics*, 41(10), pp.1088–1093.

- Harrison, F.E., Hosseini, A.H. & McDonald, M.P., 2009. Endogenous anxiety and stress responses in water maze and Barnes maze spatial memory tasks. *Behavioural brain research*, 198(1), pp.247–251.
- Hartman, R.E. et al., 2005. Treatment with an amyloid-beta antibody ameliorates plaque load, learning deficits, and hippocampal long-term potentiation in a mouse model of Alzheimer's disease. *The Journal of Neuroscience*, 25(26), pp.6213–20.
- Hébert, F. et al., 2013. Cortical atrophy and hypoperfusion in a transgenic mouse model of Alzheimer's disease. *Neurobiology of Aging*, 34(6), pp.1644–1652.
- Hefti, F. et al., 2013. The case for soluble A β oligomers as a drug target in Alzheimer's disease. *Trends in Pharmacological Sciences*, 34(5), pp.261–266.
- Heneka, M.T. et al., 2006. Locus Ceruleus Degeneration Promotes Alzheimer Pathogenesis in Amyloid Precursor Protein 23 Transgenic Mice. *The Journal of Neuroscience*, 26(5), pp.1343–1354.
- Heneka, M.T. et al., 2013. NLRP3 is activated in Alzheimer's disease and contributes to pathology in APP/PS1 mice. *Nature*, 493(7434), pp.674–8.
- Henriksen, K. et al., 2014. The future of blood-based biomarkers for Alzheimer's disease. *Alzheimer's & Dementia*, 10(1), pp.115–131.
- Herrmann, A. & Spires-Jones, T., 2015. Clearing the way for tau immunotherapy in Alzheimer's disease. *Journal of neurochemistry*, 132(1), pp.1–4.
- Hitt, B. et al., 2012. β -Site amyloid precursor protein (APP)-cleaving enzyme 1 (BACE1)-deficient mice exhibit a close homolog of L1 (CHL1) loss-of-function phenotype involving axon guidance defects. *Journal of Biological Chemistry*, 287(46), pp.38408–38425.
- Ho, G.J. et al., 2005. Altered p59Fyn kinase expression accompanies disease progression in Alzheimer's disease: implications for its functional role. *Neurobiology of aging*, 26(5), pp.625–35.
- Hoaglin, D.C. & Iglewicz, B., 1987. Fine-tuning some resistant rules for outlier labeling. *Journal of the American Statistical Association*, 82(400), pp.1147–1149.
- Hodges, H., 1996. Maze procedures: the radial-arm and water maze compared. *Cognitive Brain Research*, 3(3-4), pp.167–181.
- Hodges, J.R., Salmon, D.P. & Butters, N., 1990. Differential impairment of semantic and episodic memory in Alzheimer's and Huntington's diseases: a controlled prospective study. *Journal of Neurology, Neurosurgery & Psychiatry*, 53(12), pp.1089–1095.
- Holcomb, L. et al., 1998. Accelerated Alzheimer-type phenotype in transgenic mice carrying both mutant amyloid precursor protein and presenilin 1 transgenes. *Nature medicine*, 4(1), pp.97–100.

- Holden, H.M. et al., 2012. Spatial pattern separation in cognitively normal young and older adults. *Hippocampus*, 22(9), pp.1826–1832.
- Holmes, C. et al., 2008. Long-term effects of A β 42 immunisation in Alzheimer's disease: follow-up of a randomised, placebo-controlled phase I trial. *The Lancet*, 372(9634), pp.216–223.
- Holsinger, R.M. et al., 2002. Increased expression of the amyloid precursor β secretase in Alzheimer's disease. *Annals of neurology*, 51(6), pp.783–786.
- Honig, W.K., 1978. Studies of working memory in the pigeon. *Cognitive processes in animal behavior*, pp.211–248.
- Hook, H. et al., 2002. β Amyloid peptide in regulated secretory vesicles of chromaffin cells: evidence for multiple cysteine proteolytic activities in distinct pathways for β secretase activity in chromaffin vesicles. *Journal of neurochemistry*, 81(2), pp.237–256.
- Hsiao, K. et al., 1996. Correlative Memory Deficits, A β Elevation, and Amyloid Plaques in Transgenic Mice. *Science*, 274 (5284), pp.99–103.
- Hu, X. et al., 2013. BACE1 regulates hippocampal astrogenesis via the Jagged1-Notch pathway. *Cell reports*, 4(1), pp.40–49.
- Hu, X. et al., 2008. Genetic deletion of BACE1 in mice affects remyelination of sciatic nerves. *The FASEB Journal*, 22(8), pp.2970–2980.
- Hughes, R.N., 2004. The value of spontaneous alternation behavior (SAB) as a test of retention in pharmacological investigations of memory. *Neuroscience and biobehavioral reviews*, 28(5), pp.497–505.
- Huitron-resendiz, S. et al., 2002. Age-independent and age-related deficits in visuospatial learning, sleep – wake states, thermoregulation and motor activity in PDAPP mice. *Brain Research*, 928, pp.126–137.
- Huitrón-Reséndiz, S. et al., 2002. Age-independent and age-related deficits in visuospatial learning, sleep-wake states, thermoregulation and motor activity in PDAPP mice. *Brain research*, 928(1-2), pp.126–37.
- Hunt, C.E. & Turner, A.J., 2009. Cell biology, regulation and inhibition of β -secretase (BACE-1). *FEBS Journal*, 276(7), pp.1845–1859.
- Hussain, I. et al., 2007. Oral administration of a potent and selective non-peptidic BACE-1 inhibitor decreases beta-cleavage of amyloid precursor protein and amyloid-beta production in vivo. *Journal of neurochemistry*, 100(3), pp.802–9.
- Hyde, L. a et al., 2005. Age-progressing cognitive impairments and neuropathology in transgenic CRND8 mice. *Behavioural brain research*, 160(2), pp.344–55.
- Hyde, L.A., Hoplight, B.J. & Denenberg, V.H., 1998. Water version of the radial-arm maze: Learning in three inbred strains of mice. *Brain Research*, 785(2), pp.236–244.

- Hyman, B.T. et al., 1984. Alzheimer's disease: cell-specific pathology isolates the hippocampal formation. *Science*, 225(4667), pp.1168–1170.
- Hyman, B.T. et al., 1986. Perforant pathway changes and the memory impairment of Alzheimer's disease. *Annals of Neurology*, 20(4), pp.472–481.
- Iglewicz, B. & Hoaglin, D.C., 1993. *How to detect and handle outliers*, Asq Press.
- Iordanova, M.D., Good, M. a & Honey, R.C., 2008. Configural learning without reinforcement: integrated memories for correlates of what, where, and when. *Quarterly journal of experimental psychology (2006)*, 61(12), pp.1785–92.
- Iordanova, M.D., Good, M. & Honey, R.C., 2011. Retrieval-mediated learning involving episodes requires synaptic plasticity in the hippocampus. *The Journal of neuroscience : the official journal of the Society for Neuroscience*, 31(19), pp.7156–62.
- Irizarry, M.C. et al., 1997. Abeta deposition is associated with neuropil changes, but not with overt neuronal loss in the human amyloid precursor protein V717F (PDAPP) transgenic mouse. *The Journal of neuroscience : the official journal of the Society for Neuroscience*, 17(18), pp.7053–9.
- Irizarry, M.C. et al., 1997. APPSW Transgenic Mice Develop Age-related A [beta] Deposits and Neuropil Abnormalities, but no Neuronal Loss in CA1. *Journal of Neuropathology & Experimental Neurology*, 56(9), pp.965–973.
- Ittner, L.M., Ke, Y.D., Delerue, F., Bi, M., Gladbach, A., van Eersel, J., Wölfing, H., Chieng, B.C., Christie, M.J., Napier, I. a, et al., 2010. Dendritic function of tau mediates amyloid-beta toxicity in Alzheimer's disease mouse models. *Cell*, 142(3), pp.387–97.
- Ittner, L.M., Ke, Y.D., Delerue, F., Bi, M., Gladbach, A., van Eersel, J., Wölfing, H., Chieng, B.C., Christie, M.J. & Napier, I.A., 2010. Dendritic function of tau mediates amyloid- β toxicity in Alzheimer's disease mouse models. *Cell*, 142(3), pp.387–397.
- Ittner, L.M. & Götz, J., 2011. Amyloid- β and tau — a toxic pas de deux in Alzheimer's disease. *Nature Reviews. Neuroscience*, 12, pp.67–72.
- Ivanov, A.I. & Romanovsky, A.A., 2006. Putative dual role of ephrin Eph receptor interactions in inflammation. *IUBMB life*, 58(7), pp.389–394.
- Jack, C. et al., 2013. Personal View Tracking pathophysiological processes in Alzheimer's disease : an updated hypothetical model of dynamic biomarkers. *Lancet Neurology*, 12, pp.207–216.
- Jack, C.R. et al., 2010. Hypothetical model of dynamic biomarkers of the Alzheimer's pathological cascade. *Lancet neurology*, 9(1), pp.119–28.
- Jack, C.R. et al., 1992. MR based hippocampal volumetry in the diagnosis of Alzheimer's disease. *Neurology*, 42(1), p.183.

- Jack, C.R. et al., 2013. Tracking pathophysiological processes in Alzheimer's disease: an updated hypothetical model of dynamic biomarkers. *The Lancet Neurology*, 12(2), pp.207–216.
- Jack Jr., C.R. et al., 2011. Introduction to the recommendations from the National Institute on Aging-Alzheimer's Association workgroups on diagnostic guidelines for Alzheimer's disease. *Alzheimer's & Dementia*, 7(3), pp.257–262.
- Jacobsen, J.S. et al., 2006. Early-onset behavioral and synaptic deficits in a mouse model of Alzheimer's disease. *Proceedings of the National Academy of Sciences of the United States of America*, 103 (13), pp.5161–5166.
- Jacobsen, K.T. & Iverfeldt, K., 2009. Amyloid precursor protein and its homologues: a family of proteolysis-dependent receptors. *Cellular and molecular life sciences*, 66(14), pp.2299–2318.
- Janus, C., 2004a. Search Strategies Used by APP Transgenic Mice During Navigation in the Morris Water Maze. *Learning & Memory*, 11, pp.337–346.
- Janus, C., 2004b. Search Strategies Used by APP Transgenic Mice During Navigation in the Morris Water Maze. *Learning & memory (Cold Spring Harbor, N.Y.)*, pp.337–346.
- Jarrett, J.T., Berger, E.P. & Lansbury, P.T., 1993. The carboxy terminus of the beta amyloid protein is critical for the seeding of amyloid formation: implications for the pathogenesis of Alzheimer's disease. *Biochemistry*, 32, pp.4693–4697.
- Jawhar, S. et al., 2012. Motor deficits, neuron loss, and reduced anxiety coinciding with axonal degeneration and intraneuronal A β aggregation in the 5XFAD mouse model of Alzheimer's disease. *Neurobiology of aging*, 33(1), pp.196.e29–40.
- Jeong, Y.H. et al., 2006. Chronic stress accelerates learning and memory impairments and increases amyloid deposition in APPV717I-CT100 transgenic mice, an Alzheimer's disease model. *FASEB journal : official publication of the Federation of American Societies for Experimental Biology*, 20(6), pp.729–31.
- Jin, M. et al., 2011. Soluble amyloid β -protein dimers isolated from Alzheimer cortex directly induce Tau hyperphosphorylation and neuritic degeneration. *Proceedings of the National Academy of Sciences*, 108 (14), pp.5819–5824.
- Johnson, C.T., McDonald, R.J. & White, L.H., 1996. Dissociation of Hippocampal and Striatal Contributions to Spatial Navigation in the Water Maze 1. *Neurobiology of learning and memory*, 323, pp.305–323.
- Johnson-Wood, K., Lee, M., Motter, R., Hu, K., Gordon, G., Barbour, R., Khan, K., Gordon, M., Tan, H., Games, D., et al., 1997. Amyloid precursor protein processing and A β 42 deposition in a transgenic mouse model of Alzheimer disease. *Proceedings of the National Academy of Sciences of the United States of America*, 94(4), pp.1550–5.
- Johnson-Wood, K., Lee, M., Motter, R., Hu, K., Gordon, G., Barbour, R., Khan, K., Gordon, M., Tan, H. & Games, D., 1997. Amyloid precursor protein processing and A β 42

- deposition in a transgenic mouse model of Alzheimer disease. *Proceedings of the National Academy of Sciences*, 94(4), pp.1550–1555.
- Jones, L., Harold, D. & Williams, J., 2010. Genetic evidence for the involvement of lipid metabolism in Alzheimer's disease. *Biochimica et Biophysica Acta (BBA)-Molecular and Cell Biology of Lipids*, 1801(8), pp.754–761.
- Jordán, J. et al., 1997. p53 Expression Induces Apoptosis in Hippocampal Pyramidal. *The Journal of Neuroscience*, 17(4), pp.1397–1405.
- Kakuda, N. et al., 2006. Equimolar production of amyloid β -protein and amyloid precursor protein intracellular domain from β -carboxyl-terminal fragment by γ -secretase. *Journal of Biological Chemistry*, 281(21), pp.14776–14786.
- Kamenetz, F. et al., 2003. APP processing and synaptic function. *Neuron*, 37(6), pp.925–37.
- Karlnoski, R.A. et al., 2008. Deglycosylated anti-A β antibody dose–response effects on pathology and memory in APP transgenic mice. *Journal of Neuroimmune Pharmacology*, 3(3), pp.187–197.
- Karran, E. & Hardy, J., 2014. A critique of the drug discovery and phase 3 clinical programs targeting the amyloid hypothesis for Alzheimer disease. *Annals of neurology*, 76(2), pp.185–205.
- Kawarabayashi, T. et al., 2001. Age-dependent changes in brain, CSF, and plasma amyloid β protein in the Tg2576 transgenic mouse model of Alzheimer's disease. *The Journal of Neuroscience*, 21(2), pp.372–381.
- Kawarabayashi, T. et al., 2004. Dimeric Amyloid β Protein Rapidly Accumulates in Lipid Rafts followed by Apolipoprotein E and Phosphorylated Tau Accumulation in the Tg2576 Mouse Model of Alzheimer's Disease. *The Journal of Neuroscience*, 24 (15), pp.3801–3809.
- Kelly, J.F. et al., 1996. Amyloid β -peptide disrupts carbachol-induced muscarinic cholinergic signal transduction in cortical neurons. *Proceedings of the National Academy of Sciences*, 93(June), pp.6753–6758.
- Kelly, P. et al., 2003. Progressive age-related impairment of cognitive behavior in APP23 transgenic mice. *Neurobiology of Aging*, 24(2), pp.365–378.
- Kemp, A. & Manahan-Vaughan, D., 2012. Passive spatial perception facilitates the expression of persistent hippocampal long-term depression. *Cerebral cortex (New York, N.Y. : 1991)*, 22(7), pp.1614–21.
- Kiddle, S.J. et al., 2015. Plasma protein biomarkers of Alzheimer's disease endophenotypes in asymptomatic older twins: early cognitive decline and regional brain volumes. *Transl Psychiatry*, 5, p.e584.
- Kim, J. et al., 2007. A β 40 inhibits amyloid deposition in vivo. *The Journal of neuroscience*, 27(3), pp.627–633.

- Kim, S. et al., 2015. Evidence that the rab5 effector APPL1 mediates APP- β CTF-induced dysfunction of endosomes in Down syndrome and Alzheimer's disease. *Molecular psychiatry*, (January), pp.1–10.
- Kimura, R. et al., 2012. Beta amyloid-induced depression of hippocampal long-term potentiation is mediated through the amylin receptor. *The Journal of Neuroscience*, 32(48), pp.17401–17406.
- Kimura, R. & Ohno, M., 2009. Impairments in remote memory stabilization precede hippocampal synaptic and cognitive failures in 5XFAD Alzheimer mouse model. *Neurobiology of Disease*, 33(2), pp.229–235.
- Kimura, T. et al., 2005. Design and synthesis of highly active Alzheimer's beta-secretase (BACE1) inhibitors, KMI-420 and KMI-429, with enhanced chemical stability. *Bioorganic & medicinal chemistry letters*, 15(1), pp.211–5.
- King, D.L. et al., 1999. Progressive and gender-dependent cognitive impairment in the APP SW transgenic mouse model for Alzheimer's disease. , 103, pp.145–162.
- Kinoshita, A. et al., 2003. Demonstration by FRET of BACE interaction with the amyloid precursor protein at the cell surface and in early endosomes. *Journal of cell science*, 116(16), pp.3339–3346.
- Klein, A.M., Kowall, N.W. & Ferrante, R.J., 1999. Neurotoxicity and oxidative damage of beta amyloid 1–42 versus beta amyloid 1–40 in the mouse cerebral cortex. *Annals of the New York Academy of Sciences*, 893(1), pp.314–320.
- Klunk, W.E. et al., 2004. Imaging brain amyloid in Alzheimer's disease with Pittsburgh Compound B. *Annals of neurology*, 55(3), pp.306–319.
- Klyubin, I. et al., 2005. Amyloid β protein immunotherapy neutralizes A β oligomers that disrupt synaptic plasticity in vivo. *Nature medicine*, 11(5), pp.556–561.
- Knight, E.M. et al., 2013. Age-related changes in core body temperature and activity in triple-transgenic Alzheimer's disease (3xTgAD) mice. *Disease Models and Mechanisms*, 6(1), pp.160–170.
- Knopman, D.S. et al., 2003. Neuropathology of cognitively normal elderly. *Journal of Neuropathology & Experimental Neurology*, 62(11), pp.1087–1095.
- Knowles, J.K. et al., 2009. The p75 Neurotrophin Receptor Promotes Amyloid- β (1-42)-Induced Neuritic Dystrophy In Vitro and In Vivo. *The Journal of Neuroscience* , 29 (34), pp.10627–10637.
- Kobayashi, D.T. & Chen, K.S., 2005. Behavioral phenotypes of amyloid-based genetically modified mouse models of Alzheimer's disease. *Genes, Brain and Behavior*, 4(3), pp.173–196.
- Kojro, E. & Fahrenholz, F., 2005. The non-amyloidogenic pathway: structure and function of α -secretases. In *Alzheimer's Disease*. Springer, pp. 105–127.

- Kok, E. et al., 2009. Apolipoprotein E-dependent accumulation of Alzheimer disease-related lesions begins in middle age. *Annals of neurology*, 65(6), pp.650–657.
- Kopelman, M.D., 1985. Rates of forgetting in Alzheimer-type dementia and Korsakoff's syndrome. *Neuropsychologia*, 23(5), pp.623–638.
- Kotilinek, L.A. et al., 2002a. Reversible Memory Loss in a Mouse Transgenic Model of Alzheimer's Disease. *The Journal of Neuroscience*, 22(15), pp.6331–6335.
- Kotilinek, L.A. et al., 2002b. Reversible memory loss in a mouse transgenic model of Alzheimer's disease. *The Journal of neuroscience*, 22(15), pp.6331–6335.
- Kounnas, M.Z. et al., 2010. Modulation of γ -secretase reduces β -amyloid deposition in a transgenic mouse model of Alzheimer's disease. *Neuron*, 67(5), pp.769–780.
- Kraemer, P.J., Gilbert, M.E. & Innis, N.K., 1983. The influence of cue type and configuration upon radial-maze performance in the rat. *Animal Learning & Behavior*, 11(3), pp.373–380.
- Kurt, M.A. et al., 2003. Hyperphosphorylated tau and paired helical filament-like structures in the brains of mice carrying mutant amyloid precursor protein and mutant presenilin-1 transgenes. *Neurobiology of disease*, 14(1), pp.89–97.
- Kurup, P. et al., 2010. A β -Mediated NMDA Receptor Endocytosis in Alzheimer's Disease Involves Ubiquitination of the Tyrosine Phosphatase STEP61. *The Journal of Neuroscience*, 30(17), pp.5948–5957.
- Lamar, M. et al., 1997. Perseverative behavior in Alzheimer's disease and subcortical ischemic vascular dementia. *Neuropsychology*, 11(4), p.523.
- Lambert, J.-C. et al., 2013. Genome-wide haplotype association study identifies the FRMD4A gene as a risk locus for Alzheimer's disease. *Molecular psychiatry*, 18(4), pp.461–470.
- Lambert, J.-C. et al., 2015. PLD3 and sporadic Alzheimer's disease risk. *Nature*, 520(7545), pp.E1–E1.
- Lambert, M.P. et al., 1998. Diffusible, nonfibrillar ligands derived from A β 1–42 are potent central nervous system neurotoxins. *Proceedings of the National Academy of Sciences*, 95(11), pp.6448–6453.
- Lanz, T.A., Carter, D.B. & Merchant, K.M., 2003. Dendritic spine loss in the hippocampus of young PDAPP and Tg2576 mice and its prevention by the ApoE2 genotype. *Neurobiology of Disease*, 13(3), pp.246–253.
- Larson, J. et al., 1999. Alterations in synaptic transmission and long-term potentiation in hippocampal slices from young and aged PDAPP mice. *Brain research*, 840(1), pp.23–35.
- Lasagna-Reeves, C. a, Castillo-Carranza, D.L., Sengupta, U., Guerrero-Munoz, M.J., et al., 2012. Alzheimer brain-derived tau oligomers propagate pathology from endogenous tau. *Scientific reports*, 2, p.700.

- Lasagna-Reeves, C. a, Castillo-Carranza, D.L., Sengupta, U., Sarmiento, J., et al., 2012. Identification of oligomers at early stages of tau aggregation in Alzheimer's disease. *FASEB journal : official publication of the Federation of American Societies for Experimental Biology*, 26(5), pp.1946–59.
- Lau, C.G. & Zukin, R.S., 2007. NMDA receptor trafficking in synaptic plasticity and neuropsychiatric disorders. *Nature Reviews Neuroscience*, 8(6), pp.413–426.
- Lauderback, C.M. et al., 2001. The glial glutamate transporter, GLT₁, is oxidatively modified by 4-hydroxy-2-nonenal in the Alzheimer's disease brain: the role of A β 1–42. *Journal of neurochemistry*, 78(2), pp.413–416.
- Laurén, J. et al., 2009. Cellular prion protein mediates impairment of synaptic plasticity by amyloid- β oligomers. *Nature*, 457(7233), pp.1128–1132.
- Lee, E.B. et al., 2005. BACE overexpression alters the subcellular processing of APP and inhibits A β deposition in vivo. *The Journal of cell biology*, 168(2), pp.291–302.
- Lee, G. et al., 1998. Tau interacts with src-family non-receptor tyrosine kinases. *Journal of Cell Science*, 111, pp.3167–3177.
- Lee, J.-E. & Han, P.-L., 2013. An update of animal models of Alzheimer disease with a reevaluation of plaque depositions. *Experimental neurobiology*, 22(2), pp.84–95.
- Lee, M. et al., 2005. A β 42 immunization in Alzheimer's disease generates A β N-terminal antibodies. *Annals of Neurology*, 58(3), pp.430–435.
- Lefterov, I. et al., 2009. Memory deficits in APP23/Abca1 \pm mice correlate with the level of A β oligomers. *ASN neuro*, 1(2), pp.65–76.
- Leibson, C.L. et al., 1997. Risk of dementia among persons with diabetes mellitus: a population-based cohort study. *American Journal of Epidemiology*, 145(4), pp.301–308.
- Lemere, C. et al., 2000. Nasal A β Treatment Induces Anti-A β Antibody Production and Decreases Cerebral Amyloid Burden in PD-APP Mice. *Annals of the New York Academy of Sciences*, 920(1), pp.328–331.
- Lemere, C. a, 2013. Immunotherapy for Alzheimer's disease: hoops and hurdles. *Molecular neurodegeneration*, 8(1), p.36.
- Lemere, C. a & Masliah, E., 2010. Can Alzheimer disease be prevented by amyloid-beta immunotherapy? *Nature reviews. Neurology*, 6(2), pp.108–19.
- Lemere, C.A., 2013. Immunotherapy for Alzheimer's disease: hoops and hurdles. *Mol Neurodegener*, 8(1), p.36.
- Lesné, S. et al., 2006. A specific amyloid- β protein assembly in the brain impairs memory. *Nature*, 440(7082), pp.352–357.
- Lesné, S. et al., 2005. NMDA Receptor Activation Inhibits α -Secretase and Promotes Neuronal Amyloid- β Production. *The Journal of Neuroscience*, 25(41), pp.9367–9377.

- Lesné, S.E. et al., 2013. Brain amyloid- β oligomers in ageing and Alzheimer's disease. *Brain*, p.awt062.
- Levitan, D. et al., 2001. PS1 N-and C-terminal fragments form a complex that functions in APP processing and Notch signaling. *Proceedings of the National Academy of Sciences*, 98(21), pp.12186–12190.
- Levy, E. et al., 1990. Mutation of the Alzheimer's disease amyloid gene in hereditary cerebral hemorrhage, Dutch type. *Science*, 248(4959), pp.1124–1126.
- Levy-Lahad, E. et al., 1995. Candidate gene for the chromosome 1 familial Alzheimer's disease locus. *Science*, 269, pp.973–977.
- Lewis, J. et al., 2001. Enhanced neurofibrillary degeneration in transgenic mice expressing mutant tau and APP. *Science (New York, N.Y.)*, 293(5534), pp.1487–91.
- Li, S. et al., 2009. Soluble oligomers of amyloid β protein facilitate hippocampal long-term depression by disrupting neuronal glutamate uptake. *Neuron*, 62(6), pp.788–801.
- Lim, G.P. et al., 2005. A Diet Enriched with the Omega-3 Fatty Acid Docosahexaenoic Acid Reduces Amyloid Burden in an Aged Alzheimer Mouse Model. *The Journal of Neuroscience*, 25 (12), pp.3032–3040.
- Lin, Y. et al., 2004. Postsynaptic density protein-95 regulates NMDA channel gating and surface expression. *The Journal of neuroscience*, 24(45), pp.10138–10148.
- Lippa, C.F. et al., 1992. Alzheimer's disease and aging: Effects on perforant pathway perikarya and synapses. *Neurobiology of Aging*, 13(3), pp.405–411.
- Lippa, C.F. et al., 1996. Familial and sporadic Alzheimer's disease Neuropathology cannot exclude a final common pathway. *Neurology*, 46(2), pp.406–412.
- Liu, C.-C. et al., 2013. Apolipoprotein E and Alzheimer disease: risk, mechanisms and therapy. *Nature reviews. Neurology*, 9(2), pp.106–18.
- Liu, G.-P. et al., 2013. Silencing PP2A Inhibitor by Lenti-shRNA Interference Ameliorates Neuropathologies and Memory Deficits in tg2576 Mice. *Molecular Therapy*, 21(12), pp.2247–2257.
- Liu, L. et al., 2012. Trans-synaptic spread of tau pathology in vivo. *PloS one*, 7(2), p.e31302.
- Liu, P. et al., 2015. Characterization of a Novel Mouse Model of Alzheimer's Disease—Amyloid Pathology and Unique β -Amyloid Oligomer Profile M. Ohno, ed. *Plos One*, 10(5), p.e0126317.
- Liu, Y. et al., 2009. Intracellular trafficking of presenilin 1 is regulated by beta-amyloid precursor protein and phospholipase D1. *J Biol Chem*, 284, pp.12145–12152.
- Lleó, A. et al., 2004. Nonsteroidal anti-inflammatory drugs lower A β 42 and change presenilin 1 conformation. *Nature medicine*, 10(10), pp.1065–1066.

- Lovasic, L., Bauschke, H. & Janus, C., 2005. Working memory impairment in a transgenic amyloid precursor protein TgCRND8 mouse model of Alzheimer's disease. *Genes, brain, and behavior*, 4(3), pp.197–208.
- Luo, Y. et al., 2001. Mice deficient in BACE1, the Alzheimer's beta-secretase, have normal phenotype and abolished beta-amyloid generation. *Nat Neurosci*, 4, pp.231–232.
- Lupien, S.J. & McEwen, B.S., 1997. The acute effects of corticosteroids on cognition: integration of animal and human model studies. *Brain research reviews*, 24(1), pp.1–27.
- Lynch, D.K. et al., 2003. A Cortactin-CD2-associated protein (CD2AP) complex provides a novel link between epidermal growth factor receptor endocytosis and the actin cytoskeleton. *Journal of Biological Chemistry*, 278(24), pp.21805–21813.
- Magarin, A.M. & McEwen, B.S., 1995. Stress-induced atrophy of apical dendrites of hippocampal CA3c neurons: involvement of glucocorticoid secretion and excitatory amino acid receptors. *Neuroscience*, 69(1), pp.89–98.
- Magdesian, M.H. et al., 2008. Amyloid- β binds to the extracellular cysteine-rich domain of Frizzled and inhibits Wnt/ β -catenin signaling. *Journal of Biological Chemistry*, 283(14), pp.9359–9368.
- Maia, L.F. et al., 2013. Changes in amyloid- β and tau in the cerebrospinal fluid of transgenic mice overexpressing amyloid precursor protein. *Science translational medicine*, 5(194), pp.194re2–194re2.
- Mandelkow, E.-M. et al., 1992. Glycogen synthase kinase-3 and the Alzheimer-like state of microtubule-associated protein tau. *FEBS letters*, 314(3), pp.315–321.
- Mandelkow, E.-M. & Mandelkow, E., 1998. Tau in Alzheimer's disease. *Trends in Cell Biology*, 8(11), pp.425–427.
- Mangialasche, F. et al., 2010. Alzheimer's disease: clinical trials and drug development. *The Lancet Neurology*, 9(7), pp.702–716.
- Martins, I.C. et al., 2008. Lipids revert inert Abeta amyloid fibrils to neurotoxic protofibrils that affect learning in mice. *The EMBO journal*, 27(1), pp.224–33.
- Masliah, E. et al., 1996. Comparison of neurodegenerative pathology in transgenic mice overexpressing V717F β -amyloid precursor protein and Alzheimer's disease. *The Journal of neuroscience*, 16(18), pp.5795–5811.
- Masters, C.L. et al., 1985. Amyloid plaque core protein in Alzheimer disease and Down syndrome. *Proceedings of the National Academy of Sciences*, 82(12), pp.4245–4249.
- Mattson, M.P. et al., 1992. beta-Amyloid peptides destabilize calcium homeostasis and render human cortical neurons vulnerable to excitotoxicity. *The journal of neuroscience*, 12(2), pp.376–389.

- Mattson, M.P., Engle, M.G. & Rychlik, B., 1991. Effects of elevated intracellular calcium levels on the cytoskeleton and tau in cultured human cortical neurons. *Molecular and chemical neuropathology*, 15(2), pp.117–142.
- McClellan, P.L. & Hölscher, C., 2014. Liraglutide can reverse memory impairment, synaptic loss and reduce plaque load in aged APP/PS1 mice, a model of Alzheimer's disease. *Neuropharmacology*, 76, Part A, pp.57–67.
- McConlogue, L. et al., 2007. Partial reduction of BACE1 has dramatic effects on Alzheimer plaque and synaptic pathology in APP Transgenic Mice. *The Journal of biological chemistry*, 282(36), pp.26326–34.
- McKhann, G. et al., 1984. Clinical diagnosis of Alzheimer's disease Report of the NINCDS ADRDA Work Group* under the auspices of Department of Health and Human Services Task Force on Alzheimer's Disease. *Neurology*, 34(7), p.939.
- McKhann, G.M. et al., 2011. The diagnosis of dementia due to Alzheimer's disease: Recommendations from the National Institute on Aging-Alzheimer's Association workgroups on diagnostic guidelines for Alzheimer's disease. *Alzheimer's & Dementia*, 7(3), pp.263–269.
- McLaurin, J. et al., 2006. Cyclohexanehexol inhibitors of Aβ aggregation prevent and reverse Alzheimer phenotype in a mouse model. *Nature medicine*, 12(7), pp.801–8.
- McLaurin, J. et al., 1998. Phosphatidylinositol and inositol involvement in Alzheimer amyloid-β fibril growth and arrest. *Journal of molecular biology*, 278(1), pp.183–194.
- Means, L.W., Alexander, S.R. & O'Neal, M.F., 1992. Those cheating rats: male and female rats use odor trails in a water-escape “working memory” task. *Behavioral and Neural Biology*, 58(2), pp.144–151.
- Meilandt, W.J. et al., 2009. Neprilysin overexpression inhibits plaque formation but fails to reduce pathogenic Aβ oligomers and associated cognitive deficits in human amyloid precursor protein transgenic mice. *The Journal of neuroscience : the official journal of the Society for Neuroscience*, 29(7), pp.1977–86.
- Middei, S. et al., 2010. Learning discloses abnormal structural and functional plasticity at hippocampal synapses in the APP23 mouse model of Alzheimer's disease. *Learning & memory (Cold Spring Harbor, N.Y.)*, 17(5), pp.236–40.
- Mills, S.M. et al., 2013. Preclinical trials in autosomal dominant AD: implementation of the DIAN-TU trial. *Revue neurologique*, 169(10), pp.737–743.
- Minkeviciene, R. et al., 2008. Age related decrease in stimulated glutamate release and vesicular glutamate transporters in APP/PS1 transgenic and wild type mice. *Journal of neurochemistry*, 105(3), pp.584–594.
- Minkeviciene, R. et al., 2009. Amyloid β-Induced Neuronal Hyperexcitability Triggers Progressive Epilepsy. *The Journal of Neuroscience*, 29 (11), pp.3453–3462.

- Moechars, D. et al., 1999. Early Phenotypic Changes in Transgenic Mice That Overexpress Different Mutants of Amyloid Precursor Protein in Brain. *Journal of Biological Chemistry*, 274(10), pp.6483–6492.
- Moir, R.D. et al., 1998. Relative increase in Alzheimer's disease of soluble forms of cerebral A β amyloid protein precursor containing the Kunitz protease inhibitory domain. *Journal of Biological Chemistry*, 273(9), pp.5013–5019.
- Morgan, D. et al., 2000. A b peptide vaccination prevents memory loss in an animal model of Alzheimer's disease. *Letters to Nature*, 408(December), pp.982–985.
- Morris, J.C. et al., 2001. Mild cognitive impairment represents early-stage Alzheimer disease. *Archives of neurology*, 58(3), pp.397–405.
- Morris, R.G.M. et al., 1990. Ibotenate Lesions of Hippocampus and/or Subiculum: Dissociating Components of Allocentric Spatial Learning. *European Journal of Neuroscience*, 2(12), pp.1016–1028.
- Morris, R.G.M., Hagan, J.J. & Rawlins, J.N.P., 1986. Allocentric spatial learning by hippocampectomised rats: A further test of the “spatial mapping” and “working memory” theories of hippocampal function. *The Quarterly Journal of Experimental Psychology Section B*, 38(4), pp.365–395.
- Mucke, L. et al., 2000. High-level neuronal expression of abeta 1-42 in wild-type human amyloid protein precursor transgenic mice: synaptotoxicity without plaque formation. *The Journal of neuroscience : the official journal of the Society for Neuroscience*, 20(11), pp.4050–8.
- Mullan, M. et al., 1992. pathogenic mutation for probable Alzheimer's disease in the APP gene at the N-terminus of bold beta-amyloid. *Nature genetics*, 1, pp.345–347.
- Murray, A.J. et al., 2011. Parvalbumin-positive CA1 interneurons are required for spatial working but not for reference memory. *Nature neuroscience*, 14(3), pp.297–299.
- Murrell, J. et al., 1991. A mutation in the amyloid precursor protein associated with hereditary Alzheimer's disease. *Science*, 254 (5028), pp.97–99.
- Musiek, E.S. & Holtzman, D.M., 2015. Three dimensions of the amyloid hypothesis: time, space and 'wingmen'. *Nature neuroscience*, pp.800–806.
- Nadel, L. & Moscovitch, M., 1997. Memory consolidation, retrograde amnesia and the hippocampal complex. *Current Opinion in Neurobiology*, 7, pp.217–227.
- Nader, K., Schafe, G.E. & Le Doux, J.E., 2000. Fear memories require protein synthesis in the amygdala for reconsolidation after retrieval. *Nature*, 406(6797), pp.722–726.
- Naj, A.C. et al., 2011. Common variants at MS4A4/MS4A6E, CD2AP, CD33 and EPHA1 are associated with late-onset Alzheimer's disease. *Nature genetics*, 43(5), pp.436–441.
- Nalbantoglu, J. et al., 1997. Impaired learning and LTP in mice expressing the carboxy terminus of the Alzheimer amyloid precursor protein. *Nature*, 387(6632), pp.500–505.

- Nalivaeva, N.N. & Turner, A.J., 2013. The amyloid precursor protein: a biochemical enigma in brain development, function and disease. *FEBS letters*, 587(13), pp.2046–2054.
- Nasreddine, Z.S. et al., 2005. The Montreal Cognitive Assessment, MoCA: a brief screening tool for mild cognitive impairment. *Journal of the American Geriatrics Society*, 53(4), pp.695–699.
- Nguyen, T.-H., Liu, J. & Lombroso, P.J., 2002. Striatal enriched phosphatase 61 dephosphorylates Fyn at phosphotyrosine 420. *The Journal of biological chemistry*, 277(27), pp.24274–9.
- NICE, NHS & Guidelines, N., 2011. *Donepezil, galantamine, rivastigmine and memantine for the treatment of Alzheimer 's disease (review)*,
- Nilsberth, C. et al., 2001. The “ Arctic ” APP mutation (E693G) causes Alzheimer 's disease by enhanced A β protofibril formation. *Nature*, 9(4), pp.18–23.
- Nitta, A. et al., 1994. β -Amyloid protein-induced Alzheimer's disease animal model. *Neuroscience Letters*, 170(1), pp.63–66.
- Nixon, R.A., 2005. Endosome function and dysfunction in Alzheimer's disease and other neurodegenerative diseases. *Neurobiology of aging*, 26(3), pp.373–382.
- Noble, W. et al., 2003. Cdk5 Is a Key Factor in Tau Aggregation and Tangle Formation In Vivo. *Neuron*, 38(4), pp.555–565.
- Oakley, H. et al., 2006. Intraneuronal beta-amyloid aggregates, neurodegeneration, and neuron loss in transgenic mice with five familial Alzheimer's disease mutations: potential factors in amyloid plaque formation. *J Neurosci*, 26, pp.10129–10140.
- Oddo, S. et al., 2004. A β immunotherapy leads to clearance of early, but not late, hyperphosphorylated tau aggregates via the proteasome. *Neuron*, 43(3), pp.321–332.
- Oddo, S., Vasilevko, V., et al., 2006. Reduction of soluble Abeta and tau, but not soluble Abeta alone, ameliorates cognitive decline in transgenic mice with plaques and tangles. *The Journal of biological chemistry*, 281(51), pp.39413–23.
- Oddo, S., Caccamo, A., et al., 2006. Temporal profile of amyloid-beta (Abeta) oligomerization in an in vivo model of Alzheimer disease. A link between Abeta and tau pathology. *The Journal of biological chemistry*, 281(3), pp.1599–604.
- Oddo, S. et al., 2003. Triple-transgenic model of Alzheimer's disease with plaques and tangles: intracellular Abeta and synaptic dysfunction. *Neuron*, 39, pp.409–421.
- Ognibene, E. et al., 2005. Aspects of spatial memory and behavioral disinhibition in Tg2576 transgenic mice as a model of Alzheimer's disease. *Behavioural Brain Research*, 156(2), pp.225–232.
- Ohno, M. et al., 2004. BACE1 deficiency rescues memory deficits and cholinergic dysfunction in a mouse model of Alzheimer's disease. *Neuron*, 41, pp.27–33.

- Ohno, M. et al., 2007. BACE1 gene deletion prevents neuron loss and memory deficits in 5XFAD APP/PS1 transgenic mice. *Neurobiol Dis*, 26, pp.134–145.
- Olson, M.I. & Shaw, C.-M., 1969. Presenile dementia and Alzheimer's disease in mongolism. *Brain*, 92(1), pp.147–156.
- Olton, D.S., Becker, J.T. & Handeiraann, G.E.-, 1979. Hippocampus , space , and memory. *The Behavioural And Brain Sciences*, 2, pp.313–365.
- Olton, D.S. & Collison, C., 1979. Intramaze cues and “odor trails” fail to direct choice behavior on an elevated maze. *Animal Learning & Behavior*, 7(2), pp.221–223.
- Olton, D.S., Collison, C. & Werz, M.A., 1977. Spatial memory and radial arm maze performance of rats. *Learning and Motivation*, 8(3), pp.289–314.
- Olton, D.S. & Feustle, W.A., 1981. Hippocampal function required for nonspatial working memory. *Experimental Brain Research*, 41(3-4), pp.380–389.
- Olton, D.S. & Paras, B.C., 1979. Spatial memory and hippocampal function. *Neuropsychologia*, 17(6), pp.669–682.
- Olton, D.S. & Samuelson, R.J., 1976. Animal Behavior Processes Remembrance of Places Passed : Spatial Memory in Rats. *Journal of Experimental Psychology*, 2(2), pp.97–116.
- Olton, D.S. & Schlosberg, P., 1978. Food-searching strategies in young rats: Win-shift predominates over win-stay. *Journal of Comparative and Physiological Psychology*, 92(4), p.609.
- Olton, D.S. & Werz, M.A., 1978. Hippocampal function and behavior: Spatial discrimination and response inhibition. *Physiology & Behavior*, 20(5), pp.597–605.
- Organization, W.H., 1992. *The ICD-10 classification of mental and behavioural disorders: clinical descriptions and diagnostic guidelines*, Geneva: World Health Organization.
- Özdemir, M.B. et al., 2013. Injection of specific amyloid-beta oligomers (beta1-40:beta1-42=10:1) into rat medial septum impairs memory retention without inducing hippocampal apoptosis. *Neurological Research*, 35(8), pp.798–803.
- Palmer, A. & Good, M., 2011. Hippocampal synaptic activity, pattern separation and episodic-like memory: implications for mouse models of Alzheimer's disease pathology. *Biochemical Society Transactions*, 39(4), p.902.
- Palop, J.J. et al., 2007. Aberrant excitatory neuronal activity and compensatory remodeling of inhibitory hippocampal circuits in mouse models of Alzheimer's disease. *Neuron*, 55(5), pp.697–711.
- Parvathy, S. et al., 1999. Cleavage of Alzheimer's amyloid precursor protein by α -secretase occurs at the surface of neuronal cells. *Biochemistry*, 38(30), pp.9728–9734.

- Pearce, J.M. et al., 2005. The influence of hippocampal lesions on the discrimination of structure and on spatial memory in pigeons (*Columba livia*). *Behavioral neuroscience*, 119(5), pp.1316–30.
- Pearson, H. a & Peers, C., 2006. Physiological roles for amyloid beta peptides. *The Journal of physiology*, 575(Pt 1), pp.5–10.
- Pedersen, J.T. & Sigurdsson, E.M., 2015. Tau immunotherapy for Alzheimer’s disease. *Trends in molecular medicine*.
- Pedersen, W. a, Kloczewiak, M. a & Blusztajn, J.K., 1996. Amyloid beta-protein reduces acetylcholine synthesis in a cell line derived from cholinergic neurons of the basal forebrain. *Proceedings of the National Academy of Sciences of the United States of America*, 93(15), pp.8068–71.
- Pedersen, W.A. et al., 2006. Rosiglitazone attenuates learning and memory deficits in Tg2576 Alzheimer mice. *Experimental Neurology*, 199(2), pp.265–273.
- Perez-Nievas, B.G. et al., 2013. Dissecting phenotypic traits linked to human resilience to Alzheimer’s pathology. *Brain*, p.awt171.
- PERRY, E.K. et al., 1978. CHANGES IN BRAIN CHOLINESTERASES IN SENILE DEMENTIA OF ALZHEIMER TYPE. *Neuropathology and Applied Neurobiology*, 4(4), pp.273–277.
- Petersen, R.C. et al., 1999. Mild cognitive impairment: clinical characterization and outcome. *Archives of neurology*, 56(3), pp.303–308.
- Petersen, R.C., 2002. Mild cognitive impairment: transition from aging to Alzheimer’s disease. *Alzheimer’s disease: Advances in etiology, pathogenesis and therapeutics*, pp.141–151.
- Petersen, R.C. et al., 2006. Neuropathologic features of amnesic mild cognitive impairment. *Archives of neurology*, 63(5), pp.665–672.
- Phillips, R.G. & LeDoux, J.E., 1992. Differential contribution of amygdala and hippocampus to cued and contextual fear conditioning. *Behavioral neuroscience*, 106(2), p.274.
- Pike, C., Overman, M.J. & Cotman, C., 1995. Amino-terminal Deletions Enhance Aggregation of beta-Amyloid Peptides in Vitro. *Journal of Biological Chemistry*, 270(41), pp.23895–23898.
- Pike, C.J. et al., 1991. In vitro aging of β -amyloid protein causes peptide aggregation and neurotoxicity. *Brain Research*, 563(1–2), pp.311–314.
- Pimplikar, S.W. et al., 2010. Amyloid-independent mechanisms in Alzheimer’s disease pathogenesis. *The Journal of neuroscience : the official journal of the Society for Neuroscience*, 30(45), pp.14946–54.
- Plant, L.D. et al., 2006. Amyloid beta peptide as a physiological modulator of neuronal “A”-type K⁺ current. *Neurobiol Aging*, 27, pp.1673–1683.

- Plant, L.D. et al., 2003. The production of amyloid beta peptide is a critical requirement for the viability of central neurons. *J Neurosci*, 23, pp.5531–5535.
- Plucińska, K. et al., 2014. Knock-in of human BACE1 cleaves murine APP and reiterates Alzheimer-like phenotypes. *The Journal of neuroscience : the official journal of the Society for Neuroscience*, 34(32), pp.10710–28.
- Podlisny, M.B. et al., 1998. Oligomerization of endogenous and synthetic amyloid β -protein at nanomolar levels in cell culture and stabilization of monomer by Congo red. *Biochemistry*, 37(11), pp.3602–3611.
- Pooler, A.M. et al., 2012. Dynamic association of tau with neuronal membranes is regulated by phosphorylation. *Neurobiology of aging*, 33(2), pp.431.e27–38.
- Pooler, A.M., Phillips, E.C., et al., 2013. Physiological release of endogenous tau is stimulated by neuronal activity. *EMBO reports*, 14(4), pp.389–394.
- Pooler, A.M., Polydoro, M., et al., 2013. Propagation of tau pathology in Alzheimer's disease: identification of novel therapeutic targets. *Alzheimer's research & therapy*, 5(5), p.49.
- Pooler, A.M., Noble, W. & Hanger, D.P., 2014. A role for tau at the synapse in Alzheimer's disease pathogenesis. *Neuropharmacology*, 76, pp.1–8.
- Pouzet, B. et al., 2002. Hippocampal lesioned rats are able to learn a spatial position using non-spatial strategies. *Behavioural Brain Research*, 133(2), pp.279–291.
- Price, J.L. & Morris, J.C., 1999. Tangles and plaques in nondemented aging and "preclinical" Alzheimer's disease. *Annals of neurology*, 45(3), pp.358–368.
- Prince, M. et al., 2014. *World Alzheimer Report 2014 Dementia and Risk Reduction*,
- Prut, L. et al., 2007. Aged APP23 mice show a delay in switching to the use of a strategy in the Barnes maze. *Behavioural brain research*, 179(1), pp.107–10.
- Prybylowski, K. et al., 2005. The synaptic localization of NR2B-containing NMDA receptors is controlled by interactions with PDZ proteins and AP-2. *Neuron*, 47(6), pp.845–857.
- Puoliväli, J. et al., 2002. Hippocampal A β 42 levels correlate with spatial memory deficit in APP and PS1 double transgenic mice. *Neurobiology of disease*, 9(3), pp.339–347.
- Qian, X., Hamad, B. & Dias-Lalcaca, G., 2015. The Alzheimer disease market. *Nature Reviews Drug Discovery*, 14(10), pp.675–676.
- Rabinovich-Nikitin, I. et al., 2012. Beneficial Effect of Antibodies against β - Secretase Cleavage Site of App on Alzheimer's-Like Pathology in Triple-Transgenic Mice. *PLoS one*, 7(10), p.e46650.
- Rabinovich-Nikitin, I. & Solomon, B., 2014. Inhibition of Amyloid Precursor Protein Processing Leads to Downregulation of Apoptotic Genes in Alzheimer's Disease Animal Models. *Neurodegenerative Diseases*, 13(2-3), pp.107–109.

- Racke, M.M. et al., 2005. Exacerbation of Cerebral Amyloid Angiopathy-Associated Microhemorrhage in Amyloid Precursor Protein Transgenic Mice by Immunotherapy Is Dependent on Antibody Recognition of Deposited Forms of Amyloid β . *The Journal of Neuroscience*, 25 (3), pp.629–636.
- Raffaele, K.C. & Olton, D.S., 1988. Hippocampal and amygdaloid involvement in working memory for nonspatial stimuli. *Behavioral Neuroscience*, 102(3), pp.349–355.
- Rakover, I., Arbel, M. & Solomon, B., 2007. Immunotherapy against APP β -Secretase Cleavage Site Improves Cognitive Function and Reduces Neuroinflammation in Tg2576 Mice without a Significant Effect on Brain A β Levels. *Neurodegenerative Diseases*, 4(5), pp.392–402.
- Rammes, G. et al., 2011. Therapeutic significance of NR2B-containing NMDA receptors and mGluR5 metabotropic glutamate receptors in mediating the synaptotoxic effects of β -amyloid oligomers on long-term potentiation (LTP) in murine hippocampal slices. *Neuropharmacology*, 60(6), pp.982–990.
- Rasool, S. et al., 2013. Systemic vaccination with anti-oligomeric monoclonal antibodies improves cognitive function by reducing A β deposition and tau pathology in 3xTg-AD mice. *Journal of neurochemistry*, 126(4), pp.473–82.
- Rauch, T.M., Welch, D.I. & Gallego, L., 1989. Hypothermia impairs performance in the Morris water maze. *Physiology & behavior*, 46(2), pp.315–320.
- Razay, G. & Vreugdenhil, A., 2005. Obesity in middle age and future risk of dementia: midlife obesity increases risk of future dementia. *BMJ*, 331(7514), p.455.
- RC, P. et al., 1999. Mild cognitive impairment: Clinical characterization and outcome. *Archives of Neurology*, 56(3), pp.303–308.
- Reardon, S., 2015. Alzheimer antibody drugs show questionable potential. *Nature Reviews Drug Discovery*, 14(9), pp.591–592.
- Redwine, J.M. et al., 2003. Dentate gyrus volume is reduced before onset of plaque formation in PDAPP mice: a magnetic resonance microscopy and stereologic analysis. *Proceedings of the National Academy of Sciences of the United States of America*, 100(3), pp.1381–6.
- Reed, M.N. et al., 2009. Cognitive effects of cell-derived and synthetically derived A β oligomers. *Neurobiology of Aging*, 32(10), pp.1784–1794.
- Reilly, J.F. et al., 2003. Amyloid deposition in the hippocampus and entorhinal cortex: quantitative analysis of a transgenic mouse model. *Proceedings of the National Academy of Sciences of the United States of America*, 100(8), pp.4837–42.
- Reiman, E.M. et al., 2011. Alzheimer's Prevention Initiative: a plan to accelerate the evaluation of presymptomatic treatments. *Journal of Alzheimer's Disease*, 26(Suppl 3), p.321.
- Reitz, C. & Mayeux, R., 2014. Alzheimer disease: epidemiology, diagnostic criteria, risk factors and biomarkers. *Biochemical pharmacology*, 88(4), pp.640–51.

- Renner, M. et al., 2010. Deleterious effects of amyloid β oligomers acting as an extracellular scaffold for mGluR5. *Neuron*, 66(5), pp.739–754.
- Revilla, S. et al., 2014. Physical exercise improves synaptic dysfunction and recovers the loss of survival factors in 3xTg-AD mouse brain. *Neuropharmacology*, 81, pp.55–63.
- Ribé, E.M. et al., 2005. Accelerated amyloid deposition, neurofibrillary degeneration and neuronal loss in double mutant APP/tau transgenic mice. *Neurobiology of disease*, 20(3), pp.814–822.
- Richter, S.H. et al., 2013. Where have I been? Where should I go? Spatial working memory on a radial arm maze in a rat model of depression. *PloS one*, 8(4), p.e62458.
- Rinne, J.O. et al., 2010. 11 C-PiB PET assessment of change in fibrillar amyloid- β load in patients with Alzheimer's disease treated with bapineuzumab: a phase 2, double-blind, placebo-controlled, ascending-dose study. *The Lancet Neurology*, 9(4), pp.363–372.
- Roberson, E.D. et al., 2011. Amyloid- β /Fyn-induced synaptic, network, and cognitive impairments depend on tau levels in multiple mouse models of Alzheimer's disease. *The Journal of neuroscience*, 31(2), pp.700–11.
- Roberson, E.D. et al., 2007. Reducing endogenous tau ameliorates amyloid beta-induced deficits in an Alzheimer's disease mouse model. *Science*, 316(5825), pp.750–4.
- Roder, S. et al., 2003. Electrophysiological studies on the hippocampus and prefrontal cortex assessing the effects of amyloidosis in amyloid precursor protein 23 transgenic mice. *Neuroscience*, 120(3), pp.705–720.
- Roe, C.M. et al., 2013. Amyloid imaging and CSF biomarkers in predicting cognitive impairment up to 7.5 years later. *Neurology*, 80(19), pp.1784–1791.
- Rogaev, E.I. et al., 1995. Familial Alzheimer's disease in kindreds with missense mutations in a gene on chromosome 1 related to the Alzheimer's disease type 3 gene. *Nature*, 376(6543), pp.775–778.
- Rogers, K. et al., 2012. Modulation of γ -secretase by EVP-0015962 reduces amyloid deposition and behavioral deficits in Tg2576 mice. *Molecular Neurodegeneration*, 7(61), pp.1–18.
- Rolls, E.T., 2013. The mechanisms for pattern completion and pattern separation in the hippocampus. *Front. Syst. Neurosci*, 7(74), pp.10–3389.
- Romberg, C. et al., 2012. False recognition in a mouse model of Alzheimer's disease: rescue with sensory restriction and memantine. *Brain*, 135(7), pp.2103–2114.
- Romberg, C. et al., 2011. Impaired Attention in the 3xTgAD Model of Alzheimer's Disease Assessed Using a Translational Touchscreen Method for Mice: Rescue by Donepezil (Aricept). *The Journal of neuroscience: the official journal of the Society for Neuroscience*, 31(9), p.3500.

- Rosen, W.G., Mohs, R.C. & Davis, K.L., 1984. A new rating scale for Alzheimer's disease. *The American journal of psychiatry*.
- Rothblat, L.A. & Hayes, L.L., 1987. Short-term object recognition memory in the rat: Nonmatching with trial-unique junk stimuli. *Behavioral Neuroscience*, 101(4), p.587.
- Saganich, M.J. et al., 2006. Deficits in synaptic transmission and learning in amyloid precursor protein (APP) transgenic mice require C-terminal cleavage of APP. *The Journal of neuroscience : the official journal of the Society for Neuroscience*, 26(52), pp.13428–36.
- Sahay, A. et al., 2011. Increasing adult hippocampal neurogenesis is sufficient to improve pattern separation. *Nature*, 472(7344), pp.466–470.
- Salloway, S. et al., 2011. A phase 2 randomized trial of ELND005, scyllo-inositol, in mild to moderate Alzheimer disease. *Neurology*, 77(13), pp.1253–1262.
- Salmon, D.P. & Bondi, M.W., 2009. Neuropsychological assessment of dementia. *Annual review of psychology*, 60, p.257.
- Salter, M.W. & Kalia, L. V., 2004. Src kinases: a hub for NMDA receptor regulation. *Nature reviews. Neuroscience*, 5(4), pp.317–28.
- Sanderson, D.J. et al., 2010. Spatial working memory deficits in GluA1 AMPA receptor subunit knockout mice reflect impaired short-term habituation: evidence for Wagner's dual-process memory model. *Neuropsychologia*, 48(8), pp.2303–15.
- Sasahara, M. et al., 1991. PDGF B-chain in neurons of the central nervous system, posterior pituitary, and in a transgenic model. *Cell*, 64(1), pp.217–227.
- Satoh, Y. et al., 2007. Extracellular signal-regulated kinase 2 (ERK2) knockdown mice show deficits in long-term memory; ERK2 has a specific function in learning and memory. *The Journal of Neuroscience*, 27(40), pp.10765–10776.
- Saura, C. et al., 2005. Conditional Inactivation of Presenilin 1 Prevents Amyloid Accumulation and Temporarily Rescues Contextual and Spatial Working Memory Impairments in Amyloid Precursor Protein Transgenic Mice. *Journal of Neuroscience*, 25(29), pp.6755–6764.
- Scarmeas, N. et al., 2009. Mediterranean diet and mild cognitive impairment. *Archives of neurology*, 66(2), pp.216–225.
- Scarpini, E., Schelterns, P. & Feldman, H., 2003. Treatment of Alzheimer's disease; current status and new perspectives. *The Lancet Neurology*, 2(9), pp.539–547.
- Schenk, D., 2002. Amyloid- β immunotherapy for Alzheimer's disease: the end of the beginning. *Nature Reviews Neuroscience*, 3(10), pp.824–828.
- Schenk, D. et al., 1999. Immunization with amyloid-beta attenuates Alzheimer-disease-like pathology in the PDAPP mouse. *Nature*, 400(6740), pp.173–7.

- Scheuner, D. et al., 1996. Secreted amyloid beta-protein similar to that in the senile plaques of Alzheimer's disease is increased in vivo by the presenilin 1 and 2 and APP mutations linked to familial Alzheimer's disease. *Nat Med*, 2, pp.864–870.
- Schmitt, F.A. et al., 2000. "Preclinical" AD revisited Neuropathology of cognitively normal older adults. *Neurology*, 55(3), pp.370–376.
- Schmitt, W.B. et al., 2003. A within-subjects, within-task demonstration of intact spatial reference memory and impaired spatial working memory in glutamate receptor-A-deficient mice. *The Journal of neuroscience*, 23(9), pp.3953–3959.
- Schroeter, S. et al., 2008. Immunotherapy Reduces Vascular Amyloid- β in PDAPP Mice. *The Journal of Neuroscience*, 28 (27), pp.6787–6793.
- Schwab, C., Hosokawa, M. & McGeer, P.L., 2004. Transgenic mice overexpressing amyloid beta protein are an incomplete model of Alzheimer disease. *Experimental Neurology*, 188(1), pp.52–64.
- Scott, L. & Goa, K., 2000. Galantamine: a review of its use in Alzheimer's Disease. *Drugs*, 60(5), pp.1095–1122.
- Selkoe, D.J., 2001. Alzheimer's Disease : Genes , Proteins , and Therapy. *Physiological Reviews*, 81(2).
- Selkoe, D.J., 2002. Alzheimer's disease is a synaptic failure. *Science (New York, N.Y.)*, 298(5594), pp.789–91.
- Selkoe, D.J., 2013. The therapeutics of Alzheimer's disease: Where we stand and where we are heading. *Annals of neurology*, 74(3), pp.328–336.
- Serrano-Pozo, A. et al., 2011. Neuropathological alterations in Alzheimer disease. *Cold Spring Harbor perspectives in medicine*, 1(1), p.a006189.
- Seshadri, S. et al., 2010. Genome-wide analysis of genetic loci associated with Alzheimer disease. *Jama*, 303(18), pp.1832–1840.
- Shankar, G.M. et al., 2008. Amyloid- β protein dimers isolated directly from Alzheimer's brains impair synaptic plasticity and memory. *Nature medicine*, 14(8), pp.837–842.
- Shankar, G.M. et al., 2007. Natural Oligomers of the Alzheimer Amyloid- β Protein Induce Reversible Synapse Loss by Modulating an NMDA-Type Glutamate Receptor-Dependent Signaling Pathway. *The Journal of Neuroscience*, 27 (11), pp.2866–2875.
- Sherrington, R. et al., 1995. Cloning of a gene bearing missense mutations in early-onset familial Alzheimer's disease. *Nature*, 375, pp.754–760.
- Shi, J.-Q. et al., 2011. Anti-TNF- α reduces amyloid plaques and tau phosphorylation and induces CD11c-positive dendritic-like cell in the APP/PS1 transgenic mouse brains. *Brain research*, 1368, pp.239–247.

- Shih, I.-M. & Wang, T.-L., 2007. Notch signaling, gamma-secretase inhibitors, and cancer therapy. *Cancer research*, 67(5), pp.1879–82.
- Shukla, V. et al., 2013. A truncated peptide from p35, a Cdk5 activator, prevents Alzheimer's disease phenotypes in model mice. *The FASEB Journal*, 27(1), pp.174–186.
- Singh, T.J., Grundke Iqbal, I. & Iqbal, K., 1995. Phosphorylation of τ Protein by Casein Kinase 1 Converts It to an Abnormal Alzheimer Like State. *Journal of neurochemistry*, 64(3), pp.1420–1423.
- Sinha, S. et al., 1999. Purification and cloning of amyloid precursor protein beta-secretase from human brain. *Nature*, 402, pp.537–540.
- Şık, A. et al., 2003. Performance of different mouse strains in an object recognition task. *Behavioural Brain Research*, 147(1–2), pp.49–54.
- Snyder, E.M. et al., 2005. Regulation of NMDA receptor trafficking by amyloid- β . *Nature Neuroscience*, 8(8), pp.1051–1058.
- Snyderman, D. & Rovner, B., 2009. Mental status exam in primary care: a review. *American family physician*, 80(8), pp.809–814.
- Society, A., 2014. *Dementia UK: Update*,
- Solomon, B. et al., 1997. Disaggregation of Alzheimer β -amyloid by site-directed mAb. *Proceedings of the National Academy of Sciences*, 94(8), pp.4109–4112.
- Solomon, B. et al., 1996. Monoclonal antibodies inhibit in vitro fibrillar aggregation of the Alzheimer beta-amyloid peptide. *Proceedings of the National Academy of Sciences*, 93(1), pp.452–455.
- Solomon, B. & Frenkel, D., 2010. Immunotherapy for Alzheimer's disease. *Neuropharmacology*, 59(4-5), pp.303–9.
- Sperling, R. et al., 2012. Amyloid-related imaging abnormalities in patients with Alzheimer's disease treated with bapineuzumab: a retrospective analysis. *The Lancet Neurology*, 11(3), pp.241–249.
- Sperling, R.A. et al., 2011. Toward defining the preclinical stages of Alzheimer's disease: Recommendations from the National Institute on Aging-Alzheimer's Association workgroups on diagnostic guidelines for Alzheimer's disease. *Alzheimer's & Dementia*, 7(3), pp.280–292.
- Spires, T.L. et al., 2006. Region-specific dissociation of neuronal loss and neurofibrillary pathology in a mouse model of tauopathy. *The American journal of pathology*, 168(5), pp.1598–1607.
- Srivareerat, M. et al., 2009. Chronic psychosocial stress exacerbates impairment of cognition and long-term potentiation in β -amyloid rat model of Alzheimer's disease. *Biological psychiatry*, 65(11), pp.918–926.

- Stark, S.M. et al., 2013. A task to assess behavioral pattern separation (BPS) in humans: data from healthy aging and mild cognitive impairment. *Neuropsychologia*, 51(12), pp.2442–2449.
- Stark, S.M., Yassa, M.A. & Stark, C.E.L., 2010. Individual differences in spatial pattern separation performance associated with healthy aging in humans. *Learning & Memory*, 17(6), pp.284–288.
- Steele, J.W. et al., 2014. Early fear memory defects are associated with altered synaptic plasticity and molecular architecture in the TgCRND8 Alzheimer's disease mouse model. *Journal of Comparative Neurology*, 522(10), pp.2319–2335.
- Steele, R.J. & Morris, R.G.M., 1999. Delay dependent impairment of a matching to place task with chronic and intrahippocampal infusion of the NMDA antagonist D AP5. *Hippocampus*, 9(2), pp.118–136.
- Stein, T.D. et al., 2004. Neutralization of transthyretin reverses the neuroprotective effects of secreted amyloid precursor protein (APP) in APPSW mice resulting in tau phosphorylation and loss of hippocampal neurons: support for the amyloid hypothesis. *The Journal of neuroscience*, 24(35), pp.7707–7717.
- Steiner, H. et al., 2002. PEN-2 is an integral component of the γ -secretase complex required for coordinated expression of presenilin and nicastrin. *Journal of Biological Chemistry*, 277(42), pp.39062–39065.
- Van Strien, N.M., Cappaert, N.L.M. & Witter, M.P., 2009. The anatomy of memory: an interactive overview of the parahippocampal-hippocampal network. *Nature reviews. Neuroscience*, 10(4), pp.272–82.
- De Strooper, B. et al., 1999. A presenilin-1-dependent γ -secretase-like protease mediates release of Notch intracellular domain. *Nature*, 398(6727), pp.518–522.
- De Strooper, B., 2003. Aph-1, Pen-2, and nicastrin with presenilin generate an active γ -secretase complex. *Neuron*, 38(1), pp.9–12.
- De Strooper, B. et al., 1998. Deficiency of presenilin-1 inhibits the normal cleavage of amyloid precursor protein. *Nature*, 391(6665), pp.387–390.
- De Strooper, B., 2010. Proteases and proteolysis in Alzheimer disease: a multifactorial view on the disease process. *Physiological reviews*, 90(2), pp.465–94.
- De Strooper, B., Vassar, R. & Golde, T., 2010a. The secretases: enzymes with therapeutic potential in Alzheimer disease. *Nature Reviews Neurology*, 6(2), pp.99–107.
- De Strooper, B., Vassar, R. & Golde, T., 2010b. The secretases: enzymes with therapeutic potential in Alzheimer disease. *Nature reviews. Neurology*, 6(2), pp.99–107.
- Sturchler-Pierrat, C. et al., 1997. Two amyloid precursor protein transgenic mouse models with Alzheimer disease-like pathology. *Proceedings of the National Academy of Sciences*, 94(24), pp.13287–13292.

- Su, Y. & Ni, B., 1998. Selective Deposition of Amyloid- β Protein in the Entorhinal-Dentate Projection of a Transgenic Mouse Model of Alzheimer's Disease. *Journal of Neuroscience Research*, 53(2), pp.177–186.
- Sutherland, G.T. et al., 2013. Oxidative stress in Alzheimer's disease: Primary villain or physiological by-product? *Redox report : communications in free radical research*, 18(4), pp.134–41.
- Suzuki, N. et al., 1994. An increased percentage of long amyloid beta protein secreted by familial amyloid beta protein precursor (beta APP717) mutants. *Science*, 264(5163), pp.1336–1340.
- Swerdlow, R.H., Burns, J.M. & Khan, S.M., 2014. The Alzheimer's disease mitochondrial cascade hypothesis: progress and perspectives. *Biochimica et biophysica acta*, 1842(8), pp.1219–31.
- Sydow, a. et al., 2011. Tau-Induced Defects in Synaptic Plasticity, Learning, and Memory Are Reversible in Transgenic Mice after Switching Off the Toxic Tau Mutant. *Journal of Neuroscience*, 31(7), pp.2511–2525.
- Tai, H.-C. et al., 2012. The synaptic accumulation of hyperphosphorylated tau oligomers in Alzheimer disease is associated with dysfunction of the ubiquitin-proteasome system. *The American journal of pathology*, 181(4), pp.1426–1435.
- Takashima, A. et al., 1998. Activation of tau protein kinase I/glycogen synthase kinase-3 β by amyloid β peptide (25–35) enhances phosphorylation of tau in hippocampal neurons. *Neuroscience Research*, 31(4), pp.317–323.
- Tamayev, R. et al., 2012. β - but not γ -secretase proteolysis of APP causes synaptic and memory deficits in a mouse model of dementia. *EMBO molecular medicine*, 4(3), pp.171–9.
- Tanaka, S. et al., 1989. Tissue-specific expression of three types of β -protein precursor mRNA: enhancement of protease inhibitor-harboring types in Alzheimer's disease brain. *Biochemical and biophysical research communications*, 165(3), pp.1406–1414.
- Tanzi, R.E. et al., 1987. Amyloid beta protein gene: cDNA, mRNA distribution, and genetic linkage near the Alzheimer locus. *Science*, 235(4791), pp.880–884.
- Tariot, P.N. et al., 2003. Memantine/donepezil dual therapy is superior to placebo/donepezil therapy for treatment of moderate to severe Alzheimer's disease. In *INTERNATIONAL PSYCHOGERIATRICS*. SPRINGER PUBLISHING CO 536 BROADWAY, NEW YORK, NY 10012 USA, p. 289.
- Tateno, H. et al., 2007. Distinct endocytic mechanisms of CD22 (Siglec-2) and Siglec-F reflect roles in cell signaling and innate immunity. *Molecular and cellular biology*, 27(16), pp.5699–5710.
- Tebar, F., Bohlander, S.K. & Sorkin, A., 1999. Clathrin assembly lymphoid myeloid leukemia (CALM) protein: localization in endocytic-coated pits, interactions with clathrin, and the

- impact of overexpression on clathrin-mediated traffic. *Molecular Biology of the Cell*, 10(8), pp.2687–2702.
- Tekirian, T.L. et al., 1999. Toxicity of Pyroglutaminated Amyloid β -Peptides 3(pE)-40 and -42 Is Similar to That of A β 1-40 and -42. *Journal of Neurochemistry*, 73(4), pp.1584–1589.
- Thal, D.R. et al., 2002. Phases of A β -deposition in the human brain and its relevance for the development of AD. *Neurology*, 58(12), pp.1791–1800.
- Thomas, R.S. et al., 2006. An antibody to the beta-secretase cleavage site on amyloid-beta-protein precursor inhibits amyloid-beta production. *Journal of Alzheimer's disease : JAD*, 10(4), pp.379–90.
- Thomas, R.S. et al., 2013. Inhibition of amyloid- β production by anti-amyloid precursor protein antibodies in primary mouse cortical neurones. *NeuroReport*, 24(18).
- Thomas, R.S., Liddell, J.E. & Kidd, E.J., 2011. Anti-amyloid precursor protein immunoglobulins inhibit amyloid- β production by steric hindrance. *FEBS Journal*, 278(1), pp.167–178.
- Timberlake, W. & White, W., 1990. Winning isn't everything: Rats need only food deprivation and not food reward to efficiently traverse a radial arm maze. *Learning and Motivation*, 21(2), pp.153–163.
- Tinsley, C.J. et al., 2011. Differing time dependencies of object recognition memory impairments produced by nicotinic and muscarinic cholinergic antagonism in perirhinal cortex. *Learning & memory (Cold Spring Harbor, N.Y.)*, 18(7), pp.484–92.
- Townsend, M., Shankar, G.M., et al., 2006. Effects of secreted oligomers of amyloid β -protein on hippocampal synaptic plasticity: a potent role for trimers. *The Journal of Physiology*, 572(2), pp.477–492.
- Townsend, M., Cleary, J.P., et al., 2006. Orally available compound prevents deficits in memory caused by the Alzheimer amyloid-beta oligomers. *Annals of neurology*, 60(6), pp.668–76.
- Trinchese, F. et al., 2004. Progressive age related development of Alzheimer like pathology in APP/PS1 mice. *Annals of neurology*, 55(6), pp.801–814.
- Tulving, E., 1972. Episodic and semantic memory 1. *Organization of Memory. London: Academic*, 381(4).
- Um, J.W. et al., 2012. Alzheimer amyloid- β oligomer bound to postsynaptic prion protein activates Fyn to impair neurons. *Nature neuroscience*, 15(9), pp.1227–35.
- Um, J.W., Kaufman, A.C., Kostylev, M., Heiss, J.K., Stagi, M., Takahashi, H., Kerrisk, M.E., Vortmeyer, A., Wisniewski, T. & Koleske, A.J., 2013. Metabotropic glutamate receptor 5 is a coreceptor for Alzheimer β oligomer bound to cellular prion protein. *Neuron*, 79(5), pp.887–902.

- Um, J.W., Kaufman, A.C., Kostylev, M., Heiss, J.K., Stagi, M., Takahashi, H., Kerrisk, M.E., Vortmeyer, A., Wisniewski, T., Koleske, A.J., et al., 2013. Metabotropic glutamate receptor 5 is a coreceptor for Alzheimer $\text{A}\beta$ oligomer bound to cellular prion protein. *Neuron*, 79(5), pp.887–902.
- Vassar, R. et al., 1999. Beta-secretase cleavage of Alzheimer's amyloid precursor protein by the transmembrane aspartic protease BACE. *Science*, 286, pp.735–741.
- Vassar, R. et al., 2009. The beta-secretase enzyme BACE in health and Alzheimer's disease: regulation, cell biology, function, and therapeutic potential. *J Neurosci*, 29, pp.12787–12794.
- Vassar, R. & Citron, M., 2000. $\text{A}\beta$ -Generating Enzymes: Recent Advances in β - and γ -Secretase Research. *Neuron*, 27(3), pp.419–422.
- Venkitaramani, D. V et al., 2007. Beta-amyloid modulation of synaptic transmission and plasticity. *The Journal of neuroscience : the official journal of the Society for Neuroscience*, 27(44), pp.11832–7.
- Venkitaramani, D. V et al., 2011. Striatal-enriched protein tyrosine phosphatase (STEP) knockout mice have enhanced hippocampal memory. *European Journal of Neuroscience*, 33(12), pp.2288–2298.
- Vloeberghs, E. et al., 2006. APP23 mice display working memory impairment in the plus-shaped water maze. *Neuroscience letters*, 407(1), pp.6–10.
- Võikar, V. et al., 2001. Strain and gender differences in the behavior of mouse lines commonly used in transgenic studies. *Physiology & Behavior*, 72(1–2), pp.271–281.
- Vorhees, C. V & Williams, M.T., 2014. Assessing spatial learning and memory in rodents. *ILAR journal / National Research Council, Institute of Laboratory Animal Resources*, 55(2), pp.310–32.
- Vos, S.J.B. et al., 2013. Preclinical Alzheimer's disease and its outcome: a longitudinal cohort study. *The Lancet Neurology*, 12(10), pp.957–965.
- Walsh, D.M. et al., 2005. Certain inhibitors of synthetic amyloid β -peptide ($\text{A}\beta$) fibrillogenesis block oligomerization of natural $\text{A}\beta$ and thereby rescue long-term potentiation. *The Journal of neuroscience*, 25(10), pp.2455–2462.
- Walsh, D.M. et al., 2002. Naturally secreted oligomers of amyloid β protein potently inhibit hippocampal long-term potentiation in vivo. *Nature*, 416(6880), pp.535–539.
- Walsh, D.M. et al., 2005. The role of cell-derived oligomers of Abeta in Alzheimer's disease and avenues for therapeutic intervention. *Biochemical Society Transactions*, 33(5), p.1087.
- Walsh, D.M. & Selkoe, D.J., 2007. A beta oligomers - a decade of discovery. *Journal of neurochemistry*, 101(5), pp.1172–84.

- Walsh, D.M. & Selkoe, D.J., 2004. Deciphering the molecular basis of memory failure in Alzheimer's disease. *Neuron*, 44(1), pp.181–193.
- Wang, G.-W. & Cai, J.-X., 2006. Disconnection of the hippocampal-prefrontal cortical circuits impairs spatial working memory performance in rats. *Behavioural brain research*, 175(2), pp.329–36.
- Wang, H. et al., 2000. Amyloid Peptide A β 1–42 Binds Selectively and with Picomolar Affinity to α 7 Nicotinic Acetylcholine Receptors. *Journal of neurochemistry*, 75(3), pp.1155–1161.
- Warburton, E.C., Barker, G.R.I. & Brown, M.W., 2013. Investigations into the involvement of NMDA mechanisms in recognition memory. *Neuropharmacology*, 74, pp.41–7.
- Warburton, E.C. & Brown, M.W., 2010. Findings from animals concerning when interactions between perirhinal cortex, hippocampus and medial prefrontal cortex are necessary for recognition memory. *Neuropsychologia*, 48(8), pp.2262–72.
- Warburton, E.C. & Brown, M.W., 2015a. Neural circuitry for rat recognition memory. *Behavioural Brain Research*, 285, pp.131–139.
- Warburton, E.C. & Brown, M.W., 2015b. Neural circuitry for rat recognition memory. *Behavioural brain research*, 285, pp.131–9.
- Washbourne, P. et al., 2004. Cycling of NMDA receptors during trafficking in neurons before synapse formation. *The Journal of neuroscience*, 24(38), pp.8253–8264.
- Webster, S.J. et al., 2014. Using mice to model Alzheimer's dementia: an overview of the clinical disease and the preclinical behavioral changes in 10 mouse models. *Frontiers in genetics*, 5(April), p.88.
- Webster, S.J., Bachstetter, A.D. & Van Eldik, L.J., 2013. Comprehensive behavioral characterization of an APP/PS-1 double knock-in mouse model of Alzheimer's disease. *Alzheimers Res Ther*, 5(3), p.28.
- Wechsler, D., 1997. *WMS-III: Wechsler memory scale administration and scoring manual*, Psychological Corporation.
- Weiss, C. et al., 2002. Impaired eyeblink conditioning and decreased hippocampal volume in PDAPP V717F mice. *Neurobiology of disease*, 11(3), pp.425–433.
- West, M.J. et al., 1994. Differences in the pattern of hippocampal neuronal loss in normal ageing and Alzheimer's disease. *The Lancet*, 344(8925), pp.769–772.
- Westerman, M.A. et al., 2002. The Relationship between A_{NL} and Memory in the Tg2576 Mouse Model of Alzheimer's Disease. *The Journal of Neuroscience*, 22(5), pp.1858–1867.
- Whishaw, I.Q. & Tomie, J.-A., 1997. Perseveration on place reversals in spatial swimming pool tasks: Further evidence for place learning in hippocampal rats. *Hippocampus*, 7(4), pp.361–370.

- Whitmer, R.A. et al., 2005. Midlife cardiovascular risk factors and risk of dementia in late life. *Neurology*, 64(2), pp.277–281.
- Wilcock, D.M. et al., 2006. Deglycosylated Anti-Amyloid- β Antibodies Eliminate Cognitive Deficits and Reduce Parenchymal Amyloid with Minimal Vascular Consequences in Aged Amyloid Precursor Protein Transgenic Mice. *The Journal of Neuroscience* , 26 (20), pp.5340–5346.
- Wilcock, D.M., Rojiani, A., Rosenthal, A., Levkowitz, G., et al., 2004. Passive amyloid immunotherapy clears amyloid and transiently activates microglia in a transgenic mouse model of amyloid deposition. *The Journal of Neuroscience*, 24(27), pp.6144–51.
- Wilcock, D.M., Rojiani, A., Rosenthal, A., Subbarao, S., et al., 2004. Passive immunotherapy against A β in aged APP-transgenic mice reverses cognitive deficits and depletes parenchymal amyloid deposits in spite of increased vascular amyloid and microhemorrhage. *Journal of neuroinflammation*, 1(1), p.24.
- Wilson, C.R.E. et al., 2008. Addition of fornix transection to frontal-temporal disconnection increases the impairment in object-in-place memory in macaque monkeys. *European Journal of Neuroscience*, 27(7), pp.1814–1822.
- Wilson, J.J. et al., 2015. Spatial learning by mice in three dimensions. *Behavioural brain research*, 289, pp.125–132.
- Winblad, B. et al., 2014. Active immunotherapy options for Alzheimer's disease. *Alzheimer's research & therapy*, 6(1), p.7.
- Winblad, B. et al., 2012. Safety, tolerability, and antibody response of active A β immunotherapy with CAD106 in patients with Alzheimer's disease: randomised, double-blind, placebo-controlled, first-in-human study. *The Lancet Neurology*, 11(7), pp.597–604.
- Winters, B.D. et al., 2004. Double Dissociation between the Effects of Peri-Postrhinal Cortex and Hippocampal Lesions on Tests of Object Recognition and Spatial Memory: Heterogeneity of Function within the Temporal Lobe. *The Journal of Neuroscience* , 24 (26), pp.5901–5908.
- Winters, B.D. & Bussey, T.J., 2005. Transient Inactivation of Perirhinal Cortex Disrupts Encoding, Retrieval, and Consolidation of Object Recognition Memory. *The Journal of Neuroscience* , 25 (1), pp.52–61.
- Wirhns, O. et al., 2008. Deficits in working memory and motor performance in the APP/PS1ki mouse model for Alzheimer's disease. *Neurobiology of Aging*, 29(6), pp.891–901.
- Wisniewski, T. & Goñi, F., 2015. Immunotherapeutic Approaches for Alzheimer's Disease. *Neuron*, 85(6), pp.1162–1176.
- Wolfe, M.S., Xia, W. & Ostaszewski, B.L., 1999. Two transmembrane aspartates in presenilin-1 required for presenilin endoproteolysis and g-secretase activity. , 117(1907), pp.513–517.

- Xu, N.-G. et al., 2015. Ameliorative effects of physcion 8-O- β -glucopyranoside isolated from *Polygonum cuspidatum* on learning and memory in dementia rats induced by A β 1–40. *Pharmaceutical Biology*, 53(11), pp.1632–1638.
- Xu, W. et al., 2015. Early hyperactivity in lateral entorhinal cortex is associated with elevated levels of A β PP metabolites in the Tg2576 mouse model of Alzheimer's disease. *Experimental neurology*, 264, pp.82–91.
- Yamada, K. et al., 2009. Abeta immunotherapy: intracerebral sequestration of Abeta by an anti-Abeta monoclonal antibody 266 with high affinity to soluble Abeta. *The Journal of neuroscience : the official journal of the Society for Neuroscience*, 29(36), pp.11393–8.
- Yamashima, T., 2013. Reconsider Alzheimer's disease by the “calpain-cathepsin hypothesis”-a perspective review. *Progress in neurobiology*, 105, pp.1–23.
- Yan, R. & Vassar, R., 2014. Targeting the β secretase BACE1 for Alzheimer's disease therapy. *Lancet neurology*, 13(3), pp.319–29.
- Yancopoulou, D. & Spillantini, M., 2003. Tau protein in familial and sporadic diseases. *NeuroMolecular Medicine*, 4(1-2), pp.37–48.
- Yang, S. et al., 2012. A peptide binding to the β -site of APP improves spatial memory and attenuates A β burden in Alzheimer's disease transgenic mice. *PloS one*, 7(11), p.e48540.
- Yankner, B.A. et al., 1989. Neurotoxicity of a fragment of the amyloid precursor associated with Alzheimer's disease. *Science*, 245, pp.417–420.
- Yankner, B.A., Caceres, A. & Duffy, L.K., 1990. Nerve growth factor potentiates the neurotoxicity of beta amyloid. *Proceedings of the National Academy of Sciences*, 87 (22), pp.9020–9023.
- Yassa, M. a & Stark, C.E.L., 2011. Pattern separation in the hippocampus. *Trends in neurosciences*, 34(10), pp.515–25.
- Yassa, M.A. et al., 2010. High-resolution structural and functional MRI of hippocampal CA3 and dentate gyrus in patients with amnesic Mild Cognitive Impairment. *NeuroImage*, 51(3), pp.1242–1252.
- Yassine, N. et al., 2013. Detecting spatial memory deficits beyond blindness in tg2576 Alzheimer mice. *Neurobiology of Aging*, 34(3), pp.716–730.
- Yoon, T. et al., 2008. Prefrontal cortex and hippocampus subserve different components of working memory in rats. *Learning & Memory*, 15, pp.97–105.
- Yoshiyama, Y. et al., 2007. Synapse loss and microglial activation precede tangles in a P301S tauopathy mouse model. *Neuron*, 53(3), pp.337–351.
- You, H. et al., 2012. A β neurotoxicity depends on interactions between copper ions, prion protein, and N-methyl-d-aspartate receptors. *Proceedings of the National Academy of Sciences*, 109 (5), pp.1737–1742.

- Zanetti, O., Solerte, S.B. & Cantoni, F., 2009. Life expectancy in Alzheimer's disease (AD). *Archives of gerontology and geriatrics*, 49, pp.237–243.
- Zerbinatti, C. V et al., 2004. Increased soluble amyloid-beta peptide and memory deficits in amyloid model mice overexpressing the low-density lipoprotein receptor-related protein. *Proc Natl Acad Sci USA*, 101, pp.1075–1080.
- Zhang, Y. et al., 2014. A lifespan observation of a novel mouse model: in vivo evidence supports a β oligomer hypothesis. *PloS one*, 9(1).
- Zhang, Y. et al., 2011. APP processing in Alzheimer's disease. *Molecular Brain*, 4(1), p.3.
- Zhang, Y. et al., 2010. Genetic reduction of striatal-enriched tyrosine phosphatase (STEP) reverses cognitive and cellular deficits in an Alzheimer's disease mouse model. *Proceedings of the National Academy of Sciences*, 107 (44), pp.19014–19019.
- Zhang, Y. et al., 2008. The tyrosine phosphatase STEP mediates AMPA receptor endocytosis after metabotropic glutamate receptor stimulation. *The Journal of Neuroscience*, 28(42), pp.10561–10566.
- Zhao, G. et al., 2004. Identification of a new presenilin-dependent zeta-cleavage site within the transmembrane domain of amyloid precursor protein. *J Biol Chem*, 279, pp.50647–50650.
- Zhao, G. et al., 2007. The same gamma-secretase accounts for the multiple intramembrane cleavages of APP. *J Neurochem*, 100, pp.1234–1246.
- Zhuo, J.-M. et al., 2008. An Increase in A β 42 in the Prefrontal Cortex is Associated with a Reversal-Learning Impairment in Alzheimer's Disease Model Tg2576 APPsw Mice. *Current Alzheimer Research*, 5(4), pp.385–391.

